To the Graduate Council:

I am submitting herewith a dissertation written by Mahmood Ghazizadeh entitled "Petrology, Depositional Environments, Geochemistry, and Diagenetic History of Lower and Middle Chickamauga Group (Middle Ordovician) Along Highway 58, East Tennessee." I have examined the final copy of this dissertation for form and content and recommend that it be accepted in partial fulfillment of the requirements for the degree of Doctor of Philosophy, with a major in Geology.

Kenneth R. Walker

Kenneth R. Walker, Major Professor

We have read this dissertation
and recommend its acceptance:

Robert E. McLaughlin

Thomas M. Broadhead

Edward E.C. Clebsch

Accepted for the Council:

Lewinkel

Vice Provost
and Dean of The Graduate School

PETROLOGY, DEPOSITIONAL ENVIRONMENTS, GEOCHEMISTRY, AND DIAGENETIC HISTORY OF LOWER AND MIDDLE CHICKAMAUGA GROUP (MIDDLE ORDOVICIAN) ALONG HIGHWAY 58, EAST TENNESSEE

A Dissertation

Presented for the

Doctor of Philosophy

Degree

The University of Tennessee, Knoxville

Mahmood Ghazizadeh

August 1987

DEDICATION

This volume is dedicated with love to my wife, Shahnaz; without her, none of my successes could have been possible.

ACKNOWLEDGMENTS

I wish to thank my committee chairman, Dr. Kenneth R. Walker, Carden Professor and Head, Department of Geological Sciences, for his encouragement and advice on this dissertation and throughout my graduate studies at The University of Tennessee.

I would also like to acknowledge my other committee members, Dr. R. E. McLaughlin, Dr. T. W. Broadhead, and Dr. E. C. Clebsch, for their time and useful suggestions during the preparation of this work.

Finally, special thanks go to my brother, M. R. Ghazizadeh; my brother-in-law, S. A. Davani; and to my friends, Mr. and Mrs. C. J. Claffey, R. Asreen, W. Borowski, and fellow members of the "Carbonate Bank" and "Paleo-Room" in the Department of Geological Sciences, The University of Tennessee.

This research has been supported by a National Science Foundation Grant (EAR-792-27268) to Dr. Walker and Dr. Broadhead, a grant from The University of Tennessee Department of Geological Sciences Professors Honor Fund, and a grant from the Appalachian Basin Industrial Associates. Additional support was provided to me by a grant from Atlantic Richfield Oil Company.

ABSTRACT

The Middle Ordovician carbonate rocks which are exposed along Highway 58 in southeastern Tennessee (measured stratigraphic sections are: Goodfield, Center Point, Ten Mile, and Barnardsville), were deposited in a very complex tidal flat and subtidal-lagoonal array of environments on a gently sloping platform-shelf. Fluctuation in sea level, basin subsidence, tectonic activity, and geometry of the basin caused lateral migration of the environments, resulting in a pattern-less series of complex facies which repeated several times during deposition of the entire Middle Ordovician in the study area.

The most volumetrically important lithofacies and the inferred depositional environments within these Middle Ordovician carbonate rocks are: (1) cherty dolostone-dolostone (supratidal dolomitic flat), (2a) green and red silty mudstone (supratidal mudflat), (2b) greenish gray micrite-biomicrite (supratidal mudflat), (3a) red silty, intra-pelbiosparite (intertidal channel), (3b) green and red, loosely packed ostracod rich pelbiomicrite (intertidal pond), (3c) stromatolitic mudstone (intertidal levee), (4a) bryozoan-ostracod-brachiopod rich pelbiomicrite (subtidal "intrabasinal lagoon" or pond, type 1), (4b) silty, packed pelbiomicrite-pelbiosparite (subtidal "intrabasinal lagoon" or pond, type 2), (4c) ostracod-gastropod rich, bioturbated pelbiomicrite (subtidal "intrabasinal lagoon" or pond, type 3), (4d) bioturbated brachiopod-molluscan rich biomicrite (subtidal "intrabasinal lagoon" or pond, type 4), (5a) bioturbated green and red sity mudstone-silty sparse biomicrite (subtidal quiet-protected

lagoon), (5b) greenish gray-tan mudstone-sparse biomicrite (subtidal protected lagoon), (6) intrapelbiosparite-pelbiosparite-pelbiomicrite (subtidal channel), and (7) Tetradium rich packstone (subtidal "wave baffle").

At one locality (Center Point), where 40 samples were selected for geochemical study, based on the inferred depositional environments of the lithofacies, Sr, Na, Mn, Mg, and Fe were determined for the soluble fraction of each sample by atomic absorption spectrometyr, and calcium by titration. Local variations in elemental composition showed that Na, Mn, and Fe (partially) are controlled by detrital minerals, high Mg content of some samples by stylolitization and dolomitization. The inverse relationship between Sr and insoluble residue may indicate the close association of Sr with the original mineralogy (aragonite and calcite) and the influx of terrigenous clastic materials into the depositional environment. Discriminant function analysis and Mn vs Fe plot both showed that carbonate rocks were statistically different and can be divided into two distinct groups and one transitional group. Depositional environment, sediment type, and diagenesis are believed to be responsible for differences between groups and variation in the trace element content.

Distinct diagenetic features recognized within the Middle Ordovician in the study area include: (1) biological activity (burrowing, boring, micritization), (2) crystal silt, (3) fringe cement, (4) syntaxial overgrowth cement, (5) equant-drusy calcite mosaics, (6) neomorphism, (7) physical compaction, (8) pressure

solution, and (9) replacement. Primary and secondary porosity in these rocks includes: (1) inter- and intraparticle porosity, (2) moldic, (3) shelter, (4) fenestral, (5) fracture, (6) dissolution, (7) boring, (8) burrowing, and (9) shrinkage cracks. However, much of the porosity of the original sediment as well as secondary porosity types is now occluded and these rocks could not act as a reservoir for hydrocarbon (oil and gas) entrapment.

The Markov model of Gingerich (1969), and the modified Markov method of Carr (1982), were applied to test the presence or the absence of "orderly events, or cyclic pattern" within these rocks. The Gingerich method has shown the presence of a very complex facies transition or "cyclic pattern," which is very hard, if not impossible, to interpret in the context of the inferred depositional environments and may also be statistically meaningless. However, Carr's method has only shown two important facies transitions: (1) subtidal channel to intertidal channel, and (2) intertidal channel to intertidal pond. These facies transitions are not surprising because channels within this complex depositional system may have traversed subtidal to intertidal environments and connected to intertidal ponds which were adjacent to the intertidal channels.

TABLE OF CONTENTS

CHAPTER		PAGE
I.	INTRODUCTION	1
	General Background	1
	Previous Study	1
	Purpose and Significance	5
	Study Area and Method of Investigation	7
	Limitation of Study and Stratigraphic Problems	10
II.	STRATIGRAPHY AND SEDIMENTOLOGY	12
	Introduction	12
	Stratigraphic Nomenclature Usage	14
	Lithofacies	18
	Environment of Deposition	75
	Stratigraphic Relationships	94
	Conceptual Sedimentation Model	108
	Summary and Conclusions	114
III.	ENVIRONMENTAL SIGNIFICANCE OF SOME TRACE AND MAJOR ELEMENTS	118
	Introduction	118
	Computer Analysis	121
	Summary and Conclusions	162
IV.	DIAGENESIS AND PORE SYSTEMS	165
	Introduction	165
	Diagenesis	166
	Discussion of Sequential Diagenetic Events (Paragenesis) and Related Diagenetic Environments	189
	Pore Systems	192
	Conclusions	207
V.	AN APPLICATION OF MARKOV CHAIN ANALYSIS IN TESTING FOR POSSIBLE CYCLICITY IN CARBONATE SEDIMENTS OF THE MIDDLE ORDOVICIAN OF THE STUDY AREA	210
	Statistical Methods; Markov Chain Analysis	210
	Results and Discussion	213
	Summary and Conclusions	229
VI.	CONCLUSIONS	232

PAGE

REFERENCES 235

APPENDICES 256

A. DESCRIPTION OF MEASURED STRATIGRAPHIC SECTIONS 257
B. PETROGRAPHIC CONSTITUENT ANALYSIS 311
C. FACIES ASSIGNMENT OF SAMPLES IN THE FOUR MEASURED STRATIGRAPHIC SECTIONS 351
D. PROCEDURE AND SAMPLE PREPARATION FOR ATOMIC ABSORPTION ANALYSIS 354
E. TWO DIMENSIONAL DIAGRAM OF TRACE ELEMENT IN RELATION TO VARIMAX ROTATION FACTORS 359

VITA 363

LIST OF TABLES

TABLE		PAGE
3.1	Selected samples from Center Point stratigraphic section used in geochemical analysis	120
3.2.	Correlation coefficient for the Center Point stratigraphic section samples	123
3.3.	Concentration of the trace elements: Mn, Fe, Mg, Sr, Ca, and Na in bulk samples of Center Point section	124
3.4.	The characters of the hypersaline samples based on Na frequency distribution and boundary assignment	132
3.5.	Percentages and average of insoluble residue and Mn/Fe ratio of samples of Center Point section	142
3.6.	Mg content based on atomic absoprtion values, and dolomite percentages based on point count data, in Center Point section	148
3.7.	Varimax rotated factor matrix for 38 selected samples of Center Point sections	153
3.8.	Discriminant function analysis grouping of samples based on three parameters; insoluble residue, manganese, and strontium	157
3.9.	Discriminant function analysis grouping of samples based on six parameters; insoluble residue, manganese, strontium, sodium, magnesium, and iron	158
3.10.	Grouping of samples, using three and six parameters for discriminant function analysis, and grouping based on Mn-Fe plot	159
4.1.	Summary of terms used for morphological configurations	178
5.1.	Facies transition selected as significance level changes from $\alpha = 0.4$ to $\alpha = 0.9$ after analysis of Figure 5.1	230

TABLE PAGE

B.1. Center Point section point count analysis of samples 1A-1E 313

B.2. Center Point section point count analysis of samples 1F-5_1A 314

B.3. Center Point section point count analysis of samples 5A-6A 315

B.4. Center Point section point count analysis of samples 6_1A-11A 316

B.5. Center Point section point count analysis of samples 12B-15A 317

B.6. Center Point section point count analysis of samples 16A-$16E_2$ 318

B.7. Center Point section point count analysis of samples 17A-$20A_2$ 319

B.8. Center Point section point count analysis of samples $21A_1$-25A 320

B.9. Center Point section point count analysis of samples 25B-27R 321

B.10. Center Point section point count analysis of samples 28A-28H 322

B.11. Center Point section point count analysis of samples 29A-29G 323

B.12. Center Point section point count analysis of samples 29J-31 324

B.13. Goodfield section point count analysis of samples 1A-9 325

B.14. Goodfield section point count analysis of samples 10-22 326

B.15. Goodfield section point count analysis of samples 24-32 327

B.16. Goodfield section point count analysis of samples 34-41 328

TABLE PAGE

B.17. Goodfield section point count analysis of samples 44-53 329

B.18. Goodfield section point count analysis of samples 57-64 330

B.19. Goodfield section point count analysis of samples 65-74 331

B.20. Goodfield section point count analysis of samples 75-81 332

B.21. Goodfield section point count analysis of samples 82-95 333

B.22. Goodfield section point count analysis of samples 97 & 99 334

B.23. Barnardsville section point count analysis of samples 1-18 335

B.24. Barnardsville section point count analysis of samples 22-40 336

B.25. Barnardsville section point count analysis of samples 45-56 337

B.26. Barnardsville section point count analysis of samples 59-70 338

B.27. Barnardsville section point count analysis of samples 75-86 339

B.28. Barnardsville section point count analysis of samples 87-101 340

B.29. Barnardsville section point count analysis of samples 103-105 341

B.30. Ten Mile section point count analysis of samples 1-8 342

B.31. Ten Mile section point count analysis of samples 10 through 19-1 343

B.32. Ten Mile section point count analysis of samples 20 through 23-4B 344

TABLE		PAGE
B.33.	Ten Mile section point count analysis of samples 27-37	345
B.34.	Ten Mile section point count analysis of samples 38-39M	346
B.35.	Ten Mile section point count analysis of samples 39N-40	347
B.36.	Ten Mile section point count analysis of samples 41A-42B	348
B.37.	Ten Mile section point count analysis of samples 42C-45B	349
B.38.	Ten Mile section point count analysis of samples 45E-46K	350
C.1.	Stratigraphic section samples	352
D.1.	Analytical conditions	356
D.2.	Chemical interferences for selected elements, and the recommended releasing agent/ionization buffer	358

LIST OF FIGURES

FIGURE		PAGE
1.1.	Palinspastic map of East Tennessee showing areal distribution of Middle and Upper Ordovician strata (modified after Walker, 1980)	2
1.2.	Strike belt map showing selected previous studies north of the Saltville Fault in the vicinity of the study area	4
1.3.	Proposed environmental arrays during Porterfieldian time (from Walker, Shanmugam, and Ruppel, 1983)	6
1.4.	Location of study area and stratigraphic sections	8
2.1.	Stratigraphic nomenclature for Middle Ordovician rocks of the valley and ridge north of the Saltville Fault	16
2.2.	Stratigraphic nomenclature of Middle Ordovician rocks of the Tennessee Central Basin and part of the valley and ridge province	17
2.3.	Features of facies 1	21
2.4.	Features of lithofacies 2a and 2b	27
2.5.	Skeletal allochem preservation, cement types, and sedimentary structures of facies 3a	32
2.6.	Skeletal allochem of lithofacies 3b	37
2.7.	Thin-section negative prints of the characteristic sedimentary structures of lithofacies 3c and 4a	40
2.8.	Features observed in lithofacies 4b	47
2.9.	Features of lithofacies 4c	53
2.10.	Characteristic fabric of lithofacies 4d and 5a	58
2.11.	Characteristic fabrics observed in lithofacies 5b and 6	64

FIGURE		PAGE
2.12.	Characteristic features of lithofacies 7	73
2.13.	Diagnostic physical, chemical, and biological characteristics of lithofacies in the Middle Ordovician carbonate sediments in the study area	95
2.14.	Distribution of lithofacies in Goodfield, Center Point, Ten Mile, and Barnardsville measured stratigraphic sections	98
2.15.	Sample locations, lithologic column, paleo-bathymetry, rock types, and facies distributions for Goodfield measured section	100
2.16.	Sample locations, lithologic column, paleo-bathymetry, rock types, and facies distributions for Barnardsville measured section	101
2.17.	Sample locations, lithologic column, paleo-bathymetry, rock types, and facies distributions for Ten Mile measured section	102
2.18.	Sample locations, lithologic column, paleo-bathymetry, rock types, and facies distributions for Center Point measured section	103
2.19.	Facies relations in the Middle Ordovician, lower and middle Chickamauga Group in the study area from southwest to northeast	105
2.20.	Generalized setting (regional, plan, and cross-sections) of environments and subenvironments of northern Andros Island (from Ginsburg, 1975)	109
2.21.	Hypothetical representation of inferred paleoenvironments of the Middle Ordovician sediments in the area	112
3.1.	Trace elements distribution in facies at Center Point section	128
3.2.	Analytical results, Mn/Fe ratio, rock types, facies distribution and paleobathymetric curve for samples from Center Point section	129

FIGURE PAGE

3.3. Frequency distribution of Na concentration in samples from the Center Point stratigraphic section showing brackish and hypersaline divisions based on Na values 130

3.4. Correlation of insoluble residue and Na in Center Point samples; r = coefficient of correlation 134

3.5. Correlation of insoluble residue and Sr in the Center Point samples; r = coefficient of correlation 138

3.6. Correlation of insoluble residue and Mn in Center Point samples; r = coefficient of correlation 140

3.7. Correlation of insoluble residue and Fe in Center Point samples; r = coefficient of correlation 143

3.8. Fe vs Mn for Center Point section 146

3.9. Correlation of insoluble residue and Mg in Center Point samples 149

3.10. Grouping of samples from Center Point section based on three and six parameters, using discriminant function analysis 161

4.1. Basic porosity types in sedimentary carbonates (from Choquette and Pray, 1970) 167

4.2. Cementation fabrics of Middle Ordovician carbonate rocks (a) 168

4.3. Petrographic features observed in selected thin sections from the Middle Ordovician rocks 172

4.4. Cementation fabrics of Middle Ordovician carbonate rocks (b) 180

4.5. Cementation fabrics of Middle Ordovician carbonate rocks (c) 186

4.6. Timing of diagenetic events in the Middle Ordovician "Chickamauga Group" carbonate rocks in the study area 190

FIGURE		PAGE
4.7.	Porosity types of Middle Ordovician carbonate rocks (a)	195
4.8.	Porosity types of Middle Ordovician carbonate rocks (b)	199
4.9.	Shrinkage cracks porosity in Middle Ordovician carbonate rocks	205
5.1.	Facies transition count matrix for the Middle Ordovician rocks in the study area	215
5.2.	Facies transition probability matrix for the Middle Ordovician rocks in the study area	216
5.3.	Facies independent trial matrix for the Middle Ordovician rocks in the study area	217
5.4	Mathematical equations for calculation of x^2_y statistics and the degrees of freedom in this study	219
5.5.	Difference matrix for the Middle Ordovician rocks in the study area	220
5.6.	Lithofacies transitions of Middle Ordovician rocks	221
5.7.	Probabilities of facies transition	225
5.8.	Facies transitions selected as significant after analysis of Figure 5.1	228
5.9.	Facies transitions, using modified Markov Analysis	230
E.1.	Varimax rotation of Middle Ordovician data	360

CHAPTER I

INTRODUCTION

General Background

The Middle Ordovician ("Chickamauga Group") of East Tennessee includes all the strata between the top of the Knox Group and the base of the Sequatchie and Juniata formations (Milici, 1973), not including the "Martinsburg" Formation. The diverse lithologies of this group display a complex sequence of carbonate and terrigenous clastic lithologies ranging in thickness up to 2500 meters or more. These rocks are exposed in a series of strike belts (Fig. 1.1) which have a regional northeast-southwest trend (Rodgers, 1953). Despite many geological investigations carried out during the last century concerning the nature and interrelationship of these rocks, this group has been the subject of much controversy (Twenhofel et al., 1954).

Previous Study

Middle Ordovician strata in East Tennessee have been studied by Safford (1869), Hays (1891), Ulrich (1911), Butts (1926), Prouty (1946) Cattermole (1958), Cooper (1956) and Swingle (1964) among others, and correlated with strata in Central Tennessee by Bassler (1932) and Wilson (1949). Keith (1895), Rodgers (1953), and Newman (1955) have studied the structural and stratigraphic aspects of these rocks. In 1969, Milici and Smith redefined and described the Chickamauga Supergroup in its type area and have correlated Middle Ordovician

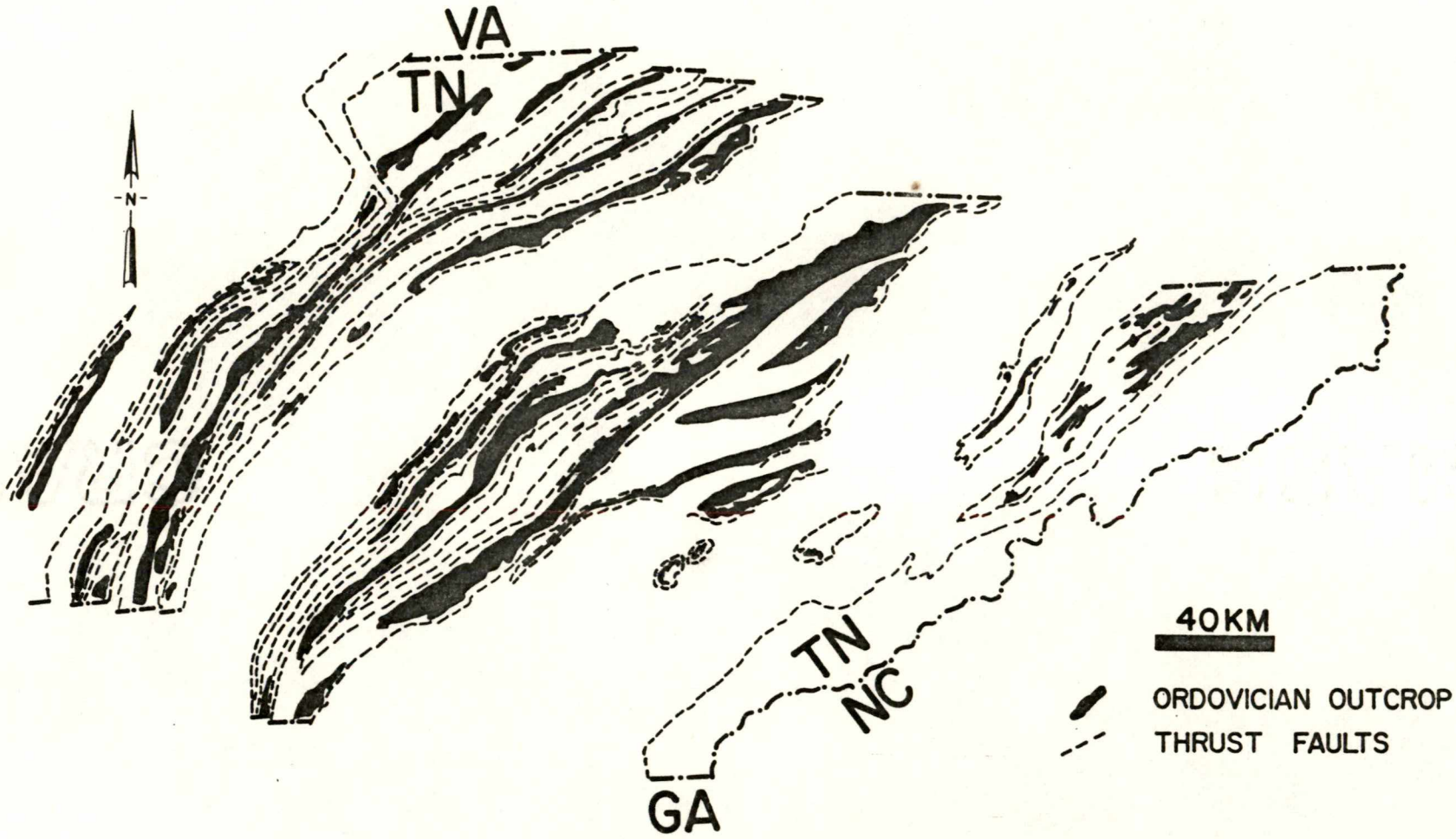


Figure 1.1. Palinspastic map of East Tennessee showing areal distribution of Middle and Upper Ordovician strata (modified after Walker, 1980). Palinspastic base after Roeder and Witherspoon, 1978.

strata in Chickamauga, Georgia, with those in the Sequatchie Valley and Central Tennessee.

Beginning in the 1970's, K. R. Walker and co-workers at the University of Tennessee, Knoxville, have studied and reevaluated the complex stratigraphic relationships of these Middle Ordovician strata in east Tennessee, using modern stratigraphic concepts and techniques. Walker and Alberstadt (1973) proposed a facies model for the Middle Ordovician deposits of east Tennessee. This model has been refined by later work (Walker, 1977, 1980) and has been continuously updated as new data become available (e.g., Walker, Shanmugam, and Ruppel, 1983). This model includes three major environmental zones: (1) a northwestern, shallow water bank with a southeasterly facing shelf edge, (2) a slope environment grading southeastward into, (3) a deeper-water basin southeast of the shelf edge, and (4) a shallow water nearshore area southeast of the basin, containing a mixture of terrigenous clastic and carbonate sediments (Ruppel and Walker, 1977; Walker, Broadhead and Keller, 1980; Walker, Shanmugam and Ruppel, 1983).

In addition to the present study on the most northwesterly carbonate shelf sequences in east Tennessee, a similar shelf sequence in the same strike belt was studied near Clinton, Tennessee, by Borowski (Fig. 1.2). No other studies have considered the area covered by the present investigation.

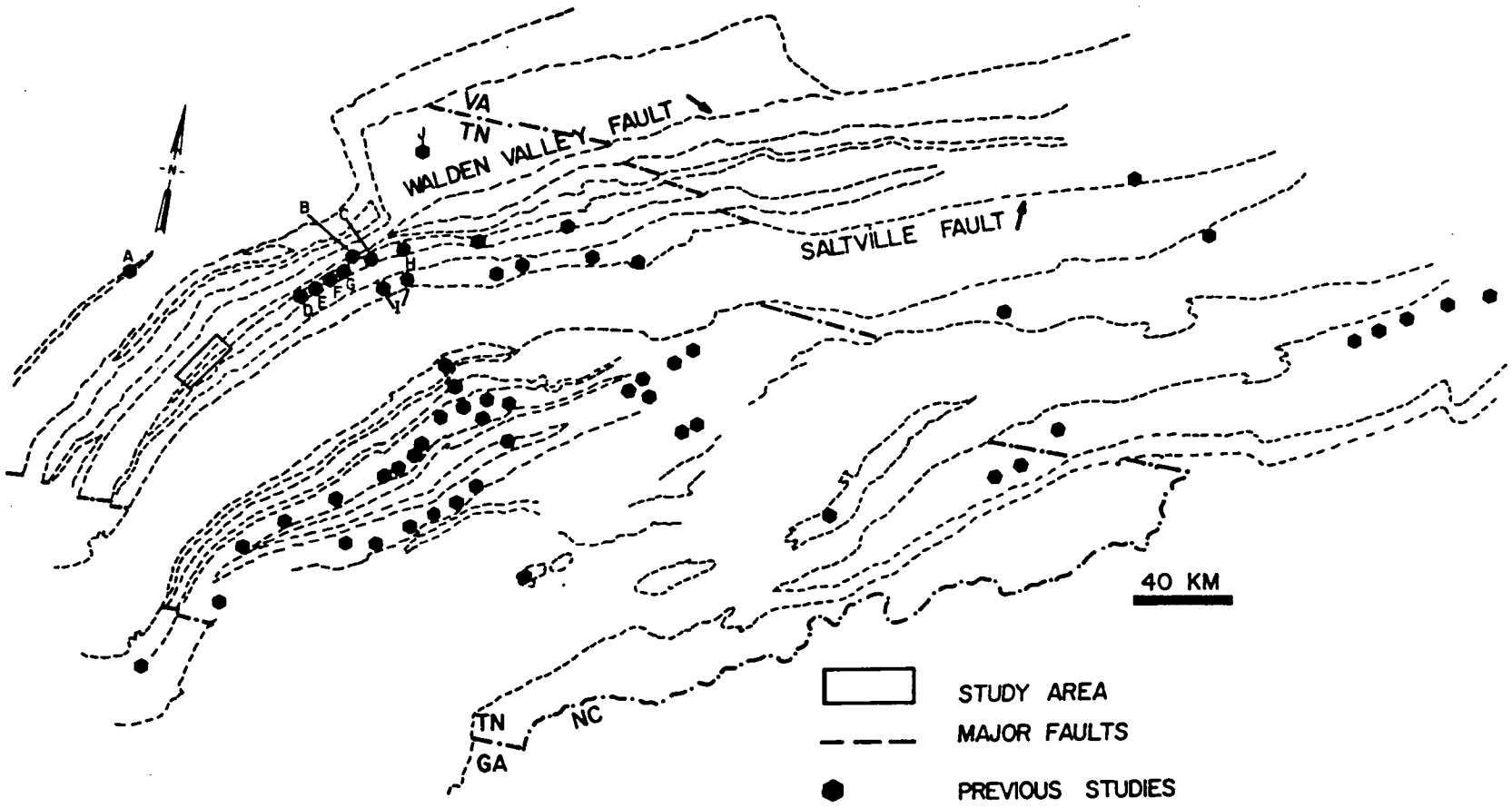


Figure 1.2. Strike belt map showing selected previous studies north of the Saltville Fault in the vicinity of the study area.

A. Blythe (1974)
B. Borowski (1982)
C. Lomenick (1958)
D. Weiss (1981)
E. Belvin (1975)
F. Harvell (1954)
G. Causey (1956)
H. Ashworth (1982)
I. Breland (1980)
J. Blythe (1967)

Purpose and Significance

Although a large amount of data has been collected by Walker and his colleagues which has led to a better understanding of the depositional environment and distribution of carbonate sequences in east Tennessee, much more needs to be done in the northwestern parts of the east Tennessee region (northwest of Athens). According to Walker's model (Walker et al., 1983), these areas were characterized by shelf lagoon subenvironment such as mud banks, and subtidal sand/mud flats and peritidal deposits (Fig. 1.3).

In the absence of detailed studies of these areas, several problems with regard to stratigraphy, paleoenvironments, and correlation are unsolved. The northwesternmost belts also contain units transitional between the Central Basin Ordovician sequence studied by Wilson (1962), Milici (1970), and Alberstadt and his students (e.g., 1973) and the east Tennessee Ordovician sequences.

The major objectives of the present investigation were as follows:

1. To analyze the lithologic and facies character of these carbonate sediments in the northwestern part of the Ridge and Valley of east Tennessee (northwest of Athens), based upon outcrop description and thin-section studies;
2. To determine the nature of the paleoenvironments through a macroscopic and microscopic examination of biota, sedimentary structures, and petrography;
3. To develop a stratigraphic and environmental framework for the sequence in the study area;

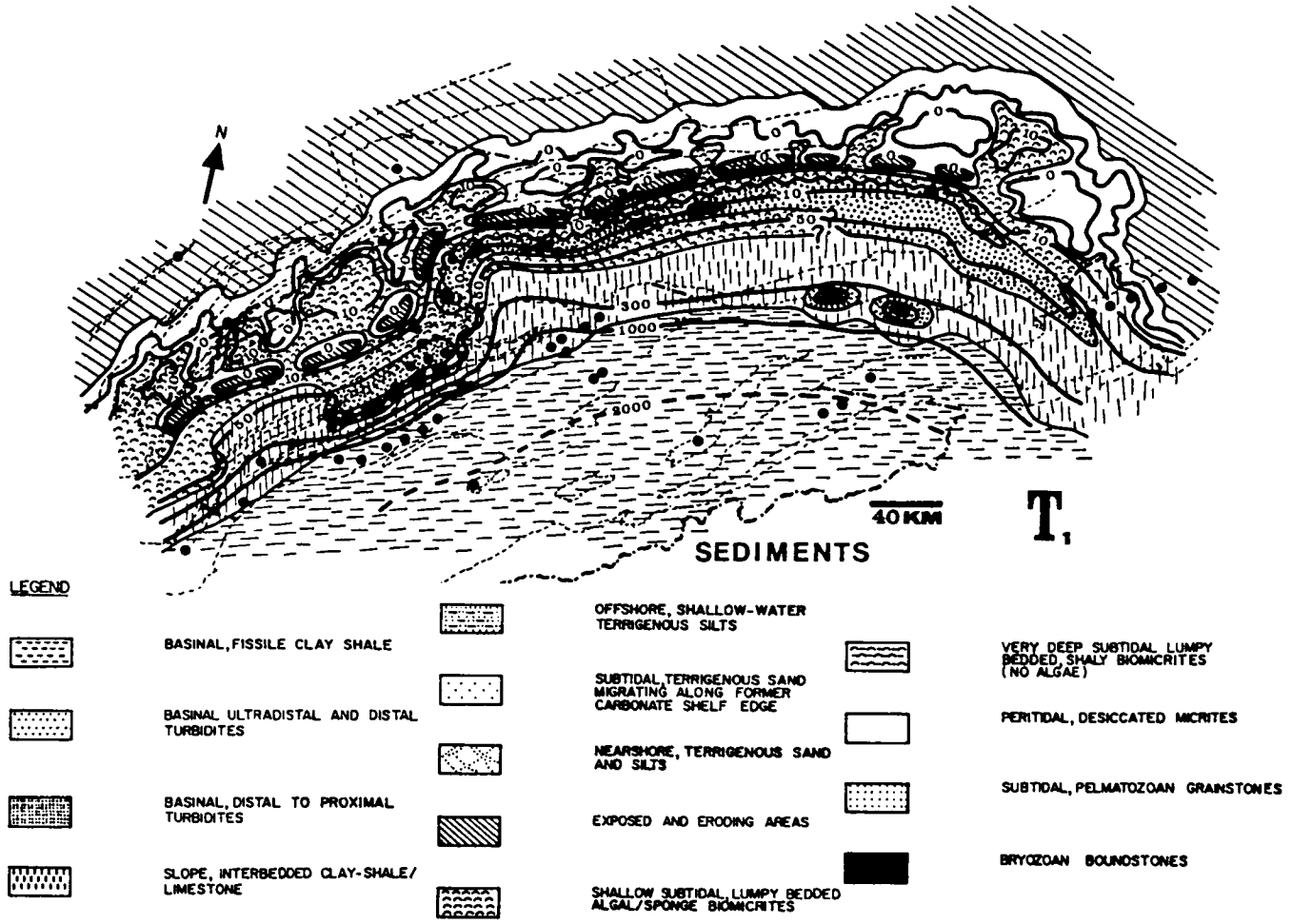


Figure 1.3. Proposed environmental arrays during Porterfieldian time (from Walker, Shanmugam, and Ruppel, 1983).

4. To analyze the vertical succession of depositional environments in detail, using a two-way frequency table and combining data from all four sections in order to recognize cyclical events and lateral relationships between th lithologies and to determine the arrangement and migration of environments and subenvironments within these sequences;
5. To study details of the diagenetic history including cementation, micritization, silicification, stylolitization and porosity occlusion;
6. To analyze trace element distributions in one of the stratigraphic sections (Center Point), using Atomic Absorption Spectrophotometry.

Study Area and Method of Investigation

Carbonate rocks of the Chickamauga Group (Rodgers, 1953) are exposed adjacent to Tennessee State Highway 58, in Meigs and Roane Counties, Tennessee (referred to as Barnardsville, Ten Mile, Center Point, and Goodfield sections), and were chosen on the basis of the quality of exposures.

Measurement of two sections (Goodfield and Center Point, Fig. 1.4) was done from the basal contact of each section at the post-Knox unconformity (Lower Ordovician) to the base of the Upper Middle Ordovician Moccasin Formation. The outcrops of the Ten Mile and Barnardsville sections lie near the axis of Ten Mile-Bacon Ridge Syncline (Fig. 1.4), so measurement of these two sections represents

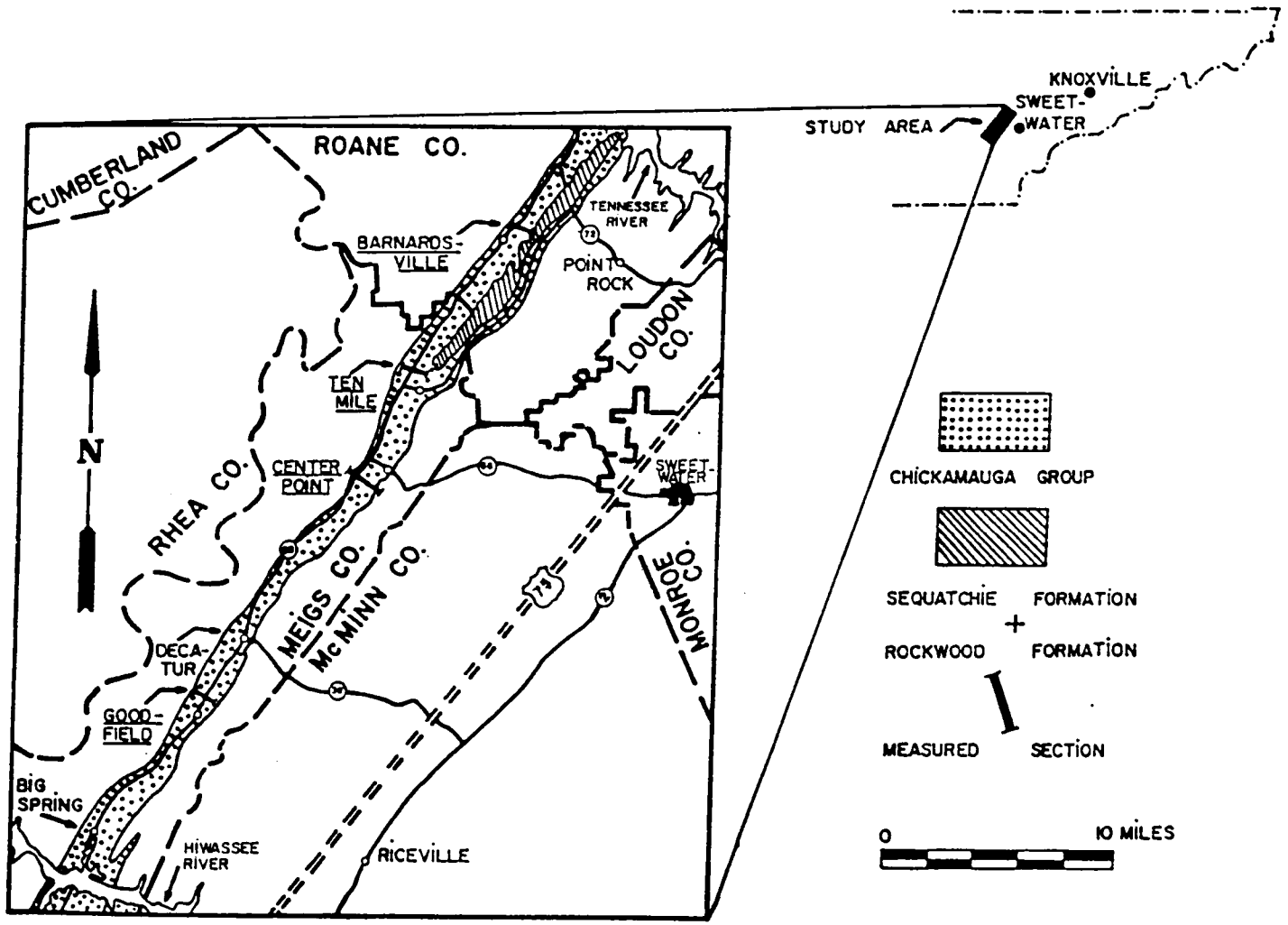


Figure 1.4. Location of study area and stratigraphic sections. Study sections are underlined and located at Goodfield, Center Point, Ten Mile, and Barnardsville.

transverse sections perpendicular to the axis of the syncline (from the post-Knox unconformity to the base of Moccasin Formation).

Rocks in this strike belt are within the Kingston Allochthon bounded on the north by the Kingston Fault and on the south by the White Oak Mountain/Walden Valley Fault (Fig. 1.2). In most areas, the sequence dips gently (up to 25°) to the southeast. The distance between sections is approximately seven miles and each ranges between 458 and 592 meters in thickness.

Paleoenvironmental interpretation was based on close field examination and description of measured sections, laboratory analysis of thin sections and analysis of polished slabs. Approximately 600 samples were collected, where there was a change in lithotype in the field. Field observation, polished slabs, and thin section data were used to assign informal units described in Appendix A. Thin sections (standard five by eight centimeters) were stained with alizarine red-S (modified from Friedman, 1959) and potassium ferricyanide (modified from Lindholm and Finkelman, 1972) to determine the presence of dolomite and iron-rich carbonate minerals. This staining aided in the study of the diagenetic history including cementation, compaction, and paragenesis (Bathurst, 1971; MacIntrye, 1977; Longman, 1980; Meyers, 1980). Cathodoluminescence was also applied to determine cement morphology and to identify different generations of cements as well as their relationship to each other.

Of the 600 samples prepared, 205 thin sections were point counted (after the technique outlined by Chayes, 1954). Approximately 350-450

points/slide were counted to determine lithologic and paleontologic compositions (Appendix B). These data were then plotted to illustrate the abundance of constituents in relation to their stratigraphic and geographic distribution as a reflection of change in environmental patterns.

Trace element study was done on 40 selected samples from the Center Point section (Chapter III). The resultant geochemical data were interpreted by correlation with lithologies, depositional environments, diagenetic history and biota.

Limitation of Study and Stratigraphic Problems

There are several major limitations of this study which must be recognized. First, because of the poor quality of exposure of Middle Ordovician rocks in the area of this study, detailed field examination and sampling is limited. Second, as a consequence of poor exposure, recovery of macrofossils and biostratigraphic study is constrained and proved to be very difficult. Third, because of rarity of any previous, detailed, environmental study of the Middle Ordovician rocks northwest of the Hunter Valley allochthon for comparison with the present study (see, however, Borowski, 1982), facies assignment and environmental interpretation involved many assumptions and speculations.

The stratigraphy of Middle Ordovician rocks of the Southern Appalachians is in a state of uncertainty and has been the subject of much controversy over the last century. The Knox unconformity represents the boundary between the Lower and Middle Ordovician, but

rocks of the basal Chickamauga Group are not synchronous over this unconformable surface (McLaughlin, 1973). Several different stratigraphic terminologies have been proposed for and applied to the Southern Appalachian region (Safford, 1869; Hayes, 1891; Prouty, 1946; Rodgers, 1953; Cooper, 1956; Wilson, 1948, 1949; Milici and Smith, 1969).

Formal rock units recognized and described by various workers in Tennessee, Georgia, and Alabama do not correspond to the rocks of the present study area. Therefore, to prevent further confusion for future workers, the approach of this investigation is to look at the rocks in terms of their depositional environments rather than to assign formal stratigraphic names. However, more environmental and biostratigraphical studies need to be completed in this and neighboring strike belts for a better understanding of stratigraphy, facies distribution, environmental patterns, and the time-correlative relationship between rocks over a wide area. Only the lower and middle parts of the Chickamauga are examined in the present study; the upper part (Moccasin Formation) was excluded.

CHAPTER II

STRATIGRAPHY AND SEDIMENTOLOGY

Introduction

The Middle Ordovician, "Chickamauga Limestone," extends over a large area of the Southern Appalachian region of the Eastern United States, covering thousands of square kilometers of Northwestern Georgia, Northeastern Alabama, East and Central Tennessee, Western Virginia and Central Kentucky. This unit consist of limestone, dolomite, sandy limestone, calcareous sandstone, siltstone, bedded chert, silty limestone, and calcareous shale. The dominant carbonates are pelloid and ooid grainstones, cryptalgal boundstone and laminites, flat pebble conglomerates, echinoderm grainstone, pelloid and skeletal packstone-wackestone, and lime mudstones. These carbonate types are variable and repeatedly interbedded throughout the sequence.

The most complete section in surface exposure occurs in the vicinity of Chattanooga, in Chickamauga Valley, near the southern edge of the town of Chickamauga in Catoosa and Walker Counties, Georgia (type sections described by Milici and Smith, 1969). The "Chickamauga Limestone" in its type area is exposed for up to 1450 feet continuously along the western bank of Chickamauga Creek. The sequence has a general northeast-southwest strike and dips gently to the northwest.

The subsurface extent of the "Chickamauga" remains speculative due to the paucity of drilling and seismic data particularly between East and Central Tennessee (around the Nashville Dome). The transition from

"Chickamauga" facies of eastern Tennessee, to those more typical of Sequatchie Valley and Central Tennessee (Nashville Dome), is least known where the Cambrian and Ordovician sequences plunge below the onlapping Upper Paleozoic Mississippian and Pennsylvanian rocks.

The thickness of the "Chickamauga" ranges from 100 to 600 meters (although correlatives nearby are up to several thousand meters thick). The belts of maximum preserved sequence are located southeast of the Saltville Fault (Fig. 1.1, p. 2). Northwest of the Saltville Fault, the sections are thinner due in part to erosion and to the greater effect of thrust faults, which have sliced a greater portion of the upper part of the "Chickamauga." It is unlikely that the thickness of the sequence in the region between Sequatchie Valley and the Central Basin of Tennessee (around Nashville Dome) ever equaled that of the east (east of the Saltville Fault).

A distinct unconformity and erosional surface exists between the Lower Ordovician sequences (Knox Group) and the Middle Ordovician (Chickamauga Group) limestone and shale. In many places, one or two younger members of the Lower Ordovician are absent beneath the Middle Ordovician rocks due to post-Early Ordovician erosion, and the Chickamauga Group overlies a regolithic surface where chert and siliciclastic detritus have accumulated from subareal weathering and karst development on the Knox Group.

Regardless of the fact that Middle Ordovician limestone, shales and dolomites are widely, and in some localities excellently, exposed in strike belts northwest of the Saltville Fault, there has been less

detailed lithostratigraphic work in the area. As information has gradually accumulated during the past few years through the evaluation of sediments in various part of the Middle Ordovician depositional system, based on modern analogues, the necessity for more detailed lithostratigraphic, facies analysis, and paleoenvironmental interpretation to construct a comprehensive depositional model for the entire Middle Ordovician has become more obvious. The area of this study is unique with respect to the previous investigations of the Middle Ordovician carbonate rocks northwest of the Saltville Fault in Tennessee because:

1. Previous studies have largely been east of a N-S line through Knoxville; and
2. The area of present study is in a transition between the facies pattern typical of East Tennessee and that characteristic of the Central Basin of Tennessee.

Stratigraphic Nomenclature Usage

The name "Chickamauga" was originally defined by Hayes (1891) for the entire Middle Ordovician and part of the Upper Ordovician. The term "Chickamauga" has been redefined by various workers since it was first proposed by Hayes: Rodgers (1953), as a formation, Swingle (1964) and Milici (1973), as a group; Milici and Smith (1969), as a supergroup.

Subsequent work was based on lithologic evidence (e.g., Wilson, 1949; Milici and Smith, 1969; Rodgers, 1953), paleontologic evidence

(e.g., Cooper, 1956), and a combination of both lithologic and paleontologic evidence (e.g., Prouty, 1946), thus resulting in subdivision, correlation and development of several stratigraphic schemes in Virginia, Alabama, and Tennessee (East and Central Tennessee).

There are thirty or more different stratigraphic names which have been applied to these Middle Ordovician rocks in East Tennessee. Figures 2.1 and 2.2 represent the most commonly used names which have received the most attention, and illustrate the wide range of nomenclature. The majority of the names on Figures 2.1 and 2.2 were derived from localities in northeastern Tennessee and Virginia (Fig. 2.1), or Georgia and Central Tennessee (Fig. 2.2).

The development of different nomenclatural schemes has resulted from research being done in widely separated areas within a single block or a few adjacent fault blocks. Also, due to the lack of knowledge of the overall environmental pattern in the past, no two columns employing these schemes represent correlative parts of the original regional facies pattern. This is because previous investigators have looked at lithostratigraphy with the conception that rock units are separate entities, bounded and separated by disconformities. They also have used single taxa for biostratigraphic correlation without considering the degree of environmental control on the faunas.

Due to the complex facies distribution of lithic units throughout the belts north of the White Oak Mountain/Walden Valley Fault, to the

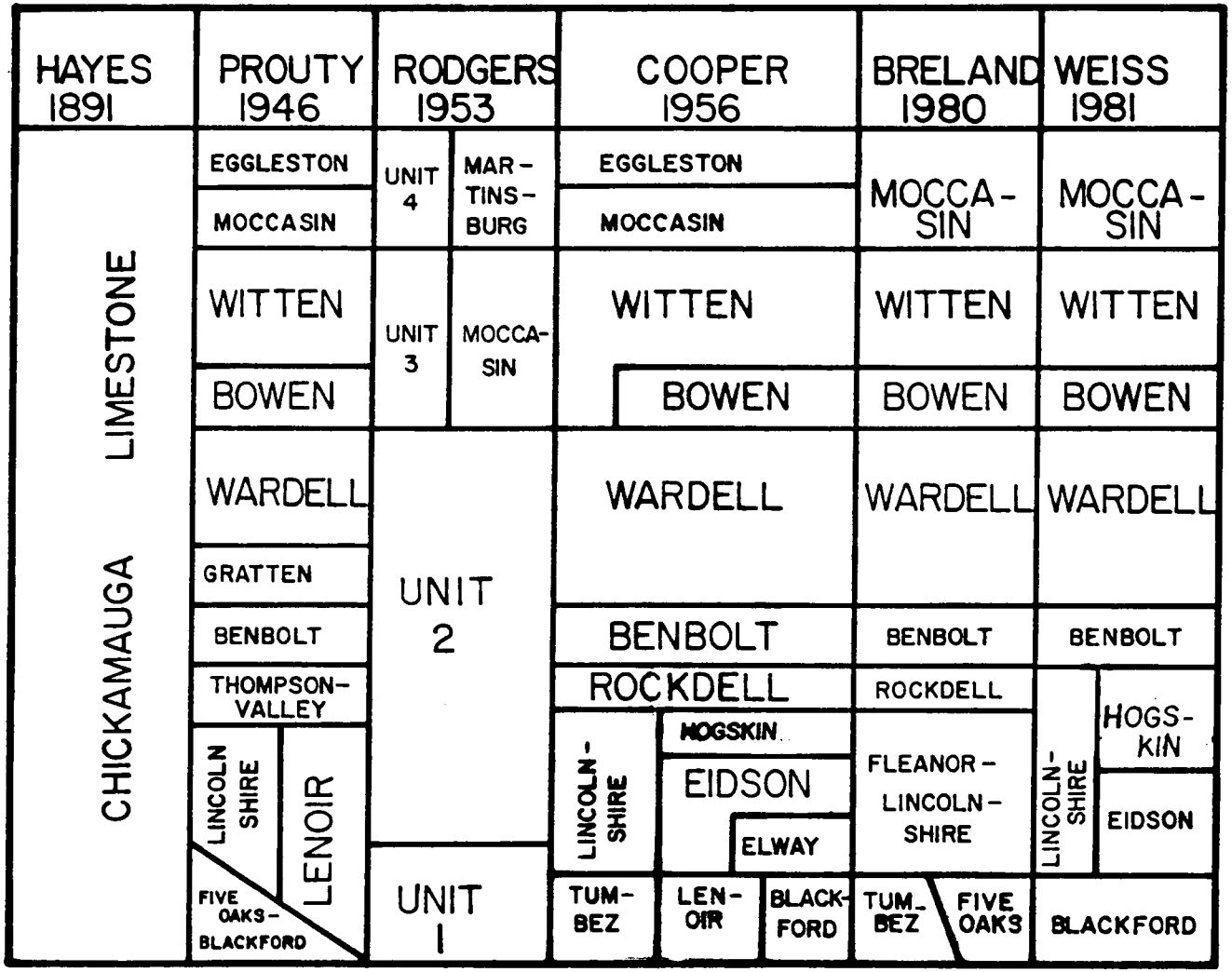


Figure 2.1. Stratigraphic nomenclature for Middle Ordovician rocks of the valley and ridge north of the Saltville Fault.

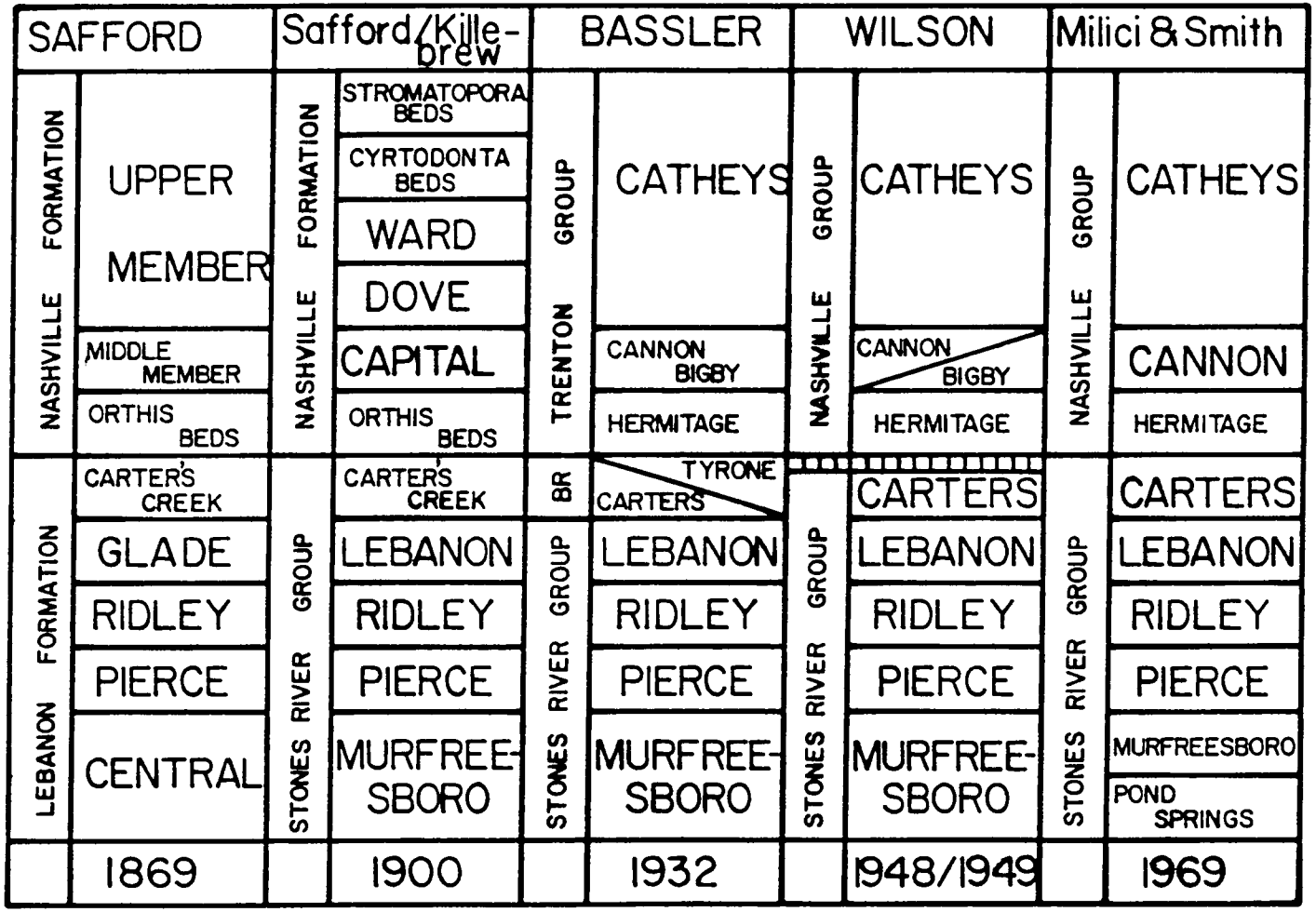


Figure 2.2. Stratigraphic nomenclature of Middle Ordovician rocks of the Tennessee Central Basin and part of the valley and ridge province.

lack of evidence of a persistent and synchronous time-marker (e.g., bentonite beds), and to the repetitive occurrence of similar rock units, nomenclature is not emphasized in this study. Instead emphasis was placed on careful subdivision in terms of lithologies and on environmental analysis in a more local context. The study's purpose is not to establish new stratigraphic terminology or to force application of previous workers' terms from other areas.

Lithofacies are described and interpreted, and correlation of these lithofacies is made through the physical extent of their lithology using particle types, sedimentary structure, and faunal content. Fourteen lithofacies and subfacies are recognized and are compared to the members of the earlier stratigraphic work in the area, but no attempt is made to correlate the rock units in this study with the sections in Georgia or the Central Basin of Tennessee.

Lithofacies

The lithofacies recognized in the Middle Ordovician carbonate sediments in the study area are as follows (Appendix C):

1: Cherty Dolostone-Dolostone

2a: Green and red silty mudstone (silty biomicrite, silty calcareous shale)

2b: Greenish gray micrite-biomicrite (wackestone)

3a: Red silty, Intrapelbiosparite-Biosparite (packstone)

3b: Green and red, loosely packed ostracod-rich pelbiomicrite (wackestone and packstone)

3c: Stromatolotic mudstone (dismicrite)

4a: Bryozoan-ostracod-brachiopod-rich pelbiomicrite (wackestone, packstone)

4b: Silty, packed pelbiomicrite-pelbiosparite (wackestone and packstone)

4c: Ostracod-gastropod-rich, bioturbated pelbiomicrite (wackestone and packstone)

4d: Bioturbated brachiopod-molluscan-rich biomicrite (wackestone and packstone)

5a: Bioturbated green and red silty mudstone-silty sparse biomicrite

5b: Greenish gray-tan mudstone, sparse biomicrite

6: Intrapelbiosparite, pelbiosparite-pelbiomicrite (packstone and grainstone)

7: Tetradium-rich packstone

What follows is a detailed descriptive discussion for each of these lithofacies. A brief mention of stratigraphic distribution of each facies is included with each description, but a full treatment of facies distribution is contained in a latter section of the dissertation.

1. Cherty Dolostone-Dolostone Lithofacies:

Facies 1 embraces the lowermost strata of the Middle Ordovician "Chickamauga Group" in the study area. This facies is easily recognized in thin section because constituent particle analysis (Appendix B) shows dolomite (approximately 90% by volume), chert clasts

(up to 5%), fossils (2%), and micrite (3%). Physical (mechanical) processes had little effect on stratification within facies 1. Storms and/or low amplitude tides and waves probably brought in fossil debris which is found within this facies. Burrowing was more common and had greater influence on the stratification, and in places destroyed any lamination that might have existed. Internal stratification and other large scale sedimentary structures may be indicated by differential weathering or crystal size variation, but commonly fracturing and karst artifacts obliterate these features on outcrop. In places, dolostone weathers so extensively that it forms vuggy surfaces.

The dolostones are light greenish-gray, light gray, and sometimes purple (GF-2A), and fracture concoidally. The lowermost contact of facies 1 is placed at the top of the uppermost beds of the Knox Group, but the lowermost portion of facies 1 is generally poorly exposed, and the exact nature of the contact in places is not known. Where observable, the lowermost 50 cm to 1.0 meter of facies 1 is made up of cherty dolostone which possibly suggests the presence of a hiatus (nondeposition-erosion) between the Middle Ordovician "Chickamauga Group" and the Knox Group (Lower Ordovician). Chert clasts up to 20 cm in length are chaotically arranged in a dolomitic matrix. The chert clasts are poorly sorted and unoriented (Fig. 2.3A). This chert or "breccia" horizon in the lowermost portion of facies 1 is never found more than 5 meters above the contact between the lower Middle Ordovician and the Knox Group (Walker, per. comm.).

Figure 2.3. Features of facies 1.

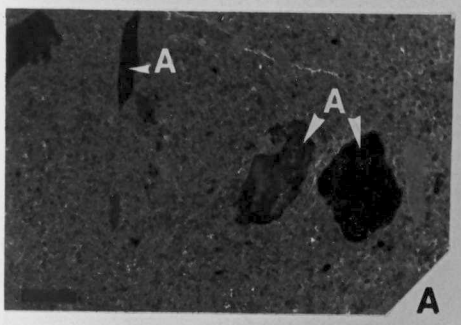
A. Negative print of thin section showing chert clasts (A) in dolomitic matrix in unit immediately above the Knox/Chickamauga contact. Bar scale is 1 cm (Sample CP1A, facies 1).

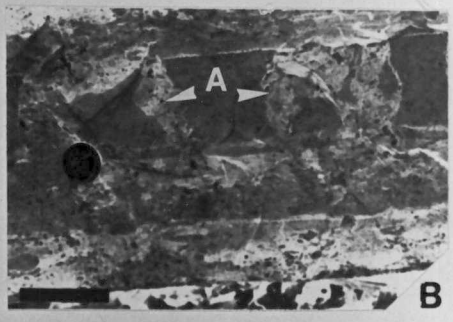
B. Negative print of thin section showing well developed mudcracks filled with sediment, and spar (A). Bar scale 1 cm (Sample GF29, facies 1).

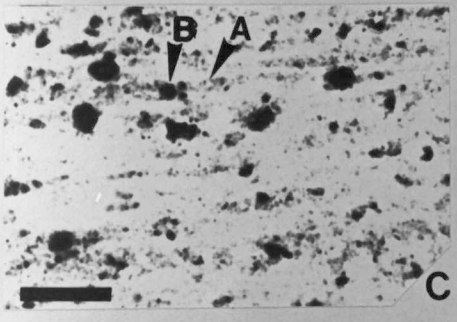
C. Negative print of thin section of laminar fenestrae (birdseyes, A), cut by irregular fenestrae (B). Bar scale is 0.5 cm (Sample GF34, facies 1).

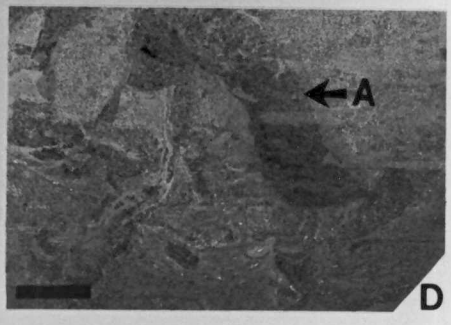
D. Negative print of thin section showing large vertical burrows (A) in burrowed lime mudstone lithofacies. Burrow tubes are filled with skeletal debris, pelloids, mud, and dolomite. Bar scale is 0.5 cm (Samples CP18, facies 1).

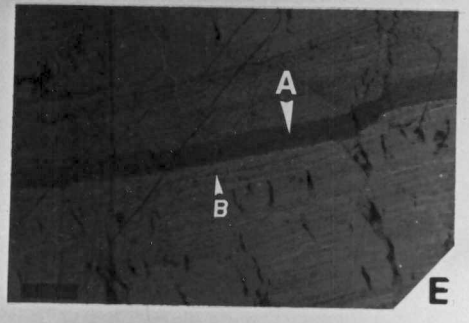
E. Negative print of thin section showing alternating lamination of coarse (A) and fine (B) dolomite. Bar scale is 1 cm (Sample GF1A, facies 1).


A
A
A


A
B


B
A
C


A
D


A
B
E

In the study area, this facies is gradational with other lithofacies and most commonly overlain by facies 4 in the southwestern section (measured section--Goodfield) and by unexposed intervals in the measured section at Ten Mile. This facies is only present at the base of two measured stratigraphic sections (Goodfield and Ten Mile), with the exception of the Goodfield section where dolostone is also present (at the 190, 250, and 325 meter intervals) and is overlain by facies 4 and a comparatively thin unit (1 meter) of facies 2.

The lowermost 5 meters of facies 1 contain medium-beds of dolostone with abundant mudcracks. Mudcracks are not very deep (up to 5 centimeters) and are filled with sediment (Fig. 2.3B). Beds show spar-filled laminoids and irregular fenestrae. The laminoid fenestrae are usually 0.5 to 1.0 millimeter wide, but sometimes extend to several centimeters. These laminoid fenestrae are generally parallel to bedding and, in places, are gently curved or jagged in shape. In many instances, they help to define the laminae of heavily weathered beds. Irregular fenestrae (irregular or vertical-tubular) vary in size, but they are usually 5 millimeters in diameter, are oriented with long axis vertical, and have crossing laminoid fenestrae. Some irregular fenestrae may intersect or coalesce with laminoid fenestrae (Fig. 2.3C). Many of these fenestrae have geopetal pelloids or micrite internal sediments.

Recognizable fossils comprise less than 2% of the rock volume and are limited to a few concentrations of leperditid ostracods, unidentifiable species of trilobite and broken-unidentifiable fossil

debris with no apparent, preferred orientation. Ostracod valves range in length from 1 to 7 millimeters. Valves occur mainly as whole, disarticulated ones, but fragmented debris is also present.

Bioturbation was limited in facies 1, and only a few vertical burrows are present. Burrow tubes are up to 1.0 cm in length and are filled with skeletal debris, pellets, and dolomite rhombs derived from surrounding sediment (Fig. 2.3D).

Dolomitized intraclasts and superficial ooids are present as patches in the dolomite matrix and comprise a small fraction of allochems (less than 1% by volume). Intraclasts are angular and range in size from 1 to 7 cm. Dolomite has three modes of occurrence:

1. A mosaic of interlocking fine and coarse grains (anhedral to subhedral) in completely dolostone beds.
2. Scattered coarse rhombs floating in a groundmass of lime mud, especially common in stylolitic seams.
3. Scattered crystals, partially to completely filling fractures and burrow tubes.

Dolomite in the dolostone beds replaced fossils and fossil fragments as well as intraclasts and pellets, indicating that it is partially a replacement product. The dolomite crystals are usually 30 to 80 microns in size and always rhombohedral in outline. Observation with a luminoscope revealed that all of the dolomite is generally the "clear" type (not zoned) and does not show any signs of rounding and transportation. In places, dolomite forms fine laminae, mostly 3 to 7 millimeters thick and consisting of alternate layers of coarse and

fine dolomite rhombs (Fig. 2.3E). These laminae are generally planar; some are crinkled and are obvious on weathered surfaces and in the thin-sections.

The last feature of facies 1 is dissolution surfaces. These irregular surfaces in many places can be traced laterally for several meters, are roughly bedding parallel, and sometimes display a vertical relief of up to 20 to 30 cm. The smaller dissolution surfaces, which are coated with micrite can be seen in thin-sections where they truncate sedimentary particles such as ostracod valves and pellets.

2a. Green and Red Silty Mudstone (silty micrite, silty calcareous shale, silty biomicrite) Lithofacies:

This facies is characteristically composed of fine-grained, green and red silty mudstone (silty micrite, silty calcareous shale, silty biomicrite). Lithofacies 2a is known only in the lower part of the Ten Mile Creek and Center Point sections where they are thin to medium bedded. Fossils are sparse (less than 2%) and are mostly fragmented, rounded, of microscopic size, and chaotically distributed in the micritic matrix. Identifiable fossils are ostracod valves (disarticulated) and debris (only occasionally articulated leperditid ostracods are preserved). These fossil fragments are severely abraded and fragmented, do not show any sign of preferred orientation, and have an average size of less than 1 mm.

Micrite within this facies, which is almost devoid of fossils, is the most abundant carbonate matrix material, varying in abundance from 58% to 64%, averaging about 61 volume percent of the rock. Sparry

calcite comprises an average of 15% of thin-sections which were point counted, but may vary from less than 4% to greater than 15% (maximum of 19%).

Medium sand size quartz grains are one of the major constituents within this facies. They vary from 23% to 36% in thin-section with the average approximately 27 volume percent. Quartz grains are subangular to subrounded and range in diameter from 0.3 to 0.7 mm (Fig. 2.4A).

Facies 2a also contains inclined-vertical burrows, irregular birdseyes, and desiccation cracks. Burrow tubes are present throughout and have an average diameter of 0.5 to 1.0 centimeters. These vertical-inclined tubes are filled with blocky calcite, peloids, quartz silt, and micrite. Burrowing activity has also destroyed any evidence of relict lamination (algal laminae, Fig. 2.4B).

Irregular birdseye structures are also common, which may indicate either biogenic activity or trapped gas which was produced from decaying organic materials. These voids which are discontinuous and which have average diameters of 7 millimeters were later infilled with sparry calcite cement.

Desiccation (shrinkage) cracks occur either as polygon-bounded mudcracks or as small, spar-sediment filled (carbonate lime mud, quartz silts, peloids) "V" shaped vugs similar to birdseye structures. The majority of these cracks are filled with nonlaminated sediments and are covered by massive (homogeneous) lime mud that is continuous across the cracks.

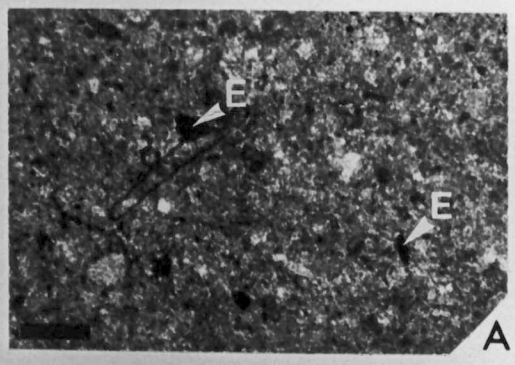
Figure 2.4. Features of lithofacies 2a and 2b.

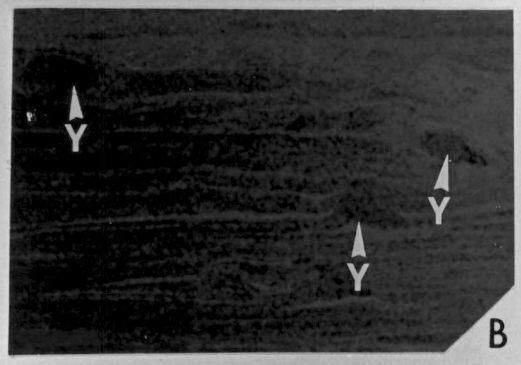
A. Photomicrograph of quartz (E) rich mudstone lithofacies. Bar scale is 1 mm (Sample CP1E, facies 2a).

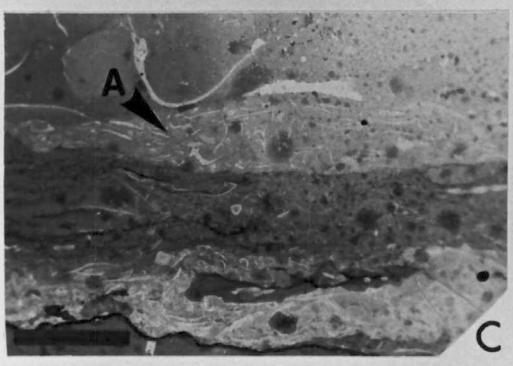
B. Negative print of thin section displaying lamination of possible cryptalgal origin with small burrows destroying lamination (Y). Bar scale is 1 cm (Sample TM14, facies 2a).

C. Negative print of thin section of Sample B96. Note concentration of fossil debris and fragmentation of skeletal allochems in micrite matrix (A). Bar scale is 1 cm (Sample B96, facies 2b).

D. Negative print of thin section showing scalloped, erosional surface (A) over an indurated mudstone (B). Note the horizontal fenestrae above the scalloped surface. Bar scale is 1 cm (Sample TM42A, facies 2b).


E
E
A


Y
Y
Y
B


A
C


B
A
D

2b. Greenish Gray Micrite-Biomicrite (wackestone):

Rocks of facies 2b include green color micrite-biomicrite (wackestone), bioturbated mudstone and dismicrite. Facies 2b is overlain by facies 3 in the northeastern sections of the outcrop belt (Ten Mile and Barnardsville), and by facies 5 and 6 in sections from the southwestern outcrop belt (Center Point and Goodfield).

Facies 2b consists of 49% micrite, 32% sparry calcite, and 19% allochems. Of the 19% allochems 2% are terrigenous quartz silts grains, 12% are bioclasts and 4% are peloids. Bioclasts are disarticulated and broken ostracod valves, worm tubes, and a minor fragmented trilobites (Fig. 2.4C). Facies 2b is sparsely fossiliferous (fossils concentrated in patches) and contains very little dolomite (less than 0.5%). Dolomite rhombs are small (about 0.3 mm) and are randomly scattered throughout the micrite matrix. Facies 2b is a mud-supported rock with no apparent internal stratification. Allochems (skeletal and nonskeletal) have no preferred orientation. Biogenic sedimentary structures, vertical-inclined, with diffused walls, are present, and in some instances sediment was strongly bioturbated (Samples: B96, CP27R). There are also abundant mud-cracks and birdseye structures (irregular, horizontal and tubular-vertical). Mudcrack polygons are very small (3 cm across), and cracks are filled with spar, mud, and fossil debris. These cracks are very shallow and have a maximum width of a few millimeters. Vertical-tubular birdseyes are more abundant than horizontal ones and sometimes reach a maximum diameter of 3 millimeters. Both vertical and horizontal fenestrae observed in this facies have equant calcite mosaic cement.

Another important though rare feature of facies 2b is the presence of scalloped-erosional surfaces. These surfaces are present only at Ten Mile (Samples: TM30T, TM42A) and appear to be continuous laterally for the width of the exposed outcrop (4 mm). In places, these surfaces reach a maximum vertical relief of 20 centimeters (Fig. 2.4D). In thin-sections, these surfaces lie between pelbiomicrite (wackestone) at the bottom, and dismicrite on top. Although the sediment above and below these surfaces is micrite, they are identifiable in the field because of the presence of different fenestrae types in the sediments. Lower sediments generally contain irregular fenestrae, whereas upper sediments have laminoid fenestrae (Grover and Read, 1978; Logan et al., 2974; Tebbut et al., 1965).

Matrix within facies 2b is restricted to burrow-filled mud, sparry calcite and peloids. In places, micrite has been neomorphically altered to microspar. This microspar consists of very small interlocking crystals, ranging in size up to 0.008 mm. Pressure solution features are rare and are in the form of nonsutured seam solution, producing microstylolites. Also equant calcite mosaic cement, which is inclusion-free, fills birdseye structures.

3a. Red Silty, Intrapelbiosparite-Biosparite (packstone):

Lithofacies 3a consists of skeletal carbonate fragments, mixed with peloids and intraclastic carbonate grains. This lithofacies is heterogeneous, with thin beds (5-10 cm thick) that are dominated by wackestone but with gradational variations. Thus, it is impractical to separate these into subfacies or smaller units of lithofacies 3a.

Lithofacies 3a occurs in all of the four measured stratigraphic sections in the study area. Rocks of this facies are randomly distributed throughout the measured stratigraphic columns, but in general show a greater abundance to the northeast (Barnardsville and Ten Mile) than to the southwest (Center Point and Goodfield).

This facies is dominantly sorted packstone (pelbiosparite) with a rare occurrence of wackestones-pelbiomicrite. Fossils comprise 24% of constituents of these sediments. Tetradium fragments (6%), pelmatozoan debris (4%), brachiopods (4%), ostracods (4%), and molluscan fragments (2.5%), are the predominant fossils in order of decreasing abundance. Gastropods, trilobites, bryozoans, algae, and worm tubes are present only in minor amounts (less than 2%). Skeletal allochems are generally moderately sorted and are usually abraded and fragmented, although occasional ostracods and molluscs are articulated and do not appear to be abraded (Fig. 2.5A).

Intraclasts and peloids comprise 26% of the rock volume. Both intraclasts and peloids are rounded, well sorted, and are oriented parallel to bedding (Fig. 2.5B). Peloids in this facies appear to be broken pieces of intraclasts which have been eroded, rounded, and transported into the final depositional site.

Unidentifiable fossil debris (3.6% of rock by volume), dolomite crystals (0.72%), and quartz silt grains (2.7%) are also found within this facies. The quartz grains, dolomite crystals and fossil debris are randomly scattered throughout.

Figure 2.5. Skeletal allochem preservation, cement types, and sedimentary structures of facies 3a.

A. Negative print of thin section showing skeletal allochem distribution and fragmentation. Note articulated bivalve and unabraded gastropods. Bar scale is 1.5 cm (Sample B24, facies 3a).

B. Negative print of thin section of Sample B46. The grains are sorted and rounded intraclasts and pelloids. Note parallel orientation of grains. Bar scale is 1 cm (Sample B46, facies 3a).

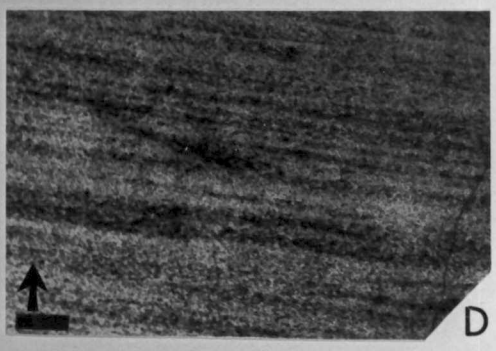
C. Negative print of thin section displaying fining upward structure. Bar scale is 1 cm (Sample TM41F, facies 3a).

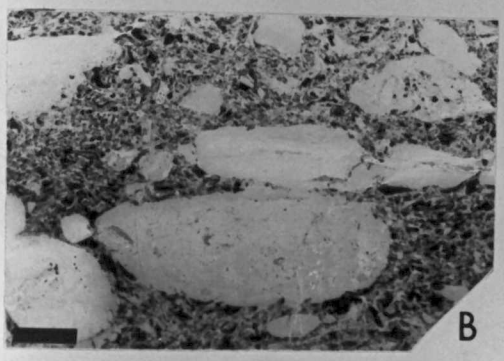
D. Negative print of thin section showing ripple cross lamination of skeletal and nonskeletal allochems. Bar scale is 1 cm (Sample B44, facies 3a).

E. Photomicrograph showing early fringe cement (F) on molluscan shell. Bar scale is 0.5 mm (Sample B43, facies 3a).

F. Photomicrograph showing equant-drusy calcite mosaic cement filling shelter area under brachiopod shell. Bar scale is 500 μm (Sample B44, facies 3a).

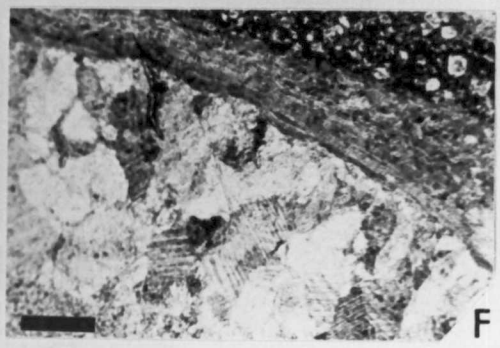

A


D


B


F
E


C


F

Both physical and biogenic sedimentary structures are present within this facies. Mechanically induced structure are the predominant type observed and consist of planar cross-beds, fining upward sequences, sorting of skeletal allochems, parallel orientation of skeletal grains (convex up) such as ostracod and brachiopod shells, and ripple marks (Fig. 2.5C and D). Burrows are present in the muddy portions but are not common and include both horizontal and vertical tubes. The strongly bioturbated sediments appear to be homogenized with no preferred grain orientation. Burrow tubes have distinct walls and are completely filled with carbonate lime mud (micrite), dolomite rhombs, sparry calcite, peloids, and skeletal grains.

Cements within facies 3a are inclusion-free fringe calcite, syntaxial overgrowth calcite, coarsely crystalline equant-drusy mosaic calcite. Other diagenetic features are vadose silt, silica replacement of calcite, and micrite envelopes. Syntaxial overgrowth cement is the predominant cement type, occurring as an overgrowth on echinoderm grains. Fringe calcite cement is restricted to one sample (Sample: B43) (Fig. 2.5E). Coarse-grained, equant-drusy mosaic calcite is found in pore spaces (interparticle), in the shelter areas under fossil fragments (ostracods and brachiopods), and in some burrows and microfractures (Fig. 2.5F).

Micrite envelopes on molluscan grains, neomorphism of aragonitic molluscan fragments to coarse-grained blocky calcite mosaic (mainly gastropod shell), dolomite rhombs (especially in burrow tubes and along stylolite seams), vadose silt (Sample: B43), and boring of brachiopod

shells (Sample: TM41F) are also present. Silicified skeletal grains occur in some samples (Sample: B43). Brachiopod shells are the major skeletal grains which have been partially replaced by silica in the form of chalcedony.

Other types of sedimentary features such as mud-cracks, geopetal structures, fining upward sequences, irregular and parallel stylolites are also present in minor amounts. The neomorphic alteration of micrite to microspar was a common alteration process within this facies.

3b. Green and Red, Loosely Packed Ostracod Rich Pelbiomicrite (wackestone and packstone):

Lithofacies 3b consist of biomicrite (loosely packed ostracod rich micrite, packstone and wackestone) with lesser amounts of peloids, intraclast, and planar-cross lamination. This lithofacies occurs in all four measured stratigraphic sections and interfingers with and overlies lithofacies 4 and 5. It is made up of 59% micrite, 25% sparry calcite, 9% skeletal allochems (brachiopods, trilobite, molluscs, pelmatozoans, and algae, each less than 1%). Other constituents such as ostracods (4%) unidentifiable fossil debris (3%), and worm tubes (1%) make up about 8% of the rock volume. Nonskeletal allochems are also present and consist of intraclasts and peloids (3% of rock volume). Dolomite crystals are present in some horizons, generally associated with stylolite seams, or filling burrow tubes, and locally make up to 33% of the sediment. Angular, silt size quartz grains are also present and make up to 2% of the rock volume in some samples.

These allochems are scattered throughout the fine-grained carbonate lime mud but the sediment is not grain supported.

Bioclasts (skeletal allochems) are poorly sorted, fragmented, and abraded with an average grain size of 0.5 mm. Ostracods are the predominant fossil type and are generally disarticulated except in a few samples (Sample: TM42B), where they are articulated and filled with mud (Fig. 2.6A). In general, the total percentage and association of ostracods and worm tubes with no sign of transportation indicate that a very limited restricted water fauna was more abundant than open-marine organisms. Open-marine organisms such as bryozoans and brachiopods are badly broken and fragmented and are very rare. Solenopora and Hedstroemia are present, but are rounded and abraded, suggesting transportation from surrounding environments (Fig. 2.6B).

Volumetrically, bioclasts within this facies are much rarer than in lithofacies 3a. Peloids occur as rounded grains and are very rare in this facies.

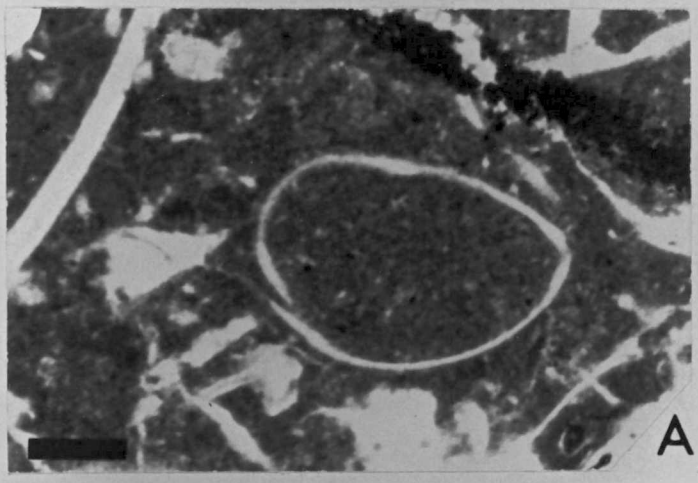
Very thin packstone beds are randomly intercalated with wackestone lithologies. Grains within these packstones are the same as bioclasts in the wackestone, but are occasionally larger in size and moderately sorted.

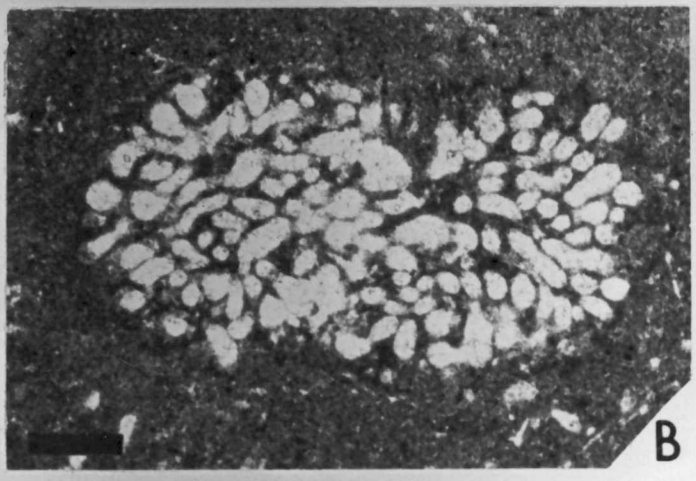
Primary physical sedimentary structures include coarsening and fining-upward sequences. The coarsening upward sequences have a bioturbated mud at the bottom, followed by molluscan-bryozoan-echinoderm rich pelbiosparite (with planar lamination) on top. The contact between these two lithologies is erosional and in places

Figure 2.6. Skeletal allochem of lithofacies 3b.

A. Articulated ostracod filled with mud in lithofacies 3b. Bar scale is 2.5 cm, TM42B.

B. Fragmented and rounded Hedstroemia (alga) in lithofacies 3b. Bar scale is 1.3 mm, TM45D.


A


B

represents scour and filled surfaces (Samples: B25, B22). On the other hand, fining-upward sequences consist of a lower fossil debris zone and an upper bioturbated mud with birdseye structures.

Both vertical-inclined and horizontal burrows are present, but horizontal burrows outnumbered the vertical burrows. Some horizontal burrows have no definite wall boundary and are filled with micrite, spar, dolomite, and fossil debris (ostracods). The lack of a distinct burrow wall is a good indication of the high water content of the original sediment. In places, sediment of this facies is strongly bioturbated where the sediment appears massive and homogenized with no preferred grain orientation.

Cement within this facies is restricted to burrow tubes. Equant-drusy calcite mosaic cement generally fills burrow tubes and worm tubes. Cement is inclusion-free, and crystals sometimes reach a length as large as 100 to 500 microns. Neomorphic alteration is in the form of recrystallization of micrite to microspar. However, this process has been very limited in this facies. Pressure solution has also occurred and forms irregular stylolite seams. Other features such as geopetal structures, irregular and horizontal birdseyes, and vertical calcite stringers are also present but in minor amounts.

3c. Stromatolitic Mudstone (dismicrite) Lithofacies:

Although from a volumetric standpoint lithofacies 3c is insignificant, it represents a readily identifiable lithology (Fig. 2.7A). Thicker units of this lithofacies are restricted and are

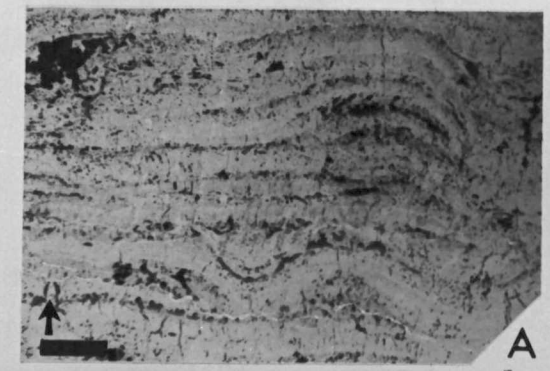
Figure 2.7. Thin-section negative prints of the characteristic sedimentary structures of lithofacies 3c and 4a.

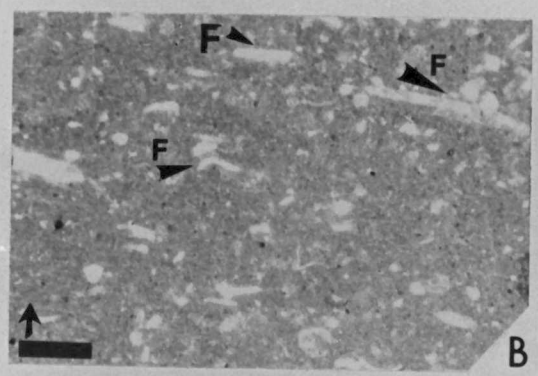
A. Thin section negative print of Sample B75 (lithofacies 3c). Note thin, crinkled, millimeter scale laminae of algal origin (stromatolite structure). Bar scale is 0.5 cm.

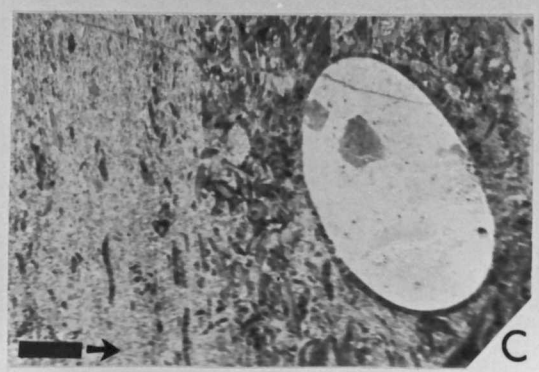
B. Fragmented and abraded fossil debris (F) in lithofacies 4a, B50. Bar scale is 0.5 cm.

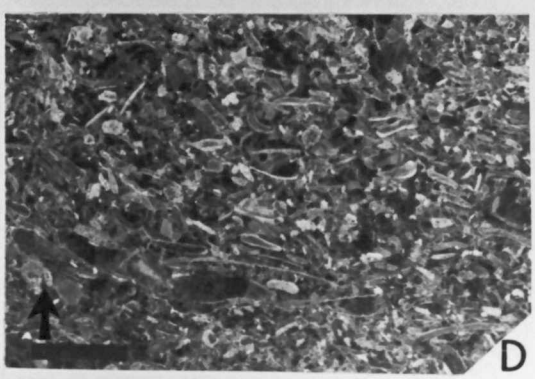
C. Negative print of thin section showing the general coarsening upward sequence in the fossil-pelloid packstone. Bar scale is 0.5 cm, TM45D.

D. Negative print of thin section of Sample TM46B (lithofacies 4a). Note the parallel orientation of allochems. Bar scale is 0.5 cm.


A


F
F
F
B


C


D

only present at Barnardsville. Although thin beds of the facies occur occasionally at other localities (Fig. 2.7A). Fossil allochems are rare and are limited to ostracods (2% by volume) which are abraded, broken, and disarticulated valves. Other constituents of this facies include micrite (58%) and sparry calcite (40%). Associated structures include desiccation cracks, fenestral fabric, and vertical burrows. Fenestral structures are mostly continuous horizontal birdseyes. Vertical burrows are very few in number; tubes have distinct walls and are filled with coarse sparry calcite. These burrows may cross-cut a number of very thin beds. Alternate mud and birdseye laminae are present throughout this facies, ranging in thickness up to 0.5 mm. These laminae are generally wavy and thickest on topographic highs, but for the most part they are crinkled with low relief (1 to 1.5 cm). Mud cracks with 2 to 5 cm polygons are also present.

4a. Bryozoan-Ostracod-Brachiopod-Rich Pelbiomicrite (wackestone, packstone):

Lithofacies 4a, bryozoan-ostracod-brachiopod-rich pelbiomicrite (wackestone and packstone), is present in all four measured stratigraphic sections and consists of approximately 58% micrite, 15% sparry calcite, 3% intraclasts and peloids, 19% skeletal allochems, 2% terrigenous quartz silt, and 3% unidentifiable fossil debris. Bioclasts in decreasing order of abundance are: bryozoan (9%), ostracod (3+%), brachiopod (3%), trilobite (2%), pelmatozoan, gastropod, and algae (Hedostroemia, Solenopora), each less than 1% by volume.

Bioclasts are poorly sorted and tend to be abraded with a wide range of grain sizes (up to 2.0 mm). Brachiopods occur as fragmented, articulated shells, and disarticulated valves. Molluscs are rare and are only present as articulated bivalve shells, and whole or fragmented gastropods; algae are found only in a few samples of this lithofacies, appearing to be transported or derived from close-by environments. Bryozoans occur as fragments where zoecia are filled with mud and sparry calcite cement. Echinoderm grains and peloids are well-rounded and sorted whenever they are present. Skeletal and nonskeletal fragments including terrigenous quartz silt within this facies are supported by a micritic matrix (Fig. 2.7B). Packing within this facies is not close enough to cause distortion of grains at grain contacts.

In general, rocks of this facies are classified as wackestone (Dunham, 1962), but packstone beds are intercalated with the wackestones. Bioclasts within these packstone beds are generally the same as those in wackestones with no systematic increase or decrease in any portion of the facies. These bioclasts are slightly larger than those of wackestone and are moderately sorted.

Sedimentary structures include both horizontal and vertical-inclined burrows, geopetal structures, shell orientation (convex up), and fining upward and/or coarsening upward sequences. The wackestones display both burrow types where tubes are filled with micrite, spar, dolomite rhombs, and skeletal fragments. These structures indicate that the substrate water content was variable

because some burrows have diffuse walls. Horizontal burrows are the predominant type and outnumber the vertical burrows.

Many samples of packstone also contain biogenic structures, but they are not as abundant as they are in wackestones. These packstone layers occasionally contain fining or coarsening upward sequences. The fining upward sequences have a debris lag of unidentifiable fossils at the base that grades upward into bioturbated mud (Sample: GF32). In coarsening upward sequences, pelbiomicrite lies at the bottom and is succeeded by a biosparite horizon (brachiopod, bryozoan, and echinoderms) over a scour surface (Fig. 2.7C).

Other features such as current-oriented allochems (convex up, e.g., Sample: TM46B) and/or parallel orientation of elongate shells such as brachiopods (Sample: GF59) are also present within the packstone layers (Fig. 2.7D). However, since biogenic activity was greater than physical activity in the depositional environment at the time of the formation of sediments of this facies, any physical structures which might have formed have been destroyed shortly after their formation.

Diagenetic features including cements within this facies are inclusion-free, pore-filling, equant-drusy mosaic calcite, silica replacement of calcite, neomorphism of micrite to microspar, alteration of aragonitic shells, syntaxial overgrowth, compactionally produced features such as horizontal and irregular stylolites, and formation of hardgrounds.

Neomorphic alteration has occurred especially in packstone layers. This alteration has caused the inversion of aragonitic shells (molluscan shells and fragments) to a coarse equant calcite (Samples: TM46B, GF69, TM46C). Neomorphic alteration of micrite to microspar, has been observed within this facies, but was restricted to a few samples (Sample: TM46K).

Silicification commonly is evidenced by chalcedony as a nonselective replacement of calcite within trilobite, ostracods, brachiopod and other shells. In many instances, silicification also replaced calcite along microstylolite seams and overgrowth cements. Chert nodules also are found within some zones. However, the origin of these chert nodules is uncertain and is beyond the scope of this study.

Pressure solution has produced hummocky stylolites (horizontal and irregular). Dolomite crystals and insoluble particles are generally concentrated along these stylolites seams.

Inclusion-free calcite, in the form of drusy crystals, is restricted to pore spaces between skeletal allochems and beneath shells, especially brachiopods, ostracods and bryozoan fragments (Samples: TM46K, TM46B, GF69). This calcite cement generally fringes the inner walls of shells, and the rest of the pore space is filled by equant calcite cement. Syntaxial calcite cement is restricted to echinoderm grains and is only observed in packstone layers.

At Goodfield, hardgrounds are evidenced by impregnated and eroded grains, and bored surfaces (Sample: GF63). Geopetal structures in the bored tubes, in burrow tubes, and on the inside of skeletal fragments

(ostracod and gastropods), and encrustation of skeletal fragments (molluscs, brachiopods) by bryozoan and unidentifiable algae, are also present sporadically (Samples: TM46B, GF74).

4b. Silty, Packed Pelbiomicrite-Pelbiosparite (wackestone and packstone):

Lithofacies 4b, silty, packed Pelbiomicrite-Pelbiosparite (wackestone and packstone), is present at all four stratigraphic sections in the study area. This facies characteristically comprises two groups of lithologies: (1) beds of molluscan-ostracod-rich wackestone (Fig. 2.8A), and (2) beds of bryozoan-brachiopod-pelmatozoan rich packstone (Fig. 2.8B). Rocks assigned to this lithofacies range in color from light-green to greenish-gray to light brown-tan. Skeletal fragments are the most abundant allochems within the packstone beds (45%). Other constituent (making 55% of the rock volume) include: micrite (29%), spar (16%), intraclasts and peloids (3%), terrigenous quartz silt grains (3%), and dolomite (1%).

The most noticeable fossils in decreasing order of abundance are: bryozoans, brachiopods, gastropods, Tetradium, molluscs, ostracods, unidentifiable fossil debris, worm tubes, pelmatozoans, and trilobites. A stromatoporoid is also present in one sample (B60) (Fig. 2.8C). In general, open-marine faunal elements (25%), including brachiopods, pelmatozoans, and bryozoans are slightly more abundant than restricted-water elements (19%, including ostracods, trilobites, molluscs, and worm tubes). Sorting and abrasion among the skeletal and nonskeletal grains appear to be minimal with a wide range of grain

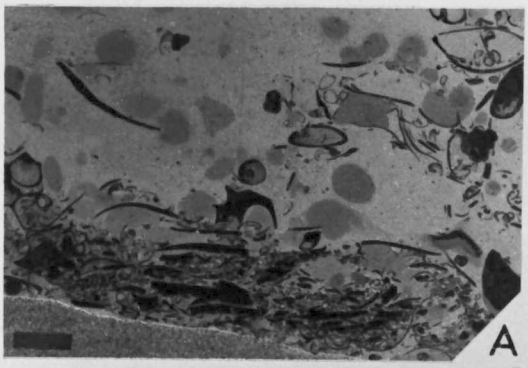
Figure 2.8. Features observed in lithofacies 4b.

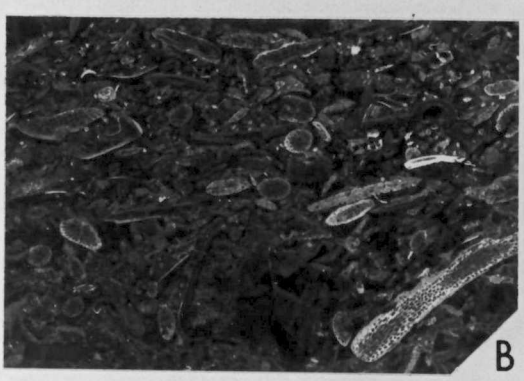
A. Negative print of thin section of Sample B79 showing abundance of molluscan-ostracod (broken and whole) valves in a micrite matrix. Bar scale is 1 cm, facies 4b.

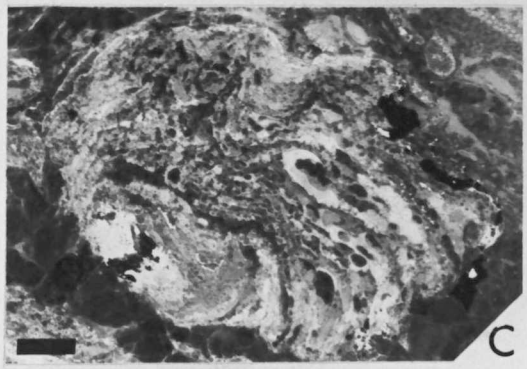
B. Negative print of thin section showing preservation and abundance of bryozoan and pelmatozoan grains in packstone of lithofacies 4c. Bar scale is 0.5 cm, facies 4b.

C. Photomicrograph of Sample GF12A showing a specimen of Stromatoporoid. Bar scale is 1 cm, facies 4b.

D. Photomicrograph showing articulated ostracod partially filled with internal sediments in a geopetal position. Drusy-equant calcite filled the rest of the pore. Bar scale is 0.9 mm, TM46K, facies 4b.


A


B


C


D

sizes. However, some samples occasionally display fair to moderate sorting and abrasion. Bryozoans are fragmented but not rounded or abraded, and their internal structures are filled with mud and sparry calcite. Brachiopod and ostracods are both articulated and disarticulated brachiopods in a few samples (CP10A) retain skeletal spine. Gastropods are as whole or broken fragments but are not abraded. Tetradium is present as broken fragments in a few samples (TM18, 39D, 38, 17b) and comprise 5% of rock volume. These corals sometimes occur as fingerlike longitudinal section of colonies, but transverse sections are more common. These fragments always form moldic porosity due to exposure to fresh-water (meteoritic water) and dissolution-recrystallization of skeletal material. However, corallites are filled with carbonate mud. According to Walker (1970), these corals had various growth forms and could live in environments where agitation was low, salinity fluctuated rapidly, and fine-grained carbonate mud was abundant.

Worm tubes, possibly of serpulid (?) origin, are present in a few samples (TM18, 41A, 17) where Tetradium is present. Laporte (1967) has also noted the presence of serpulid worm tubes in tidal flat rocks of Devonian age in New York.

Unidentifiable fossil debris (rounded and abraded, 4%) and pelmatozoan grains (2%) are also present within this lithofacies.

Nonskeletal allochems such as peloids, intraclasts and terrigenous quartz silt are also present. Peloids and intraclasts comprise 3% of the rock volume in a few samples (TM41E, *41A, 39D, *38, B9, 84, 97,

GF71, *CP10A, *19. Note: Asterisks represent samples with intraclasts). Peloids are rounded, sorted, and are about 0.70 mm in length. Terrigenous quartz silt is rare in a few samples (B76, 97, 19, TM6, 16). These quartz grains are angular and randomly distributed throughout the rocks.

Horizontal and vertical burrows with distinct walls are present. These burrow tubes are filled with peloids (0.1 mm diameter), skeletal fragments, mud, and sparry calcite.

Other sedimentary structures such as fining or coarsening upwards sequences are also observed. Occasionally, large fossils such as disarticulated ostracod valves and brachiopod shells, are aligned parallel to bedding, is present (Samples: TM46J, 46K, CP28E). Micrite envelopes which possibly indicate algal, bacterial, or fungal boring are also present (Samples: TM16, 46ER, GF79, CP10A). The coarsening upward sequences consist of bioturbated mud with occasional ostracod shells at the bottom, which are succeeded by an ostracod packstone with planar lamination on top (Sample: B19). Fining sequences are less common and consist of pelbiomicrite at bottom followed by sparse biomicrite on top (Sample: CP28G). Encrustation by algae on molluscan and bryozoan grains, is present in few samples (TM6, 46E, 46J). Geopetal structures are common in some samples (Samples: GF60, TM46K) and formed inside of ostracod valves (Fig. 2.8D).

Pore filling calcite cement is present in minor amounts as a filling of void spaces, as rim cement around skeletal allochems such as brachiopods and molluscan grains with sawtooth terminations on crystals

whose c-axis is oriented perpendicular to the molluscan wall, as filling in burrow tubes, and in shelter areas beneath ostracod, brachiopod, and trilobite grains.

Silica, in the form of chalcedony, replaces calcite in brachiopod shells (Sample: TM41A). Syntaxial overgrowth cement on crinoid fragments is also present, but is very rare. Neomorphism is only present as micrite to microspar in a few samples (GF79). Microspar crystals reach an average size of 0.01 to 0.3 mm. Also within this facies, the alteration of original aragonitic composition of molluscan fragments to a coarse calcite mosaic and the recrystallization of Tetradium skeletal fragments are common features.

4c. Ostracod-Gastropod-Rich, Bioturbated Pelbiomicrite (wackestone-packstone):

Rocks of lithofacies 4c are typically greenish gray to light gray in color, fine- to medium-grained, mud-supported ostracod-gastropod-rich, bioturbated pelbiomicrite (wackestone-packstone). Fine-grained materials which include micrite and detrital quartz silt vary in abundance; micrite ranges from 23% to 67% (average of 49%), and detrital quartz silt from 4% to 20% (average of 3%).

Skeletal fragments, in decreasing order of abundance, are: articulated and disarticulated ostracods (8%), whole or broken gastropods (3%), sponge spicules (3%), longitudinal and transverse sections of Tetradium (1%), broken fragments of trilobites (1%),

pelmatozoan debris (1%), molluscs (<1%), disarticulated brachiopods (<1%), and very rare worm tubes.

Fossil grains comprise 32% of the rock volume in thin sections (32% includes unidentifiable fossil debris which makes up 13% of the rock). Sorting among skeletal allochems is poor. Fossil grains are generally abraded (except ostracods and gastropods), and show some signs of rounding, especially among the pelmatozoans, algae (Hedstroemia and Girvanella), and bryozoans (Fig. 2.9A). However, skeletal fragments do not show any sign of preferred orientation except in fining or coarsening upward sequences. Micrite coatings are present around brachiopod fragments.

Nonskeletal allochems include intraclasts and peloids. Intraclasts are rounded, abraded, and comprise an average of 1% of rock volume. Peloids are generally rounded and sorted, making an average of 1% of the rock.

Sparry calcite is in the form of neomorphic spar, spar inside of or beneath skeletal fragments, and between grains (interstitial spaces). The neomorphic spar is in the size range of microspar and is commonly observed in thin sections. Dolomite is a very rare constituent and is generally found within the fine-grained constituents (micrite), around fossil allochems, and within stylolite seams.

Burrows are common; both vertical and horizontal burrows are present. Burrow walls have distinct or diffuse boundaries and tubes are mud- and/or spar-filled. Dolomitization has been a very common process within the burrow tubes. Vertical burrows are short and stubby

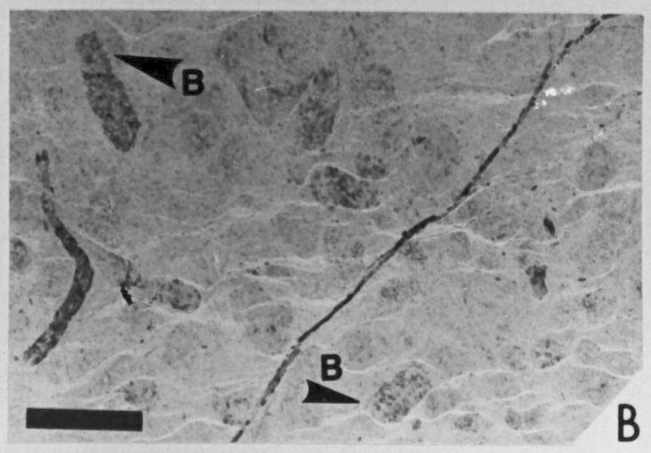
Figure 2.9. Features of lithofacies 4c.

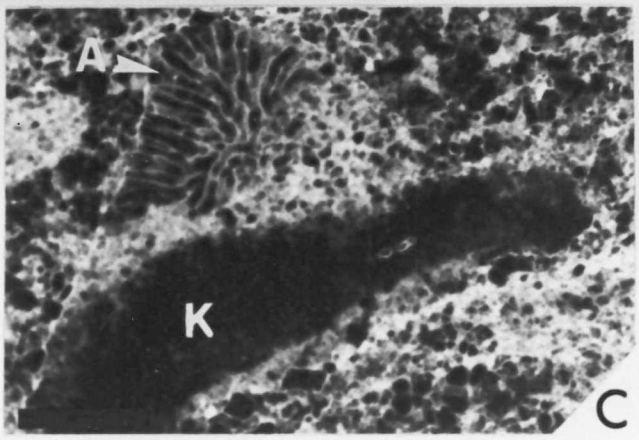
A. Thin section negative print of Sample CP28H (lithofacies 4c). The grains are sorted fossils, mainly gastropods, bivalves, and ostracods. Bar scale is 1 cm.

B. Negative print of thin section showing short-stubby, vertical-inclined burrows (B). Bar scale is 1 cm, CP26B (lithofacies 4c).

C. Hedstroemia (A) (alga) encrusting a molluscan fragment (K) in lithofacies 4c, CP25A. Bar scale is 0.7 mm.


A


B
B
B


A
K
C

and in places cross-cut laminae within beds (Fig. 2.9B). The presence of both horizontal and vertical burrows, distinct and diffuse walls, cross-cut laminae (in places), and dolomitized sediments within the tubes all indicate the variability in sediment water content at the time of burrowing.

This lithofacies exhibits features which are the products of primary physical sedimentary processes. Among the most common are: shelter cavity (convex up), coarsening and fining upward sequences, oncolites, and geopetal structures. The fining and coarsening upward sequences are very rare and are only observed in packstone horizons. The fining upward sequences have a lower plane-laminated pelmabiomicrite (fossils are: molluscs, ostracods, brachiopods) which grades into intrabiosparite which is overlain by a bioturbated micrite (Sample: TM44C). On the other hand, coarsening upward sequences start with a bioturbated mud and grade into a horizon of biomicrite and biosparite which is rich in unidentifiable fossil debris (Sample: CP28H). The contact between these two lithologies appears to be a scour surface where relief is very small (less than 3 cm) and fossils lie in current-oriented positions (convex up). However, a few oncolites (?) are also present within thin sections of the rocks of this facies (CP 25A).

Other features such as algal encrustation on Tetradium and brachiopods (Fig. 2.9C), vertical calcite stringers, and corroded skeletal grains (ostracod and trilobite) are present in a few samples (Samples: GF3, CP14B).

Cement within lithofacies 4c is very rare and includes: syntaxial cement, silica replacement, drusy-equant calcite, neomorphism, and radial fibrous cement. Syntaxial overgrowth cement occurs on crinoidal fragments and tends to envelop nearby grains as well. Equant-drusy mosaic calcite cement generally fills pore spaces and skeletal cavities (beneath skeletal fragments such as brachiopods, ostracods and bivalves). The most common diagenetic feature within this facies is the alteration of the original micrite to microspar and the conversion of aragonitic and high magnesium calcite of molluscan and Tetradium fragments to low magnesium calcite mosaics (Samples: GF3, CP14B, GF15).

Chert is not found within rocks of this facies, but some brachiopod fragments and pelmatozoan grains have been replaced by fibrous chalcedony. Silica replacement in pelmatozoan grains has taken place inside of the grain and within the overgrowth cements.

Pressure solution is indicated by the presence of nonsutured seams. Both horizontal and irregular stylolites with stylocumulate (clays) are common (Sample: CP14B). Other features such as micrite envelopes and radial fibrous cements are rarely observed. The fine-grained, prismatic calcite cements occur as a fringe around bivalves. These crystals are about 60 microns long and grew normal to bivalve shells (only observed in one sample (GF15). Formation of micrite envelopes was more common than radial fibrous cementation, and formed around brachiopod and bivalve shells (Sample: TM5).

4d. Bioturbated Brachiopod-Molluscan-Rich Biomicrite (wackestone packstone):

Lithofacies 4d, bioturbated brachiopod-mollusc-rich biomicrite (wackestone and packstone) is present in three measured stratigraphic sections (Ten Mile, Center Point, Barnardsville). In hand specimens and thin sections the most characteristic feature of the rocks is that they contain horizons characteristic of storm accumulated fossil-peloid packstone (Fig. 2.10A). The interbedding of wackestone and these storm deposits (packstone) is not common, but whenever present, packstone layers exhibit fining and coarsening upward sequences with basal scour surfaces. Bioclastic fragments are observed a very minor constituent of these rocks except in the storm deposits. Skeletal allochem distribution within thin sections is in many instances irregular and patchy and these grains comprise approximately 34% of the rock volume. Identifiable skeletal allochems in decreasing order of abundance are: brachiopods (8%), gastropods (<8%), molluscs (6%), ostracods (4%), trilobite (2%), pelmatozoan debris (1%). Unidentifiable fossil debris makes up to 4% of rock volume. Other fossil allochems such as worm tubes (<1%), and bryozoans (trace) are also present within rocks of this facies. Peloids are generally absent, except in storm deposits (fining and coarsening upward sequences), making an average of 1% of those rock. These peloids are very small (0.1 mm), and are sorted.

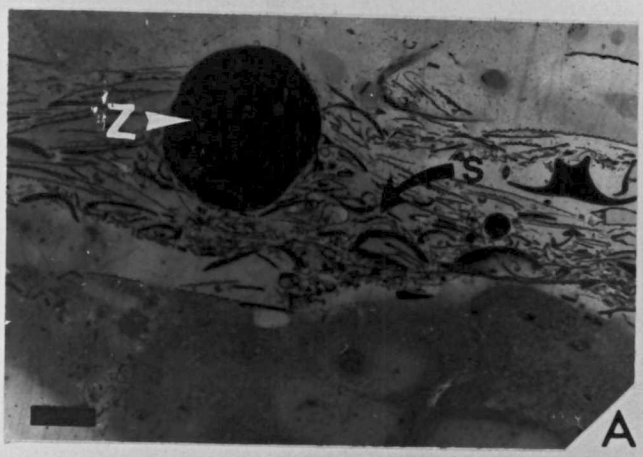
Skeletal fragments except brachiopods, ostracods, and bivalves are generally severely abraded and fragmented and show signs of sorting and transportation.

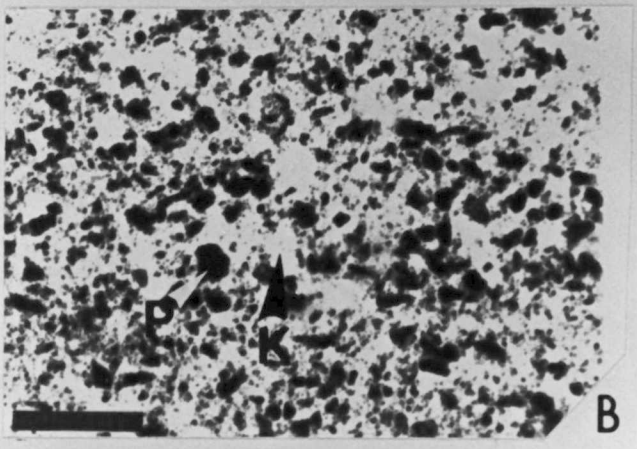
Figure 2.10. Characteristic fabric of lithofacies 4d and 5a.

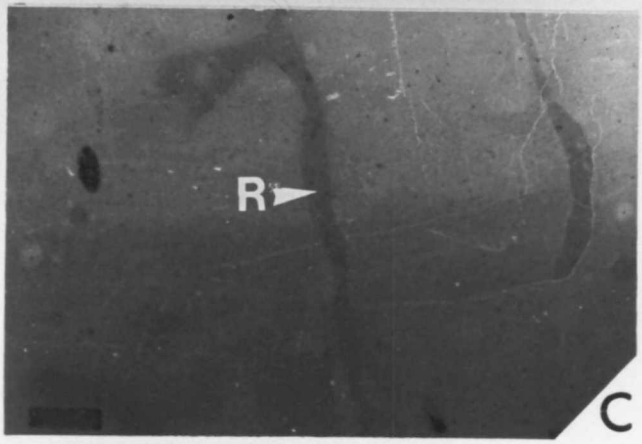
A. Thin section negative print of sample CP28H. Note the storm accumulated fossil debris horizon in the photograph (S). Also notice the probable cephalopod (Z) in the middle of photograph. Bar scale is 1 cm, CP28H, facies 4d.

B. Photomicrograph showing poorly developed alternate laminae of carbonate lime mud (K) and quartz silt (P). Bar scale is 900 μm, CP1H, facies 5a.

C. Negative print of thin section showing vertical burrow (R). Bar scale is 1 cm, TM39, facies 5a.


Z
S
A


P
K
B


R
C

Carbonate mud (micrite) is the most abundant carbonate matrix material and averages about 48% of the rock. Dolomite comprises less than 1% of the rock in the thin sections and is associated with stylolite seams and/or filling of burrow tubes. Sparry calcite is mostly of neomorphic origin (microspar) with minor amounts as pore fillings and fillings of shelter areas beneath the skeletal allochems. It comprises 26% of the rock in this facies.

The wackestone in this facies is bioturbated and displays both horizontal and rare vertical burrows. Burrow walls are distinct, and tubes are filled with mud and dolomite crystals. The biogenic activity in some samples was so extensive that fossils within the sediment are randomly oriented. The packstone horizons or tongues of fossiliferous sediments are present throughout this lithofacies, but are generally discontinuous over a short distance (30 cm). These packstones exhibit features such as fining and coarsening upward sequences, characteristic of high energy conditions (storm deposits). Fossils within these deposits include both fragmented and abraded open-marine elements, and fragmented but not abraded restricted water forms. Elongated skeletal allochems such as brachiopods, ostracods and bivalves lie parallel to bedding (convex up). Also fining upward sequences are commonly observed within these packstone layers. These sequences have a basal fossiliferous packstone (ostracod, brachiopod, pelmatozoan), followed by bioturbated mudstone. In many instances, the contact between these two lithologies exhibits a scour surfaces, but is sometimes gradational (Samples: B78, 79, 63).

Blocky calcite cement in the form of replaced and skeletal fragments (molluscs) and as filling of shelter areas beneath brachiopod, ostracod, and bivalve shells, is generally present but rare. Also evidence of chemical destruction (corrosion) of skeletal fragments is occasionally observed in some samples (TM19).

5a. Bioturbated Green and Red Silty Mudstone-Silty Sparse Biomicrite:

Lithofacies 5a is a terrigenous quartz silt and carbonate lime mud-rich facies and occurs commonly in all four measured sections (Fig. 2.10B). This lithofacies includes green and red bioturbated mudstone and silty sparse biomicrite. In general, fossil allochems within this facies are rare, comprising only about 5% of the rock volume. Stratigraphically, lithofacies 5a occurs most frequently with lithofacies 4 and 3 and is always sandwiched between rocks of facies 4. Occasionally, it is overlain or underlain by lithofacies 2 and 6 especially at Ten Mile and Barnardsville where the facies pattern is much more complex than at the two southern sections (Center Point and Goodfield).

Internal structure is lacking. This lithofacies is almost void of fossil materials except for ostracod (1%), bryozoan (trace), and unidentifiable fossil debris (4%). Ostracods are both articulated and disarticulated but not broken or abraded. Bryozoans are fragmented, rounded, and abraded. Unidentifiable fossil debris is generally rounded, abraded and in a few instances, exhibits a weak parallel orientation. Other fossil allochems such as worm tubes, trilobites, and algae (Hedstroemia and Solenopora) are occasionally present in thin

sections (generally less than 0.5% of the rock volume). Dolomite is present only in burrow tubes and is present only in trace amount. Sparry calcite which is found in the form of burrow filling and filling of shelter areas comprises 26% of the rock. Detrital quartz silt is an important inorganic constituent of this facies. This silt, which is present in all samples, comprises 28% of rock volume and ranges in size from coarse silt to very fine sand. Grains are angular to subangular and are not sorted. A number of samples have a series of laminae consisting of alternating carbonate mud and quartz silt (Fig. 2.10B).

Biogenic activity (burrowing) was present; a few samples are homogenized mudstone. Both horizontal- and vertical-inclined burrows are present. Horizontal burrows outnumber vertical burrows, and are filled with spar, mud, dolomite crystals, and ostracod fragments. Burrow walls are distinct and sharp. The lack of diffuse burrow walls indicates that the sediment water content was low. Also, some samples (TM39B) show evidence of extensive biogenic activity where in places, horizontal and vertical burrow tubes are connected and appear to have been formed by a single organism (Fig. 2.10C).

Incipient stylolites are present within carbonate mud laminae but not within quartz silt laminae. Vertical fracturing and drusy-equant, pore filling, calcite mosaics are also present in this lithofacies. Drusy-equant calcite cement is very rare and is only found within burrow tubes.

5b. Greenish Gray-Tan Mudstone-Sparse Biomicrite:

Rocks assigned to this lithofacies range in color from greenish gray to tan. Very fine lamination is present but is faint. In hand specimens the most noticeable characteristic of these rocks is that they are very indurated and break with concoidal fracture. Silty laminae which were common in lithofacies 5a are rare to absent in this facies. Bioclastic fragments are present in hand samples but are a minor characteristic. Fossil allochems comprise 3% of the rock and include gastropods, ostracods, trilobites, and unidentifiable fossil debris, all in trace amounts. Other fossils such as algae (Solenopora), pelmatozoan debris, and bryozoans are occasionally present in some samples (CP16E, TM20), but are severely abraded and fragmented (Fig. 2.11A).

Micrite is the most abundant matrix material and makes an average of 78% of the rock. Sparry calcite is also present (16%) in the form of microspar, spar filling of burrow tubes, and spar filling of shelter areas beneath skeletal fragments. Dolomite comprises 3% of the thin sections and always is associated with stylolite seams and burrow tube fillings. Terrigenous quartz silt is a minor constituent and comprises an average of less than 1% of the rock. These quartz grains are randomly distributed throughout the rocks within this facies.

Biogenic activity was very rare and is indicated by both horizontal and vertical burrows. In places, bed interiors are homogenized with an occasional occurrence of discrete burrows. Horizontal burrows are more numerous than vertical burrows throughout the micritic layers

Figure 2.11. Characteristic fabrics observed in lithofacies 5b and 6.

A. Photomicrograph showing severe abrasion and fragmentation of skeletal fragments. Bar scale is 0.2 cm, CP16E-1 (lithofacies 5b).

B. Photomicrograph showing pelmatozoan-bryozoan packstone-grainstone. Bar scale is 900 μm, 18B, lithofacies 6.

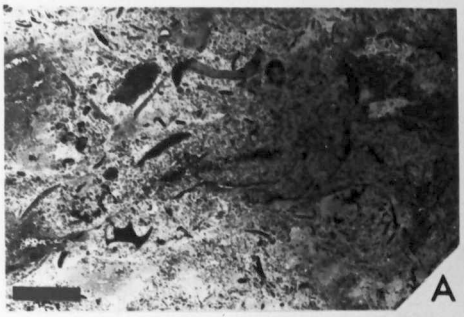
C. Negative print of thin section showing gastropod-molluscan rich packstone. Bar scale is 0.5 cm, 10B, lithofacies 6.

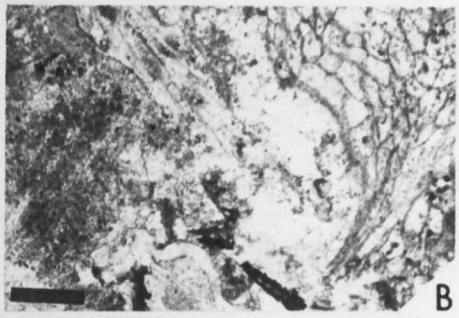
D. Photomicrograph of Sample TM23-1. Note the mixture of skeletal (A) and nonskeletal (B) grains in photograph. Bar scale is 1.2 mm, lithofacies 6.

E. Photomicrograph of Sample TM23-3. Note the rounded intraclast which is composed of transverse section of Tetradium. Bar scale is 5 mm, lithofacies 6.

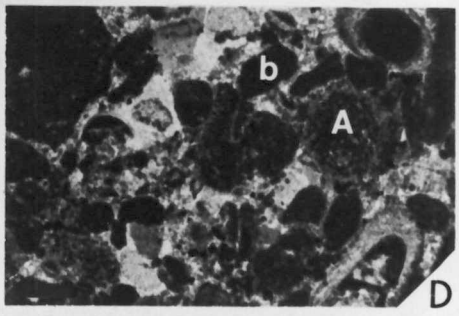
F. Thin section negative print of Sample B45. Note the pelloid-fossil planar lamination. Bar scale is 1 cm, lithofacies 6.

G. Photomicrograph showing dogtooth (scalenohedral) morphology of calcite cement filling the shelter area under brachiopod shell. Bar scale is 700 μm, CP30, lithofacies 6.

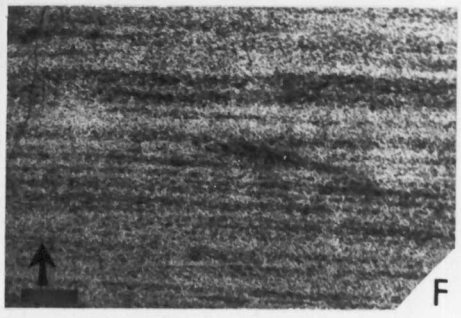

A

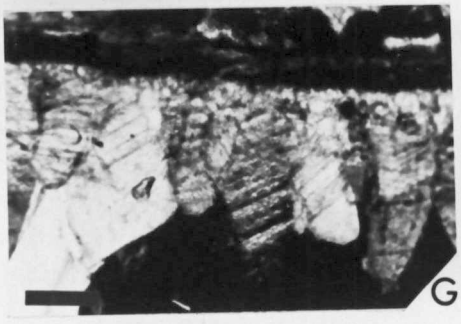

B


C


b
A
D


E


F


G

and have a diameter of 0.5 cm. These burrow tubes are filled with spar, micrite, peloids, and dolomite crystals. Burrow tubes generally have distinct walls.

Geopetal structures in articulated ostracod valves are present only in one sample (CP25B). Horizontal and vertical stylolite and vertical fractures are also present (GP84).

Cementation is restricted to pore filling, sparry calcite cement which fills burrow tubes, and neomorphic alterations of micrite to microspar (CP16D). Lamination is also present in a few samples (GF16, TM11). These laminae exhibit interlaminar fenestral (?) structures. Upper surfaces of laminae are wavy, characteristic of those which are formed by algal activity in modern environments as described by Davies (1970b), and Hardie and Ginsburg (1975). However, due to the scarcity of these features in this facies, their origin cannot be established.

6. Intrapelbiosparite, Pelbiosparite-Pelbiomicrite (packstone and grainstone):

Rocks of lithofacies 6 are medium to coarse-grained, grain supported, and range in color from light gray to medium gray. Skeletal allochems are large and are the most abundant constituent within this lithofacies (52% of rock volume). The most abundant and noticeable fossil fragments in both hand specimens and thin sections are brachiopods, bryozoans, and pelmatozoan debris. Based on the dominant skeletal and nonskeletal allochems, there are three different rock types within this facies as follows: (1) pelmatozoan-bryozoan-rich packstone-grainstone with minor amounts of brachiopods, ostracods,

trilobites and peloids (Fig. 2.11B), (2) gastropod-molluscan-rich packstone with minor amounts of brachiopods, intraclasts, and peloids (Fig. 2.11C), and (3) mixed packstone, consisting of subequal amounts of skeletal and nonskeletal allochems, and containing ostracods, brachiopods, molluscs, bryozoans, trilobite, and peloids (Fig. 2.11D).

Sorting of skeletal allochems is poor to fair except in pelmatozoan debris which displays sorted to well sorted grains. Roundness of skeletal and nonskeletal allochems varies, but grains are generally subrounded to subangular.

Intraclasts are observed only in minor amounts in a small number of samples (1% of rock volume). These intraclasts are sometimes contain small fossil fragments such as brachiopods, algae, and Tetradium coral, which are also present in the surrounding matrix (Fig. 2.11E). Peloids are more abundant than intraclasts and make up an average of 7.5% of rocks. They are generally poorly sorted but are not abraded. Many of these peloids are clearly intraclastic in origin because they have an internal fabric. Others may be fecal in origin, or were originally skeletal fragments that have been micritized; many of the skeletal grains such as bryozoans and brachiopods show partial micritization and have uneven micrite envelopes. Micritization of skeletal grains is the work of boring algae and fungi, and may completely obliterate the original skeletal microstructures if the process goes to completion (Bathurst, 1966, 1976).

The fauna of lithofacies 6 is very diverse. Unabraded and unfragmented biofoliated bryozoans (10%), articulated and

disarticulated brachiopods (14%) and ostracods (4%), algae (including Hedstroemia, Solenopora, Kazahkstanelia, and Nuia, (G99, 100, B87), trilobites (GF41, B87, 3.15%), whole and broken gastropods (3%), pelmatozoan debris with micrite envelopes (11%), broken fragments of Tetradium (1%), bivalves (2%), and cephalopod (only in Sample GF68) are among the fossil allochems in this facies.

Many of the horizontally (parallel to bedding) oriented skeletal fragments such as brachiopods, molluscs, ostracods, and trilobites, and porous grains such as pelmatozoans, bryozoans and Tetradium within this facies are coated or filled with micrite. This micrite coating tends to give the particles rounded outlines. Nonskeletal allochems such as oncoids also are present only in a few samples (GF17, 57, B87). Skeletal grains and intraclasts are always the core for these oncoids which exhibit an unlayered micrite cortex.

Rounded and abraded unidentifiable fossil debris (5%), dolomite (5%), and terrigenous quartz silt (1%) are also present. Dolomite crystals are always associated with mud, which fills the skeletal fragments, and with stylolite seams. Quartz silt is angular and randomly scattered throughout the rocks.

Biogenic sedimentary structures within this facies are rare but include both horizontal and vertical burrows. These burrows are generally preserved within the muddy portions of fining or coarsening upwards sequences. Burrow tubes have diffuse walls and are filled with fossil debris, mud, peloids, dolomite, and sparry calcite. Primary physical sedimentary structures are the predominant feature of this

facies and include fining and coarsening upwards sequences, planar-cross bedding, ripple-cross lamination, erosional surfaces, and current-induced parallel orientation of elongate skeletal fragments such as brachiopods and bivalves. Erosional surfaces are generally planar but may also have scallops with a relief of up to 3-5 cm. These surfaces can be traced for up to 2 m in outcrops and are seen to repeat vertically in thin sections. Skeletal and nonskeletal allochems in the underlying beds are always truncated, but beds do not show extensive scouring. The sediments on both sides of these surfaces are identical and contain the diverse marine and restricted biota characteristic of this lithofacies (CP30).

Sediments of this lithofacies contain abundant evidence of moderate to high energy, current-induced features. Ripple marks are generally present at the base of sediments and are followed by planar-cross beds with internal current-laminated fossils, and peloids (GF30, 35, 95, 78, B27, 37) (Fig. 2.11F). Fining and coarsening upward sequences also are common. In fining upward sequences the basal layer is composed of coarse peloids and skeletal materials, overlain by plain-laminae consisting of fossils, peloids, or unidentifiable fossil debris; these laminae are succeeded by bioturbated mud (B64, TM41E). On the other hand, coarsening upward sequences have a basal bioturbated mud which is overlain by granular or sand-sized skeletal debris (gastropod, molluscs, and brachiopods) or unidentifiable fossil debris which exhibits planar and cross lamination. The contact between these two lithologies is erosional and in places scoured (B64, 57, 36, 24, 34, CP5C, GF78).

Cements within these packstones and grainstones are drusy-equant calcite mosaic, syntaxial calcite, fibrous fringe calcite, vadose silts, neomorphism calcite (micrite to microspar and recrystallization of high magnesium calcite and aragonite to low magnesium calcite), and silica replacement. The drusy-equant calcite mosaic cement is the dominant type of cement and generally fills the shelter area beneath skeletal fragments and between the skeletal and nonskeletal fragments (interstitial). Crystals range in size from 30 to 250 μm and increase in size toward the center of the voids (in shelter areas or interstitial pore spaces). This pore filling cement type in a few samples (GF71, 62, CP30) shows dogtooth-scalenohedral morphology, characteristic of fresh-water phreatic precipitates (Fig. 2.11G). The syntaxial calcite cement occurs as overgrowths on crinoid grains and in places envelopes the nearby grains as well (B18, GF62).

Fine-grained, prismatic fringe cement is also observed around the periphery of echinoderm grains (B87). This cement is only present in minor amounts and generally occupies the first stage in the paragenetic sequence of cementation (see Chapter V for details). Neomorphism which has occurred within the sediments of this lithofacies, exists in two basic forms: (1) neomorphic alteration of micrite to microspar (Sample: G30); and (2) replacements of original aragonitic and high magnesium calcite molluscan and Tetradium fragments (Samples: GF71, 73) to low magnesium calcite probably by solution/redeposition.

Silicification also occurred within some skeletal allochems; brachiopods, pelmatozoan debris, and bryozoans are among the common

fragments which have been replaced by fibrous chalcedony (Samples: B87, 18). This silica replacement is always last in the paragenetic sequence and replaced both grains and overgrowth syntaxial cement on crinoid grains.

Chemical processes (solution) evidenced by skeletal corrosion have occurred in a few samples, but were very rare in this lithofacies (Samples: GF95, 73). Other features such as encrustation of skeletal grains (Tetradium, bryozoans and trilobites) by algae, horizontal and vertical stylolites, and geopetal structures in bivalves, brachiopods and ostracods are also present but rare.

7. Tetradium-Rich Packstone:

Lithofacies 7, Tetradium-rich packstone, is present in all four measured stratigraphic sections and is easily distinguished from other lithofacies by its characteristic skeletal allochems. This lithofacies is comprised of massive skeletal limestone with trace amounts of peloids and intraclasts and occasional cross stratified carbonate units.

The dominant skeletal fragment is the coral Tetradium which comprises 31% of the rock volume. Other skeletal allochems within this facies include ostracods (7%), pelmatozoan debris (3%), and unidentifiable fossil debris (<3%). Minor skeletal components which comprise less than 1% (each group) are: brachiopods, gastropods, trilobites, bryozoans, aglae (Hedostroemia and Solenopora), and molluscan debris. Ostracods are articulated, disarticulated, and broken and show varying degrees of the effects of transportation.

Pelmatozoan debris is heavily abraded and rounded. Bivalves are both articulated and disarticulated. Other skeletal allochems display a wide spectrum of transportation history. However, the restricted water fauna appears to exhibit less abrasion suggesting it is the indigenous fauna of this lithofacies.

Tetradium is present either as individual colonies as isolated heads or as both longitudinal and transverse sections in thin sections (Fig. 2.12A). In the outcrop, the coral heads have been observed to reach a diameter of 30 to 50 cm and a height of 10 to 20 cm. Interhead material consists of skeletal fragments, mainly articulated and disarticulated ostracods, and rounded pelmatozoan debris. Tetradium heads in the outcrop were also found to be either right-side up or toppled, but they do not display any signs of transportation. Therefore, based on their complete preservation, they are suggested to be in situ. The Tetradium coralites are filled with mud, spar, and in places with skeletal fragments such as ostracods.

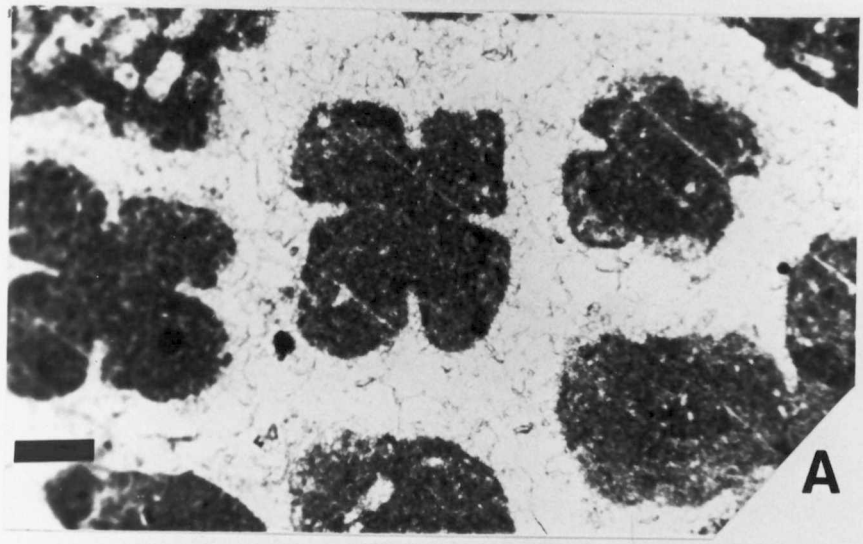
Dolomite crystals are also present (1%) and are always associated with stylolite seams and/or burrow tubes. Carbonate mud is a major constituent of matrix materials and comprises 43% of the rock volume. Sparry calcite is only present as a minor constituent in this facies (7%).

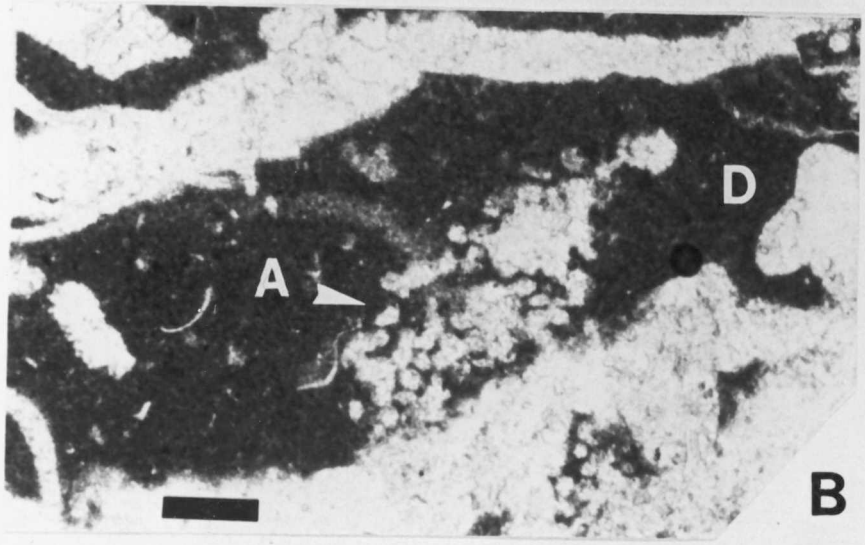
Biogenic activity and burrowing are present and include only horizontal burrows with diffuse walls. These burrow tubes are filled with micrite, skeletal fragments, and dolomite crystals. Encrustation of skeletal grains, such as Tetradium and ostracods by algae

Figure 2.12. Characteristic features of lithofacies 7.

A. Transverse section through a Tetradium corallite. Bar scale is 0.3 mm, B83.

B. Solenopora (?) (alga, A) encrusting a Tetradium corallite (D). Bar scale is 0.7 mm, B83.


A


D
A
B

(Solenopora) is a very common feature in this lithofacies (Samples: B26, 72, Fig. 2.12B). Geopetal structures within the ostracod valves (Sample: GF28), micrite envelope development on ostracods, and molluscs, and vertical calcite stringers are also present.

Cement within this lithofacies is limited to syntaxial overgrowth calcite and drusy-equant calcite mosaics. Syntaxial cement is observed only on crinoid grains. Drusy-equant calcite mosaic cement always fills Tetradium coralites and bryozoan zoecia. Silicification of skeletal grains in the form of chalcedony is also present (GF28), but is limited to a few brachiopod and Tetradium fragments (B72). Neomorphism of original aragonitic and high magnesium calcite molluscan and Tetradium fragments to low magnesium calcite, is also present.

Environment of Deposition

1. Lithofacies 1:

Interpretation of facies 1 is dependent primarily on the identification and interpretation of features such as: burrows (horizontal and vertical), matrix, fenestral structures, mud cracks, biota, and other physical sedimentary structures. This facies occurs at the base of two measured sections (Goodfield and Center Point), and also at the middle of the stratigraphic section at Goodfield.

The majority of features observed in facies 1 strongly suggest that sediment of this facies accumulated on a supratidal dolomitic flat. One of the most important characteristics of supratidal environments is the scarcity, or the total absence of fauna. This

phenomenon is mainly due to the highly stressful conditions (chemical and physical) within these environments associated with high salinity, intense evaporation and frequent subaerial exposure. Skeletal material present in this facies was probably carried in from the surrounding environments (intertidal and subtidal) by storms, tides, and/or waves. The restricted fauna observed, essentially one species of leperditid ostracod, is evidence for the restricted conditions and possibly greater than 50% exposure time to subaerial conditions (Ginsburg and Hardie, 1977).

Dolomite in the matrix probably formed in situ as a result of the evaporation of water on the exposed supratidal flats. Dolomite formation in tidal flat environments is due to the high concentration of magnesium and calcium ions by capillary action where calcium has higher solubility than magnesium, leading to dolomite formation (Shinn et al., 1965). Dolomitized intraclasts are evidence of early dolomitization. These intraclasts are parts of supratidal mud flats that were ripped up by storms, waves or tides shortly after initial deposition.

Chert clasts which were observed in the lower portion of the measured sections within this facies were probably derived from the exposed Knox Group rocks in the study area. These chert clasts do not exhibit any signs of sedimentary structures, such as imbrication, to indicate conditions of transportation.

The common laminoid fenestrae presumably formed as a result of one of, or a combination of the following mechanisms: (1) desiccation and

shrinkage of sediment (Shinn, 1968; Tebbut et al., 1965), (2) molds of algal mats (Logan et al., 1974), (3) gas generation (Cloud, 1962), and horizontal burrows. Desiccation-shrinkage of sediment and/or gas generation are the most likely mechanisms responsible in forming fenestral structures in this facies. The fact that these fenestrae are regular with matching sides and the lack of flat bottom and jagged top, characteristic of the void left after the decay of algal mats, disproves the algal mat possibility of origin (Tebbut et al., 1965; Logan et al., 1974; Hardie and Ginsburg, 1975). Likewise, due to the high stress conditions and the scarcity of fauna within a supratidal environment, the burrowing mechanism can be also disregarded as being responsible for the formation of the regular fenestrae. However, the origin of irregular fenestrae is much more difficult to determine. The experimental study by Shinn (1968) and Cloud (1962) on modern carbonate sediment on the Bahamian Banks attributed these irregular fenestrae to the generation and migration of gas. Since these irregular fenestrae are commonly associated with laminoid fenestrae, other possibilities such as the enlargement of sheet cracks or laminoid fenestrae by dissolution or desiccation of muddy sediment (Grover and Read, 1978) due to exposure are possible. All of these possible interpretation support the supratidal origin of facies 1.

The dissolution surfaces formed as a result of the exposure of sediments to meteoric water which was the only source of undersaturated water (with respect to Ca/Mg) in an environment with an exposure greater than 50% (Ginsburg et al., 1977).

Vertical burrows are also present in facies 1. Seilacher (1964) has stated that vertical burrows are characteristic of shallow water environments and are more numerous in supratidal and intertidal environments than in subtidal environments. Rhoads (1967) has also noted the paleobathymetric distribution of burrows. He concluded that deep vertical burrows are advantageous to the organisms where physical conditions such as temperature and salinity are stressful.

This facies also possesses desiccation features. Shrinkage cracks in modern carbonate environments are typically formed in supratidal and intertidal environments. However, based on available information (Shinn, 1969; Ginsburg et al., 1977; Ginsburg, 1975), the preservation potential of these features is much greater in supratidal-high intertidal environments than lower intertidal zones. These shrinkage cracks and other feature (previously mentioned) suggest that sediments of facies 1 were deposited above mean high tidal levels in a supratidal environment.

2a. Lithofacies 2a:

The absence of intensive biogenic activity and the lack of horizontal lamination indicate that current energy was low in the environment of deposition of this facies. The small grain size (abundant carbonate lime mud), rare fossil fragments (less than 2% by volume), and the abundance of quartz silt most likely represent an area of little mechanical agitation and currents in the low areas of shallow tidal flat environments where the episodic introduction of

coarse-grained sediment (fossil debris) from deeper water into the environment was possible (Shinn, 1973).

This supratidal environment was also characterized by the abundance of mud cracks and the presence of vertical burrows. During subaerial exposure (exposure index greater than 50), mud cracks formed (Hardie and Ginsburg, 1975). During flooding episodes, burrowing organisms and mobile fauna thrived where organic debris was abundant. Therefore, the presence of vertical burrows accompanied by mud cracks and the lack of diverse fauna indicate a supratidal environment.

2b. Lithofacies 2b:

Sedimentary features within facies 2b indicate that mechanical processes were limited and had very little influence on stratification. There is only one line of evidence that supports the effect of mechanical processes on the sediments of this facies; scalloped-erosional surfaces. On the other hand, biological processes in the form of burrowing had greater influence. In places, intense bioturbation has destroyed any evidence of physical sedimentary structures that might have existed.

The environment of deposition of facies 2b is designated as supratidal for the following reasons: (1) the abundant vertical mud cracks which suggest exposure greater than 50% of the time (Shinn, 1968; Ginsburg and Hardie, 1977), (2) abundant birdseye fenestrae, both horizontal and vertical (Grover and Read, 1978), (3) concentration (very limited) of fossils of certain taxonomic varieties (gastropod, brachiopod) which were either washed in from surrounding intertidal and

subtidal environments, or represent remains of in situ organisms inhabiting an environment lacking favorable conditions for diverse organic activity (Laporte, 1967), (4) an abundance of vertical burrows (Rhoads, 1967), and (5) the presence of scalloped-erosional and scour filled surfaces (Ball et al., 1967).

Facies 2b is considered to be the lowermost portion of the supratidal mud flats, in the zone that was most likely to be covered by high water during tidal cycles (Shinn, 1973). However, prolonged periods of exposure (greater than 50%) allowed the formation of mud cracks, burrowing activity, and formation of birdseye structures. Finally, occasional, strong storm tides in this supratidal environment ripped up portions of mud flat sediments, and formed scalloped, erosional surfaces that later were filled by sediments which exhibit horizontal and vertical birdseye structures.

3a. Lithofacies 3a:

Sediment with lithofacies 3a shows abundant evidence of physical reworking, but very little of biogenic reworking. Winnowing of sediment by currents removed mud and sorted the skeletal and nonskeletal allochems. Planar-cross-lamination and ripple marks within the packstone (intrapelbiosparite) of this facies is evidence of mechanical stratification. However, quartz silt (3% of rock volume) is not hydraulically compatible with larger skeletal and nonskeletal (peloids and intraclasts) allochems. This suggests that these quartz grains were not deposited by the same processes as the carbonate allochems, but may have been deposited either by winds or were carried

to the final depositional site as a result of reciprocal sedimentation (exposure, and erosion of sediments at the regimes landward margin). However, this proposal is highly speculative and further evidence is required.

The biogenic reworking within this facies was rare and, thus, physical sedimentary structures are dominant. In addition to the above mentioned sedimentary features characteristic of well-agitated environments (intertidal), the presence of graded bedding, fining or coarsening upward sequences, which occur as thin beds or lens shaped bodies within this facies, are supportive evidence of storm activity in the area. These thin, storm-generated lenses are intercalated with the lagoonal (subtidal) deposits of lithofacies 4 and 5.

Rounded intraclasts and peloids, and abraded and sorted bioclasts (fossil debris) also indicate a deposition where the energy level was high, because fine carbonate mud was winnowed from the coarser fossil debris and fragmentation and sorting of fossils also took place. Also, the occasional presence of mud cracks within this facies indicates that sediment was exposed subaerially for short periods of time.

Based upon features of lithofacies 3a (well-rounded and sorted allochems, ripple marks, planar-cross lamination), its association with tidal flat deposits, and comparison with modern carbonate environments (Shinn, 1968), these sediments were probably deposited in an intertidal flat channel. However, portions of these intertidal channels may have extended into the subtidal zone.

3b. Lithofacies 3b:

Processes involved in the stratification of lithofacies 3b were mainly biological with only very minor mechanical/physical processes. Most of the time the environment was a low energy one in which abundant lime mud (59% by volume) accumulated. Also, occasional storms brought in sediments during periods of higher energy conditions and coarse bioclasts were mixed with lime mud. However, the initial energy level in this environment was sufficiently low that not much winnowing or sorting of allochems took place most of the time.

The characteristic features within this facies indicate that these sediments were deposited in intertidal ponds, of limited areal extent, similar to the tidal ponds of modern carbonate environments of Andros Island (Hardie et al., 1975). The presence of mixed horizontal and vertical burrows (horizontal more common than vertical) with indistinct burrow walls, restricted water fauna such as ostracods (present as articulated specimens), and the absence of open-marine biota suggest a tidal pond depositional environment. The absence of open-marine biota is probably due to the great distance from open-marine environments. Quartz silt either came from a cratonic source on the north and the west, or from the rejuvenation of the land mass to the east and southeast of the depositional basin.

Restricted water fauna also suggests a tidal pond depositional environment. The proposed tidal pond environments are solely based on the association of these sediments with tidal flat sediment, fauna, and sedimentary structures preserved in the sediments.

Finally, since these ponds were located between low and high tide and were periodically exposed subaerially, features such as small scale mud cracks, and horizontal and irregular birdseye structures were occasionally formed (Garret, 1975; Hardie and Ginsburg, 1975).

3c. Lithofacies 3c:

Sedimentary structures resulting from the activity of blue green algae have been named cryptalgal by Atkin (1966) and are laminated or nonlaminated. Their geometry has been used to classify the various cryptalgal structures in modern carbonate environments. The most distinctive algal structures are those of Shark Bay, Australia (Davies, 1970b; Logan et al., 1974). These algal structures are generally associated with intertidal environments, but they also form in the shallow subtidal.

Algal structures (small domal shaped) in this study resemble the crinkle structures which have been described by Davies (1970b) and Logan et al. (1974), and which were formed in intertidal-shallow subtidal environments. However, according to Davies (1970b), these structures are generally 1 cm thick and are expected to be preserved in the fossil record more often than other types. Algal structures in other modern carbonate environments such as in Florida and the Bahamas have been recorded to be generally less than 1 cm thick and have a patchy distribution (Newell et al., 1959; Monty, 1967; Bathurst, 1967).

Based upon the studies of modern carbonate environments, especially those by Bathurst (1971) and Newmann et al. (1970), which have suggested the greater preservation potential of intertidal algal

structures due to the partial absence of burrowing and browsing organisms which destroy these structures, the presence of small-scale mud cracks with 2-5 cm polygons, the association of rocks of this facies with other intertidal sediments (intertidal pond and channels), and the presence of restricted water fauna such as ostracods, the sediments of lithofacies 3c are interpreted to have formed in restricted environments such as intertidal levees. However, this is a rare facies, and its interpretation is problematical.

4a. Lithofacies 4a:

The stratification of sediments of facies 4a has resulted from both mechanical and biological processes. The environment of deposition of lithofacies 4a was dominated by low energy conditions most of the time, which resulted in the accumulation of lime mud. Mechanical processes were of minor importance and episodic, forming packstone layers which are intercalated with wackestone beds. These packstone layers have sedimentary structures which are indicative of high energy conditions, such as fining or coarsening upward sequences, and parallel orientation of elongated skeletal fragments such as brachiopod and ostracods.

The abundant biogenic structures in the form of horizontal and vertical burrows with distinct walls are strong evidence of the sedimentation of organic matter with carbonate lime mud and the size sorting of the sediments. However, occasional changes of the energy level for short periods of time allowed winnowing to produce packstone layers.

Other supportive evidence for the absence of mechanical processes are: the lack of preferred grain orientation, poor sorting and roundness of allochems, and abundant lime mud as matrix. Because brachiopods are preserved both as articulated and disarticulated specimens, gastropods as whole or slightly broken shells, bivalves as articulated specimens, and ostracods as articulated and disarticulated specimens, and broken fragments, it is suggested that sediment transport was of little consequence. Also, the relative increase in the diversity of organisms in comparison to lithofacies 1, 2, and 3, the greater abundance of horizontal burrows than vertical burrows, and the subequal amount of restricted low energy subtidal origin. These sediments originated in subtidal areas adjacent to a higher energy subtidal environment. The good preservation of ostracods, gastropods, trilobites and the rounded and sorted nature of open marine biota (bryozoans and pelmatozoans) indicate a relatively shallow subtidal, restricted water condition adjacent to open-marine water, where transportation of fossils into the environment was possible. The above characteristics are present within many subenvironments of subtidal zones in the modern carbonate environments near Andros Island, British Honduras (Ambergris Cay), and Western Australia (Shark Bay) (Shinn, 1968; Hardie and Ginsburg, 1975; Ebanks, 1967; Hardie et al., 1975; Garret, 1975).

Rarity of algae (less than 1%) within this facies implies that sediments were deposited in restricted, shallow, low energy subtidal environments where either salinity variation or the influx of

terrigenous quartz silt did not permit algae to survive and/or to populate.

4b. Lithofacies 4b:

The constituents of the two lithic subdivisions of facies 4b (1) mollusc-ostracod-rich wackestone and packstone, and (2) bryozoan-brachiopod-pelmatozoan-rich packstone, are considered to be the product of two closely associated subtidal environments. However, these constituents probably formed in two different subtidal environments, but accumulated together. The mollusc-ostracod-rich wackestone and packstone is believed to represent sedimentation in a quiet-restricted subtidal area. The associated rounded crinoidal fragments, articulated brachiopods and pelecypods, Tetradium with no sign of abrasion or fragmentation, and delicate bifoliate bryozoan fragments with little abrasion, indicate that these fossils have not been subjected to prolonged transportation and probably originated in a nearby, less restricted subtidal environment. These two lithic types, especially bryozoan-brachiopod-pelmatozoan packstone, show evidence of higher energy conditions (fining and coarsening upward sequences, parallel orientation of elongated shells), probably of storm or tidal current origins. Also, peloids and minor amounts of intraclasts which are present in a few samples of this facies are a good indication of a higher energy level. Samples of the first lithic type (mollusc-ostracod-rich wackestone and packstone) do not contain evidence of higher energy conditions. Contacts between the two lithic types are sharp and exhibit small scale scour and filled features. Also, the

presence of infauna is inferred from the horizontal and vertical burrows.

Although lithofacies 4b is very similar to the lithofacies 4a, it is distinctive in having a lesser abundance of lime mud (29%), presence of worm tubes, Tetradium, and overall increase in diversity of fauna. The less abundant biota of lithofacies 4a may indicate a greater variability in salinity. Also the subequal amount of open-marine and restricted fauna, the slight increase in the incidence of horizontal burrows, and the greater amount of features such as coarsening and/or fining upward sequences, and parallel lamination of elongated shells, all suggest a greater exposure to occasional higher energy conditions, closer proximity to the intertidal system or greater access to storm or high tidal activity.

The depositional environment suggested for facies 4b is a shallow, restricted subtidal one in which occasional turbulence as a result of storm or tidal current caused the concentration of the second lithic type (bryozoan-brachiopod-pelmatozoan packstone), by removing the majority of mud from the matrix. The characteristics of this lithofacies are very close to the ones described by Milici and Walker (1973) for portions of the Moccasin Formation and might have been formed in a subtidal "lake" environment. However, in the author's opinion, the proposed environment of deposition of facies 4b sediments might have been a restricted subtidal "intrabasinal lagoon," type 2 environment with variable size, physical, chemical and biological

conditions, characteristic of modern restricted "intrabasinal lagoonal" environments in Belize (Ambergris Cay, Ebank, 1967).

4c. Lithofacies 4c:

A shallow, restricted subtidal "interbasinal lagoon," is suggested for the depositional environment for wackestones of this lithofacies. These rocks contain abundant micrite and abundant restricted water fauna such as articulated ostracods and whole gastropods, which suggest an area of very little mechanical agitation and current activity. However, the presence of large and abraded fragments of diverse fossil groups, sedimentary features such as fining and coarsening upward sequences, alignment of shells such as bivalves and ostracods, and abundant unidentifiable fossil debris (12%) indicate episodes of high mechanical energy and transportation. Generally, storm deposits exhibit characteristic features such as fining and coarsening upward sequences and graded bedding resting on scour surfaces (Kumar and Sanders, 1976). The storms were insufficient in magnitude to remove all of the micrite, thus, wackestones were formed in the environment. The articulated ostracods and whole gastropod shells which are commonly present in wackestone may represent the indigenous biota of the environment.

Micrite coatings on a few fossil grains such as brachiopods, bivalves, and trilobites, the presence of Tetradium, the low diversity of the fauna, the abundance of restricted water fauna (ostracods, gastropods), the presence of sponge spicules (an average of 3%), and the presence of both horizontal and vertical burrows with both distinct

and diffuse walls, are all further evidence to suggest a restricted subtidal origin, possibly similar to lithofacies 4b ("intrabasinal lagoon," type 2) environment. The above mentioned features are also observed in some modern subtidal carbonate environments such as Shark Bay (Davies, 1970; Logan et al., 1974), and the Bahamas (Hardie et al., 1975; Monty, 1967; Garrett, 1975).

The lithofacies may be distinguished from the facies 4b by the increased amount of mud content, the number of whole and broken gastropods, the percentage of unidentifiable fossil debris, the presence of sponge spicules, the decrease in the number of sedimentary features indicating episodic events (fining or coarsening upward sequences), and the decrease in the amount of bryozoan.

4d. Lithofacies 4d:

Sediment lithofacies 4d was deposited in a restricted subtidal, "intrabasinal lagoon" environment where current action and agitation were operating on a minimum scale. The presence of alternating wackestone and packstone layers indicates that occasional minor storm events occurred in the depositional environment. However, this abundant horizontal burrows, the lack of abrasion of the ostracods and gastropods, the overall dominance of restricted water fauna over open-marine forms, and the abundant mud all suggest a low energy, relatively quiet subtidal environment. The alternation of wackestone and packstone most likely represents the episodic introduction of coarser-grained materials by storms. The packstones exhibit sequences

characteristic of storm deposits as described by Kumar and Sanders (1965).

The sediment of facies 4d is very similar to that of lithofacies 4b and 4c. It differs from lithofacies 4b in the absence of Bryozoa and Tetradium. This facies also contains higher percentages of brachiopods and gastropods, and lacks the sponge spicules and Tetradium fragments characteristic of lithofacies 4c. Other features such as horizontal and vertical burrows are present in all three facies, but horizontal burrows in facies 4d outnumbered the vertical burrows. The abundant horizontal burrows in this facies may also be an indication of a slightly deeper subtidal environment than the other two previously described facies (facies 4b, 4c).

Features observed in this facies are quite similar to the modern shelf-lagoonal environment near Andros Island and in the Florida Bay area (Ginsburg, 1956).

5a. Lithofacies 5a:

Lithofacies 5a was deposited in a low subtidal-lagoonal environment. Characterized by a very limited fossil content with low diversity; a greater number of horizontal burrows with more distinct walls than the vertical burrows, and the presence of alternate laminae of quartz silt and carbonate mud. The restricted water fauna consists of ostracods; the abraded bryozoans present were obviously transported into the depositional site. Quiet water conditions are suggested by the abundant lime mud.

These features within lithofacies 5a are similar to the quiet water, lagoonal environment in the lee side of Andros Island and in the Florida Bay area (Ginsburg, 1956; Purdy, 1963). The only difference between the lagoonal sediments of this study and those of these modern analogues is the presence of terrigenous quartz silt in the former.

5b. Lithofacies 5b:

Rocks of this lithofacies were deposited in protected, low subtidal-lagoonal environments where current action was at a minimum. The abundant lime mud (78%), rare fossil allochems with low diversity (3%), and numerous horizontal burrows in this facies all suggest a low energy, quiet-water, protected subtidal environment. The absence of quartz silt laminae in this facies indicates either lack of supply of terrigenous clastic silt or quieter water conditions (deeper than facies 5a).

In general, the paucity of biota is the striking feature of this facies and may be attributed to unfavorable chemical and biological conditions. Lithofacies 5b is similar to facies 5a, yet it is distinguished in its lack of quartz silt laminae, lesser biogenic activity, and lower fossil content. The environments of deposition of lithofacies 5a and 5b are inferred to have been adjacent to one another since rocks of these facies are interbedded. Both of these facies are associated with other subtidal deposits in this study (facies 4d, 4c, 4b) and are thus, suggestive of a subtidal origin. However, the occasional presence of interlaminar fenestrae (?) in a few samples is a puzzle. Although these features usually originate in tidal flat

environments, similar features have been observed in the lagoonal environments of Florida Bay and Bahamian subtidal zones (Newel et al., 1959; Monty, 1967; and Bathurst, 1967). As these authors have stated, the subtidal fenestrae, possibly of algal origin, are generally less than 1 mm thick and have a patchy distribution. However, based on a combination of features (mentioned above), these deposits are probably of subtidal origin.

6. Lithofacies 6:

The characteristic feature of lithofacies 6 is its diverse biota when compared to the faunal diversity in lithofacies 5b. This diverse fossil assemblage is an indication of deposition under the influence of open-marine conditions (normal salinity and abundant food supply). Features such as mud cracks and fenestral structures, characteristic of supratidal and intertidal environments which were present in facies 1 through 4, are completely absent in this facies. Also, the abundant primary sedimentary structures indicate that biogenic activity (burrowing) was not usually able to keep pace with currents and waves in reworking sediment. However, the finer parts of some fining or coarsening upward sequences show bioturbation.

This facies shows features which are indicative of reworking by waves and/or tidal currents. These include: (1) sorting and rounding of peloid and pelmatozoan debris, (2) the presence of oncoids, (3) erosional-scour surfaces, and (4) fining and coarsening upward sequences with internal planar or cross-lamination.

All of the above features of lithofacies 6 suggest a relatively high mechanical energy environment in which deposition of packstone and grainstone took place. The presence of intraclasts which show signs of transportation and abrasion, and rounded peloids and skeletal fragments such as pelmatozoans, is a good indication that currents were actively distributing, reworking, and shaping skeletal and nonskeletal grains. In general, rocks such as packstone and grainstone with grain supported fabric and close packing indicate that deposition took place in agitated water (Dunham, 1962). However, the presence of calcareous algae such as Solenopora, Hedstroemia, Kazahkstanellia, and Nuia support deposition in this zone.

Finally, the paucity of mud in this facies, the presence of interbeds with planar and cross-lamination, the fining and coarsening upward sequences, the mixed and diverse fauna, the lack of reworking of associated sediment by biogenic activity, and the presence of algae and oncoids are characteristic features of many specific environments such as platform edges, subaqueous channels, and shoals. However, since rocks of this facies are associated with subtidal sediments of lithofacies 4, 5, and 3, a subtidal channel origin for these sediments is strongly suggested.

7. Lithofacies 7:

The mechanical energy which existed at the depositional site of lithofacies 7 was low and had little effect on stratification. This is shown by the lack of preferential grain orientation, the poor sorting, and the abundance of micrite in the matrix. The absence of agitated

conditions is also supported by the fact that Tetradium colonies were found upright in the out-crop and as coralites, up to 3 cm long in thin sections with no sign of fragmentation. Walker (1970) discussed the growth forms and life orientation of similar Tetradium in his "wave baffle" community of the Ordovician in New York. According to Walker (1970) these growth forms characterized an environment with abundant mud and variable salinity. Ostracods are also present as articulated and disarticulated valves suggesting that they probably lived in the same environment as Tetradium. Other skeletal fragments (minor fossil debris) which display varying degrees of fragmentation and roundness were probably brought into the environment from surrounding environments, trapped by the baffling action of the Tetradium colonies.

The presence of horizontal burrows with diffuse walls points to a subtidal origin. The features observed in lithofacies 7 strongly suggest that these sediments have a subtidal origin possibly of a low relief "biostromal" type such as the "wave baffle" environment of Walker (1970). The similar sediment baffling mechanism by Thalassia testudinum occurs in modern carbonate environments in the Carribean area (see Walker, 1970).

Stratigraphic Relationships

In the study area, the measured sections show that these Middle Ordovician rocks (lower and middle Chickamauga Group) can be divided into 14 principal lithofacies. Figure 2.13 summarizes the characteristics of these lithofacies. Each lithofacies consists of a

Figure 2.13. Diagnostic physical, chemical, and biological characteristics of lithofacies in the Middle Ordovician carbonate sediments in the study area.

Note: _____ Features present in all samples.
------ Features present in few samples.

Explanation for Figure 2.13

Lithofacies	Depositional Environments
1	Supratidal Dolomitic Flat
2a	Supratidal Mudflat
2b	Supratidal Mudflat
3a	Intertidal Channel
3b	Intertidal Pond
3c	Intertidal Levee
4a	Subtidal "Intrabasinal Lagoon" or Pond, Type I
4b	Subtidal "Intrabasinal Lagoon" or Pond, Type II
4c	Subtidal "Intrabasinal Lagoon" or Pond, Type III
4d	Subtidal "Intrabasinal Lagoon" or Pond, Type IV
5a	Subtidal Quiet-Protected, Lagoon
5b	Subtidal Protected, Lagoon
6	Subtidal Channel
7	Subtidal "Wave Baffle"

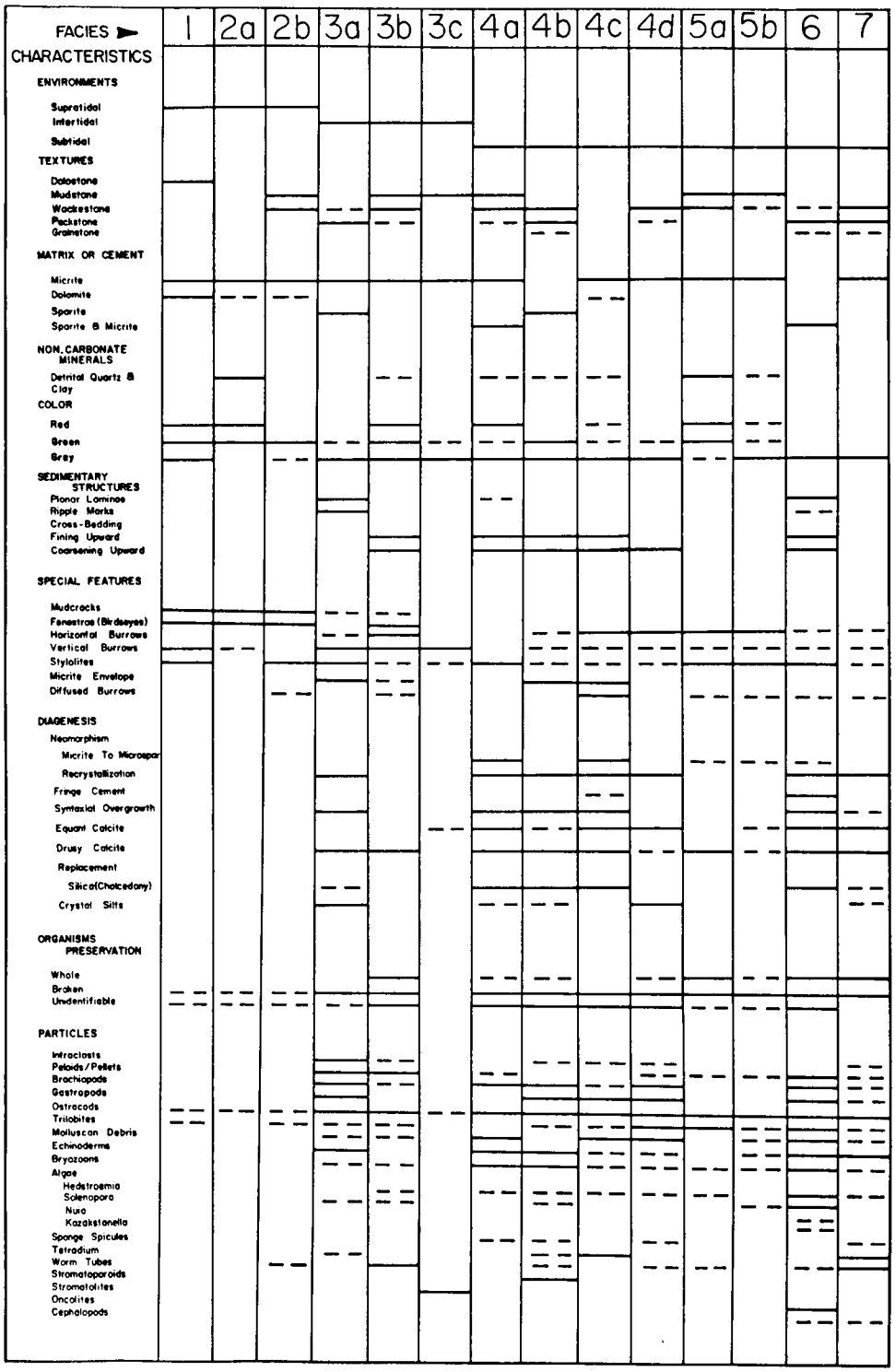

FACIES
CHARACTERISTICS
1
2a
2b
3a
3b
3c
4a
4b
4c
4d
5a
5b
6
7
ENVIRONMENTS
Supratidal
Intertidal
Subtidal
TEXTURES
Dolostone
Mudstone
Wackestone
Packstone
Grainstone
MATRIX OR CEMENT
Micrite
Dolomite
Sparite
Sparite & Micrite
NON-CARBONATE MINERALS
Detrital Quartz & Clay
COLOR
Red
Green
Grey
SEDIMENTARY STRUCTURES
Planar Laminae
Ripple Marks
Cross-Bedding
Fining Upward
Coarsening Upward
SPECIAL FEATURES
Mudcracks
Fenestrae (Birdseyes)
Horizontal Burrows
Vertical Burrows
Stylolites
Micrite Envelope
Diffused Burrows
DIAGENESIS
Neomorphism
Micrite To Microspar
Recrystallization
Fringe Cement
Syntaxial Overgrowth
Equant Calcite
Drusy Calcite
Replacement
Silica(Chalcedony)
Crystal Silts
ORGANISMS PRESERVATION
Whole
Broken
Unidentifiable
PARTICLES
Intraclasts
Peloids/Pellets
Brachiopods
Gastropods
Ostracods
Trilobites
Molluscan Debris
Echinoderms
Bryozoans
Algae
Hedstroemia
Solenopora
Nuia
Kazakstanella
Sponge Spicules
Tetradium
Worm Tubes
Stromatoporoids
Stromatolites
Oncolites
Cephalopods

Figure 2.13.

variety of lithologies, but lithofacies in the measured sections of the "Chickamauga Group" are recognized and represented by a group of samples sharing similar lithologic characters. In spite of the fact that each lithofacies occurs as a "pure" end member, mixtures of two or more lithofacies (transitional facies) are also common. Samples of transitional or mixed lithofacies can be placed into the proper subfacies by use of data derived from point counts.

This study indicates that lithofacies 2b, 3a, 3b, 4a, 4b, 4c, 5a, 5b, 6, and 7 of the measured sections are present in all four sections, whereas lithofacies 1 is only present in sections GF and CP, lithofacies 2a in sections TM and CP, lithofacies 3c in section B, and lithofacies 4d in sections TM, CP, and B (Fig. 2.14).

The data obtained from the microscopic study of thin-sections, from field observation, and from hand samples, along with the primary sedimentary structure and biota distribution and comparison with modern and ancient examples in the literature, will be used to interpret the most probable environment of deposition for each lithofacies.

Studies on Holocene carbonate sediments (Ginsburg, 1957; Shinn et al., 1965; Illing et al., 1965; Logan et al., 1970; Hardie, 1975) have provided useful criteria for recognition and delineation of modern subtidal, intertidal and supratidal depositional environments. Investigations such as those of Laporte (1967), Braun and Friedman (1969), Shinn (1968) and Walker et al. (1977, 1980) have applied these criteria in interpreting ancient carbonate sediments in various parts of North America, mainly the Eastern and Central United States.

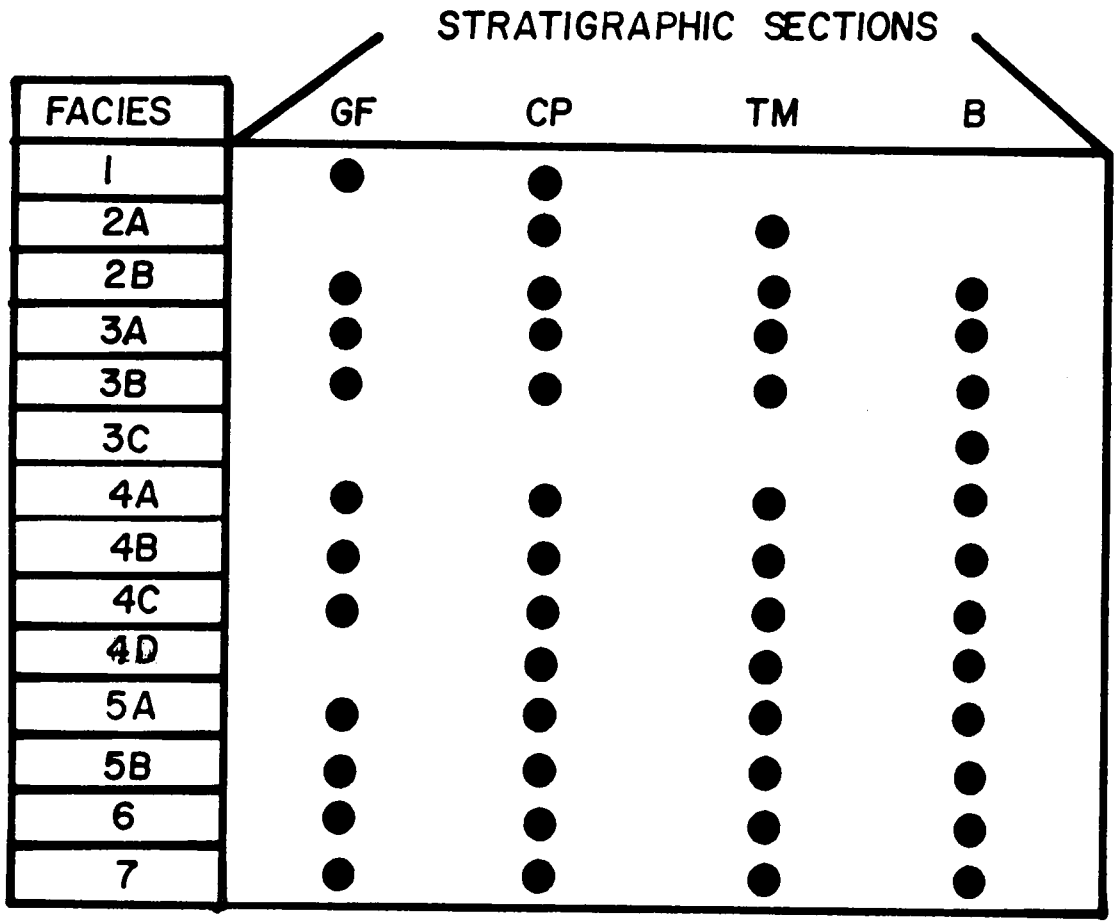


Figure 2.14. Distribution of lithofacies in Goodfield, Center Point, Ten Mile, and Barnardsville measured stratigraphic sections.

Definition of terms such as subtidal, intertidal, and supratidal used in this investigation are as follows (after Laporte, 1967 as modified by Walker, 1973):

Subtidal: The zone which is nearly always covered by marine water.

Intertidal: That strand zone which is regularly and periodically flooded by marine water at unspecific intervals for unspecific durations.

Supratidal: That strand zone only rarely flooded by marine water, but with a distinct marine influence.

Lithofacies distributions and the depositional environments assigned to the lithofacies are summarized in Figures 2.14 and 2.13 (after Laporte, 1971; Benedict and Walker, 1978; Friedman et al., 1971). Figure 2.13 lists lithologic, paleontologic, and structural (both biogenic and physical) characteristics of lithofacies in the Middle Ordovician carbonate sediments in the study area.

In order to characterize rock types (Dunham, 1962; Folk, 1959, 1962), paleobathymetric patterns, facies distribution, and for a better understanding of paleoenvironmental interpretation, graphical presentation methods have been used to simplify the large amount of data from the study (Figs. 2.15, 2.16, 2.17, and 2.18).

A workable depositional model can be constructed from the available petrologic, stratigraphic, and environmental evidence. From this model and from future work on the same strike belt, the history of tidal-flat sequences of the Middle Ordovician in the transitional area

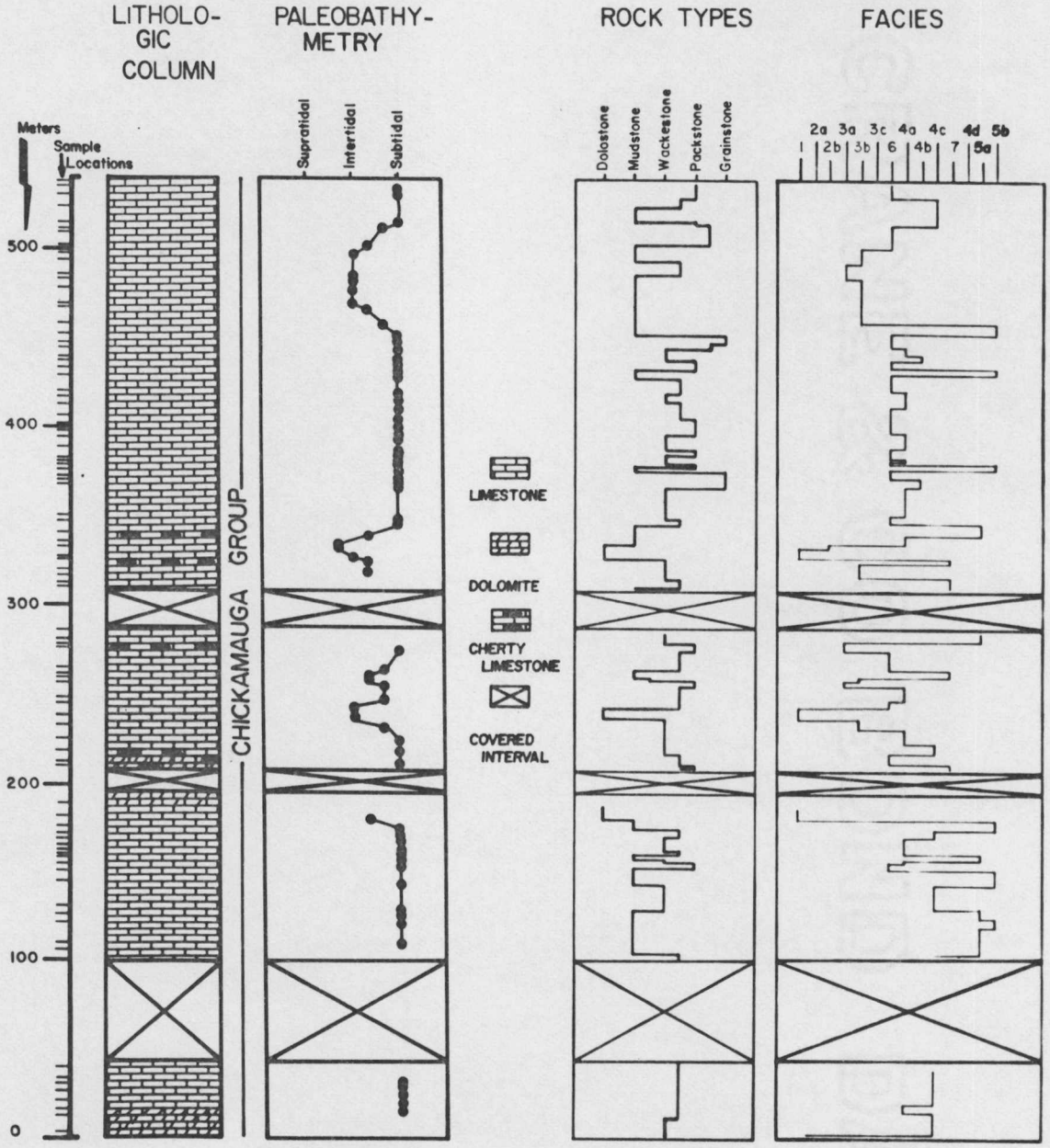


Figure 2.15. Sample locations, lithologic column, paleobathymetry, rock types, and facies distributions for Goodfield measured section.

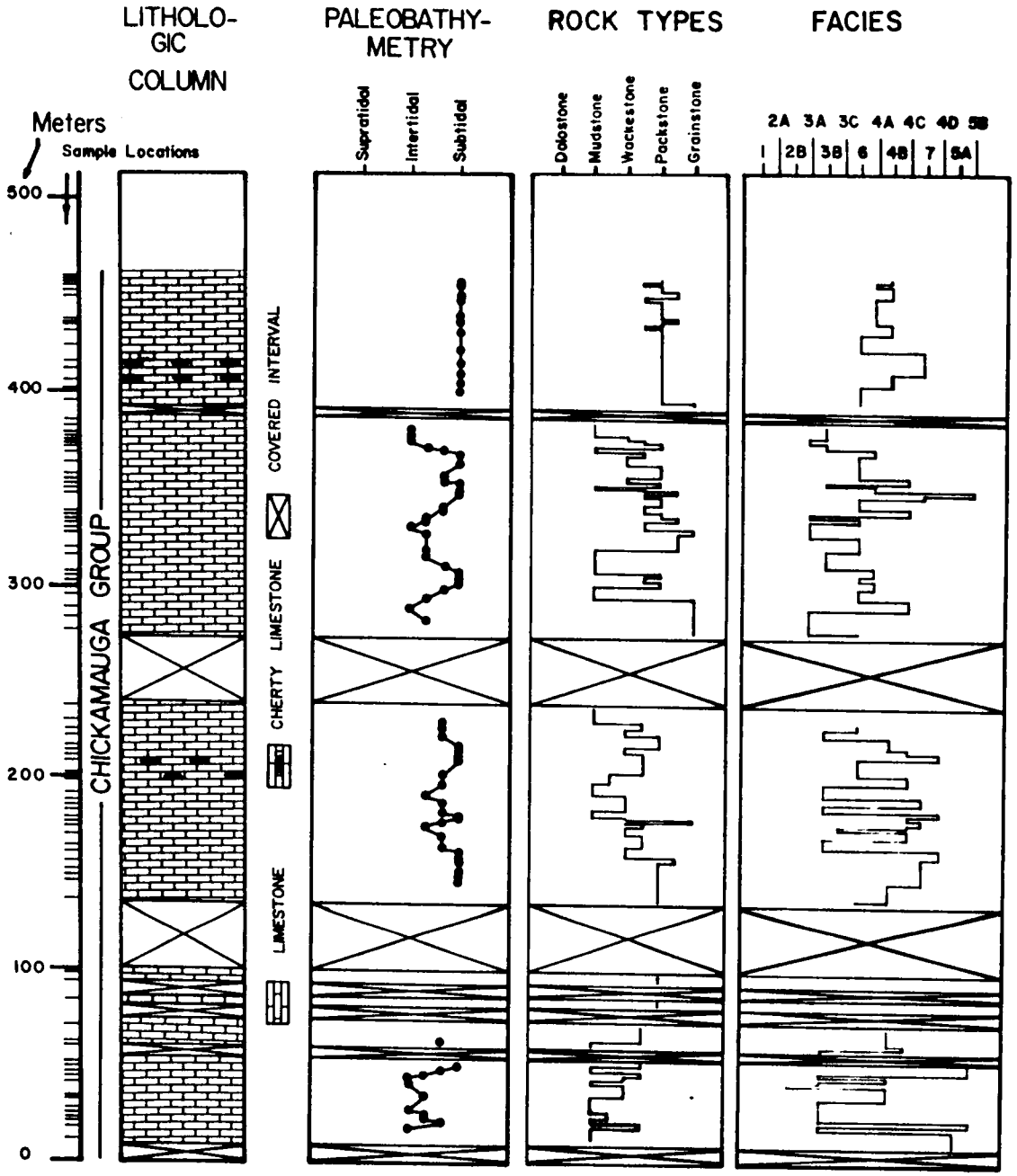


Figure 2.16. Sample locations, lithologic column, paleobathymetry, rock types, and facies distributions for Barnardsville measured section.

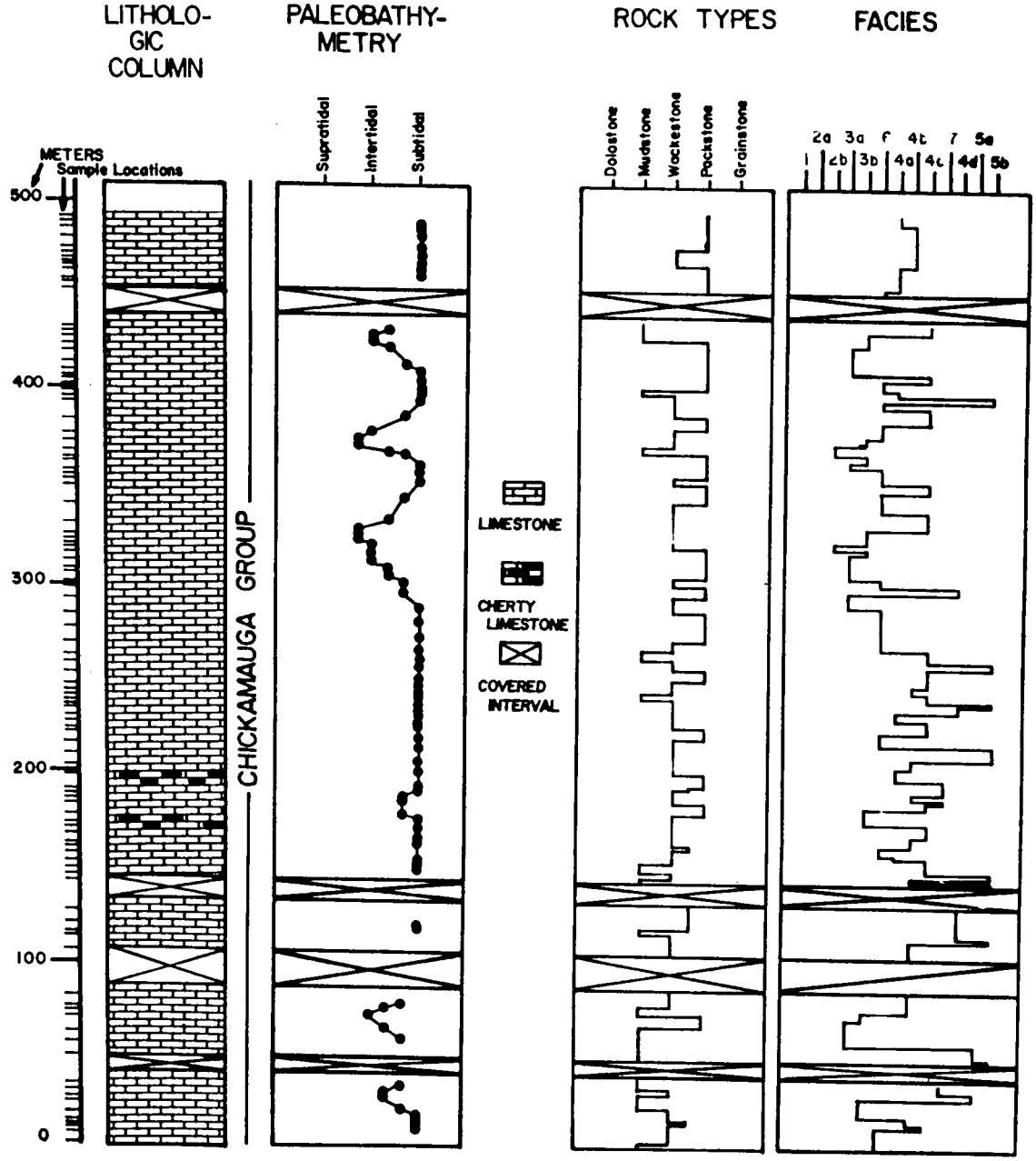


Figure 2.17. Sample locations, lithologic column, paleobathymetry, rock types, and facies distributions for Ten Mile measured section.

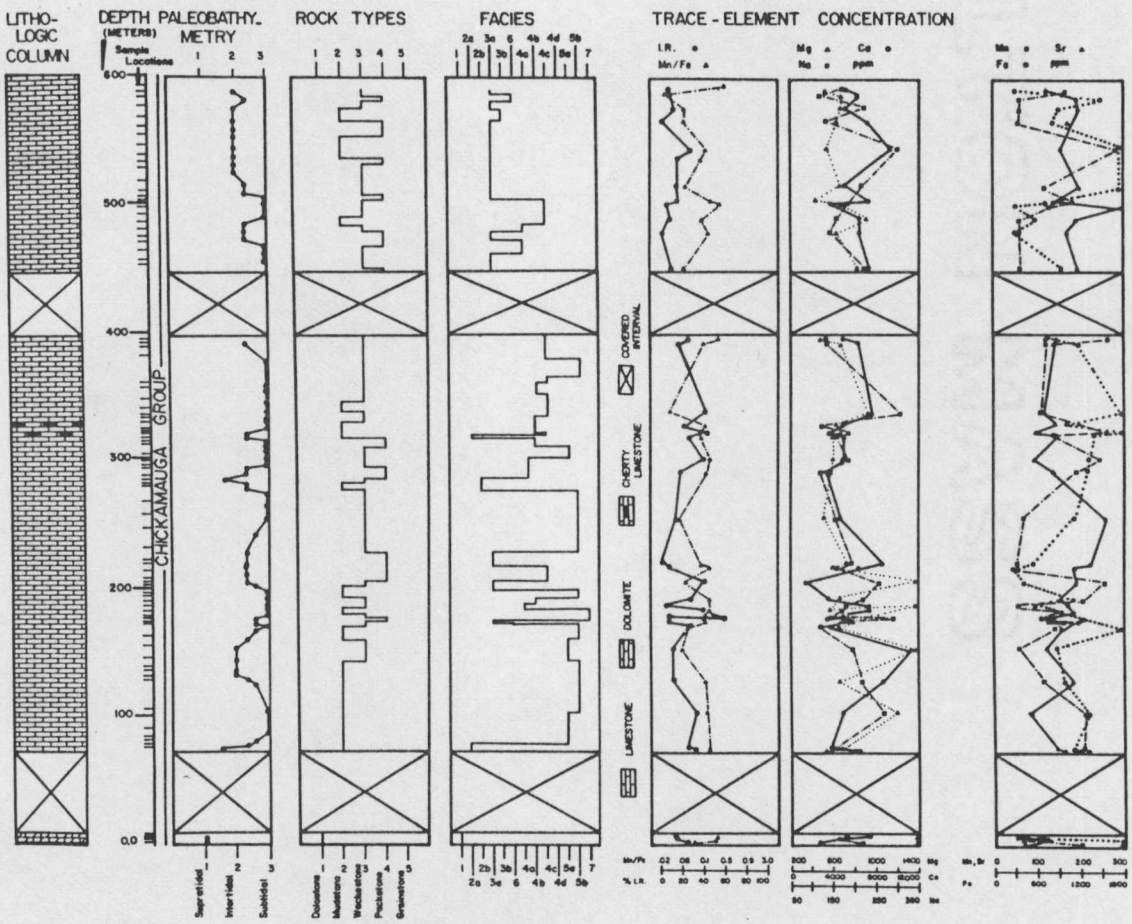


Figure 2.18. Sample locations, lithologic column, paleobathymetry, rock types, and facies distributions for Center Point measured section.

between East Tennessee and the Central Basin of Tennessee may be inferred.

The complex facies mosaic and high degree of lithological variability which characterizes the Middle Ordovician is in large part responsible for the ongoing, unsolved problems of correlation among these rocks. The stratigraphic cross-section that will be discussed is presented in Figure 2.19. The location of sections is shown in Figure 1.4 (p. 8). The stratigraphic profile is generalized, and the lithology depicted represents the major lithologies that were present within each 2 to 4 m of section.

This analysis has produced a general picture of the lateral facies relationship of these Middle Ordovician rocks along a line roughly parallel to the general, regional depositional strike (northeast-southwest). Correlation of various rocks units used in this report is based on informal units, and boundaries which are diagramatically expressed as sharp contacts are actually often gradational and/or interlaminate in outcrop. Correlation of rocks in the study area with formal names applied by various workers is much more difficult than in the areas to the east and west.

Figure 2.19 shows a fairly consistent pattern along the approximately 18 mile long line of sections. For the purpose of lithostratigraphic correlation, chert beds, lithologic packages, and similarities in these packages are used in this study. One of the significant trends that can be noted on cross-section A-A' (Fig. 2.19) is the general thickening to the southwest from 450 m to well over

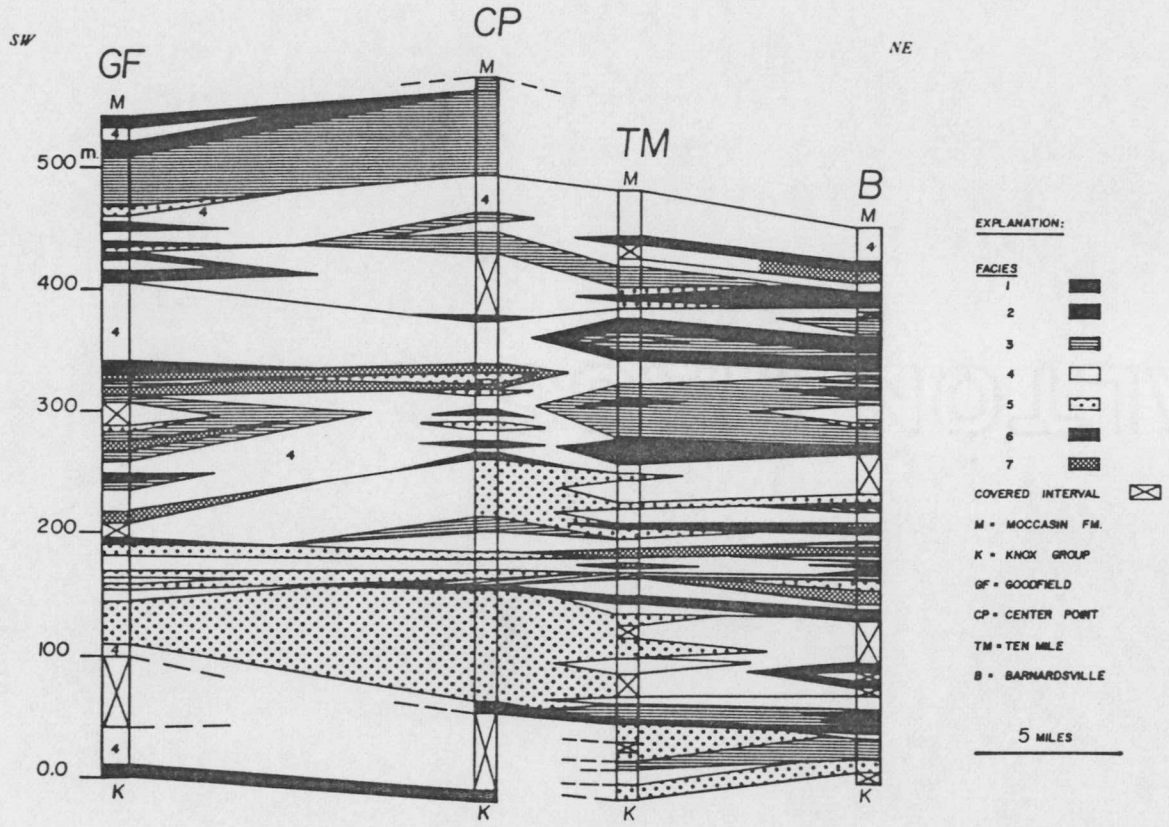


Figure 2.19. Facies relations in the Middle Ordovician, lower and middle Chickamauga Group in the study area from southwest to northeast.

500 m. Past studies suggested that the thickening of sections could be related to: (1) the amount of post-Early Ordovician (Knox) erosion, (2) the amount of disruption by faults, (3) bathymetric variation, (4) variation in major paleoenvironmental patterns, (5) differential rate of sedimentation and subsidence, and (6) variation in basin geometry. Bedded, cherty limestone and the lithologic packages (the association of cherty, bedded limestone, red-silty mudstone an homogeneous mudstone) which have been used as stratigraphic markers for the purpose of lithostratigraphic correlation also thicken toward the southwest.

The most interesting feature of Figure 2.19 is the correlation of the lower part of the sections with the Pond Spring Formation of Milici and Smith (1969). In the type section in Georgia, this formation consists of a lower chert conglomerate in red-bed sequence, light-gray limestone, green calcareous shale and mottled greenish-gray and grayish-red beds. The Pond Spring equivalent overlies the widespread unconformity on the post-Knox surface in the study area.

In the lower part of the section, the Pond Spring equivalent (Milici and Smith, 1969), the thickness of the calcareous shale unit increases from the northeast to the southwest. The increase in terrigenous silt content and red-beds with high clay content in the northeast may be accounted for by the extra supply of material from the cratonic sources to the northwest.

Interesting facies changes are also reflected in the amount of red and green calcareous shale and mottled mudstones along the strike belt

from northeast to southwest within the interval equivalent to the Murfreesboro Limestone (Milici and Smith, 1969). At the Goodfield section, the entire Murfreesboro Limestone equivalent is composed of intercalated red and green calcareous shale (predominantly green, calcareous shale) with occasional limestone layers. Toward the northeast, these beds begin to pinch out and to be replaced by light grayish-tan mudstone (wackestone), with occasional thin-bedded, green calcareous shale. This suggests a greater supply of terrigenous clastic materials due to tectonic activity to the south-southwest, or to a local sediment supply in the southwesterly area. Also, at the very base of the Center Point and Goodfield sections in the southwest, dolomite and dolomitic limestone and coarser grain lithologies (limestone) replace the red mudstone-calcareous shale of the northeast section. This could possibly indicate greater relief (more intense winnowing) and exposure on the post-Knox surfaces which might also explain the greater amount of dolomite formation (presumably supratidal) which occurs in the southwesternmost section.

The stratigraphic cross-section also shows the remaining parts of the sections (Ridley, Lebanon, Carters, Hermitage, Bigby-Cannon (?) equivalents), to be relatively continuous and to maintain consistent thicknesses along the strike belt with only a few minor, isolated changes occurring. This phenomenon is probably indicative of a period of tectonic quiescence in the study area after the formation of the Middle Ordovician sedimentary basin.

Faunal content does not show sharp changes in the northeast to southwest direction, although there is a slight increase in the amount of open-marine fauna in the southwesterly sections, which possibly indicates less restriction or more access to open-marine water. However, more regional information must be available before the true significance of these differences can be ascertained.

Conceptual Sedimentation Model

The "Chickamauga Group" rocks exposed along Highway 58, in East Tennessee (Fig. 1.4, p. 8), provide evidence for the deposition of these sediments in a complex tidal flat and shallow subtidal-lagoonal set of environments. The general pattern of depositional environments ranged from peritidal (supratidal and intertidal), tidal ponds, shallow subtidal-"interbasinal lagoon" with restricted-water subtidal channels, subtidal "wave baffles," to open-water lagoon. Water depth probably did not exceed more than 3 to 5 m (in subtidal ponds and channels), and was usually about 1 to 2 m deep in intertidal channels and ponds. The proposed depositional environment and associated water depths in the study area are based on analogy with recent carbonate environments in Florida Bay, Bahama Bank, Persian Gulf, Shark Bay, and Belize, and with various ancient analogues of carbonate sedimentation in the shallower water epeiric seas on the North American Continent during the Paleozoic (Ginsburg, 1956; Enos and Perkins, 1979; Ebanks, 1967; Davies, 1970b).

The Bahama Bank is one of the extensively studied modern carbonate environments. Figure 2.20 displays a generalized setting (plan and

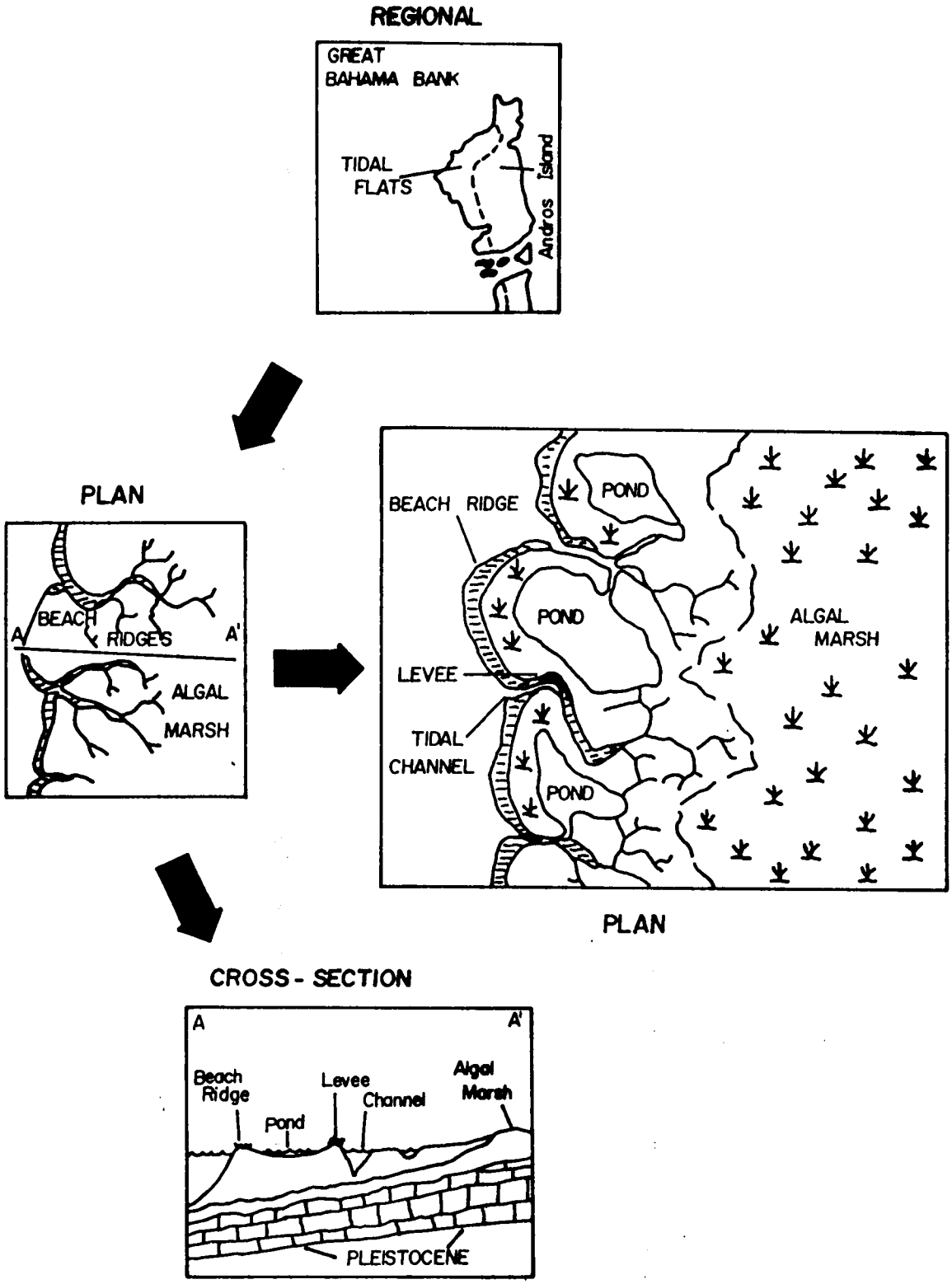


Figure 2.20. Generalized setting (regional, plan, and cross-sections) of environments and subenvironments of northern Andros Island (from Ginsburg, 1975).

cross sections) of Northwestern Andros Island (Ginsburg, 1975). The Bank can be divided into: (1) a peritidal complex, Western Andros Island, (2) a shallow interior platform, west of the peritidal complex, and (3) an oolitic shoal which separates the interior platform from the shelf break. The portion of the Bank which has been used as an analogue in this study is the peritidal complex where an extensive tidal flat system has developed on the irregular (karstic) topographic surfaces of Pleistocene Limestone (Shinn, 1969). The tidal flat system on Andros Island is about 10 to 15 miles wide, whereas the tidal flat system in the Middle Ordovician time in the East Tennessee area is proposed to have extended beyond 15 miles, possibly on the order of 40 to 50 miles (Per. Comm. K. R. Walker).

Based on petrological evidence from samples collected in the study area, the deposition of these Middle Ordovician Carbonate sediments began on the Knox unconformity surface in a supratidal environment in the Goodfield and Center Point stratigraphic sections, and in the shallow-restricted subtidal environment in the Ten Mile section. The environment for the basal portion of the Barnardsville section can not be discerned because the interval is unexposed (Fig. 2.19).

Figure 2.21 is a hypothetical representation of the inferred paleoenvironmental setting for Middle Ordovician sedimentation in the study area. The environments changed from the basal portion of sections to a more varied setting throughout the middle and upper parts of the stratigraphic sections. Within this complex tidal flat system, there were a small supratidal flats or "islands," lying just above high

Figure 2.21. Hypothetical representation of inferred paleoenvironments of the Middle Ordovician sediments in the area.

Explanation for Figure 2.21

Lithofacies	Depositional Environments
1	Supratidal Dolomitic Flat
2a	Supratidal Mudflat
2b	Supratidal Mudflat
3a	Intertidal Channel
3b	Intertidal Pond
3c	Intertidal Levee
4a	Subtidal "Intrabasinal Lagoon" or Pond, Type I
4b	Subtidal "Intrabasinal Lagoon" or Pond, Type II
4c	Subtidal "Intrabasinal Lagoon" or Pond, Type III
4d	Subtidal "Intrabasinal Lagoon" or Pond, Type IV
5a	Subtidal Quiet-Protected, Lagoon
5b	Subtidal Protected, Lagoon
6	Subtidal Channel
7	Subtidal "Wave Baffle"

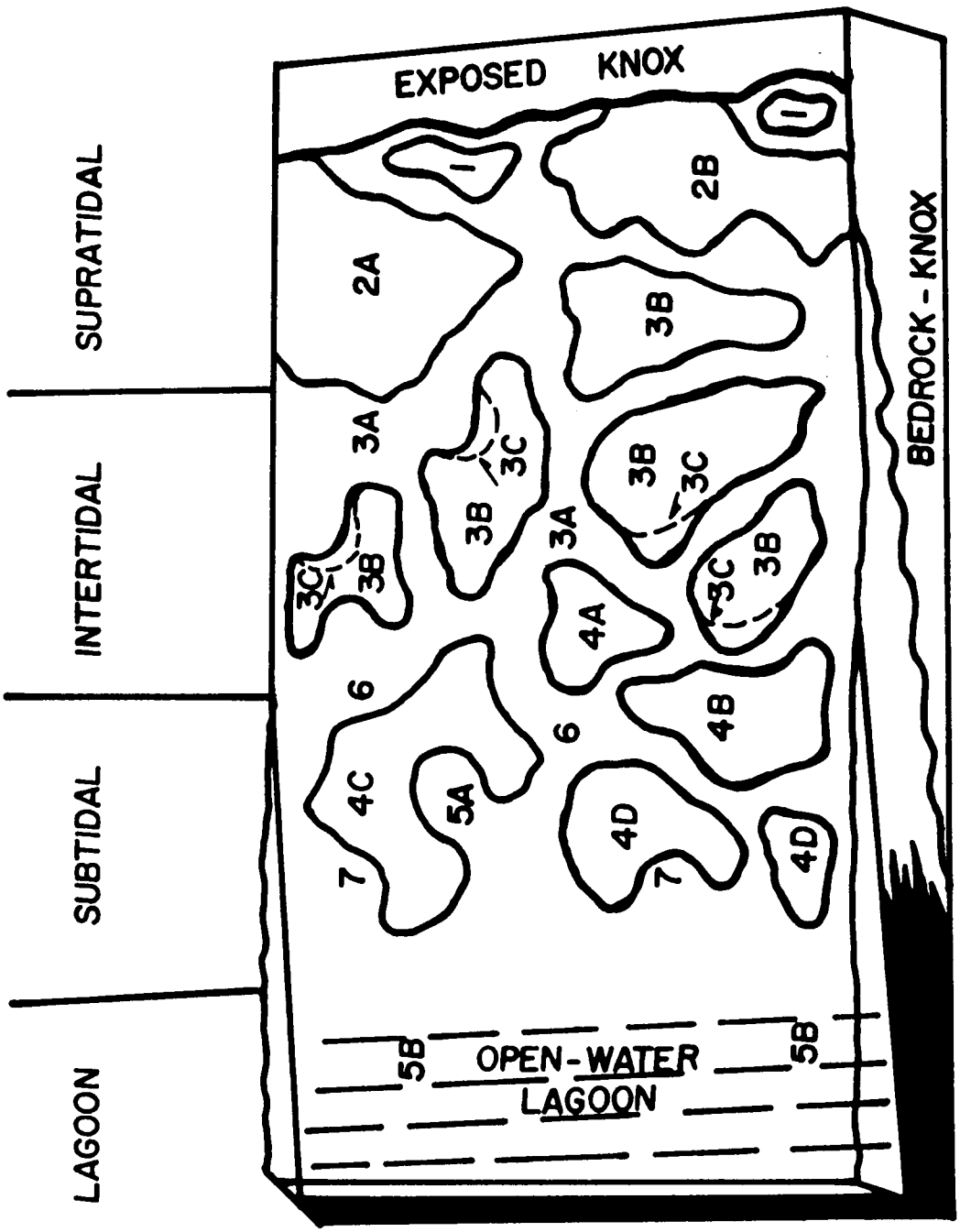

SUPRATIDAL
INTERTIDAL
SUBTIDAL
LAGOON
EXPOSED KNOX
BEDROCK - KNOX
OPEN-WATER LAGOON
1
2A
2B
3A
3B
3C
4A
4B
4C
4D
5A
5B
6
7

Figure 2.21.

tide level. These islands were formed on the remnants of the post-Knox unconformity surface similar to the mud banks found in modern Florida Bay. Intertidal flats, which flanked the supratidal environments, were more extensive areally than supratidal flats and consisted of intertidal channels, levees, and ponds. Subtidal environments consisted of "intrabasinal lagoon" or ponds, subtidal lagoons, subtidal "wave baffles," and subtidal channels. The subtidal environments became more extensive as Middle Ordovician deposition progressed, as indicated by the increasing abundance of open-marine fauna such as echinoderms, bryozoans, and brachiopods in the middle and upper portions of the sections. High energy conditions developed either as waves or tides in the channels, or as storms especially at the two central sections (Center Point and Ten Mile). The presence of extensive channelization in the central portion of the study area may be an indication of paleotopographic highs left from differential erosion on the former Knox surface which governed the pattern of sedimentation at the time, may have resulted from tectonic activity in the area that formed topographic highs. Whatever their origin, these topographic highs appear to be significant and need further study.

The presence of characteristic features of supratidal and intertidal conditions, such as mud cracks, fenestral fabric, and vertical burrows, in the middle and upper portions of the stratigraphic sections indicates that the broad and complex tidal flat system, similar to the basal portion, may have occurred during later Middle

Ordovician deposition, after which the environments changed back to more uniform subtidal and intertidal systems.

The lateral and vertical facies changes with no systematic pattern, observed in the Middle Ordovician carbonate rocks, probably indicate that the environments (supratidal, intertidal, and subtidal), and subenvironments (channels, ponds, and intrabasinal lagoons) were randomly scattered throughout the study area, and were migrating with no predictable pattern, creating a complex mosaic facies (vertical contact analysis and succession will be discussed in Chapter V). The difficulty in correlating this complex facies pattern from section to section is an indication of the independent lateral shifting of environments in each section (Fig. 2.19, p. 105).

Summary and Conclusions

The "Chickamauga Group" within the Kingston Allochthon (this study) is 458 to 592 m thick. The complex facies changes which occur throughout the area and the lack of temporal stratigraphic markers (bentonite beds, conodont zones) make correlation of these rocks difficult. The correlation of four stratigraphic sections in this study is based on informal rock units.

Carbonate rocks of this study are categorized into 14 volumetrically important major lithofacies and subfacies. The lithologic, paleontologic and sedimentary structures (both physical and biogenic) of the Middle Ordovician rocks provide evidence for establishing the environmental framework of these rocks. This framework was similar to

that of the tidal flat complex and subtidal-lagoonal environments of the Trucial Coast in the Persian Gulf, Bahama Bank (Andros Island), Shark Bay, Western Australia, and Belize (Ambergris Cay).

The lower portions of the Middle Ordovician section in the study area were interpreted as having formed on a broad tidal flat complex (supratidal dolomitic flat) with an irregular topographic surface (islands, low laying areas or "pond," and channels), and partly on the karstic surface of the Lower Ordovician Knox Group. As deposition progressed, the tidal complex was transgressed by the sea and with possible basin subsidence and tectonic activity, intertidal and subtidal conditions were introduced. Small tidal islands were separated by subtidal environments, similar to the interior of the Bahamian Bank and the Belize areas. Also, this tidal flat complex reappeared sporadically during the late Middle Ordovician. The lateral migration of these environments resulted in a series of complex and patternless three dimensional relationships between lithofacies.

Facies variation between the four measured stratigraphic sections (B, TM, CP, GF) is evident. The basal portions of the Goodfield and Center Point sections are dominated by the dolostone (facies 1), whereas the lower portion of Ten Mile section is represented by a subtidal facies (facies 5). This environmental pattern suggests that the configuration of the underlying topographic surface (karstic surface) on top of the Knox Group was irregular, and strongly influenced sediment distribution and accumulation during the basal Middle Ordovician deposition in the study area. This area was later

inundated by the sea with several minor transgressive-regressive cycles.

The Middle Ordovician supratidal deposits are the most diagnostic, but only make up a small fraction of the measured stratigraphic columns. These deposits are typified by a high micrite content, desiccation cracks, vertical burrows, laminations, and the virtual absence of fossils. Intertidal deposits consist of channels and ponds in varying proportions. Intraformational conglomerates, peloids, and sedimentary structures such as fining or coarsening upward sequences are characteristic of these intertidal sediments. Intertidal pond sediments do not contain as many sedimentary structures as in intertidal channels, but they contain abundant ostracods and gastropods. Intrabasinal lagoon and lagoonal sediments also contain a high proportion of micrite, but they are generally nonlaminated and have various proportions of "restricted" faunal assemblages mixed with open-marine fauna such as pelmatozoan, bryozoan, and brachiopods. The assemblage of organisms within these intrabasinal lagoons and lagoonal sediments differs from unit to unit, reflecting the variable physical, chemical, and biological conditions. The subtidal channels exhibit a diversity of organisms, both open-marine and restricted elements, and display several types of sedimentary structures such as small scale ripple marks, planar-cross-lamination, scour surfaces, and horizontal burrows.

In general, the lower half of these Middle Ordovician stratigraphic sections represents a very complex facies pattern,

characteristic of a mixed supratidal, intertidal, and subtidal environment, whereas the upper half indicates more uniform deposition of subtidal and intertidal sediments across the study area.

CHAPTER III

ENVIRONMENTAL SIGNIFICANCE OF SOME TRACE AND MAJOR ELEMENTS

Introduction

Due to the lack of availability of geochemical information on the "Chickamauga Group," this project was undertaken because it offered for the first time the possibility of contributing basic and fundamental geochemical information on the shallow shelf sediments of the Middle Ordovician, especially in the area northwest of the Saltville Fault in Tennessee (see Figs. 1.2 and 1.4, pp. 4 and 8). In the last decade there has been an increasing interest in the application of trace element geochemistry to the problem of paleoenvironmental interpretation. In particular, the trace element content of carbonate sediment has been used with varying degrees of success as an aid to distinguish fresh and marine waters and environments (Friedman, 1969; Veizer and Demovic, 1974; Brand and Beizer, 1980).

A study of the trace element distribution of these Middle Ordovician shallow shelf carbonate rocks within the study area is only the starting point for a detailed investigation of the relationship between trace element distribution and depositional environments. It is hoped that by collation of paleoenvironmental information and their geochemical signatures, the problem of inherited trace element content, effect of diagenesis, partition coefficients of elements, effects of facies on trace element distribution, and, finally, the effect of precursor lithology, mainly the effect of faunal content, all can be

determined. This information would also increase our understanding of certain geochemical principles governing the distribution of trace elements within shallow shelf carbonate rocks and might yield principles applicable to other Middle Ordovician rocks throughout Tennessee and in the surrounding areas.

An acid-insoluble fraction of 38 samples from the Center Point stratigraphic section was selected for this study to be analyzed for six elements (magnesium, sodium, iron, calcium, manganese, and strontium). In order to provide systematic information on the geochemical nature of the stratigraphic sequence, samples were selected from assigned lithofacies (see Table 3.1) of the sequence. The data are representative only of samples of the Center Point section. The principal purposes of this investigation were:

1. To determine the trace element concentration of samples of the Center Point section and to examine trends within the stratigraphic section.
2. To test whether samples of the various facies of the Middle Ordovician carbonate rocks of the Center Point section can be distinguished on the basis of their trace element concentrations.
3. To examine the effect of diagenesis, paleoenvironment, precursor mineralogy, insoluble residue, and sedimentation rate on the concentration of elements in the carbonate fraction of these selected samples.

Table 3.1 Selected samples from Center Point stratigraphic section used in geochemical analysis.

Facies	Sample Number
1	1A
	1B
	1C
2a	1D
	1E
2b	18A
	27R
	23A
3a	6_1A
	13A
	15A
	28A
	28F
	29C
	29G
	29J
	31
3b	29K
4a	$20A_2$
	$24A_1$
	29A
4b	10A
4c	11A
	14A
	25A
	26F
4c	28H
	29
4d	5_1B
4d	1I
	9A
5a	3A
	5B
	16C
6	30
4c	6A
7	7A
4c	25D

Atomic absorption analyses were carried out on a Varian 475 Spectrophotometer, and statistical analyses were performed on an IBM 360, model 30 computer at the University of Calgary, Canada. Sample preparation, analytical procedure and conditions are described in Appendix D.

Computer Analysis

Correlation Coefficient

Correlation analysis is a common statistical method which examines the variation of measurements made on two variables in a given sample. The correlation coefficient applied in this study is the Pearson Product Moment Correlation Coefficient. In any method, the value of r (correlation coefficient) is a measure of the amount of variation that two measurements have in common. In other words, it is a measure of the correlation between variables (trace elements, fossils, micrite, spar and insoluble residue).

In this method the value of $r = 1$ is representative of the strongest possible correlation existing between any of the two components, and $r = 0$ represents the weakest possible correlation. The values between 0 and ± 1 are approximately the square root of the total variance between two components (Krumbein and Graybill, 1965).

In any statistical analysis, numbers of samples are a major controlling factor in determining the significance level of the values obtained. For this study, the 99% significance level occurs at $r = 0.4$ based on 38 samples analyzed in this study (Dixon and Massey, 1975,

Table A-30). Also in this study in order to explain correlation coefficients to represent 50% or more of the variance, the correlation coefficient of r = 0.4 has been considered to be a weak correlation, r = 0.4-0.6 as a moderate, and r = 0.6 as a strong correlation. Table 3.2 presents the correlation coefficient values for 38 samples used in this study.

Trace Element Data

In this section I shall discuss the distribution of the trace elements in the Center Point stratigraphic section with respect to mean, correlation coefficient values, significance level of each element, correlation coefficients between pairs of variables and geological implications of r values. Table 3.3 represents ranges and means, and Figure 3.1 and 3.2 exhibits distribution of trace elements vs facies for 38 analyzed samples. In this section correlation coefficients between pairs of variables will be discussed and geological implications of the r values will be presented.

Sodium

The mean sodium concentration in Center Point samples is 183.32 ppm, while the range is 122.58-3000 ppm (Figure 3.3).

Land and Hoops (1973) and Land (1973) studied recent and Pleistocene age rocks and indicated that sodium concentration in carbonate rocks was: (1) incorporated into the skeletal materials in variable quantities, and (2) exhibited a decreasing trend with increasing exposure to diagenetic environment. The incorporation of

Table 3.2. Correlation coefficient for the Center Point stratigraphic section samples.

	Na	Mg	Fe	Mn	Sr	I.R.	Fossils	Micrite	Spar
Na	1.00000	0.17684	0.44003	0.27516	-0.09312	0.57677	-0.04176	0.08626	-0.0788
Mg	0.17684	1.00000	0.39256	0.02759	-0.26397	0.08275	-0.27266	-0.27991	-0.0685
Fe	0.44003	0.39256	1.00000	0.49123	-0.24174	0.60415	-0.40923	-0.01094	0.2343
Mn	0.27516	0.02759	0.49123	1.00000	-0.30176	0.67989	-0.43985	0.13193	0.1587
Sr	-0.09312	-0.26397	-0.24174	-0.30176	1.00000	-0.38238	0.12568	0.07380	0.0880
I.R.	0.57677	0.08275	0.60415	0.67989	-0.38238	1.00000	-0.26684	0.05142	-0.0312
Fossils	-0.04176	-0.27266	-0.40923	-0.43985	0.12568	-0.26684	1.00000	-0.27567	-0.1937
Micrite	0.08626	-0.27991	-0.01094	0.13193	0.07380	0.05142	-0.27567	1.00000	-0.4310
Spar	-0.07882	-0.06857	0.23435	0.15878	0.08807	-0.03122	-0.19377	-0.43101	1.00000

Note: Underlined values represent positive and negative correlations where correlation coefficient (r) represents moderate to strong correlation.

If $r \geq \pm.400$, r is significant.
Number of samples analyzed = 38.
Number of variables = 9.
$r \leq 0.4$ = weak correlation.
r = 0.4-0.6 = moderate correlation.
$r \geq 0.6$ = strong correlation.

Table 3.3. Concentration of the trace elements: Mn, Fe, Mg, Sr, Ca, and Na in bulk samples of Center Point section. All values stated in parts per million (ppm).

Sample Number	Facies	Mn	Fe	Mg	Sr	Ca	Na	Ins. Residue (%)
1A	1	200	2,400	6,120	73	247,686	208	33.3
1B	1	58	1,791	4,567	129	487,372	161	10.6
1C	1	113	317	4,857	62	731,059	177	16.0
		X=124	X=1,502	X=5,181	X=88	X=488,705	X=182	
1D	2a	220	1,200	540	161	611,216	200	33.3
1E	2A	202	1,100	660	148	371,529	154	27.3
		X=211	X=1,150	X=600	X=155	X=491,372	X=177	
18A	2b	185	1,290	580	135	371,529	122	17.3
27R	2b	266	714	482	146	487,372	132	25.3
23A	2b	135	1,367	615	148	487,372	157	
		X=195	X=1,124	X=559	X=143	X=448,757	X=137	
6A	3a	161	1,159	782	177	487,372	168	8.0
13A	3a	254	4,000	6,580	186	123,843	253	38.0
15A	3a	51	540	729	224	858,902	179	1.30
28A	3a	55	902	812	183	731,059	210	11.30
28F	3a	51	275	620	168	611,216	140	3.30
29C	3a	117	1,777	666	194	487,372	210	10.0
29G	3a	277	2,520	540	152	972,000	300	33.30
29J	3a	50	839	629	166	731,059	128	4.60
31	3a	163	294	529	119	487,372	158	9.30
		X=131	X=1,667	X=560	X=199	X=610,021	X=185	
29K	3b	56	895	671	187	487,372	223	10.6
		X=56	X=895	X=671	X=187	X=487,372	X=223	

Table 3.3 (continued).

Sample Number	Facies	Mn	Fe	Mg	Sr	Ca	Na	Ins. Residue (%)
20A	4a	241	1,333	600	88	487,372	182	40.0
24A	4a	263	2,962	666	96	371,529	187	46.0
29A	4a	178	707	415	130	731,059	187	13.30
		X=227	X=1,667	X=560	X=199	X=529,986	X=185	
10A	4b	52	559	2,643	173	731,059	176	4.60
		X=52	X=559	X=2,643	X=173	X=731,059	X=176	
11A	4c	208	1,090	654	152	341,161	221	26.60
14A	4c	54	273	616	181	611,216	156	2.60
25A	4c	128	1,016	610	141	487,372	125	21.30
26F	4c	119	1,185	666	130	611,216	133	10.0
28H	4c	54	571	900	181	611,216	154	6.60
29	4c	125	294	661	412	371,529	182	9.30
6A	4c	125	1,230	553	137	371	295	56.60
25D	4c	102	2,564	923	112	731	302	48.0
		X=114	X=1,028	X=698	X=181	X=517	X=196	
1I	5a	220	1,333	1,200	80	487,372	271	40.0
9A	5a	166	851	574	183	731,059	174	37.30
		X=193	X=1,092	X=887	X=132	X=609,215.5	X=222	
3A	5b	112	970	661	185	858,902	214	9.30
5B	5b	138	1,818	654	152	371,529	123	26.60
16C	5b	58	1,126	507	255	611,216	152	5.30
		X=103	X=1,305	X=607	X=197	X=613,882.33	X=163	
30	6	54	1,470	661	179	611,216	117	9.30
		X=54	X=1,470	X=661	X=179	X=611,216	X=117	

Table 3.3 (continued).

Sample Number	Facies	Mn	Fe	Mg	Sr	Ca	Na	Ins. Residue (%)
7A	7	108	805	604	119	487,372	142	0.60
		X=108	X=805	X=604	X=119	X=487,372	X=142	
5-1B	4d	56	869	4,434	123	183,364	197	8.0
		X=56	X=869	X=4,434	X=123	X=183,364	X=197	
Average		139	1,221	1,320	157	526,196	183	25.89

Note: All analysis was done by atomic absorption method except calcium (titration method).

X = Average of values in each facies.

Figure 3.1. Trace elements distribution in facies at Center Point section.

Explanation for Figure 3.1

Lithofacies	Depositional Environments
1	Supratidal Dolomitic Flat
2a	Supratidal Mudflat
2b	Supratidal Mudflat
3a	Intertidal Channel
3b	Intertidal Pond
3c	Intertidal Levee
4a	Subtidal "Intrabasinal Lagoon" or Pond, Type I
4b	Subtidal "Intrabasinal Lagoon" or Pond, Type II
4c	Subtidal "Intrabasinal Lagoon" or Pond, Type III
4d	Subtidal "Intrabasinal Lagoon" or Pond, Type IV
5a	Subtidal Quiet-Protected, Lagoon
5b	Subtidal Protected, Lagoon
6	Subtidal Channel
7	Subtidal "Wave Baffle"

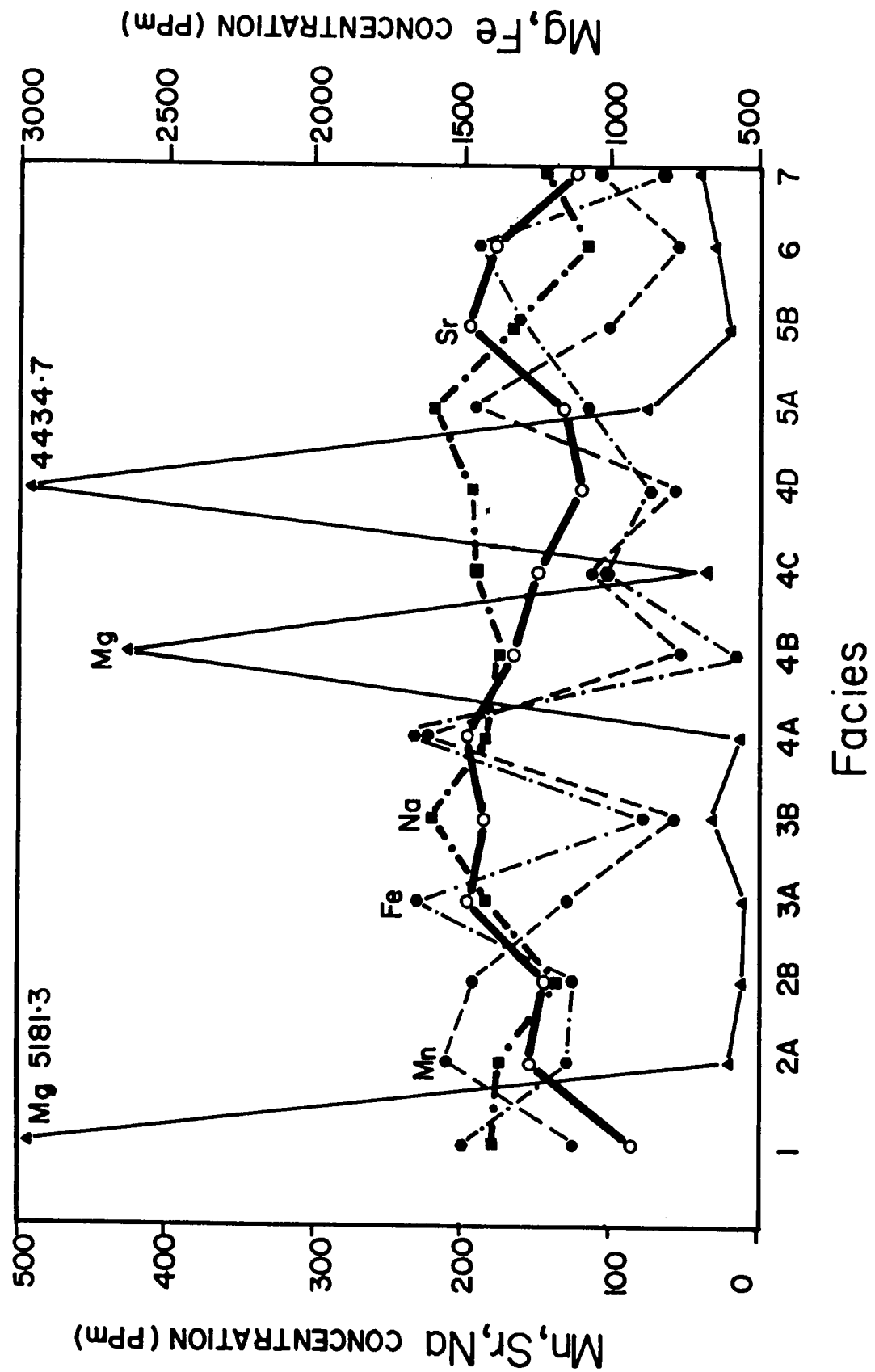

Mn, Sr, Na CONCENTRATION (PPm)
Mg, Fe CONCENTRATION (PPm)
Mg 5181·3
4434·7
Mn
Fe
Na
Mg
Sr
Facies
1
2A
2B
3A
3B
4A
4B
4C
4D
5A
5B
6
7

Figure 3.1.

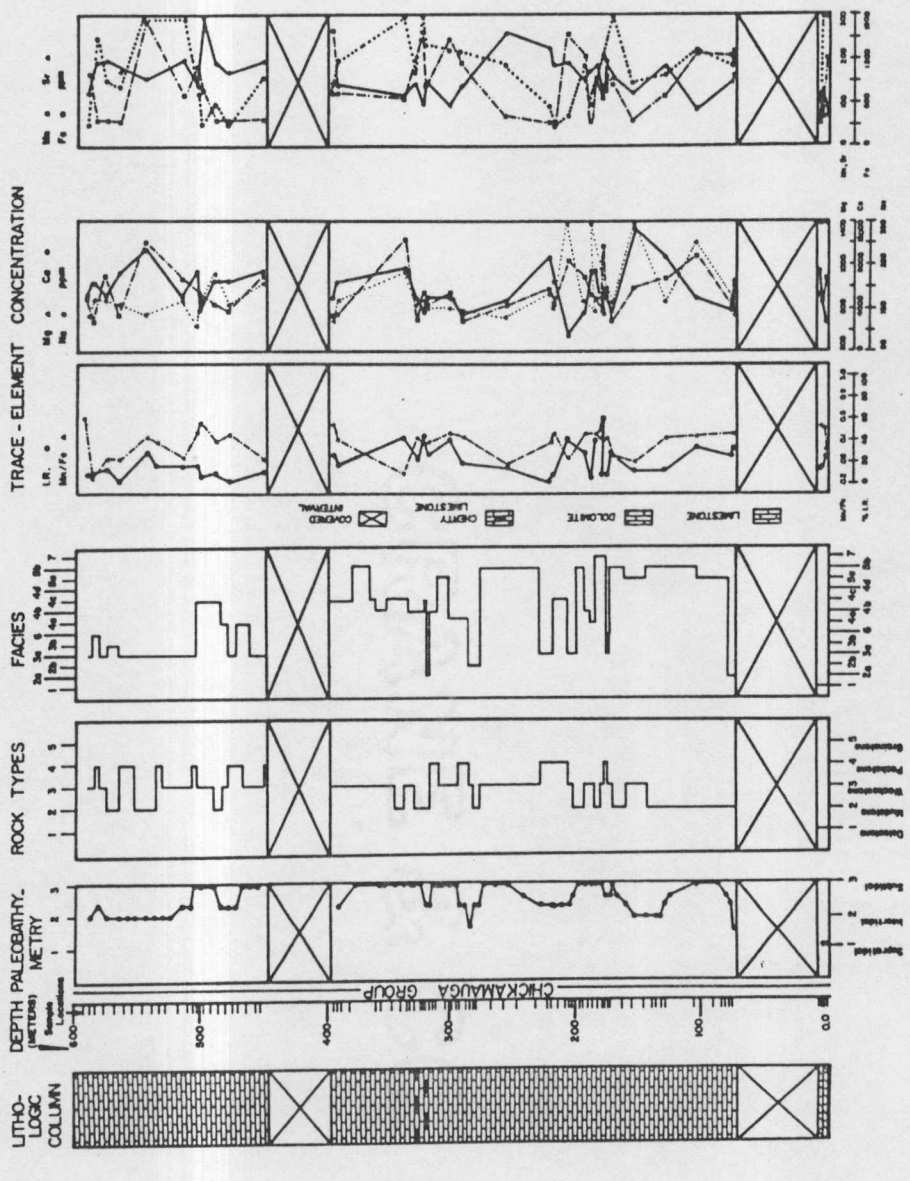


Figure 3.2. Analytical results (trace elements concentration), Mn/Fe ratio, rock types, facies distribution and paleobathymetric curve for samples from Center Point section.

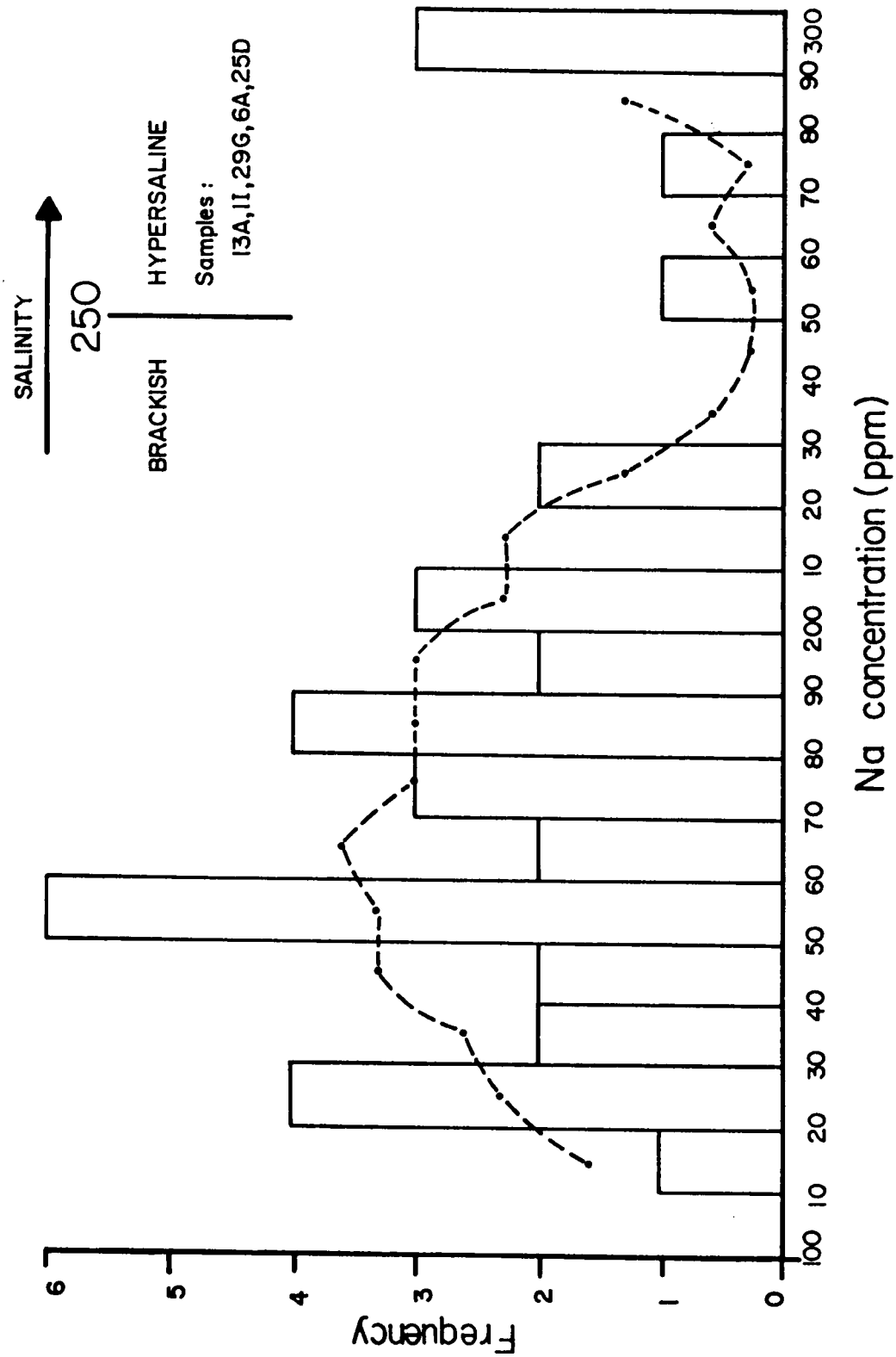


Figure 3.3. Frequency distribution of Na concentration in samples from the Center Point stratigraphic section showing brackish and hypersaline divisions based on Na values (dashed line represents a 3 by 3 moving average).

sodium into the skeleton is possibly controlled by the biological affinity (family, genus, species) of organisms.

The studies by Brand and Veizer (1980) and Veizer et al. (1978) of Peleozoic rocks revealed that decrease in sodium concentration was mainly due to equilibrium achievement with meteoric diagenetic environments, and that low values were a reflection of the paleosalinities of depositional and early diagenetic environments.

Sodium has also been used by other investigators to estimate paleosalinity of shale and ancient carbonate rocks of various geological ages (Spears, 1973; Fritz and Katz, 1972). Veizer et al. (1978) have stated that the stratigraphic distribution of Na in Paleozoic formations reflects a paleosalinity trend, and the boundary between normal and hypersaline environments can be placed a 230 ppm Na concentration in ancient carbonate sediments. However, this boundary is not fixed and should be adjusted according to the original variability of facies, leaching acid and its strength, variation in postdepositional history, analytical method, alumino-silicate concentration, and the type of carbonate involved. Badiozamani (1973) has also reported 100-300 ppm Na concentration for open-marine Ordovician carbonate sediment of Wisconsin.

The boundary obtained in this study for the Middle Ordovician shallow shelf carbonate sediments is placed at 250 ppm Na concentration (Fig. 3.3, Table 3.4). Higher sodium concentrations can only be seen in a small population of analyzed samples where petrological and paleontological evidence also indicates the high value to be due mainly

Table 3.4. The characters of the hypersaline samples based on Na frequency distribution and boundary assignment. These data are based on point count information.

Sample Number	Rock Types	Environments	Burrow Structures (H & V)	Quartz Silt %	Algae %	Ostracod %	Sponge Spicule %	Micrite %	Spar %	Pellets %	Dolomite %	Insoluble Residue %
13A	Silty-Micrite	Inter-tidal	--	37	--	--	--	6.0	44.0	11.60	--	38
29G	Dismic-rite	Supra-tidal	H & V	--	--	--	--	75.0	22.0	--	--	10
6A	Cherty Micrite	Subtidal Baffle zone	Abundant H & V	47.0	--	--	--	30.0	3.0	--	21.0	56.60
25D	Cherty Biomic-rite	Subtidal Baffle zone	--	22.0	--	2.50	--	35.0	29.0	2.0	--	48
1I	Red-Silty-Biomic-rite	Subtidal Restricted	H & V	28.0	6.0	2.50	--	36.0	26.0	--	--	40

to a high alumino-silicate content and diagenetic alteration, and not to a reflection of a hypersaline condition (Table 3.3, Samples: 1I, 13A.6A, 25D, 29G).

The average sodium content of samples in this study (180 ppm) is below the value cited by Veizer (1977) and Veizer et al. (1978) as indicative of hypersaline environments (230 ppm). Therefore, on this basis, the data suggest normal marine waters as the environment for deposition of these rocks. If this salinity boundary between normal and hypersaline environments is real, then it correlates well with the depositional model proposed for these sediments. According to my depositional model (Fig. 2.21, p. 111), sediments at Center Point were deposited in tidal flat-lagoonal environments with restricted water circulation and under tropical conditions, where salinity was in the brackish range (1-30 PPT).

The data do not illustrate a general trend of increasing or decreasing sodium values for supratidal to subtidal facies. However, small trends can be seen in portions of the section which are not a reflection of salinity differences. These trends may indicate the effect of other factors such as insoluble residue, clay content, degree of exposure to meteoric water, and recrystallization which have helped to deplete or enrich the sodium content of sediments.

Figure 3.4 is a plot of sodium concentration vs insoluble residue of the 38 analyzed samples. X-ray diffraction analysis of insoluble residue indicates that terrigenous clay and quartz are among the most important constituents. The adsorption effect of clay minerals is

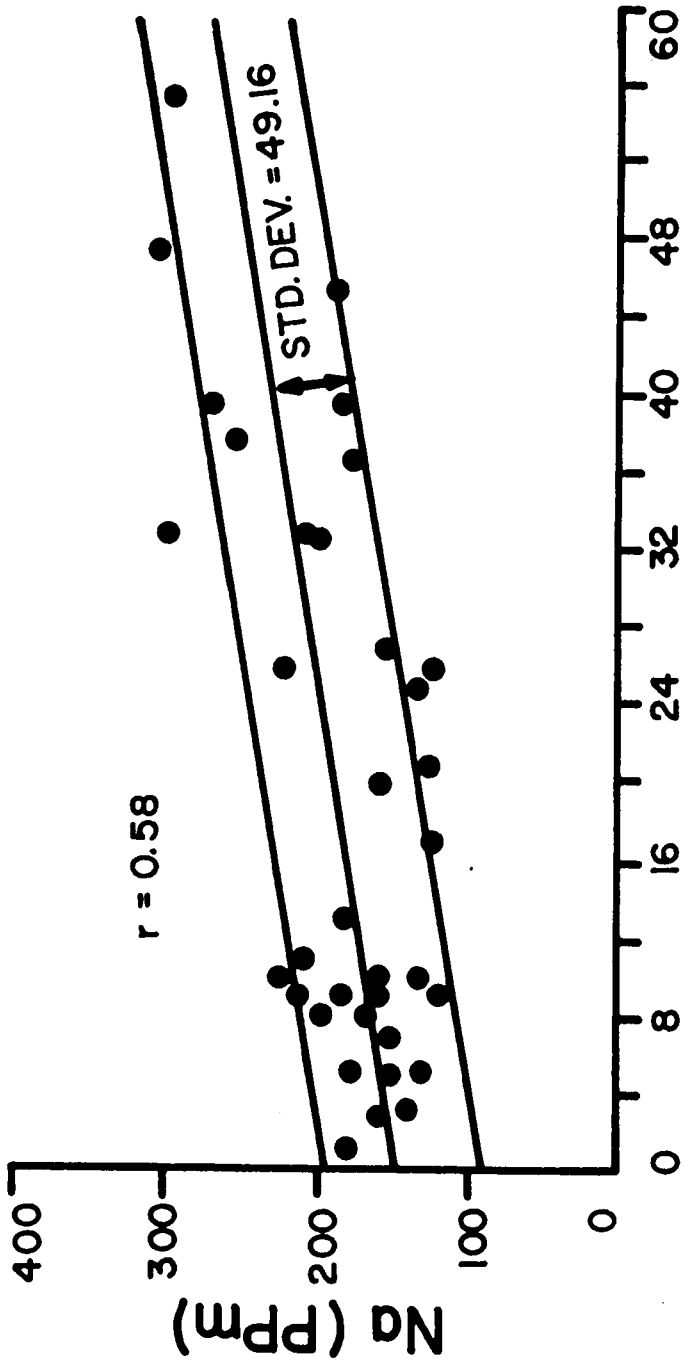


Figure 3.4. Correlation of insoluble residue (I.R.) and Na in Center Point samples; r = coefficient of correlation.

mainly responsible for the correlation of Na and I.R. with a moderate correlation coefficient value of r = 0.58. The regression line for sodium values passes through 146 ppm Na concentration with a slope of 1.95 and a standard deviation of 49. Samples with high insoluble content generally exhibit a high sodium value (Table 3.3, p. 124). This high sodium value is evidently associated with the clastic materials in the limestone.

Sodium also shows a weak correlation with Fe in the Center Point samples (Table 3.2, p. 123). This weak correlation (r = 0.44) may also be due to insoluble residue content, because Fe has also exhibited a moderate to strong correlation with I.R. (r = 0.64) and was possibly carried into the final depositional site with small particles from northwest and southeast of the study area during exposure and weathering of sediments. The relationship of Fe and I.R. will be discussed below.

Strontium

The average strontium content of all the samples of the Center Point stratigraphic section is 157.56 ppm Sr and the range is 62.5-412.5 ppm (Fig. 3.2, Table 3.3). These values are much lower than the strontium content of recent carbonate sediments.

According to studies of modern carbonate sediment (Land and Hoop, 1973; Morrow and Meyer, 1978; James et al., 1975; Land and Goreau, 1970; Pilkey et al., 1969), low magnesium calcite contains 1000 to 2000 ppm Sr, high magnesium calcite 1000 to 3000 ppm Sr, and aragonite contains 8000 to 10,000 ppm Sr. Kinsman (1969) has stated that the degree of openness or closeness of the chemical system controls the

repartitioning of strontium in ancient carbonates during recrystallization. Other studies (Veizer and Demovic, 1974; Veizer, 1977; Davies, 1972; Pingitor, 1978; Brand and Veizer, 1980, 1980) have also indicated that factors such as original mineralogy, salinity, and facies are important in controlling the strontium content in carbonate sediments. These studies have proven that the longer carbonate sediments are exposed to meteoric water, the greater the depletion of their strontium content. Therefore, the low value of strontium in Center Point samples possibly reflects the depletion of strontium from the samples as a result of exposure to meteoric water (Table 3.3, p. 124). Busch's (1968) results indicated that sediment from basinal and fore-reef environments can be easily distinguished from back-reef and lagoonal sediments, using their strontium content. The values of strontium in this study correlate well with the values given by Busch (1968) for back-reef and lagoonal sediments (100 to 400 ppm). However, studies by Veizer (1977); Bencini and Turi (1974); Veizer and Demovis (1974); Hoskin (1968); Thompson and Chow (1955) and Lowenstam (1954) indicate that the primary mineralogy and paleobathymetric position of facies also appear to be controlling factors and have a great effect on strontium distribution in sediment as a result of shallow to deep water distribution of sediments dominated by aragonite vs calcite. The strontium content in samples to correspond to the assigned facies distribution for supratidal (shallow water) to subtidal (deeper water) environments.

The most striking feature is that strontium does not show a strong positive correlation with any other element, insoluble residue, fossil types, or micrite in this study, although a very weak negative correlation of r = -0.38 exists between strontium and insoluble residue (Table 3.2, p. 123). This low correlation coefficient may be due to the fact that strontium is incorporated in aragonite and calcite phases of carbonate sediments and was expelled during diagenesis and/or aragonite to calcite transformation (Parekh et al., 1977).

The scattering of the points on Figure 3.5 may reflect the variable degree of diagenetic effects on these sediments. The negative correlation of Sr with I.R. may also indicate the slow down of carbonate production (the site of Sr fixation) into the depositional environments during times of high terrigenous input (Walker, per. comm.).

Manganese

The average Mn content of all the samples studied is 139.87 ppm. The highest concentration occurs in Sample 29G (277.77 ppm) and the lowest concentration in Sample 29J (56.50 ppm) (Fig. 3.2, p. 129). The majority of values fall within 50-160 ppm Mn with no anomalously high values. High Mn values commonly occur in samples of silty red mudstones and biomicrite, but this is not always the case. However, a high manganese content may be due to the abundance of Mn in a reducing environment. Mn, under the reducing conditions, goes into solution and can easily be substituted for Ca in the calcite structure (Lynn and Bonatti, 1965; Eaton, 1979; Davison, 1961). A reducing environment for

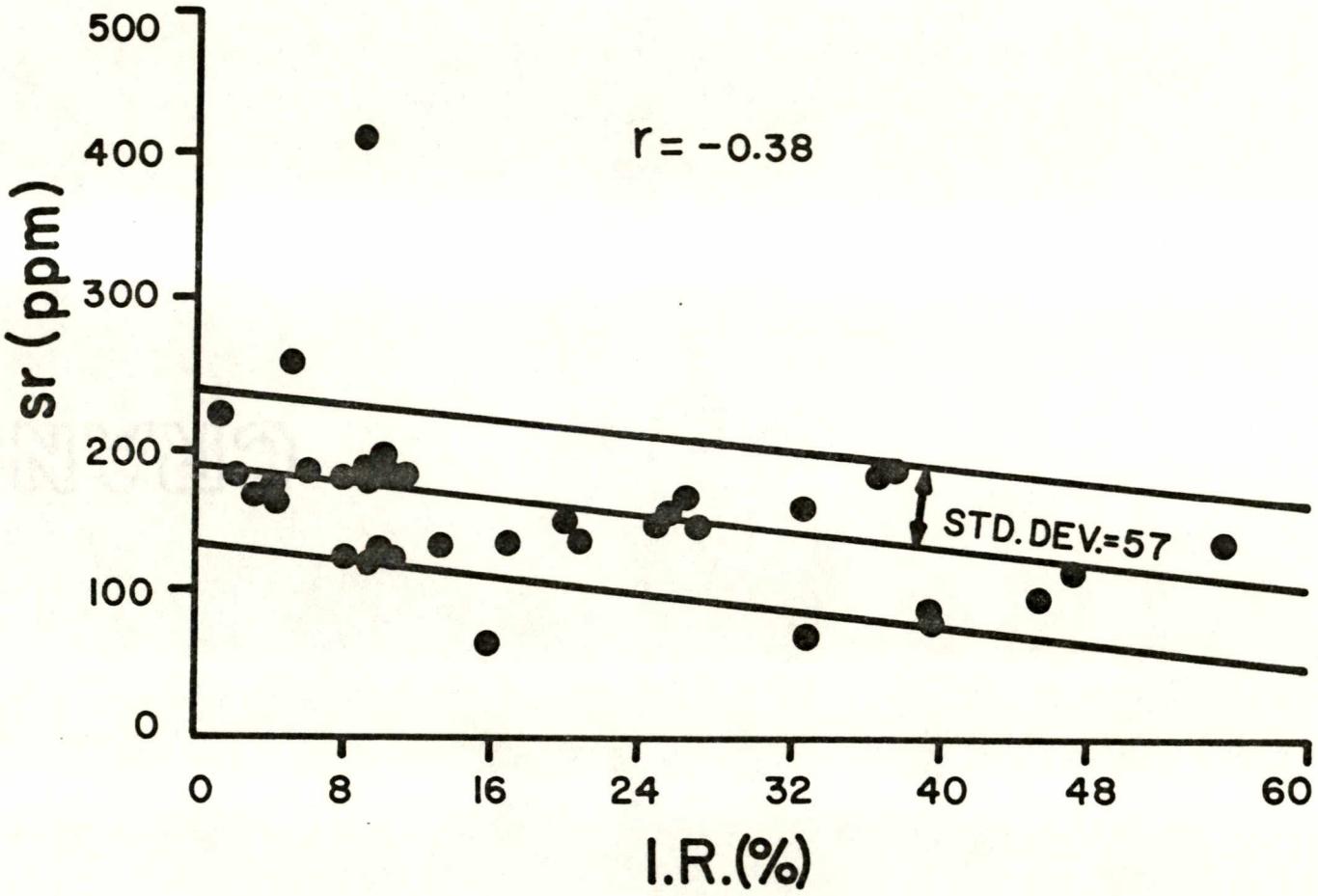


Figure 3.5. Correlation of insoluble residue (I.R.) and Sr in the Center Point samples; r = coefficient of correlation.

the samples with relatively high Mn values is also inferred from the petrographic evidence (Fig. 3.2, p. 129).

Manganese has been used extensively by various investigators as a paleobathymetric, paleoenvironmental, and diagenetic indicator. According to Bencini and Turi (1974), low Mn concentration indicates an original aragonitic mineralogy representative of shallow water, and a high Mn concentration implies an original calcite mineralogy common in deeper water and possibly more reducing conditions. The reason for this incorporation is that Mn can easily be substituted in the calcite lattice, whereas it is not easily accepted into the aragonitic lattice (Krauskopf, 1967; Kinsman, 1969). The manganese values determined in this study seem abnormally low (mean of 139 ppm) and correlate perfectly with this theory. This may be an indication of the original aragonite composition of sediments. However, Brand and Veizer 91980) have hypothesized that diagenetic equilibration (postdepositional alteration) of carbonate sediment as a result of exposure to meteoric water can lead to an increase or decrease in manganese concentration. The low values obtained here may indicate that manganese is partially controlled by exposure of sediments to meteoric water.

Manganese shows a strong positive correlation with insoluble residue ($r = 0.679$), suggesting that its concentration is probably partially controlled by insoluble residue concentration in the sediment (Fig. 3.6). Manganese fixation in the sediment can take place in various forms. It is easily substituted for calcium, iron, and magnesium in carbonates to form Mg (CO_3) (Rhodochrosite), Ca (Mn, Fe,

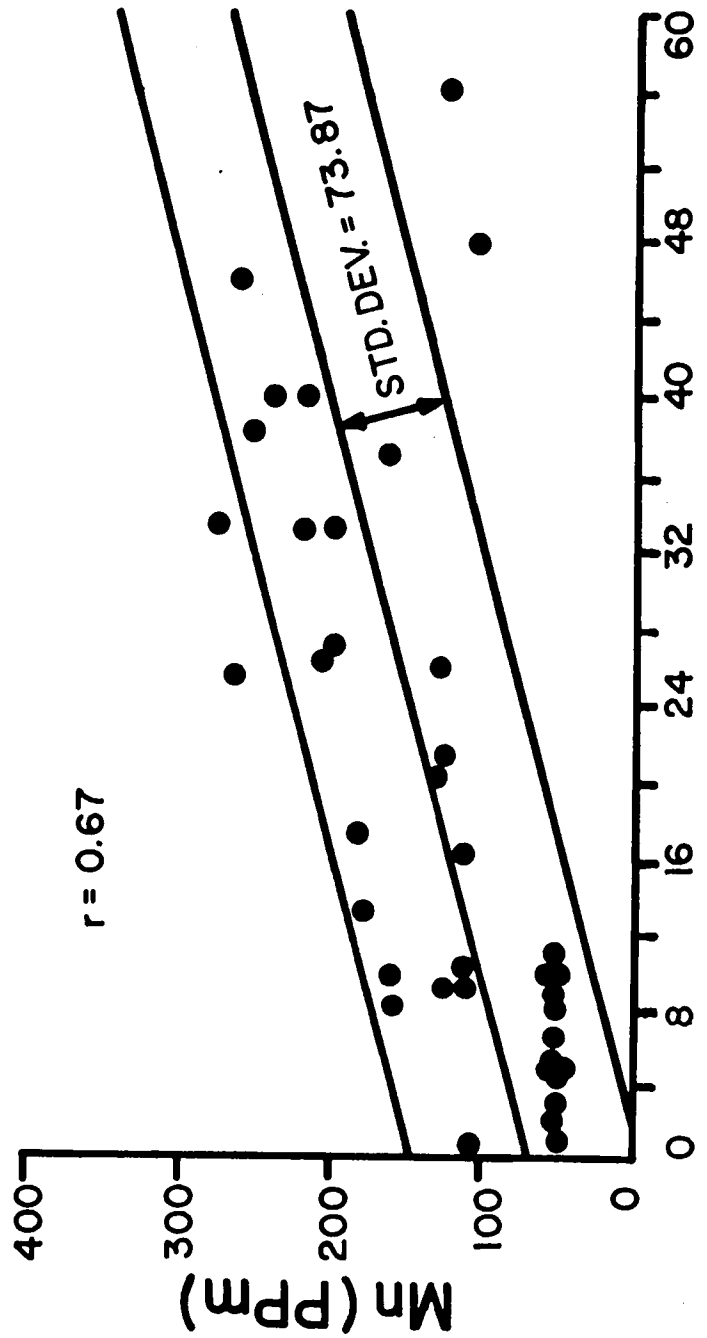


Figure 3.6. Correlation of insoluble residue (I.R.) and Mn in Center Point samples; r = coefficient of correlation.

Mg) (CO_3) (Ankerite) and CaMn (CO_3) (Kutnahorite). For 38 samples analyzed in this study (Table 3.2, p. 123), manganese shows a moderate positive correlation with Fe (r = 0.49), a weak negative correlation with Sr (r = -0.30), and a moderate positive correlation with fossil content (r = 0.43). This positive correlation with Fe and the negative correlation with Sr possibly indicates its presence in carbonate minerals. The positive moderate correlation with fossil content may reflect the original mineralogy of the skeletal material into which manganese has been incorporated (Correns, 1941).

Figure 3.2 (p. 129) also exhibits the Mn/Fe ratios plotted in stratigraphic sequence for Center Point samples. The average Mn/Fe ratio for all the samples studied is 0.154 (Table 3.5). This relatively high ratio probably reflects the presence of manganese bearing carbonate minerals in the samples studied. The high Mn/Fe ratios have also been attributed to the ease of substitution of Mn for Ca instead of Fe in the calcite lattice, because of the similar radius of the two former ions (Rankama and Sahama, 1950).

Iron

The average iron content in Center Point samples is 165 ppm, while the range obtained is from 294 to 4000 ppm.

The correlation coefficient for all of the samples shows Fe to have a significantly positive correlation with insoluble residue (r = 0.60, Fig. 3.7). Iron also shows a weak to moderate positive correlation with sodium (r = 0.44), weak positive correlation with magnesium (r = 0.39), moderate positive correlation with manganese

Table 3.5. Percentages and average of insoluble residue and Mn/Fe ratio of samples of Center Point section.

Facies	Sample Number	Ins. Residue (%)	Mn/Fe Ratio
1	1A	33.30	0.083
	1B	10.60	0.312
	1C	16.0	0.357
2a	1D	33.30	0.183
	1E	27.30	0.184
2b	18A	17.30	0.143
	27R	25.30	0.373
	23A	20.0	0.098
3a	6_1A	8.0	0.139
	13A	38.0	0.063
	15A	1.30	0.094
	28A	11.30	0.061
	28F	3.30	0.184
	29C	10.0	0.066
	29G	33.30	0.110
	29J	4.60	0.060
	31	9.30	0.550
3b	29K	10.60	0.063
4a	$20A_2$	40.0	0.181
	$24A_1$	46.0	0.088
	29A	13.30	0.252
4b	10A	4.60	0.094
4c	11A	26.60	0.190
	14A	2.60	0.200
	25A	21.30	0.126
	26F	10.0	0.010
4c	28H	6.60	0.096
	29	9.30	0.425
4d	5_1B	8.0	0.064
5a	1I	40.0	0.165
	9A	37.30	0.195
5b	3A	9.30	0.115
	5B	26.60	0.076
	16C	5.30	0.051
6	30	9.30	0.036
4c	6A	56.60	0.101
7	7A	0.60	0.134
4c	25D	48.0	0.039
Average		19.318	0.154

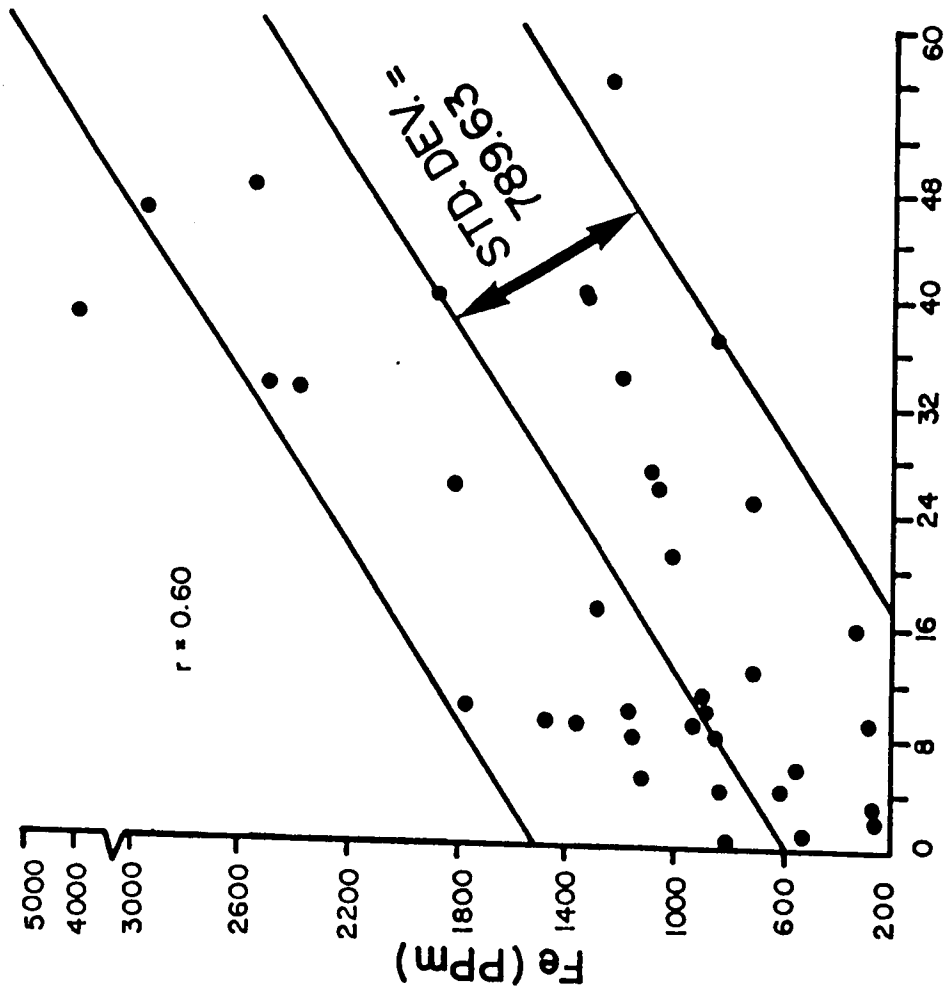


Figure 3.7. Correlation of insoluble residue (I.R.) and Fe in Center Point samples; r = coefficient of correlation.

(r = 0.49), and a weak negative correlation with fossil content (r = -0.40) (Table 3.2, p. 123). Much of the iron entering into the depositional basin may have been carried with clay and been in colloidal form in suspension, and later incorporated into the sediment. A certain amount of iron may have also been held by organic complexes in the sediment. Iron content in recent sediment is found to exist in complexes, mainly with organic matter (Baasbecking et al., 1960).

Experimental studies have also shown that sulphate reducing environments promote the formation of such complexes. Therefore, it is possible that some of the Center Point samples with high Fe concentration are due to deposition under reducing conditions where organic content was high (Fig. 3.2, p. 129).

The moderate positive correlation between iron and manganese (r = 0.49) may also indicate reducing environmental conditions because these two elements have a similar chemistry and both are mobile under these conditions. However, some other factor such as pH-Eh may also be responsible for their behavior and distribution in the sediment (Mason, 1966; Krumbein and Garrels, 1952; Ronov and Ermiskina, 1959; Urban, 1960). The weak to moderate positive correlation between iron and sodium (r = 0.40), iron and Mn (r = 0.49) and a strong positive correlation with insoluble residue (r = 0.66) may be thought to be due to the occurrence of these elements in the detrital portion of the sediment. However, because iron is present in two oxidation states and is highly reactive, it is very difficult to separate the causes and to

explain its behavior under depositional or diagenetic environmental conditions (Gavish and Friedman, 1969).

Iron and manganese have also been used by various investigators as paleobathymetric indicators (Frieman, 1969; Bencini and Turi, 1974). In this study, iron does not show an apparent increasing or decreasing trend from supratidal to subtidal facies. However, a small increasing trend can be seen from facies 4b to facies 7 (Fig. 3.1, p. 127) where water depths were greater and where there may have been reducing conditions. Also Fe and Mn can be easily incorporated into the calcite lattice due to their ionic radius and valances. Therefore, based on a general bathymetric distribution of aragonite and calcite it could be proper to propose that the small trend observed in this study may have been partially due to a mineralogical-bathymetric control. In general, fresh water contains more soluble Fe and Mn than marine water (Durum and Haffty, 1961; Ungar and Alde, 1962). Therefore, more iron and manganese is available for uptake by organisms (Friedman, 1969). Figure 3.8 demonstrates a plot of iron vs manganese content in samples from Center Point. In this figure there are there distinct groups of samples indicating the differences in the Fe and Mn concentration in carbonate sediments of various facies. Group A, which represents open-marine conditions based on petrographic evidence, has low Mn and relatively high Fe content. Group B has a wide variation in both Mn and Fe distribution, reflecting variation in the characteristic of the facies (see Chapter II) and probably the greater effect of various parameters other than bathymetry and mineralogy on concentration of

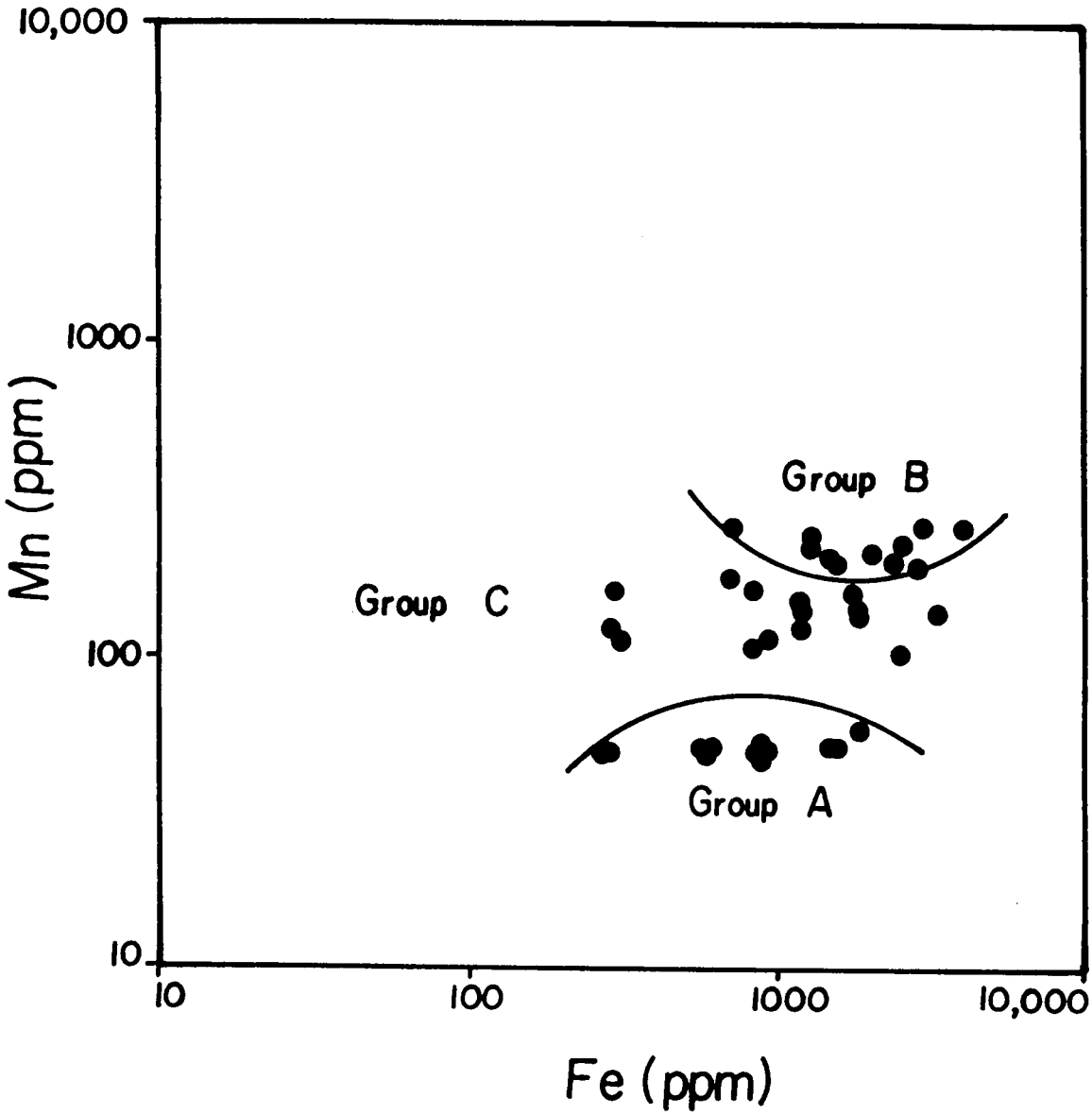


Figure 3.8. Fe vs Mn for Center Point section.

these elements. Group C is transitional where values of Mn and Fe fall between values of Group A and Group B samples.

Magnesium

An average of 1320.55 ppm and a range from 415.38 to 6580.65 ppm magnesium were found for the Center Point samples (Table 3.3, p. 124). Magnesium occurs mainly in the mineral dolomite as is shown by the close correlation of the Mg content with petrographic evidence of samples which show high dolomite percentages (Table 3.6).

Magnesium shows no strong correlation with any other element, fossil content, insoluble residue (Fig. 3.9), spar or micrite (Table 3.2, p. 123). However, a weak positive correlation ($r = 0.39$) exists between magnesium and iron. The lack of strong correlation with Fe or any other element for all the samples analyzed may indicate that the bulk of the magnesium in the samples is associated with "primary dolomite," dolomitized sediment, stylolitized sediment, and samples with high terrigenous clastic content (terrigenous clay and quartz silt). However, Figure 3.9 (Mg vs I.R.) shows two populations of samples. The first group only with six samples (Samples 1A, 1B, 1C, 13A, 10A, and 5-1B), indicating a high correlation coefficient ($r = 0.9$). The second group, where majority of samples belong to, indicate a low correlation coefficient ($r = 0.12$).

The overall magnesium content of samples in this study is very low in comparison to the available published data for recent and ancient sediment, indicating a possible leaching of carbonate minerals. According to Gavish and Friedman (1969) and Brand and Veizer (1980),

Table 3.6. Mg content based on atomic absoprtion values, and dolomite percentages based on point count data, in Center Point section.

Sample No.	Mg Content (ppm)	Dolomite (%)
1A	6120.00	74.90
1B	4567.16	44.47
1C	4857.14	46.28
1D	540	1.57
1E	660.55	0.0
18A	580.64	0.0
27R	482.14	0.0
23A	615.38	0.0
6A	553.84	0.0
13A	6580.64	0.0
15A	729.72	
28A	812.03	8.67
28F	620.68	0.0
29C	666.66	0.0
29G	540	
29J	629.37	11.20
31	529.41	0.0
29K	671.64	0.0
20A	600	0.0
24A	666.66	0.0
29A	415.38	0.0
10A	2643.35	7.54
11A	654.54	4.87
14A	616.43	1.15
25A	610.16	0.0
26F	666.66	0.0
28H	900	0.28
29	661.76	0.0
5-1A	4434.78	17.25
1I	1200	0.0
9A	574.46	0.28
3A	661.76	0.0
5B	654.54	0.0
16C	507.04	12.0
30	661.76	6.31
6-1A	782.60	0.0
7A	604.02	0.0
25D	923.07	0.0

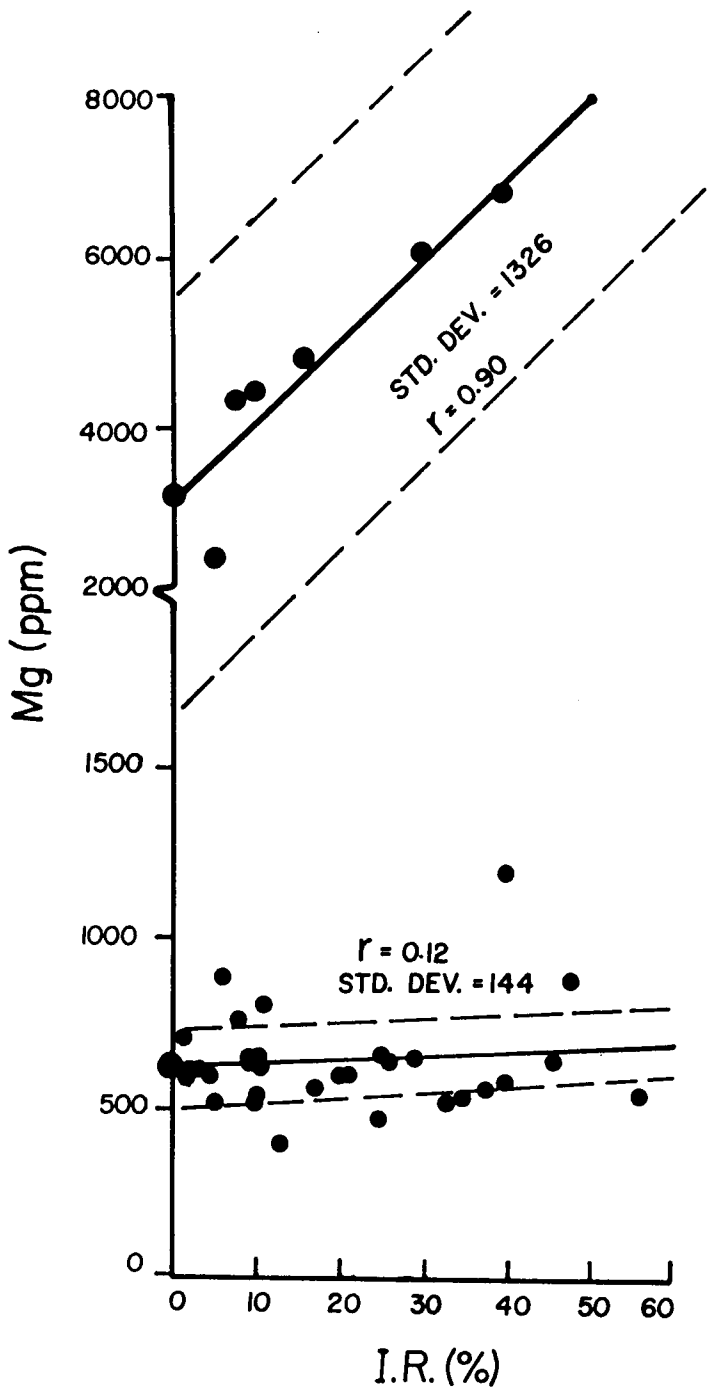


Figure 3.9. Correlation of insoluble residue (I.R.) and Mg in Center Point samples. R = coefficient of correlation. Note break in ordinate axis at 2000 ppm and the change in the scale of that axis above that value.

magnesium content of organisms skeletons varies among different biological groups. Therefore, high magnesium calcite and aragonite skeletons lose magnesium very quickly during conversion of high magnesium calcite to low magnesium calcite and transformation of aragonite to calcite. In this study, petrographic evidence (Appendix B) provides information to prove that high percentages of the fossil groups in the samples were originally of high magnesium calcite or aragonitic compositions (echinoderms, ostracodes, gastropods and pelecypods). Thus, Mg content of samples was likely much higher originally and the loss is due to diagenetic removal. Brand and Veizer (1980) have also stated that low magnesium carbonate sediments lose their magnesium content during exposure to meteoric water and subsequently exhibit a very low value. In this study there is evidence, such as presence of altered fossil grains with original high magnesium calcite composition, to indicate that this theory is applicable to these rocks.

The magnesium values plotted stratigraphically on Figure 3.2 (p. 129) vary considerably, but they do not show a trend for the section as a whole or from supratidal to subtidal facies (Fig. 3.1, p. 127). There are only three anamolously high sets of values observed in facies 1, 4b, and 4d (Fig. 3.1) which are due to "primary dolomite" formation, stylolitization and, perhaps, later dolomitization of samples within these facies.

Calcium

Calcium abundance is due mainly to its presence in the carbonate fraction of the samples. The Center POint samples have an average of 526,196 ppm and a range from 123,843 to 972,000 ppm calcium. Since calcium has a very high concentration in he samples and was not analyzed with the atomic spectrometry technique (titration method was applied), for uniformity of method and accuracy of data, it was not treated in the statistical analysis. Therefore, no correlation coefficient values have been obtained, and no comparison or interpretation was made with respect to its concentration and relationship to any other element, fossil content, spar, micrite or insoluble residue. Table 3.3 (p. 124) illustrates the concentration of calcium in all samples of the Center Point stratigraphic section.

Factor Analysis

Factor analysis is a statistical technique which when applied to a large number of variables, relates these variables to a smaller group of "new" variables or simply, factors. The distribution of these variables (trace elements, fossils, micrite, spar and insoluble residue) in the sediment can be assumed to be controlled by certain parameters or factors (depositional environments, diagenetic process, Eh-pH, original mineralogy). The relationships among these variables can be governed by either one or many factors. However, the most common application of factor analysis is to reduce the data for a better understanding of the relationship between variables and the

governing factors. It also helps to detect patterns of variable distribution and to discover new concepts (Kin, 1975).

In spite of the fact that a large number of methods of factoring are available, the principal component factoring method with interaction (PA2) is the most widely accepted one. Also, to achieve a meaningful patterning of variables and to simplify the extracted factors, rotation methods are applied to the initial factors. In this study orthogonal rotation (varimax), the most commonly accepted method, is used because it simplifies the columns of a factor matrix (Kim, 1975). Mathematical techniques, details, concepts, and procedures are described by Davies (1973), Kim (1975) and Cattell (1965a, 1965b). Also, examples of the use of factor analysis in geochemistry are given in papers by Spencer (1966) and Brand and Veizer (1980).

Table 3.7 illustrates the results of the factor loading of the elements for four factors where they explain 100.0% of the variation for all the samples. Appendix E shows the two dimensional diagrams of trace elements in relation to varimax rotation factors. Element loading of less than 0.4 is assumed to be insignificant because of the significant sample levels which fall below 80% (Kim, 1975). The communality values ("the amount of the variance of a variable that is shared by at least one other variable in the set"; Kim, 1975) of variables varies from 0.98120 for insoluble residue to 0.17368 for strontium (Table 3.7). These values indicate that the greater amount of variation of strontium is not shared by any other variable, whereas insoluble residue shared almost its total variation with other

Table 3.7. Varimax rotated factor matrix for 38 selected samples of Center Point sections.

Variable	Communality	Factor 1	Factor 2	Factor 3	Factor 4
Na	0.34046	0.56699	-0.01856	-0.09651	0.096654
Mg	0.79806	0.12260	0.11193	0.02808	0.87733
Fe	0.60799	0.60751	0.35251	0.18333	0.28469
Mn	0.58962	0.63001	0.41687	0.10089	-0.09358
Sr	0.17368	-0.34638	-0.04652	0.02174	-0.22598
I.R.	0.98120	0.98423	0.10698	-0.01810	-0.02701
Fossils	0.69344	-0.15945	-0.80075	-0.03468	-0.16002
Micrite	0.74528	0.01691	0.42438	-0.67539	-0.32975
Spar	0.72673	-0.02327	0.22643	0.81415	-0.10993

Note: Factor 1: Eigenvalue = 2.69343; Variance Accounted for = 47.6%; Cumulative Variance Accounted for = 47.6%.
Factor 2: Eigenvalue = 1.26728; Variance Accounted for = 22.4%; Cumulative Variance Accounted for = 70.0%.
Factor 3: Eigenvalue = 0.89907; Variance Accounted for = 15.9%; Cumulative Variance Accounted for = 85.9%.
Factor 4: Eigenvalue = 0.79669; Variance Accounted for = 14.1%; Cumulative Variance Accounted for = 100.0%.

variables (variation of insoluble residue is almost 1.0 or 100.0%).

Factor 1 accounted for 47.6% of the total variation in the variables used in the analysis and has a positive loading for sodium (0.56699), Fe (0.60751), Mn (0.63001) and insoluble residue (0.98423). This positive loading can be assumed to represent the detrital mineral contribution and, by a small fraction, leaching of the elements from insoluble residues during acid digestion of the samples.

Factor 2, which accounted for 22.4% of the variation, has a positive loading for Mn (0.41687), micrite (0.42438) and a negative loading for fossils (-0.80075). This factor probably represents the environmental conditions (temperature, salinity, turbulence) which govern the chemical precipitation of manganese and the negative loading relationship between fossil content and micrite. Based on petrographic analysis (Chapter II), these sediments were deposited in semiprotected environments which favored lime mud deposition. Therefore, the positive correlation between Mn and micrite may indicate that manganese in its reduced state favors substitution in calcite where lime mud is abundant.

Factor 3 has a positive loading for spar and a negative loading for micrite. This factor has some features in common with the negative aspect (loading) of factor 2 and represents the predominant control of the environmental conditions over this factor. The negative loading relationship can be easily seen petrographically in samples from Center Point stratigraphic section (see Appendix B). This phenomenon has been noted in the literature by various investigators (Dunham, 1962;

Ginsburg, 1956; Shinn, 1968) who say that a direct relationship exists between energy of the environment and the amount of mud which accumulates there. Therefore, most of this factor is controlled by energy of the depositional environment where low energy favors accumulation of mud and high energy favors removal of mud from the sediment and subsequent precipitation of spar. Factor 3 only accounts for 15.9% of the total variance (Table 3.7).

The last important factor, factor 4, accounted for 4.1% of the variation in the trace elements, fossils, spar, micrite and insoluble residue content of Center Point samples and consists principally of a high positive loading for magnesium (Table 3.7). "Primary dolomite," dolomitization, and stylolitization account for magnesium's high positive loading.

Because of the high Ca concentration in the sediment and application of different methods for calculation of calcium concentration, no calcium values were used in the statistical analysis. The data thus do not show the probably inverse relationship between calcium and magnesium which may also provide evidence in support of the dolomitization control on this factor as was predicted from petrographic studies. However, to further support this theory, no positive or negative loading was observed in the previous factors. Therefore, it indicates that a majority of magnesium must have been supplied through the dolomitization and stylolitization processes and was not carried into the depositional environment by detrital minerals (insoluble residue).

Discrimination Function Analysis

Discriminant function analysis has been used in geology, mathematics, ecology, and other fields to differentiate groups of samples on the basis of two or more measured properties. This method can also compute statistically the probability of an unknown or unidentified sample, and place it in the right group. Property measurement has been done in such a way that all properties have been considered together in the best possible way to discriminate the various groups of samples. Therefore, based on measured properties of the individuals that made up the groups, this information can be used to determine whether groups of preselected individuals are statistically different or not. Details of methods, procedures and mathematical principles are described by Krumbein and Graybill (1965) and Klovan and Billing (1967).

In this study, geochemical data (trace elements: Sr, Mg, Mn, Na, Fe and insoluble residue) were used to compute whether samples of the Center Point section can be statistically distinguished and separated into different groups. Discriminant "scores" (in this study posterior probability of membership of groups) were calculated for all samples of the Center Point section and were used to predict into which of the two groups (group 0: less restricted environment having access to open-marine conditions; and group 1: more restricted-lagoonal environment) these samples would be classified (Tables 3.8-3.10). Two discriminant function analyses were calculated in this study. The firs analysis was calculated on the basis of manganese, strontium, and insoluble residue

Table 3.8. Discriminant function analysis grouping of samples based on three parameters; insoluble residue, manganese, and strontium. Note samples with star indicate misclassified observation.

Sample No.	From Group	Classified into Group	Posterior Probability of Membership in Groups	
			G-0	G-1
5-1B	0	0	0.6236	0.3764
30	0	0	0.8093	0.1907
29C	0	0	0.4568	0.5432
29J	0	0	0.8404	0.1596
6-1A	0	1*	0.2107	0.7893
28H	0	0	0.8232	0.1768
28F	0	0	0.8459	0.1541
3A	0	0	0.4879	0.5121
16C	0	0	0.8633	0.1367
10A	0	0	0.8359	0.1641
29K	0	0	0.7974	0.2026
28A	0	0	0.7955	0.2045
14A	0	0	0.8436	0.1564
27R	1	1	0.0077	0.9923
1E	1	1	0.0379	0.9621
24A-1	1	1	0.0031	0.9969
5B	1	1	0.3003	0.6997
9A	1	1	0.0749	0.9251
25A	1	1	0.2480	0.7520
18A	1	1	0.0773	0.9227
1D	1	1	0.0202	0.9798
20A-2	1	1	0.0066	0.9934
1I	1	1	0.0110	0.9890
1B	1	0*	0.7410	0.2590
29	1	1	0.6591	0.3409
26F	1	1	0.3778	0.6222
15A	1	1	018843	0.1157
1C	1	1	0.2908	0.7092
31	1	1	0.1572	0.8428
6A	1	1	0.0877	0.9123
29A	1	1	0.1014	0.8986
11A	1	1	0.0338	0.9662
7A	1	0*	0.5166	0.4834
1A	1	1	0.0231	0.9769
23A	1	1	0.2300	0.7700
25D	1	1	0.1768	0.8232
13A	1	1	0.0080	0.9920
29G	1	1	0.0044	0.9956

Table 3.9. Discriminant function analysis grouping of samples based on six parameters; insoluble residue, manganese, strontium, sodium, magnesium, and iron. Note samples with star indicate misclassified observations.

Sample No.	From Group	Classified into Group	Posterior Probability of Membership in Groups	
			G-0	G-1
5-1B	1	1	0.1930	0.8070
30	1	1	0.0003	0.9997
29C	0	0	0.7792	0.2208
29J	0	0	0.7806	0.2194
6-1A	0	0	0.7355	0.2645
28H	1	1	0.0015	0.9985
28F	0	0	0.6735	0.3265
3A	0	0	0.7037	0.2963
16C	1	1	0.0101	0.9899
10A	1	1	0.1397	0.8603
29K	1	1	0.2778	0.7222
28A	0	0	0.7365	0.2635
14A	1	1	0.0186	0.9814
27R	1	1	0.0066	0.9934
1E	1	1	0.2330	0.7670
24A-1	0	0	0.7580	0.2420
5B	1	1	0.0438	0.9562
9A	1	1	0.2165	0.7835
25A	1	0*	0.7374	0.2626
18A	1	1	0.1807	0.8193
1D	1	1	0.0354	0.9646
20A-2	1	1	0.1577	0.8423
1I	0	0	0.8062	0.1938
1B	1	1	0.0055	0.9945
29	1	1	0.0025	0.9975
26F	1	1	0.0031	0.9969
15A	1	0*	0.7249	0.2751
1C	1	1	0.2517	0.7483
31	1	1	0.1812	0.8188
6A	1	1	0.0585	0.9415
29A	1	1	0.2047	0.7953
11A	1	1	0.0252	0.9748
7A	0	0	0.8213	0.1787
1A	1	1	0.0129	0.9871
23A	1	1	0.0014	0.9986
25D	1	1	0.1271	0.8729
13A	0	0	0.7416	0.2584
29G	1	1	0.0011	0.9989

Table 3.10. Grouping of samples, using three and six parameters for discriminant function analysis, and grouping based on Mn-Fe plot. Note: Underlined samples are classified into the same group by at least two methods.

Three Parameters

Group A:
1B, 10A, 14A, 15A, 16A, 28A, 28F, 28H, 29J, 29K, 30

Group B:
1A, 1D, 1E, 1I, 11A, 13A, 20A2, 24A, 27R, 29G

Group C:
1C, 3A, 5B, 6A, 6-1A, 7A, 9A, 18A, 25D, 25A, 26F, 29A, 29C, 31

Six Parameters

Group A:
1I, 3A, 6-1A, 7A, 13A, 15A, 24A, 25A, 28A, 28F, 29C, 29J

Group B:
1A, 1B, 1D, 5B, 6A, 11A, 14A, 16C, 23A, 26F, 27R, 28H, 29, 29G, 30

Group C:
1C, 1E, 5-1B, 9A, 10A, 18A, 20A2, 25D, 29K, 31

Mn-Fe Plot

Group A:
1B, 5-1B, 14A, 15A, 16C, 28A, 28F, 28H, 29K, 29J, 30, 10A

Group B:
1A, 1D, 1E, 1I, 11A, 13A, 20A2, 24A, 27R, 29G

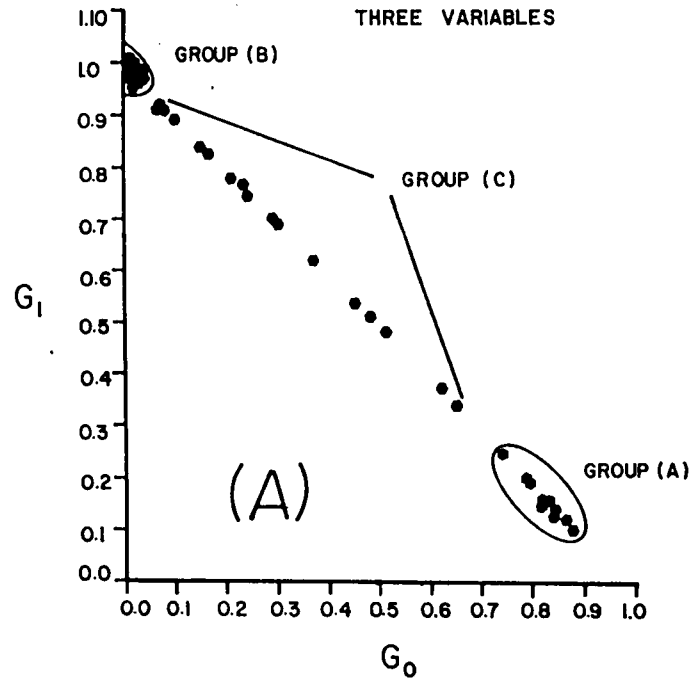
Group C:
1C, 3A, 5B, 6A, 6-1A, 7A, 9A, 18A, 23A, 25A, 25D, 26F, 29A, 29, 29C, 31

---

content and the second analysis used six parameters; strontium, sodium, manganese, iron, magnesium, and insoluble residue. Figure 3.10A and B show the distribution of the samples based on discriminant "scores" for the samples.

Figure 3.10A illustrates that on the basis of three parameters (Mn, Sr, I.R.), samples can be classified into three groups: (1) less restricted open-marine samples (Group A), (2) very restricted lagoonal samples (Group B), and (3) transitional-lagoonal samples (Group C). This grouping also corresponds to the grouping of samples based on the Mn/Fe plot (Fig. 3.8, p. 146, and Table 3.10) and petrographic classification of samples (Figs. 2.15 through 2.18, pp. 100-103).

One of the reasons for the grouping of samples in the first analysis (using three parameters) is that Mn and I.R. have a high correlation coefficient value ($r = 0.60$). Therefore, as already stated in the trace element data section, Mn distribution in the sediments is controlled by detrital mineral contribution, whereas Sr concentration has a negative correlation coefficient with insoluble residue and its distribution is not controlled by insoluble residue. Also, detrital mineral influx into the shallow water environment where calcium carbonate is forming, could slow down carbonate production (see Walker, Shanmugam, and Ruppel, 1983). Thus, negative correlation between production of calcium carbonate and detrital minerals is present. However, in the absence of carbonate production (aragonite) in shallow water strontium which favors substitution in the aragonite lattice, would be very low in the sediments and such samples represent a



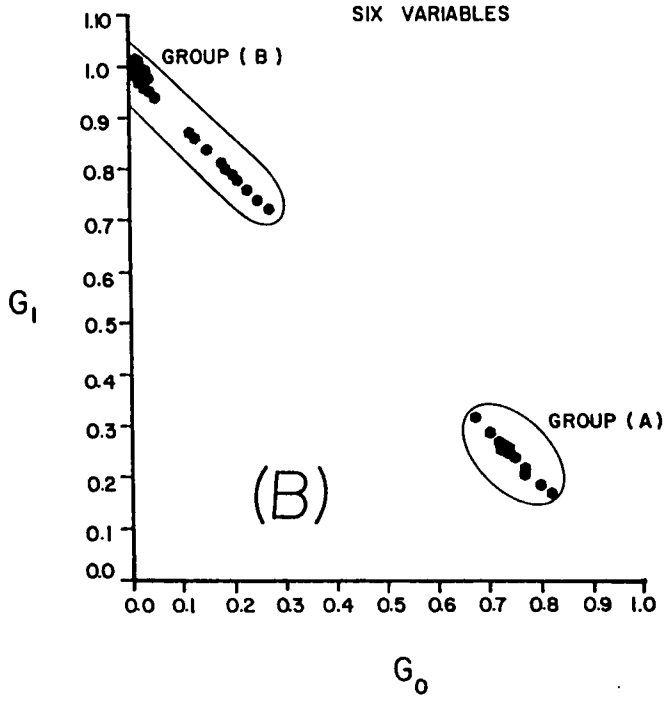


Figure 3.10. Grouping of samples from Center Point section based on three (A) and six (B) parameters, using discriminant function analysis. G_0 and G_1 are two major groupings of samples which show probability of membership of samples in each group.

distinct group which characterized periods of detrital mineral influx into the environment.

However, Figure 3.10B (using six parameters) suggests that samples from Center Point can be divided into three distinct groups which are partially correlated with the previous group assignments on Figure 3.10A and which also match with the Mn/Fe plot (Fig. 3.8, p. 146) and petrographic data. This result is slightly different from that arrived at previously by using three parameters. In this study, discriminant function analysis (using six parameters) simply demonstrates that the grouping of samples, at least in part, is not controlled by one factor as observed in Figure 3.10A; instead, several factors or parameters have been combined to result in the grouping observed in Figure 3.10B. Noteworthy is the fact that the majority of the samples in Groups A, B, and C on Figure 3.10B fall within the same groups in Figure 3.10A and the Mn/Fe plot of Figure 3.8 (Table 3.10). Thus, according to the discriminant function analysis in the study, groupings of samples can be classified statistically, but the process requires a large number of parameters as observed in Figure 3.10A and B.

Summary and Conclusions

Based on the geochemical and petrographical data derived from samples of the Center Point stratigraphic section, the following tentative conclusions concerning the chemical conditions responsible for the concentration of trace elements in the sediment can be proposed:

1. Petrographic information is useful as a supplement to the geochemical data for the best possible interpretation of the processes responsible for the concentration of trace elements in the carbonate sediments.
2. Correlation coefficient results in this study indicate that the concentrations of Na, Mn, and Fe are controlled by detrital mineral contribution into the sedimentary environment.
3. The high magnesium content of some of the samples and the lack of correlation between Mg and any other variable is the result of dolomitization and stylolitization.
4. Trace element data in this study do not show an increasing or decreasing trend from supratidal to subtidal facies; small trends are due to minor local phenomena and cannot be used to reach any kind of geochemical conclusion.
5. Sodium values in this study have proven to be useful as paleoenvironmental indicators but should be tested with petrographic data. Na concentrations suggested brackish paleosalinity for Center Point samples.
6. Strontium values indicate that facies is the major controlling factor for its concentration. However, these values are much lower than the strontium content of recent carbonate sediments which may reflect the original mineralogy of the Ordovician sediments. Variation in the values is probably due to the

varying degree of porosity and/or exposure of sediments to the diagenetic environment.

7. The high Mn/Fe ratio represents the greater tendency and the ease of substitution of Mn rather than Fe for Ca in the rhombohedral structure of calcite.
8. According to the discriminant function analysis, samples from the Center Point section consist of at least two groups where the majority of individuals of each group are the same as the one in the Mn vs Fe plot and petrographic subdivisions of the samples.

CHAPTER IV

DIAGENESIS AND PORE SYSTEMS

Introduction

The term diagenesis as used here refers to all the changes that occur in sediments and sedimentary rocks from the time of initial burial to the time when temperature and/or pressure cause the passage of rocks into the metamorphic stage (Pray and Murray, 1965). However, the original carbonate mineralogy, sedimentary structure, texture, and porosity of these carbonate sediments have been modified by several different types of physical, chemical, and organic processes after initial deposition. Although diagenesis is extensive in some instances, the original sedimentary texture has not been greatly altered. The diagenesis of "Chickamauga Group" sediments can be divided into several distinct events which will be discussed in detail later in this chapter. Attempts have been made to present these diagenetic events in the order in which they acted upon the rocks. Unfortunately, due to the complexity of the rocks and the scarcity of actual observational data on diagenetic event sequences it is difficult to produce an accurate temporal sequence. Further, some of the processes probably occurred simultaneously making differentiation of separate processes much more difficult.

In order to define the effects of diagenesis, especially the precipitation of cements, on these Middle Ordovician carbonate sediments, the classification of Choquette and Pray (1970) for basic

porosity types was used (Fig. 4.1). They stated that the record of diagenetic events can be observed in creation, modification or occlusion of porosity, and that carbonate pore systems can be useful in interpretation of geological history and physiochemical processes of depositional environments.

The purposes of this chapter are: (1) to document the various types of diagenetic features present in the Middle Ordovician "Chickamauga Group" in the study area; (2) to consider the physical, chemical, and biological processes responsible for such modification; (3) to establish the sequence of diagenetic events (paragenesis) where possible; (4) to elucidate the environments of formation of these diagenetic features; and (5) to evaluate the role of diagenesis in controlling the porosity and possibly the reservoir characteristics of these Middle Ordovician sediments for oil and gas entrapment.

Diagenesis

Biological Diagenesis

Biological activity in the Middle Ordovician "Chickamauga Group" sediments included burrowing, boring, and micritization. In some of the carbonate sediments of the study area, bioturbation is very extensive. Some horizontal and vertical burrows have sharp and distinct boundaries, whereas others lack definite burrow walls but exhibit extensive bioturbation in the form of mottles, swirled distribution of allochems, and disrupted, indiscrete laminae (Fig. 4.2A-D). The burrow tubes are completely or partially filled, in

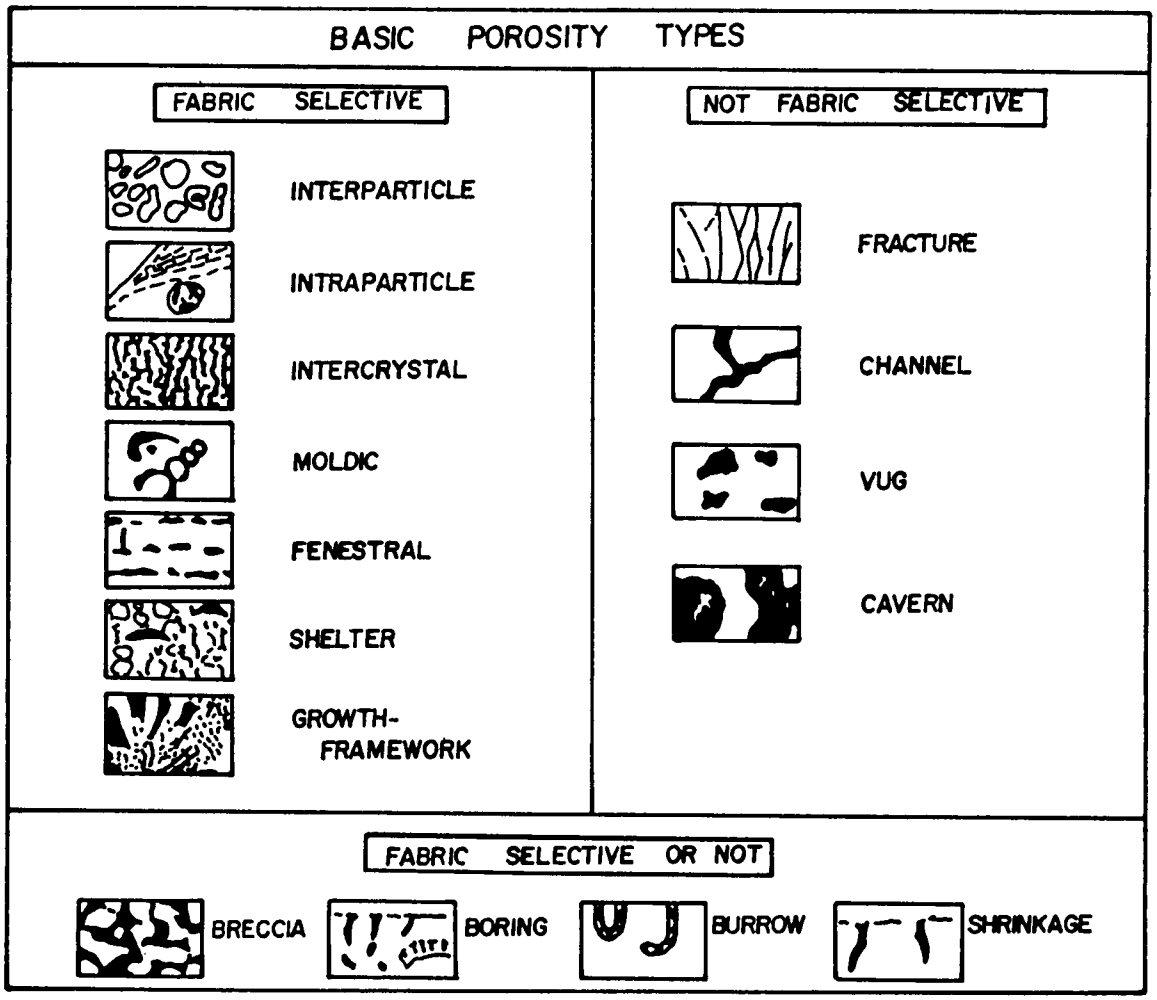


Figure 4.1. Basic porosity types in sedimentary carbonates (from Choquette and Pray, 1970).

Figure 4.2. Cementation fabrics of Middle Ordovician carbonate rocks (a).

A. Thin section negative print of sample CP27R showing burrow tube with distinct wall boundary (arrow). Bar scale is 1 cm.

B. A bioturbated mudstone. Thin section negative print of Sample B97 displays the typical mottled appearance indicative of extensive biogenic activity in the sediment. Bar scale is 5 mm.

C. Thin section negative print of Sample B2 showing evidence of biogenic activity (B) in gastropod packstone-wackestone. Note the rotated articulated brachiopod shell (arrow) with geopetal structure. Bar scale is 5 mm.

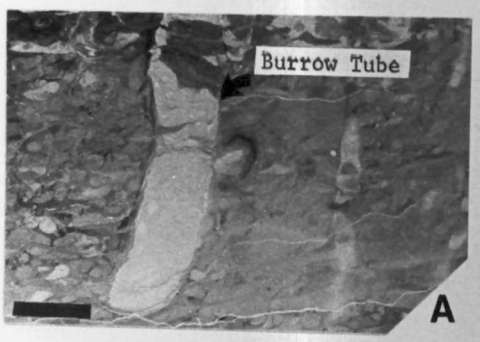
D. Thin section negative print showing the effect of bioturbation on destruction of sedimentary structures. Note the disruption of horizontal laminae on the left-hand side of slide. Bar scale is 5 mm, 9DGF.

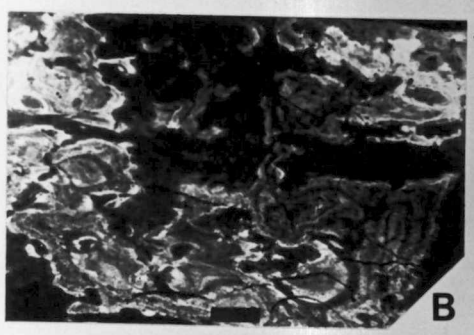
E. Photomicrograph showing a vertical burrow in bioturbated mudstone. Note the partial filling of tube by internal sediments (spar and micrite). Bar scale is 1 cm, CP1I.

F. Sharp break between two lithologies; mudstone at the bottom, and skeletal packstone on top; upper surface of mudstone is extensively bored (arrow); bores are filled with ostracod shells and spar. Bar scale is 5 mm, B67.

G. Close-up of boring into a gastropod shell (arrow). Note infilling of bore by a mosaic of small, equant calcite crystals and sediments. Bar scale is 5 mm, TM39I.

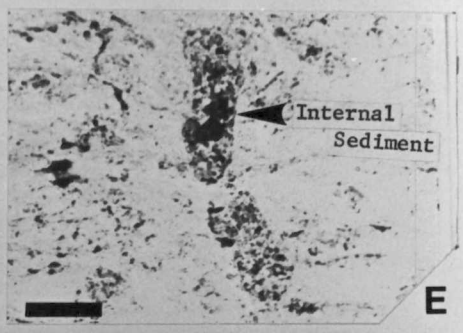
H. Molluscan grain defined by micrite rim (arrow), infilled by calcite spar. The spar consists of finely crystalline, pore filling drusy calcite mosaic. Bar scale is 900 μm, CP15A.

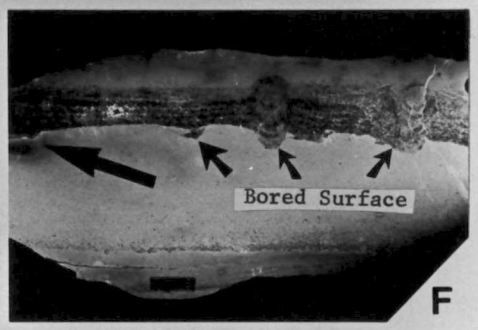

Burrow Tube
A

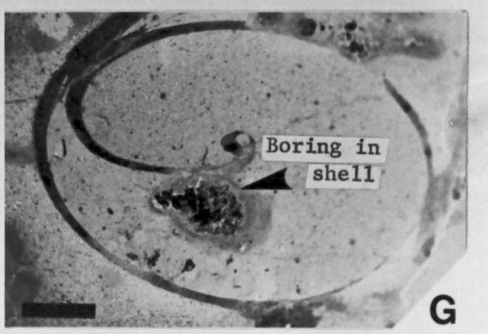

B


B
B
Swirled shell
C


Disrupted Laminae
D


Internal
Sediment
E


Bored Surface
F


Boring in
shell
G


Micrite rim
H

some instances the sediment retaining a black, possibly organic residue. Sediments filling these tubes consist of micrite, spar, skeletal fragments, and pelloids (Fig. 4.2E).

Bored surfaces are common but not as abundant as burrowing throughout the samples. The borings penetrate surfaces which range from inconspicuous breaks in sedimentation accompanied by surface erosion, to borings in skeletal fragments, to a sharply defined bore surface, with distinct and elongated circular and sometimes U-shaped borings. No attempt has been made to classify borings into groups or to assign names of organisms responsible for the excavation of these features. However, variations in the boring dimensions indicate that a variety of organisms such as "worms," algae and fungi were involved in the generation of these features.

Some borings in the rocks of the study area are straight or slightly curved, smooth to irregularly walled, and cylindrical to slightly bulbous with a circular cross-section. They attain a maximum diameter or approximately 0.8 cm, are horizontal to subhorizontal, and usually are unbranched (Fig. 4.2F and G). However, these features are only apparent in a few samples, and are of limited use.

Micritization is a common feature in both the lagoonal and the tidal flat facies. Micritization is either in the form of a thin micrite rim on skeletal grains, especially on molluscan shells, or is in the form of pelloids. Brachiopod, echinoderm, ostracod, and bivalve fragments are among the most common skeletal grains affected (Fig. 4.2H). The contact between micrite rim and skeletal fragments is

either regular or irregular. Where irregular, the grain surface was probably bored by algae and/or fungi and the borings later infilled with micrite calcium carbonate (Bathurst, 1971). When the composition of skeletal grains is either high magnesium calcite or aragonite, a micrite rim or envelope allows retention of overall shell shape after solution, and the resultant mold is later infilled by coarse, equant or drusy sparry calcite (Fig. 4.2H). In this study, grains with regular coatings have not been found, and only micrite rims with irregular contact were observed in various facies, most commonly in low intertidal to subtidal facies.

Pelloids found in the Middle Ordovician carbonate sediments are predominantly round to ellipsoidal in shape and are dark brown in color. The origin of pelloids is still the subject of much controversy, but micritization by boring processes is partially responsible for their formation (Winland, 1968; Illing, 1954). Pelloids may have resulted from: (1) excretion of pelleted mud as feces by organisms, (2) biological micritization, and/or (3) degrading neomorphism (Folk, 1965). Due to the fact that the host has been completely altered, it is very difficult to ascertain which of these mechanisms has been responsible for this alteration (Fig. 4.3C).

Neomorphism

Folk (1965) proposed the term "neomorphism" to describe all transformations between one mineral and itself or a polymorph. These processes in ancient carbonate sediments involve the formation of

Figure 4.3. Petrographic features observed in selected thin sections from the Middle Ordovician rocks.

A. Gastropod mold in gastropod packstone; shell and dissolution porosity now infilled with coarse equant calcite mosaic. Bar scale is 1 cm, CP14A.

B. Transverse section of bryozoan in a muddy matrix. Note the peripheral micrite rim and internal filling of microstructure by micrite where structures are partially destroyed (arrow). Bar scale is 587 μm, TM39I.

C. Photomicrograph of a pelloid, showing that the original carbonate mud has been neomorphosed to microspar. Bar scale is 400 μm, TM39K.

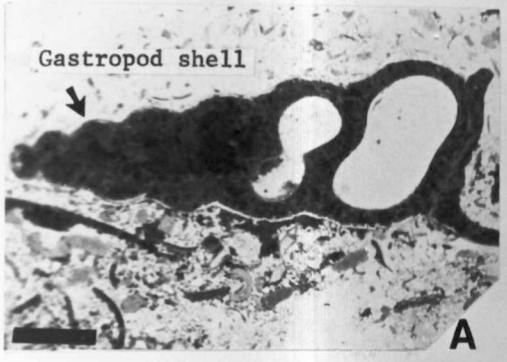
D. Photomicrograph of articulated ostracod in ostracod wackestone. Note the micrite filling in the shell (arrow) has been neomorphosed to microspar. Bar scale is 0.5 mm, CP14A.

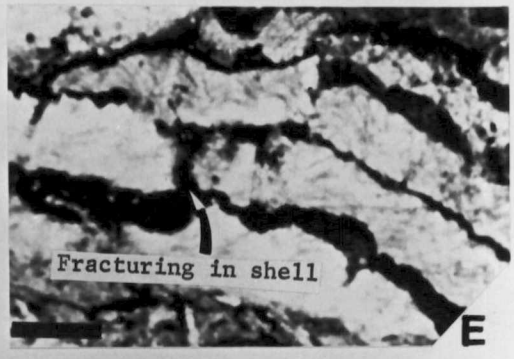
E. Near-vertical fracture development in brachiopod-bryozoan packstone; micrite rims on grains are broken and equant spar infilled along the fractures. Bar scale is 0.5 mm, GF31.

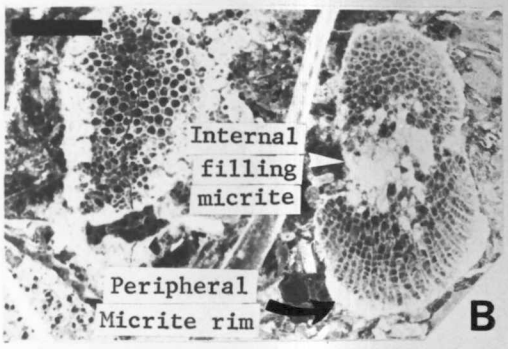
F. Microstylolite and interpenetration in echinoderm-brachiopod packstone. Note that stylolite penetrates grains, overgrowth calcite cement, and the matrix. Bar scale is 587 μm, CP15A.

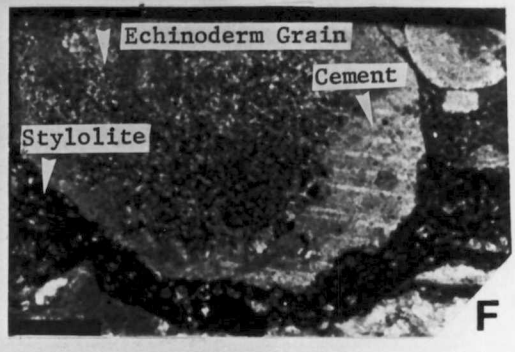
G. Microsuture boundary development in echinoderm-brachiopod wackestone. Note accumulation of insoluble residue along the suture line. Bar scale is 587 μm, B51.

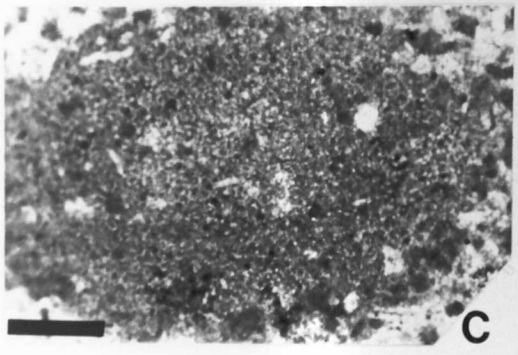
H. Photomicrograph showing echinoderm grain at extinction (crossed nicols). Note the micrite cement filling of small pores in the grain and syntaxial overgrowth cement which is in optical continuity with the grain. Bar scale is 587 μm, GF17.

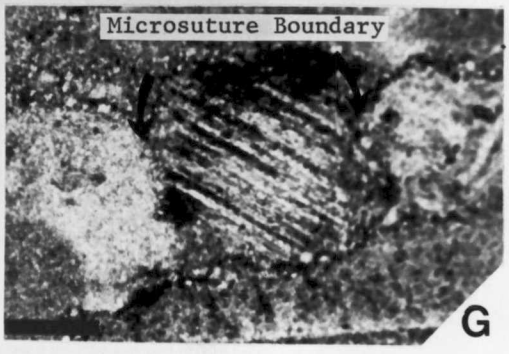

Gastropod shell
A

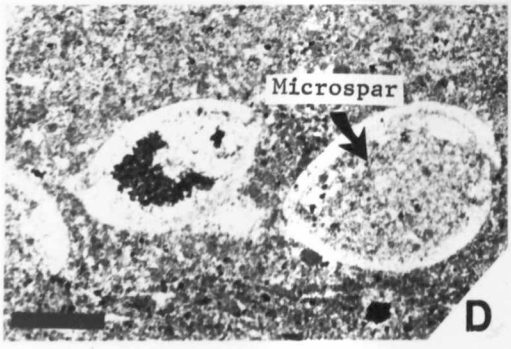

Fracturing in shell
E

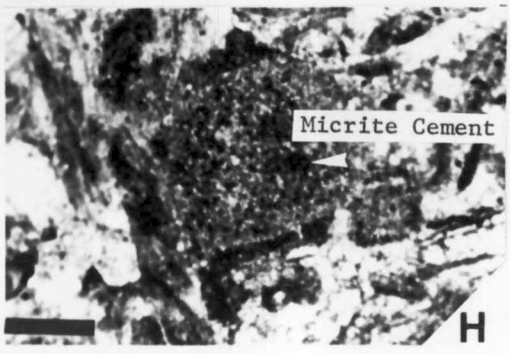

Internal
filling
micrite
Peripheral
Micrite rim
B


Echinoderm Grain
Cement
Stylolite
F


C


Microsuture Boundary
G


Microspar
D


Micrite Cement
H

larger or smaller crystals, change in shape or crystals from the previous state, and/or appearance of a new mineral species.

Middle Ordovician carbonate sediments in the study area exhibit evidence of two forms of neomorphisms: (1) inversion of aragonite to calcite, and (2) the recrystallization of micrite to microspar. Skeletal allochems such as pelecypods, gastropods, and nonskeletal allochems such as pelloids have been recrystallized so that the original microstructures have been completely destroyed (Fig. 4.3A). Molluscan fragments, especially gastropods, exhibit recrystallization fabric in the form of clear, medium to coarse-grained mosaics of equant calcite (Fig. 4.3A). The calcite spar "replacements" of originally aragonitic shells probably formed through a process involving solution of the original shell and subsequent filling of the resultant void (which was protected by the micrite envelope) by calcite.

Bryozoans and corals often have micritized edges and internal microstructures have been partly destroyed by the micrite infilling (Fig. 4.3B). The micrite infilling of these skeletal grains lacks the tubular bores that extend into the host shells, characteristic of biological micritization. It is not known whether these micrite peripheries are the result of recrystallization (neomorphism) or were due to the actual precipitation of microcrystalline micrite cement in preexisting, larger borings. The recrystallization of micrite to microspar is a common neomorphic process the results of which are observed in the studied sediments. These microspar crystals have a size ranging between 5 to 20 microns and from an interlocking network

of calcity crystals (Fig. 4.3D). The process of formation of microspar has been described by Folk (1965, 1974).

Chemical and Physical Compaction

Physical and chemical compaction are two important mechanisms responsible for reduction of the original porosity and vertical thickness of carbonate sediments. Physical compaction, such as deformation, flattening of shells, breakage of shells, close packing and rearrangement of carbonate components, is in response to the overburden pressure which results in porosity reduction. On the other hand, chemical compaction has usually taken place by pressure solution at grain to grain contacts (Bathurst, 1958, 1971). The calcium carbonate release at the point of maximum stress (grain to grain contact), provides a major source of late diagenetic cement (Bathurst, 1958; Heald, 1959). This cement possibly occludes the remaining porosity left in the sediments.

Figure 4.3E, shows a broken micrite envelope produced after leaching of a molluscan shell. The shell void was subsequently filled by equant calcite spar. The calcite spar has extended into the interparticle void space, indicating that micrite envelope formation occurred prior to the leaching and filling of the void. However, the studied sediments do not show extensive evidence of physical and chemical compaction. It is probable that these rocks were cemented early.

Stylolites are the predominant pressure solution features in the fine-grained sediments of the study area. According to Weyl (1961) and

Schlanger (1963) the presence of clay minerals appears to promote pressure solution processes. Therefore, the abundance of stylolites in the fine-grained carbonate sediments in the study area may be due in part to the presence of clay in the sediments. Bed parallel stylolites are the most common type observed. These have amplitudes ranging from 2 to 10 cm, and cut across cement, matrix, and skeletal fragments (Fig. 4.3F). Dolomite rhombs, black insoluble residue, quartz grains and skeletal fragments are commonly accumulated in the stylolite seams.

Microsuture boundaries resulting from pressure solution between skeletal grains are best seen in the echinoderm packstones-grainstones (Fig. 4.3G). These suture boundaries formed an interlocking network of echinoderm plates where syntaxial overgrowth cement occludes all of the primary porosity in the rocks.

In this study, no quantitative estimates have been made of the effect of the physical and chemical compaction processes on the reduction of vertical thickness or porosity. However, fine-grained, micrite rich carbonate sediments of this study usually exhibit greater degrees of cementation and numerous types of stylolites, whereas in the micrite free sediments, stylolites are considerably less common, and primary porosity was often preserved to be filled by later cements.

Cementation

The term cement is used here for all precipitated carbonate crystals which are filling preexisting pores and openings in the sediments or rocks and which are usually attached to a formerly free surface (Bathurst, 1971). During the early diagenesis and alteration

of sediments, cementation is important in the lithification of carbonate sediment and in the reduction of primary porosity. Cementation is always a prolonged process, can occur under different diagenetic environments, and has been proven by various investigators (Bathurst, 1971; Oldershaw, 1971) to be continuous, discontinuous, or occur in pulses. Pulsation causes the change and development of different cement morphologies, fabrics, composition and chemical "fingerprints" of the filling materials. These morphological configurations are indications of the diagenetic environments in which they were formed. However, in some instances, cement does not exhibit highly organized morphological features, which is due to either the fine crystalline nature of the cement or to the fact that the original fabric is destroyed or modified by neomorphism.

In the past fifteen years, the study of cementation has accelerated and contributed much to our understanding of the sources of cement materials, mechanics of precipitation and the processes involved (Longman, 1980; Land and Goreau, 1970; Friedman et al., 1971; James et al., 1976; Land, 1973; Steinen, 1974; Mathews, 1974; Folk, 1965; Purser, 1969). Consequently, the terminology used in the current literature to define these morphological configurations is variable and confusing. Therefore, it was necessary to define terms used in this study (Table 4.1).

Cement fabrics of the Middle Ordovician carbonate rocks in the study area include: (1) micrite cement, (2) fringe cement, (3) crystal silt, (4) syntaxial overgrowth cement, (5) equant calcite cement,

Table 4.1. Summary of terms used for morphological configurations.

1.	Drusy sparite; drusy spar, drusy calcite spar, blocky drusy sparite, equant drusy sparite, clear drusy sparite.
2.	Neomorphic cement; neomorphic spar, neomorphic sparite, neomorphic mosaic.
3.	Fringe cement; fringing cement, fringing bladed cement, bladed fringe cement, fibrous fringe cement, fringe cement with syntaxial or nonsyntaxial extinction, polycrystalline fringing cement, prism fringe, fibrous cement.
4.	Syntaxial overgrowth cement; syntaxial cement, echinoderm syntaxial overgrowth, syntaxial rim cement.
5.	Micrite cement; "micrite high-magnesium cement," originates as high-magnesium calcite.

(6) drusy mosaic cement, and (7) replacement silica and dolomite. Each of these materials is briefly treated below.

Micrite cement. Micrite cement has been suggested to be the first stage of cement in the diagenetic history of modern carbonate sediments in the Bahamas, the Persian Gulf, and the Belize Reef (Shinn et al., 1964; Ginsburg and James, 1976). The crystal size of individual micrite grains is very small and, because they are compositionally high magnesium calcite and later stabilize to low magnesium calcite, it is very difficult to observe them in ancient carbonate rocks. Pelmatozoan grains and rarely bryozoan fragments are the only skeletal elements that show this type of cement in these Middle Ordovician carbonate rocks. The cement generally fills small pores of grains and later is masked by syntaxial overgrowth cement after conversion to low magnesium calcite (Fig. 4.3H).

Fringe cement. This type of cement is not very common in these Middle Ordovician carbonate rocks. Whenever it is present, it consists of a thin fringe of calcite crystals on the periphery of allochems (skeletal and nonskeletal grains). The crystal habit within the fringe is either bladed (long axis of crystals orienting normal to the surface of grains) or equant; cement occurs either as uniform, isopachous layers, discontinuous rims, or irregular patches (Fig. 4.4A). This cement usually represents the earliest stage of cementation (generally after biological activities and micrite cement) and is clear, inclusion free, and does not show coarsening size patterns. This cement is

Figure 4.4. Cementation fabrics of Middle Ordovician carbonate rocks (b).

A. Early fringe cement on molluscan shell succeeded by pore filling equant calcite mosaic (arrow). Bar scale is 0.5 mm, GF15.

B. Crystal silts (arrow) occurring as intraparticle sediment. The crystal silts postdate micrite filling in the shell and predate clear, equant calcite mosaic cement filling. Bar scale is 400 μm, TM17-2.

C. Syntaxial overgrowth cement (arrow) is in optical continuity with echinoderm grain, completely filling the pore spaces. Note the close packing of grains in photomicrograph. Bar scale is 25 μm, TM39J.

D. Two generations of cement are present. Micrite cement infilling of pores of echinoderm grain and the later overgrowth calcite cement; both grain and overgrowth cement are in optical continuity. Bar scale is 1 cm, TM39I.

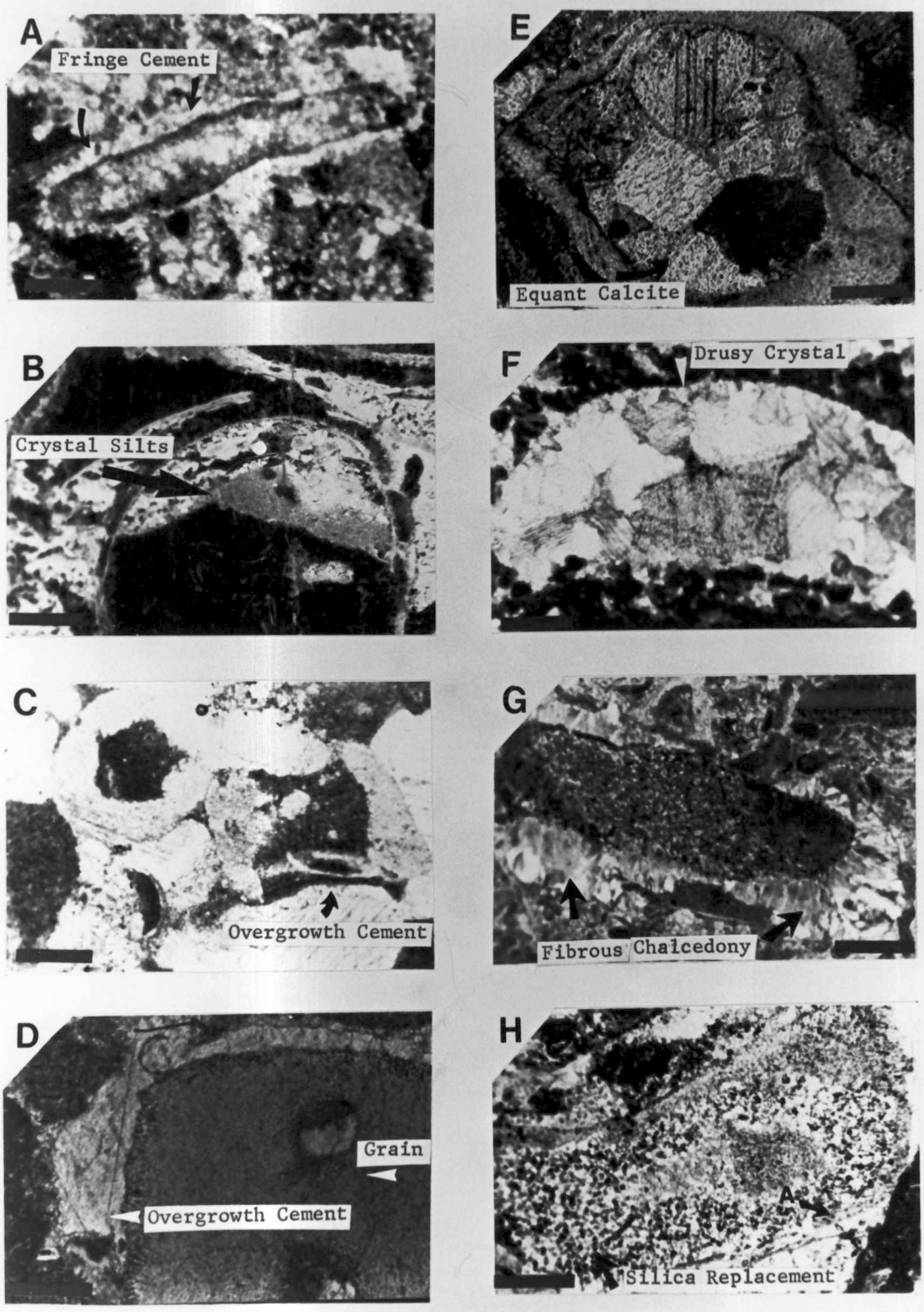
E. Molluscan grain infilled by very coarse, clear, inclusion-free equant calcite mosaic cement. Bar scale is 400 μm, B51.

F. Drusy calcite mosaic filling burrow tube in pelloidal packstone. Note the increase in the crystal size from wall toward the center of tube. Bar scale is 400 μm, B43.

G. Photomicrograph in polarized light of echinoderm grain, replaced by chalcedonic silica with fibrous morphology (arrow). Note the silica replaces both gran and the syntaxial overgrowth cement, but the micrite rim is not altered. Bar scale is 587 μm, GF7.

H. Two generations of cements are present on echinoderm grain (polarized light). Bar scale is 0.5 cm, GF7.

   (1) First generation cement is overgrowth calcite cement (A)
   (2) Second generation cement is the replacement of cement by silica (arrow).


A
Fringe Cement
B
Crystal Silts
C
Overgrowth Cement
D
Grain
Overgrowth Cement
E
Equant Calcite
F
Drusy Crystal
G
Fibrous Chalcedony
H
A
Silica Replacement

observed on ostracods, brachiopods, and trilobite fragments and exhibits both syntaxial and nonsyntaxial extinctions. Unfortunately, due to the scarcity of this type of cement in these rocks, no further conclusion can be made regarding its relationship with other types of cement, its variation in morphological configuration, its role in the lithification and porosity occlusion, and/or its abundance in various facies in this study. However, in the near shelf-edge part of this Middle Ordovician sequence, this type of cement is common and has been interpreted as early marine in origin (Jernigan, 1987).

Crystal silt. The term crystal silt was proposed by Dunham (1969) to refer to silt sized calcite particles, which fill openings and voids as internal sediment, settling on top of skeletal fragments; or which fill a portion of skeletal grains in geopetal structures in meteoric-phreatic or vadose diagenetic environments (Fig. 4.4B).

The size of individual crystals is between 20 um to 30 um, and the aggregate is generally well sorted, occasionally contains small skeletal fragments, and sometimes exhibits a high angle of repose on the upper surface of sediment grains (Fig. 4.4B). Crystal silt is most common in packstone lithofacies in the rocks of the present study. This type of silt postdates the early micrite cement and micrite rims, but predates the final, late, pore occluding cement. These silt size crystals are more common in the intertidal facies where they are associated with features probably indicative of vadose conditions.

Syntaxial overgrowth cement. Syntaxial overgrowth cement is the predominant cement type developed in the Middle Ordovician carbonate rocks in the study area. It is very common in echinoderm-bryozoan packstone and grainstone (Fig. 4.4C). The cement occurs in optical continuity with echinoderm grains, but it may also cover the nearby, nonechinoderm fragments such as trilobite fragments or ostracods (Fig. 4.4D). The overgrowth cement is usually clear, free of inclusions, nucleated on skeletal fragments, and grows outward in all directions (in optical continuity with the grain) until all pores are completely filled or until it meets overgrowth cement from the surrounding grains. When the matrix of the rock is rich in mud (micrite, 20-30%), syntaxial overgrowth cement is rare and is seldom observed to grow on echinoderm or any other skeletal grains. Even if the overgrowth cement forms in the presence of micrite, it is very thin when compared to overgrowths in micrite-free sediments.

The origin of this cement is still the subject of much controversy. Both fresh and marine environments have been proposed to be the environments where this cement formed (Purser, 1969; Longman, 1980; Cotter, 1966; Meyers, 1974). However, in this study, syntaxial overgrowth cement is generally in contact with pore filling, equant-drusy calcite mosaics, which may be suggestive of a fresh water environment. On the other hand, since syntaxial overgrowth cement is generally formed very early in diagenetic processes, it may have been generated in a very shallow marine, subtidal environment. Later in the diagenetic cycle of these sediments the remaining pore systems were

finally filled by equant-drusy calcite mosaic cements precipitated from meteoric waters.

Equant calcite mosaic cement. Equant calcite mosaic cement is generally clear, inclusion-free, and commonly occurs as finely to coarsely crystalline calcite (30 to 300 microns in size) filling all types of pore spaces. In the studied sediments, two types of equant calcite mosaic cements are distinguished: (1) mosaics with equigranular crystals, and (2) mosaics with crystals whose sizes increase from the grain surface to the center of the void (Fig. 4.4E and F). These cements are generally present where lithofacies do not show closely-packed grains. However, both of these cement types compete with syntaxial overgrowth cement in filling pore spaces. The second type of equant mosaic (coarsening crystals) fills bivalve molds and shells, gastropod shells, bryozoan zoecia, coral, burrows and shelter areas.

Staining indicates that these mosaics do not show any zoning (alternating Fe-rich and Fe-poor calcite) or growth bands. This occurrence of unzoned equant calcite mosaic possibly indicates either a semiclosed chemical system with limited flow of solution or a lack of change in the chemistry of the solution. However, not quantitative measurement (Fe content) was done in this study to elucidate the absence of petrographic zoning.

Replacement (silica and dolomite). The replacement of sediment by silica or dolomite is not very extensive in he studied samples, and is

restricted to the area under skeletal fragments (shelter cavities), within skeletal grains (mainly echinoderm and brachiopods), and occasionally in pore spaces between allochems. Replacing materials always occupy positions representing the final stage of the diagenetic cycle and were emplaced after cementation was completed.

Replacement silica is always in the form of fibrous chalcedony. This type of replacement is commonly associated with skeletal packstones, but is also found in some wackestone-packstone lithofacies where echinoderm ossicles, bryozoan fragments, and molluscan debris are set in a loosely-packed, micritic matrix. In this study, certain types of allochems show a greater tendency to be replaced by silica with a specific morphology. For example, echinoderm debris and corals (Tetradium) commonly exhibit fibrous chalcedonic replacement (Fig. 4.4G). Fibrous chalcedony may also replace carbonate overgrowth cements (Fig. 4.4H). However, bryozoan fragments and brachiopod valves are often replaced by spherulitic chalcedony (Fig. 4.5A). Silica has also concentrated along the walls of fractures where stylolites are present (Fig. 4.5B).

Sources of silica for silicification are not known. However, siliceous sponge spicules could provide enough silica for silicification of these skeletal fragments in the sediments. Meyers' (1978) work on Mississippian strata of New Mexico has suggested that silica cementation is more common in the landward side of the depositional system than in the seaward portion. He attributed this to be mainly due to the fresh-water phreatic ground water system. As he suggested,

Figure 4.5. Cementation fabrics of Middle Ordovician carbonate rocks (c).

A. Photograph under crossed polarized light of silicified echinoderm-bryozoan-brachiopod packstone. Note the spherulitic silica (chalcedony) replacement in brachiopod shell where micrite rim is intact. Bar scale is 250 μm, TM46C.

B. Silicification along fracture zone. Note the stylolite formation along the wall of fracture. Bar scale is 1 cm, B18.

C. Dolomite crystals (arrow) replaced micrite infilling of articulated ostracod in ostracod wackestone. Bar scale is 0.5 mm, TM46K.

D. Stylolite development in clay and organic rich zone in brachiopod wackestone. Note corrosion of brachiopod shell by stylolite (arrow). Bar scale is 587 μm, B43.

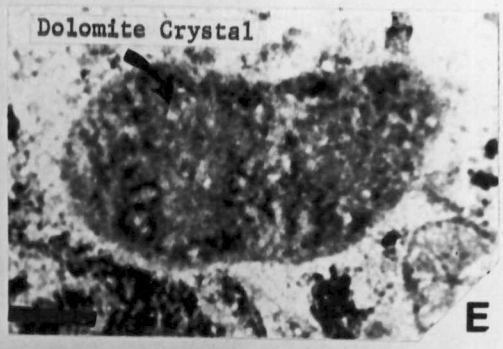
E. Euhedral dolomite (arrow) crystals replaced micrite of intraclast grain. Bar scale is 250 μm, B12.

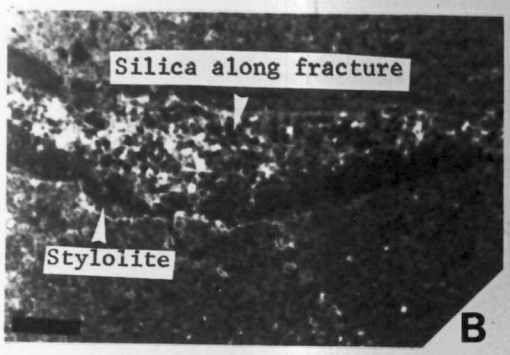
F. Loose packing of skeletal grains in molluscan wackestone-packstone. Bar scale is 5 mm, B15.

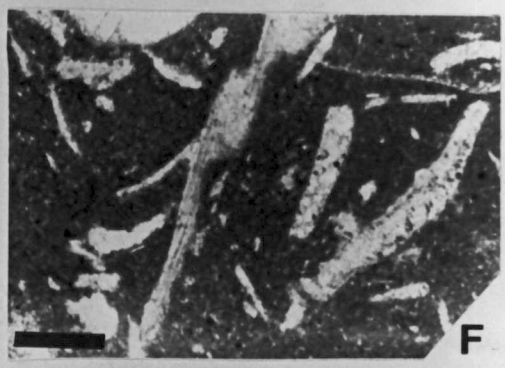
G. Extreme grain interpenetration and stylolite development in echinoderm-molluscan packstone. Note corrosion of grain and removal of overgrowth cement by stylolite (arrow). Bar scale is 400 μm, TM46I.

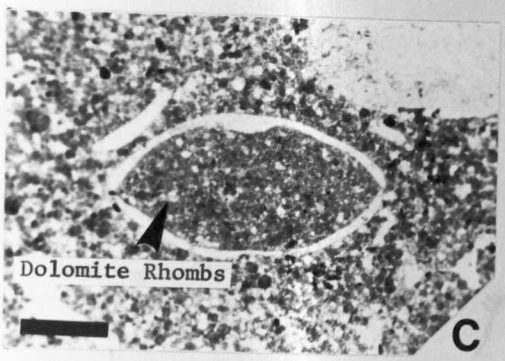
H. Close-packing arrangement of ostracod shells in ostracod packstone. Note the stacking of shells in the upper left hand side of photo due to compaction. Bar scale is 5 mm, B63.

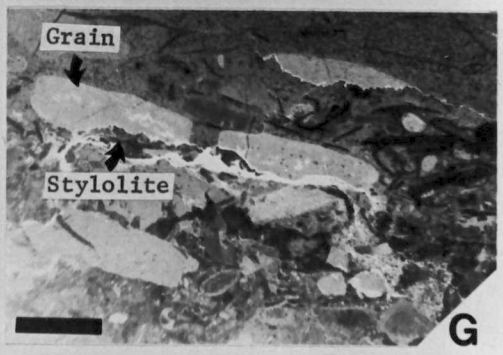

Spherulitic Chalcedony
A


Dolomite Crystal
E


Silica along fracture
Stylolite
B


F


Dolomite Rhombs
C


Grain
Stylolite
G


Clay & Organic Rich Zone
Stylolite
D


H

the fresh-water supply was saturated with respect to silica and was undersaturated in calcite. Therefore, silica cementation has occurred in Mississippian sediments through the influx of fresh-water into the depositional system. If this theory is correct and is also true for the Middle Ordovician carbonate sediments, then it would help to explain the predominant equant-drusy mosaic calcite cements present in the sediments of the study area. However, more work needs to be done on diagenesis of these sediments before one can propose a model for silicification.

Dolomite in these rocks consists of very fine crystals and has been recognized to be more common in the fine-grained wackestone and mudstone in the study area. These dolomite crystals are generally associated with microspar and are clear, euhedral to anhedral, unzoned, and free of inclusions (Fig. 4.5C). In the study area, dolomite crystals do not show preferential replacement morphology, size gradation, or zoning. They occur mainly within burrow tubes, along stylolitic seams, and in organic rich zones (Fig. 4.5D). It appears that clay and organic content are the two major controlling factors influencing the formation of these dolomite crystals. Whenever clay and/or organic matter are found to be abundant heavy dolomite concentration occurs (Fig. 4.5D). Dolomite rhombs also replace some intraclasts and pellets (Fig. 4.5E). These features (small crystal sizes, replacement of intraclasts and pellets) of dolomite rhombs suggest a replacement origin.

Discussion of Sequential Diagenetic Events (Paragenesis) and Related Diagenetic Environments

Carbonate sediments of the lower and middle Chickamauga Group in the study area were deposited in a very complex system of depositional environments, ranging from perital (supratidal and intertidal) to shallow subtidal-lagoonal. Diagenetic processes, especially in fresh-water phreatic environments, have affected these sediments, giving rise to several different diagenetic features recognizable on the microscopic scale (Fig. 4.6).

Biological activities including burrowing (producing sediment-filled tubes, indistinct bioturbation and disrupted laminae), and boring (producing micrite rims and envelope and pelloids) are the earliest diagenetic features observed in this study. These processes occurred in both peritidal and subtidal environments either very early or penecontemporaneous with sedimentation (Shinn, 1969; McIntyre et al., 1968; Ginsburg et al., 1971; Land, 1971). A succession of burrow types showing cross-cutting relationships indicate that some sediment was burrowed by different taxa during the gradual change from soft to firmer sediment consistency in the earliest stages of diagenesis (see Walker and Diehl, 1986, for discussion of criteria for these features).

Cementation within these Middle Ordovician carbonate sediments appears to have taken place early during diagenesis. The most important evidence, suggestive of early cementation, is the loose packing of allochems within packstone and wackestone lithofacies

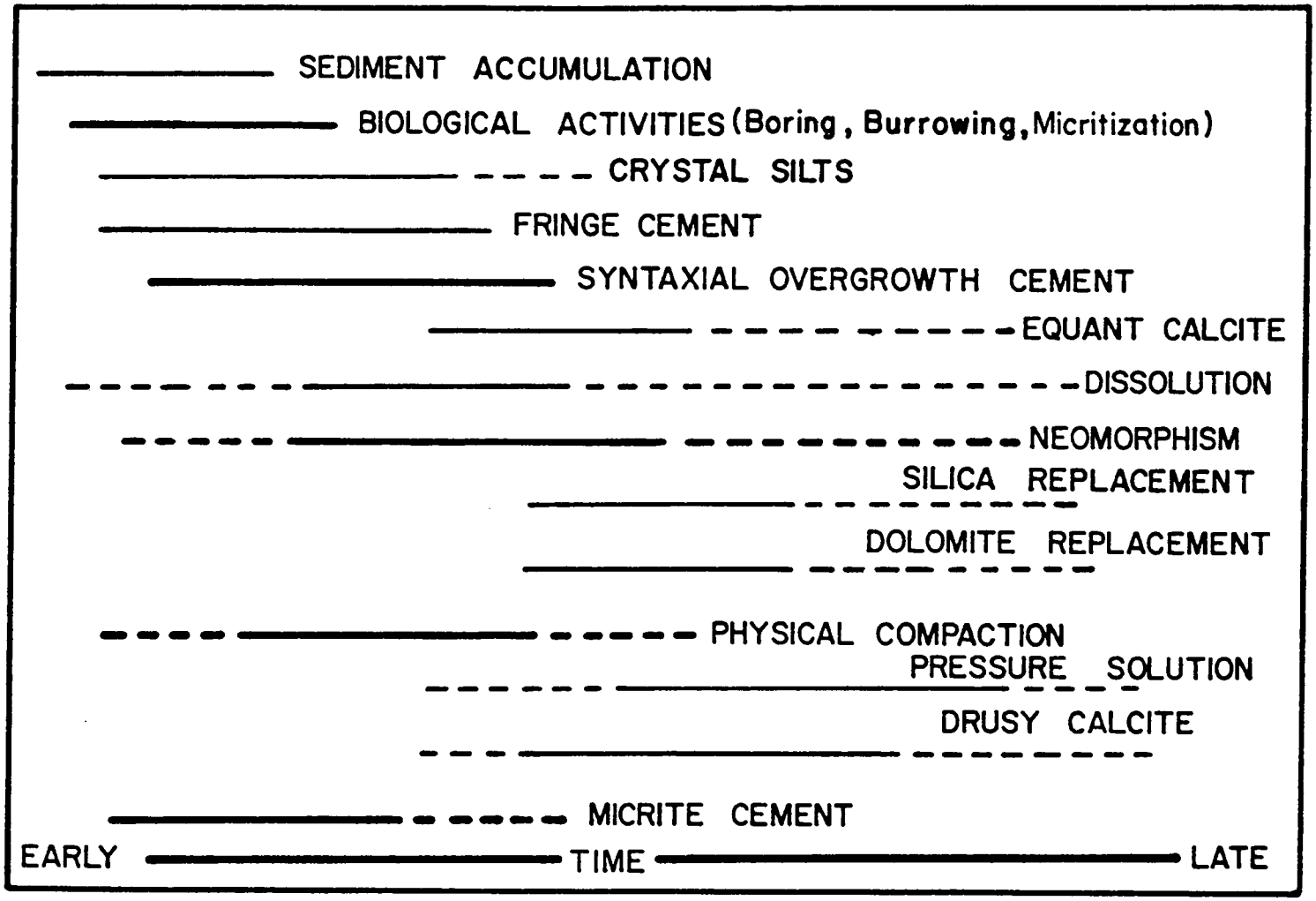


Figure 4.6. Timing of diagenetic events (paragenesis) in the Middle Ordovician "Chickamauga Group" carbonate rocks in the study area.

(Fig. 4.5F, p. 186). Loose packing indicates that cementation must have been in operation before a significant amount of compaction had taken place. Also stylolites have cut the syntaxial overgrowth cement. Thus, this relationship suggests that cementation (overgrowth) was completed before chemical compaction (pressure solution) acted upon the sediments (Fig. 4.5G).

The predominant cement types in these rocks are equant-blocky and drusy (or "coarsening outward crystal mosaics"). These cements are always associated with fresh-water phreatic zones where cements are directly precipitated from meteoric water which is low in magnesium ions (Folk, 1974). This is an indication of the early exposure of these rocks to meteoric water. The generalized order of diagenetic events in these rocks is as follows: (1) biological diagenesis (boring, burrowing and micritization), (2) micrite cement, (3) fringe cement and/or crystal silt deposition, (4) syntaxial overgrowth cement, (5) equant calcite cement, (6) drusy cement, and (7) silica and/or dolomite replacement. There are other processes such as dissolution, physical compaction (Fig. 4.5H), pressure solution, and neomorphism which appear to have taken place over a considerable period of time, either as pulses or continuously. These processes are not placed in any specific order of sequential events in the diagenetic sequence given here for these sediments.

In the absence of fringe cement, syntaxial overgrowth cement is present in the echinoderm packstone facies, forming very early, possibly shortly after biogenic activities and deposition of sediments.

These echinoderm fragments show evidence of early micritized rims around the periphery of the grains before syntaxial cement nucleated. Development of these micritized rims in modern carbonate environments has prevented formation of syntaxial overgrowth cements on rains (Evamy and Shearman, 1969; Lucia, 1962). In these Ordovician sediments micrite envelope formation was followed by syntaxial overgrowth. This latter cement has grown from the surface of the grains into the voids and in some instances has completely filled the open spaces between allochems. According to Folk (1965), the growth of a monocrystalline syntaxial cement is easier and faster than other, nonmonocrystalline cements, thus, filling the void spaces in the sediments completely if voids are open and if there is a supply of cement materials.

Pore Systems

These rocks exhibit various types of primary (original) and secondary pore spaces. Although these pores are now completely filled, their history is an important aspect of the diagenesis of these sediments. These pore systems are more common in sediments with less than 20% micrite matrix (packstone and grainstone) than sediments where the micrite matrix is greater than 20% (wackestone and mudstone). In this study, in order to examine the pore systems and to understand the mechanism of the original void space formation and its relationship to the facies, depositional environment, and fabric, the nomenclatural scheme of Choquette and Pray (1970) was used to describe and classify the observable porosity types. According to Choquette and Pray (1970),

the pore system in carbonate rocks shows evidence of geologic history, and physiochemical conditions of depositional environments through creation, modification or occlusion of pore systems. However, the majority of primary porosity within these sediments has been completely occluded or partially reduced by early diagenetic events, especially cementation processes. yet, in some lithofacies (packstone and grainstones), dissolution processes have enlarged the primary pores and developed secondary porosity.

Figure 4.1 (p. 167) illustrates basic porosity types according to Choquette and Pray (1970). They have stated that the fabric of carbonate sediments is a very important factor in recognizing and understanding the development of the pore system and the interpretation of diagenetic processes responsible for its evolution. It is evident that a direct relationship exists between porosity and fabric selectivity. Thus, based on Choquette and Pray's study (1970), primary porosity is fabric selective, whereas secondary porosity can be either fabric selective or not.

The basic porosity types present in the Middle Ordovician carbonate rocks in the study area will be discussed below.

Fabric Selective Porosity

Interpartical porosity. The void spaces between skeletal and nonskeletal grains were one of the most important pore types present in packstone and grainstone facies. Interparticle porosity depends on the type and shape of grains and the degree of sorting. Thus, the amount

of porosity was highly variable and highest in the well-sorted, well-rounded echinoderm-molluscan packstone lithofacies (Fig. 4.7A). This porosity type was not well developed in the wackestone or even in the packstone facies, where there is a great deal of variation in the grain sizes or in the presence of micrite.

Intrapartical porosity. This type of porosity was present in all of the lithofacies of this study that contained skeletal fragments such as brachiopods, gastropods, ostracods, corals, and bryozoans (Fig. 4.7B). However, it is very hard to estimate the amount of original skeletal porosity of void spaces which remained open at the time of the final deposition. Carbonate sediment of this study provided abundant evidence to support the presence of internal sediment (crystal silt) and cements which have occluded the intraskeletal pores either at syndepositional or postdepositional phases (see cementation section of Chapter IV). Also, in this study there is not enough evidence to provide information of the actual time of precipitation of cements which have occluded the intraskeletal porosities of these sediments.

Moldic porosity. Moldic porosity was formed as a result of removal or dissolution of unstable skeletal and nonskeletal grains in these sediments. Dissolution was either partial or complete and created or enlarged pore spaces. In this study, dissolution of aragonitic, molluscan shells appears to have been the predominant type of moldic porosity formation.

Figure 4.7. Porosity types of Middle Ordovician carbonate rocks (a).

A. Micrite rim on echinoderm, bryozoan, and brachiopod shells in echinoderm-molluscan packstone, interparticle porosity infilled with clear, coarsely crystalline, equant calcite mosaic. Bar scale is 6 mm, B9.

B. Irregular micrite rim development on worm tubes in Tetradium (?) packstone; intraparticle porosity (inside of worm tube) is filled with coarsely crystalline, inclusion-free, equant calcite mosaic. Bar scale is 5 mm, TM42B.

C. Gastropod with intraparticle equant calcite mosaic in shell within a gastropod packstone. Note complete infilling of the lower chambers with equant calcite mosaic and preservation of porosity in the last three whorls of shell. Bar scale is 1 cm, B18.

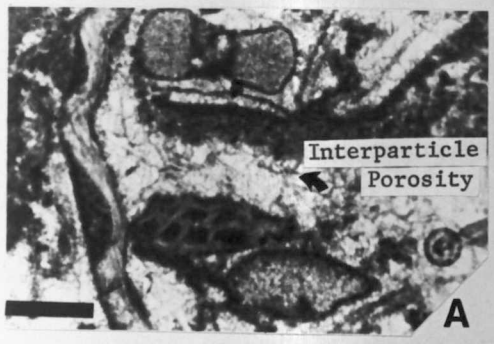
D. Pelloidal packstone; inclusion-free, clear, coarse equant calcite mosaic developed in the moldic porosity, nonskeletal fabric (arrow). Bar scale is 400 μm, TM39T.

E. Micrite rim development on gastropod shell in gastropod-brachiopod packstone; gastropod shell recrystallized and pore filled by coarse equant calcite mosaic and micrite. Bar scale is 587 μm, B2.

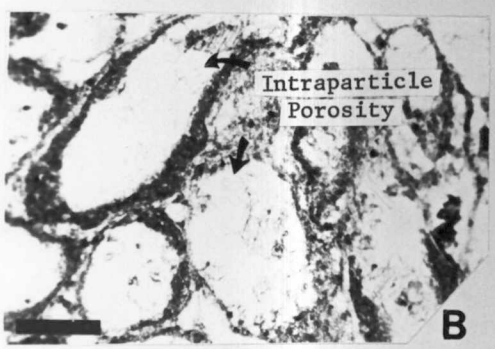
F. White, clear, coarse equant calcite mosaic (arrow) developed in shelter porosity in molluscan packstone; shells are oriented convex-up and parallel to bedding. Bar scale is 0.5 cm, CP31.

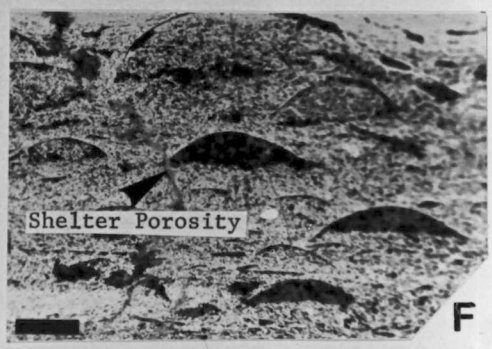
G. Dismicrite with laminar fenestral porosity; fenestral porosity infilled with clear, equant calcite mosaic (arrow). Bar scale is 0.5 cm, CP1B.

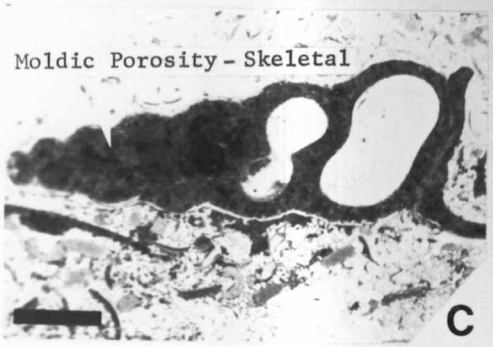
H. Dismicrite with irregular fenestral porosity; fenestral porosity infilled by coarse, clear, equant calcite mosaic (arrow). Bar scale is 0.5 cm, B24.

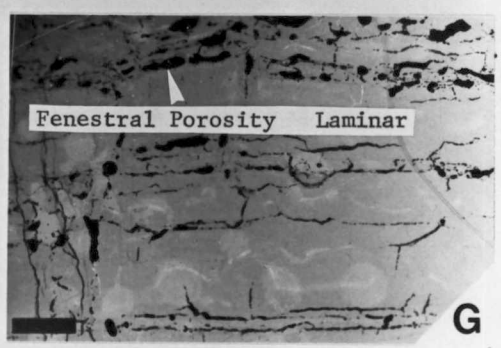

Interparticle
Porosity
A

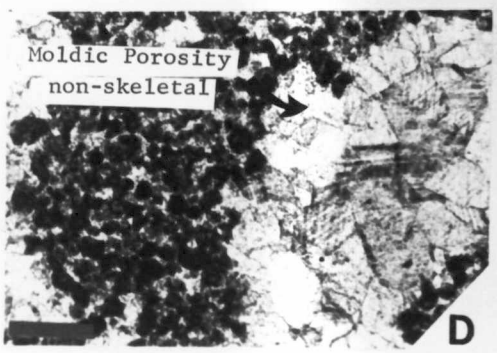

Micrite rim
E

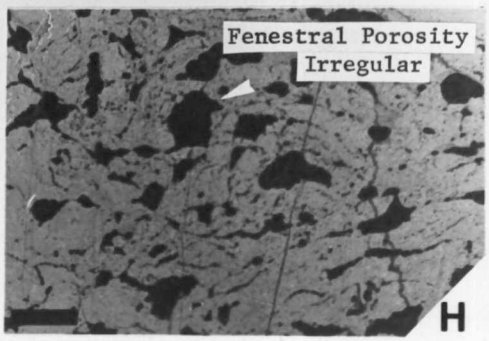

Intraparticle
Porosity
B


Shelter Porosity
F


Moldic Porosity - Skeletal
C


Fenestral Porosity Laminar
G


Moldic Porosity
non-skeletal
D


Fenestral Porosity
Irregular
H

Fabric selective or fabric nonskeletal porosity formation can take place at different times in diagenetic cycles (Choquette and Pray, 1970). In this study, both cases have been recognized, but fabric selective processes were more common (Fig. 4.7C and D). Selective dissolution generally effects individual allochems, whereas nonskeletal processes always occur along fractures and burrows, resulting in formation of cavities and vugs.

Dissolution processes were not restricted to any specific lithofacies, but were more common in skeletal packstone and grainstone. There are several lines of evidence, such as the corrosion and leaching of allochems (complete or partial leaching of micritic rims, micritic grains, and cements), to indicate the effect of dissolution processes and the formation of moldic pores in these rocks (Fig. 4.7E).

Shelter porosity. Choquette and Pray (1970) stated that this type of fabric selective porosity is created through the sheltering effect of skeletal and nonskeletal grains (intraclasts), where voids or spaces beneath the grains are protected from infiling by fine particles. In this study, cement in shelter porosity is minor and is only present in facies such as skeletal packstone and grainstone. The porosity formed under skeletal grains such as pelecypods, brachiopods, and ostracods, when disarticulated skeletal fragments were deposited in a convex-up orientation (Fig. 4.7F).

Fenestral porosity. The term fenestra was first proposed by Tebbutt et al. (1965) for gaps in rocks which were either primary or

formed penecontemporaneously with deposition. Since that time, this term has been redefined by various investigators and the origin of such features is believed to be polygenetic instead of monogenetic (Logan et al., 1974; Shinn, 1968). The fenestrae have a variety of forms and shapes. They usually have rounded forms with lenticular, spherical or in some instances, irregular shapes, where floors, roof, and margins of these features retain different morphologies.

Fenestral fabrics can form through different processes such as decay of algal tissues, desiccation of sediment, and degassing. They generally form in supratidal, intertidal and, in some cases, shallow subtidal sediments. Shinn (1968) stated that these features are formed as a result of degassing and sediment distension very early after the deposition of sediments. On the other hand, Logan et al. (1974) indicated that algal activity is responsible for the formation of these features in modern sediment. They believed that smooth algal mat coverage resulted in the laminoid fenestral fabric, whereas irregular fenestral fabrics are formed under "postular" algal mats in the sediments.

In this study, Grover and Read's classification of fenestral porosity (1978), is used to define different types of fenestral structures and their role in pore system evolution. These types of pores (laminar, irregular and tubular fenestral) were abundant in lithofacies 1, 2, and 3 of this study and occurred in "algal" rich mudstone, wackestone and pelloidal wackestone facies (Fig. 4.7G and H, and Fig. 4.8A). However, these fenestral fabrics are now occluded with

Figure 4.8. Porosity types of Middle Ordovician carbonate rocks (b).

A. Large laminar fenestral pores in dismicrite; fenestral porosity infilled with inclusion-free, coarsely crystalline equant-drusy calcite mosaic. Bar scale is 0.5 cm, GF50.

B. Large irregular fenestral pores partially infilled by internal sediments (arrows); remaining pore spaces filled by equant calcite mosaic. Bar scale is 587 μm, B69.

C. Nearly vertical, nonpersistent fracture in pelloidal packstone. Fracture cuts nonskeletal and skeletal grains (arrow). Bar scale is 250 μm, B9.

D. Macrofracture, now calcite healed, forming anastomosing pattern. Note also the displacement of laminae at the bottom of photomicrograph. Bar scale is 1 cm, GF39.

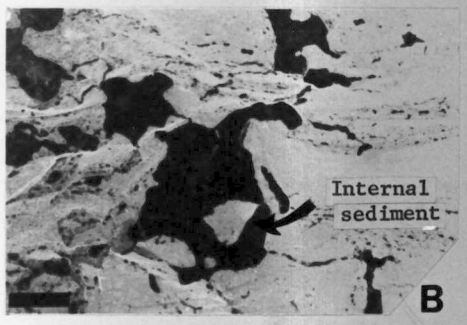
E. Large fracture cuts an early cemented shell (brachiopod). Fracture postdates early, pore-filling equant calcite mosaic cement. Bar scale is 400 μm, TM43D.

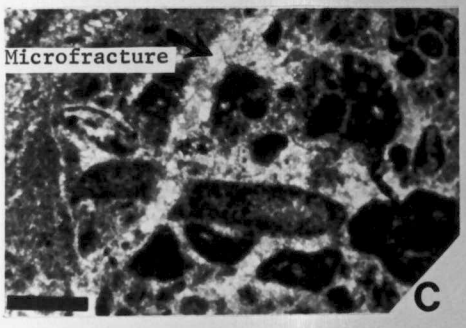
F. Micrite rim retaining mold of recrystallized molluscan shell (gastropod). Note also breakage and destruction of micrite rim by second generation of calcite mosaic cement, filling the interparticle pore spaces. Bar scale is 587 μm, B2.

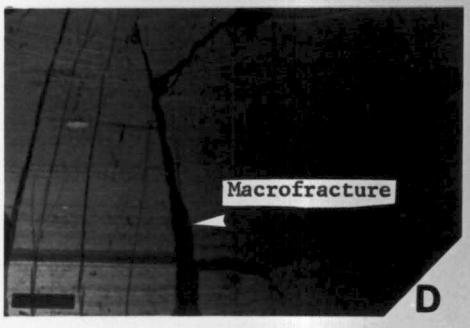
G. Penetration of sediment surface by boring organisms (arrows). Boring in the underlying sediment (mudstone) produced large cavity (holes) where lithoclasts and sediment from both the overlying and underlying layers are filling the eroded surfaces. Bar scale is 1 cm, CP29L.

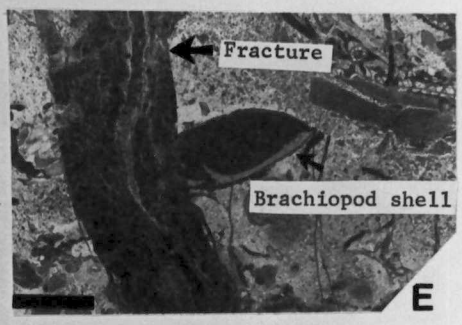
H. Extensively bioturbated (vertical and horizontal burrows) mudstone. Note the distinct wall of short tubular burrows where tubes are completely filled with sediments. Bar scale is 0.5 cm, CP26B.


A


Internal
sediment
B

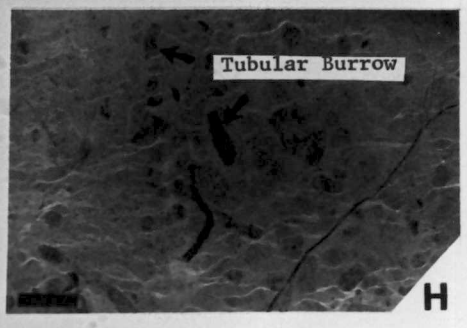

Microfracture
C


Macrofracture
D


Fracture
Brachiopod shell
E


Micrite rim
F


Bored Surface
G


Tubular Burrow
H

equant, drusy mosaic, calcite cement and in some samples, with pelloids, micrite and skeletal fragments covering the floor of the fenestrae (Fig. 4.8B).

Fabric Nonselective Porosity

Fracturing. Fracturing and dissolution are the only two types of fabric nonselective porosity processes indicated by features observed in this study. Fracturing is apparent both at microscopic (thin-section) and macroscopic (hand sample and outcrop) scales (Fig. 4.8C and D). Although fracturing has been classified by Choquette and Pray (1970) as a fabric nonselective porosity type, it may be controlled by sedimentary textures and compositions of sediments (Wanless, 1979).

These fractures are always of a late diagenetic origin (timing) and are exhibited as vertical breaks with smooth walls except when they encounter allochems such as skeletal and nonskeletal grain boundaries, where they become irregular (Fig. 4.8C). In some instances, these fractures are interconnecting and form anastomosing patterns (Fig. 4.8D).

Fluid could easily have migrated through this system and occluded or enlarged porosity. Fractures are useful in dating different periods or episodes of diagenetic processes, especially of cementation, in the rocks. Figure 4.8E exhibits a fracture system that cuts across an allochem (brachiopod shell) with internal cement (equant cement). In this study, fracturing is more common in the rocks of the upper

portions of the stratigraphic sections where wackestone and packstone lithofacies are more abundant than in the lower portions. This suggests that the fracturing may be syntectonic in origin because these stratigraphic sections are usually overlain by a thrust-fault surface. However, fracturing of fossil components in some of the grain-supported facies in this study is believed to be the result of compaction through an increase in the overburden pressure during and after burial of the sediments, and not necessarily the result of tectonic processes.

Dissolution. The importance of dissolution has already been described in detail in the cementation section of this chapter. However, this process can be instrumented in the formation of vugs, channels, and cavernous pores in the sediment. Whether complete or partial, the late removal of sediment or the modification of preexisting voids can create enormous amounts of porosity in the sediment. Dissolution processes in the Middle Ordovician carbonate sediments in this study were limited to the removal of aragonitic and high magnesium calcite minerals from molluscan, coral, and from some bryozoan zoasia, where micrite envelopes preserved molds of original skeletons (Fig. 4.8F). These molds are generally filled by drusy and/or equant calcite mosaic cement, and occasionally with internal sediment (crystal silt) which form geopetal structures. Larger vugs are always associated with fenestral porosity, were they seldom cut across any grain; this is probably due to the leaching of matrix from sediment (Dunham, 1969). It is evident that dissolution processes were not able to create large channels and vugs, or to connect pores in

these rocks. The lack of an observable channel system and cavities in these sediments may be in part due to the early lithification and cementation processes which were operating in the depositional environment and shortly thereafter.

Fabric Selective or Not

Boring. Although the discussion of boring and its character is presented in the diagenetic section of this chapter, boring produces pores that form through biological activity in the sediment, either as fabric selective or not. In spite of the fact that several widespread boring types are present in rocks and shells in modern carbonate environments (especially in modern coastlines), such information from ancient carbonate sediment is seldom reported (Warme, 1975). However, boring did not commonly produce pores in Middle Ordovician sediment, but bored surfaces and bored skeletal fragments have been observed occasionally in the rocks of the study area. Bored surfaces which show breaks in sedimentation and that are accompanied by surface erosion, are present (Fig. 4.8G). Bored skeletal fragments are a more common feature where the bore diameter is up 15 mm than sediment surface boring.

Burrowing. Various Middle Ordovician lithofacies, ranging from supratidal to subtidal, show color or textural changes, suggesting bioturbation. Burrowing activities ranged from churning of sediment and disruption of laminae, to reorientation of skeletal fragments. Secondary porosity development through burrowing activity is best

developed in skeletal wackestone facies. These burrows are isolated, individual tubes, infilled by internal sediments, pelloids, skeletal fragments and equant-drusy calcite mosaics. The net result of this process was to occlude these tubes and reduce porosity in the rocks.

Burrows are either tubes with sharp and distinct walls, or are reflected by a mottled appearance (Fig. 4.8H, and Fig. 4.9A). Burrows in this study are isolated tubes and are not connected to form effective porosity.

Shrinkage cracks. Development of shrinkage crack porosity takes place in sedimentary environments where sediments are exposed above mean high tide and are subjected to air drying. In the study area these shrinkage cracks are common in the lower portions of stratigraphic sections where micritic-matrix rocks predominate (Fig. 4.9B). Cracks have a maximum depth of 15 cm and are 2-3 cm wide. They are generally infilled by sand size debris (skeletal fragments, and pelloids) and cement, suggesting an early (synsedimentary) origin for these features. The resultant voids were never interconnected to form an effective void system in these sediments (Fig. 4.9C).

In modern carbonate environments where shrinkage cracks are forming, the resultant polygons are susceptible to breakage by either the hydraulic regime (tide and wave), or through the boring and burrowing activities by organisms.

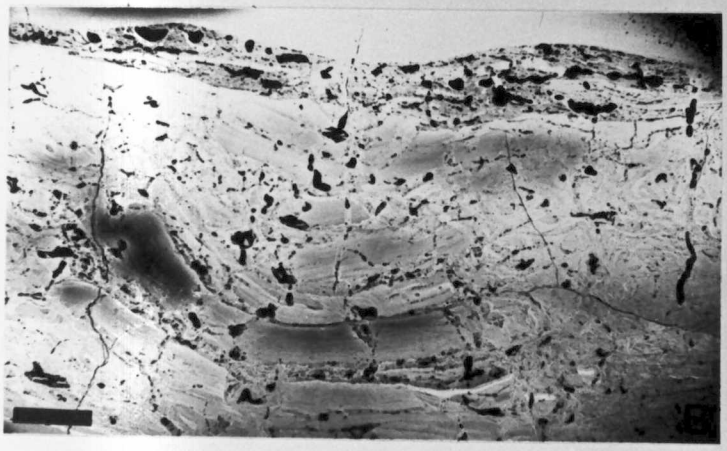
Figure 4.9. Shrinkage cracks porosity in Middle Ordovician carbonate rocks.

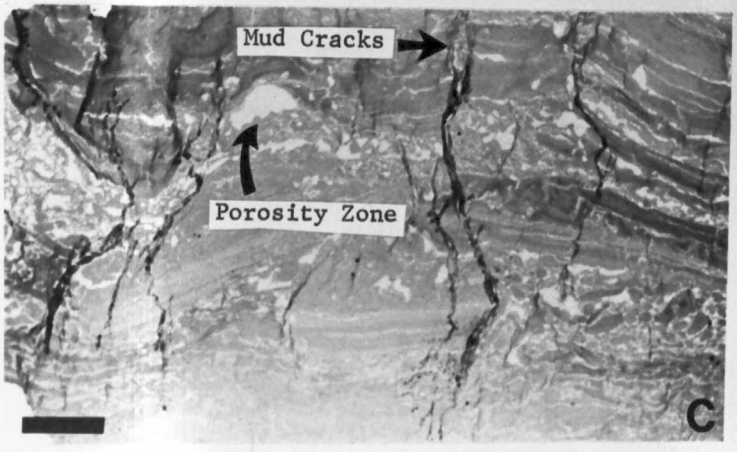
A. Mottled appearance in extensively bioturbated wackestone. Note color alteration in photomicrograph as a result of biogenic activity. Bar scale is 1 cm, B100.

B. Mudcrack development associated with irregular fenestral porosity in dismicrite. Note the curvature in mud polygons. Bar scale is 1 cm, B21.

C. Mudcrack development associated with irregular fenestral porosity. Note the isolated fenestral porosity development as a result of shrinkage of sediment (arrow). Bar scale is 1 cm, CP18A1.


A




Mud Cracks
Porosity Zone
C

Conclusions

1. Investigation into the diagenetic history of the carbonate sediments of the Middle Ordovician in the study area has indicated that the degree and type of diagenetic modification depends, for the most part, on the facies in which it occurred. The precipitation of cement was more common in the coarse grained, micrite-free facies than in micrite-rich matrix rocks.
2. Precipitation of various types of cements was either coeval or overlapped in time. Thus, it is very difficult to establish any system of temporal ordering (see, however, Fig. 4.2, p. 168).
3. Formation of micrite envelopes and rims on skeletal fragments, boring, and burrowing occurred very early in the diagenetic history of these rocks while they were still in the environment of deposition.
4. Micrite cement, possibly of high magnesium calcite composition, was probably the earliest cement type that filled voids and spaces of skeletal fragments (commonly echinoderm grains) and openings between the grains. As in modern sediments, this type of cement is probably of marine origin.
5. Following the micrite cement, fringe cement precipitation took place, although this cement is relatively rare. It is restricted to packstone and grainstone facies, free of muddy matrix.

6. Deposition of crystal silt (internal sediment) appears to have overlapped in time with fringe cement precipitation.
7. Syntaxial overgrowth cement developed at the same time as fringe cement. This cement was restricted to echinoderm grains with or without micrite rims, and destroyed a major portion of primary porosity where it is present.
8. Stabilization of high-magnesium calcite to low magnesium calcite, solution of aragonitic shells and replacement by low magnesium calcite, and neomorphism of micrite to microspar probably took place in a meteoric-phreatic diagenetic environment, but it is very difficult to place them in any paragenetic order.
9. Precipitation of equant and drusy calcite mosaic cements was apparently restricted to mud-free sediments and represents a late stage cementation process that completely occluded the remaining primary and secondary porosity. These mosaics were probably precipitated in vadose and/or meteoric-phreatic diagenetic environments.
10. Physical compactional processes such as breakage, rearrangement, and flattening of shells may have taken place before or during the cementation processes. However, breakage of skeletal fragments generally occurs early in the diagenetic history of rocks and gradually decreases with the passage of time. On the other hand, the chemical compaction process in the form of pressure solution along stylolites or at grain to

grain contacts, occurred late in the diagenetic history of these sediments.

11. Silica and dolomite replacement are the result of a late diagenetic process and always happened after the formation of various types of cements, conversion of high magnesium calcite to low magnesium calcite, and aragonite to calcite transformation.

12. In spite of the fact that there is very little or no primary or secondary porosity remaining in these Middle Ordovician carbonate sediments, porosity development was very restricted and limited to coarse-grained, mud-free facies. Thus, horizontal and vertical communication between the porous zones was very restricted. Vertical permeability barriers were mainly due to the sudden change and patchy distribution of facies and presence of insoluble residue along stylolites. Horizontal limitations were mainly controlled by variations in the facies characters and cements. Although features such as fractures do cut the horizontal and vertical barriers, they are not extensive enough to generate good vertical and horizontal communication between the available porosity in these rocks.

CHAPTER V

AN APPLICATION OF MARKOV CHAIN ANALYSIS IN TESTING FOR POSSIBLE CYCLICITY IN CARBONATE SEDIMENTS OF THE MIDDLE ORDOVICIAN OF THE STUDY AREA

Statistical Methods; Markov Chain Analysis

Markov Chain Analysis is a statistical method introduced by Vistelius in 1949, followed by Griffiths (1966) and Krumbein and Dacey (1969) to study the vertical succession of lithic units in a sedimentary sequence. The proposed method determines the probability of orderly events or cyclic events and the evolution of depositional processes within a given sedimentary basin. Orderly or cyclic events are believed to exist in sedimentary sequences, thus, an ideal order can be constructed in the study of a lithic succession. However, this ideal order has been expressed by various geologists as representative of "Walther's Law."

The Markovian process is a stochastic process in which the nature and extent of a particular state is determined by the nature of the previous state within a system, but not on all states previous to that. The presence of a Markov process within a sedimentary sequence indicate the presence of orderly or cyclic patterns within that system. An introduction to the mathematical procedures of the Markov Chain method is given in Kemeny and Snell (1960) and Krumbein (1967, 1968).

The most commonly used Markov Chain Analysis in geology is the one described by Harbough and Bonham-Carter (1970), and Gingerich (1969).

This method is a first order Markov Analysis in which they evaluation of the system (in this case, lithic units) is based on only a single step; the relationship between a given lithofacies and the next lithofacies immediately succeeding it. The first step in the Gingerich (1969) method is to count the transition frequency between the lithofacies (fi) and tabulate the data (transition count matrix, fij). The second step is to test the observed frequency of transition which could be the result of random process, against the independent trial matrix (eij), using the chi-square test. The independent trial matrix is calculated by dividing the total number of one lithofacies by the total number of facies in the row, excluding the desired lithofacies. In this method, the transition probability matrix (Pij) is the number of transitions from one facies to another facies divided by the sum of the transitions of all facies.

Gingerich (1969) also calculated the value of the x^2 statistic which is the probability that indicates the observed transition count (fij) within the sedimentary sequence is the result of random process operating within the observed frequency of lithofacies (fi) (Billingsley, 1961);

$$x^2v = \Sigma ij\ (fij - fieij)^2/fieij$$

where:

fij = transition count matrix

fi = frequency distribution of lithofacies

eij = independent trial matrix

v = degree of freedom

Thus, the value of the x^2 statistic can be used to display the presence of Markovian processes within the system. Finally, the difference matrix can be constructed by subtracting the value of the independent trial matrix (eij) from the transition probability matrix (Pij). This tally matrix includes both positive and negative elements, where positive values are representative of transitions which have a higher than random probability of occurring within the system. Therefore, a "Cyclic pattern" can be derived from the path of the positive elements through the matrix.

According to Carr (1982), the results of this commonly used Markov technique are subject to an inappropriate, if not false, conclusion due to the structural flaws within the mathematical procedure of the method. Schwarzacher (1975) has also indicted that the major problem with the Gingerich (1969) method is the presence of previously defined zeros in the transition count matrix. He stated that predefined zeros within the transition matrix are not the result of a simple independent random process; thus, the result of the facies transitions is statistically meaningless. However, the validity or rejection of this type of statistical method (Markov Chain Analysis) requires further examination which is not within the scope of this study.

The second type of Markov Analysis or the modified Markov Analysis (Log-Linear Model) which has been proposed by Bishop, Feinberg, and Holland (1975), Feinberg (1977), and Carr (1982), is provided to

evaluate the incomplete tables. The Log-Linear Model, which is accompanied by the concept of quasi-independence, can be used to predict the frequency of cells (expected cells) in multiway and incomplete tables. Using this method, a table of frequency of expected cells would be derived. If the Log-Linear Model is rejected, then a Markov process or chain may be present within the system. This method also records and processes the observed column and row tables, while maintaining the undefined cells on the diagonal (mathematical details are given in Carr, 1982).

To be able to use the Log-Linear Method for evaluation of the facies transition of the lithic succession within sedimentary sequences, Brown (1974) proposed a stepwise computer program (BMDP-2F) which expresses the Log-Linear Model mathematical procedures. Therefore, by applying this method, the selection of too many facies transitions is diminished and the selected transitions are apparently closer to the true transitions observed in the natural depositional system.

Results and Discussion

The Middle Ordovician carbonate rocks in the study area consist of fourteen lithofacies and subfacies. One hundred ninety-seven facies transitions were counted on the composites of all four measured stratigraphic sections. To reduce the number of empty cells within the tally matrix, the lithofacies transition count of all four measured

sections and a few facies within the same depositional environments were combined. The combined facies for this study are as follows:

1. Facies 2a and 2b represented as facies 2,
2. Facies 4a, 4b, and 4c represented as facies 4,
3. Facies 4d, 5a, and 5b represented as facies 5.

To determine the presence of orderly events or cyclic patterns the method of Gingerich (1969) was applied. The frequency of occurrence of units of the eight major lithofacies was:

Lithofacies 1 = 4

Lithofacies 2 = 9

Lithofacies 3a = 21

Lithofacies 3b = 25

Lithofacies 4 = 55 = fi

Lithofacies 5 = 30

Lithofacies 6 = 37

Lithofacies 7 = 14

Total = 197

Based on the 197 facies transitions, the transition count matrix can be summarized as shown in Figure 5.1. The probability form of this transition count matrix is shown in Figure 5.2. The calculated independent trial matrix shown in Figure 5.3 is based on the 197 facies transitions with regard to the assumption that the sequence of lithofacies within the study area was determined by a random process within the frequency distribution of facies.

N=197	FACIES	1	2	3a	3b	4	5	6	7
SUPRATIDAL DOLOMITIC FLAT	1	.00	1	0	0	1	0	1	1
SUPRATIDAL MUDFLAT	2	0	00	1	3	4	1	0	0
INTERTIDAL CHANNEL	3a	0	0	00	8	5	3	3	2
INTERTIDAL POND	3b	1	2	3	00	10	3	4	2
SUBTIDAL "INTRABASINAL LAGOON"	4	0	4	4	10	00	15	18	6
SUBTIDAL LAGOON	5	1	2	3	5	12	00	5	2
SUBTIDAL CHANNEL	6	0	0	10	0	22	5	00	0
SUBTIDAL "WAVE BAFFLE"	7	1	0	0	2	3	3	5	00

$=f_{iJ}$

TRANSITION COUNT MATRIX

*NOTE: i = STATE OF VARIABLES (ROWS)
J = STATE OF VARIABLES (COLUMNS)

Figure 5.1. Facies transition count matrix for the Middle Ordovician rocks in the study area.

N=197	FACIES	1	2	3a	3b	4	5	6	7
SUPRATIDAL DOLOMITIC FLAT	1	00	.25	0	0	.25	0	.25	.25
SUPRATIDAL MUDFLAT	2	0	00	.11	.33	.44	.11	0	0
INTERTIDAL CHANNEL	3a	0	0	00	.38	.23	.14	.14	.09
INTERTIDAL POND	3b	.04	.03	.12	00	.40	.12	.16	.08
SUBTIDAL "INTRABASINAL LAGOON"	4	0	.07	.07	.17	00	.26	.31	.10
SUBTIDAL LAGOON	5	.03	.06	.09	.16	.40	00	.16	.06
SUBTIDAL CHANNEL	6	0	0	.27	0	.59	.13	00	0
SUBTIDAL "WAVE BAFFLE"	7	.07	0	0	.14	.21	.21	.35	00

$=P_{iJ}$

TRANSITION PROBABILITY MATRIX

Figure 5.2. Facies transition probability matrix for the Middle Ordovician rocks in the study area.

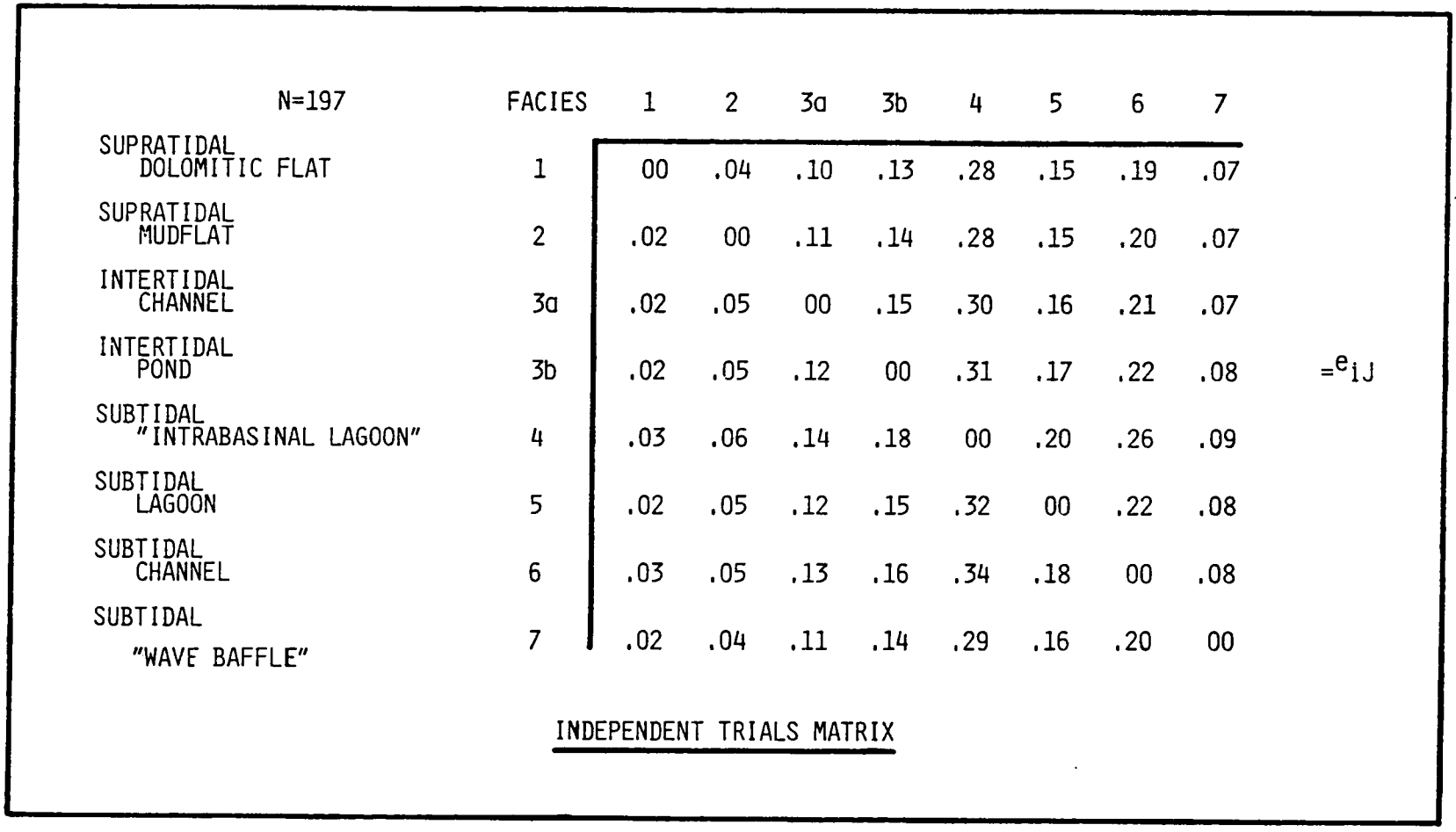


Figure 5.3. Facies independent trial matrix for the Middle Ordovician rocks in the study area.

The x^2 statistic which indicates that the observed facies transition count (fij) is the result of random process within the observed frequency of the lithofacies (fi), yields a value of 80.016 (J. Silk, 1979) with 49.223 degrees of freedom (Fig. 5.4). Therefore, according to the calculated x^2 value, deposition of these Middle Ordovician carbonate sediments has taken place by an independent, or non-Markovian mechanism. Thus, based on the Gingerich (1969) method, these carbonate sequences do not represent "cyclic sedimentation" in a complex tidal flat and subtidal environment.

The difference matrix is the result of subtraction of the independent trial matrix (eij) from the transition probability matrix (pij) (Fig. 5.5). The positive elements (values) within this difference matrix, which is representative of the lithofacies transitions which have a higher than random probability of occurring, have been taken out of the matrix and used to develop the "cyclic patterns" for these rocks (Fig. 5.6A and B). The lithofacies transition diagram (Fig. 5.6A) displays the total probability of transitions from one facies to different facies. Figure 5.6B, only exhibits the probabilities greater than 0.10.

The facies transition diagram (Fig. 5.6A) which displays the total probabilities of transitions with probability values ranging from -0.08 to +0.25, is very complex. Thus, no conclusive interpretation could be made on the observed facies transitions. However, if only the more probable facies transitions (values greater than 0.10) are used, then, a simpler and more meaningful set of facies transitions can be deduced

$$x_v^2 = \Sigma ij(f_{ij} - f_i e_{ij})^2 / f_i e_{ij}$$

where:

$$\sum_{ij}^{(n)} (1) \left(f_{ij} - f_i i_{ij}\right)^2 / f_i e_{ij} = \sum_{ij}^{(8)} (1) \left(f_{ij} - f_i e_{ij}\right)^2 / f_i e_{ij}$$

and:

$\Sigma ij(1) = 7.868$ $\Sigma ij(5) = 21.154$

$\Sigma ij(2) = 5.971$ $\Sigma ij(6) = 1.640$

$\Sigma ij(3) = 9.885$ $\Sigma ij(7) = 24.906$

$\Sigma ij(4) = 2.379$ $\Sigma ij(8) = 6.212$

Note: i and j are states of variable where i represents rows and j represents columns.

$$x_v^2 = 80.016$$

Degree of freedom:

Total number of positive entries in e_{ij} (Independent trial matrix) - Rank of e_{ij}

So:

d.f. = 56 - 6.77 = 49.23

Figure 5.4 Mathematical equations for calculation of x_v^2 statistics.

N=197	FACIES	1	2	3a	3b	4	5	6	7
SUPRATIDAL DOLOMITIC FLAT	1	00	+.21	-.10	-.13	-.03	-.15	+.09	+.18
SUPRATIDAL MUDFLAT	2	-.02	00	0	+.19	+.19	-.04	-.20	-.07
INTERTIDAL CHANNEL	3a	-.02	-.05	00	+.23	-.07	-.02	-.07	+.02
INTERTIDAL POND	3b	+.02	-.03	0	00	+.09	-.05	-.06	0
SUBTIDAL "INTRABASINAL LAGOON"	4	-.03	+.01	-.07	-.01	00	+.06	+.05	+.01
SUBTIDAL LAGOON	5	+.01	+.01	-.03	+.01	+.08	00	-.06	-.02
SUBTIDAL CHANNEL	6	-.03	-.05	+.14	-.16	+.25	-.05	00	-.08
SUBTIDAL "WAVE BAFFLE"	7	+.05	-.04	-.11	0	-.08	+.05	+.15	00

$=P_{iJ}-e_{iJ}$

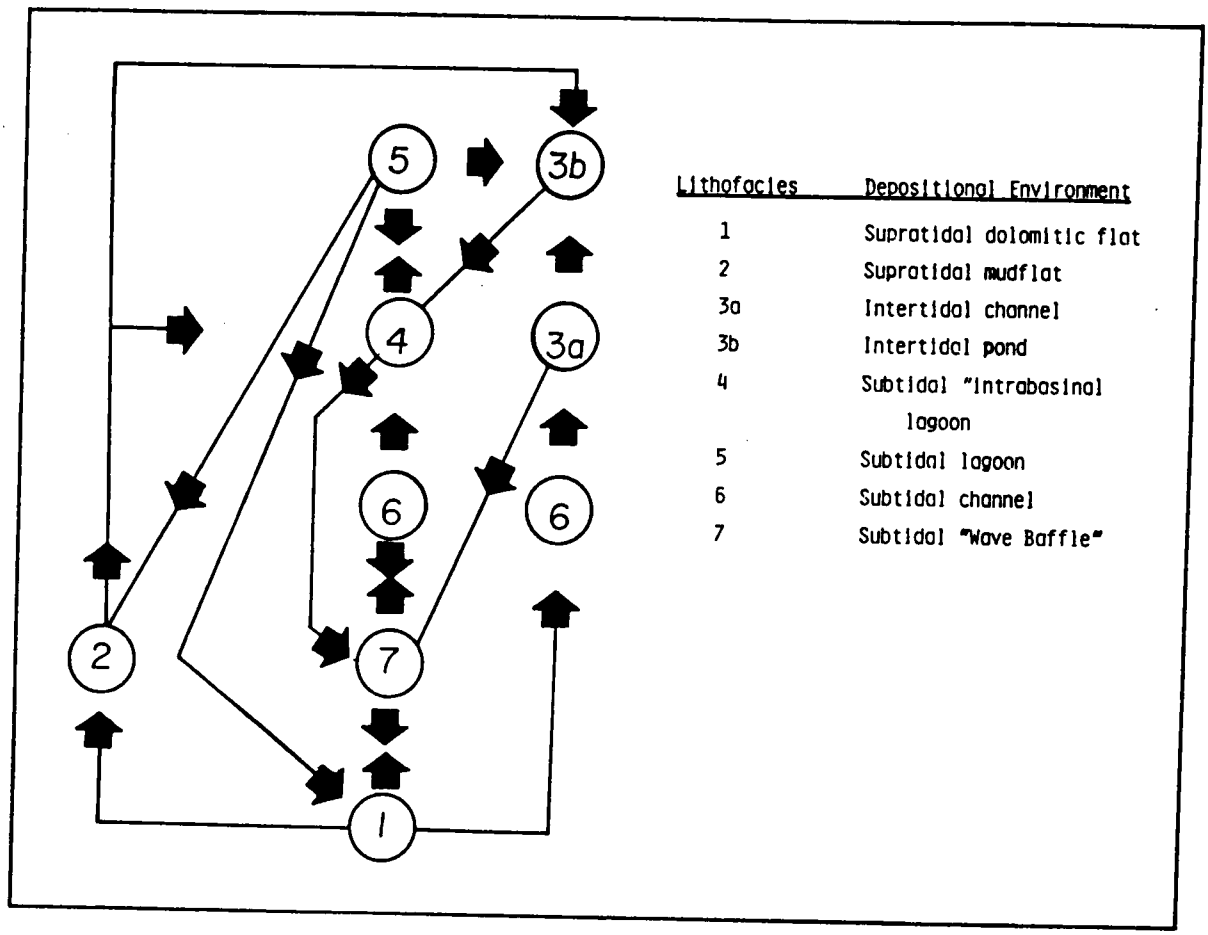
DIFFERENCE MATRIX

Figure 5.5. Difference matrix for the Middle Ordovician rocks in the study area.

Figure 5.6. Lithofacies transitions of Middle Ordovician rocks.

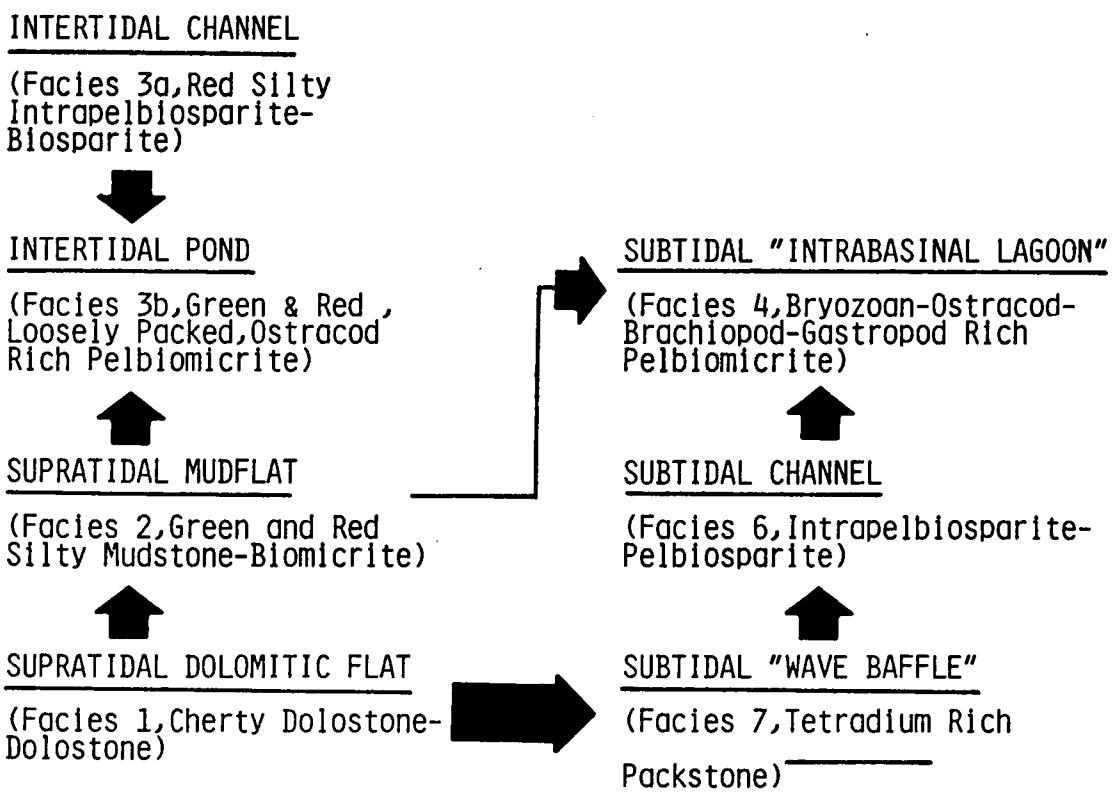
A. Lithofacies transition of Middle Ordovician rocks in the study area. Probabilities less than -0.10 and greater than +0.10 are included.

B. Lithofacies transitions diagrams of Middle Ordovician carbonate rocks in the study area. Probabilities less than 0.10 are not included.


5
3b
4
3a
6
6
2
7
1
Lithofacies
Depositional Environment
1 Supratidal dolomitic flat
2 Supratidal mudflat
3a Intertidal channel
3b Intertidal pond
4 Subtidal "intrabasinal lagoon
5 Subtidal lagoon
6 Subtidal channel
7 Subtidal "Wave Baffle"

A.

Figure 5.6.



B.

Figure 5.6 (continued)

(Fig. 5.6B). Facies 1 (supratidal dolomitic flat) has a higher probability of being overlain by facies 2a (supratidal mudflat) than facies 7 (subtidal Tetradium "wave baffle"). Facies 2 has a greater probability of being overlain by facies 3b (intertidal pond) than facies 4 (subtidal "intrabasinal lagoon or pond"); facies 3a has only probability of being overlain by facies 3b (intertidal channel). Lithofacies 7 has a greater probability of being overlain by facies 6 (subtidal channel) than any other facies. Finally, lithofacies 6 can only be overlain by facies 4 (subtidal "intrabasinal lagoon or pond").

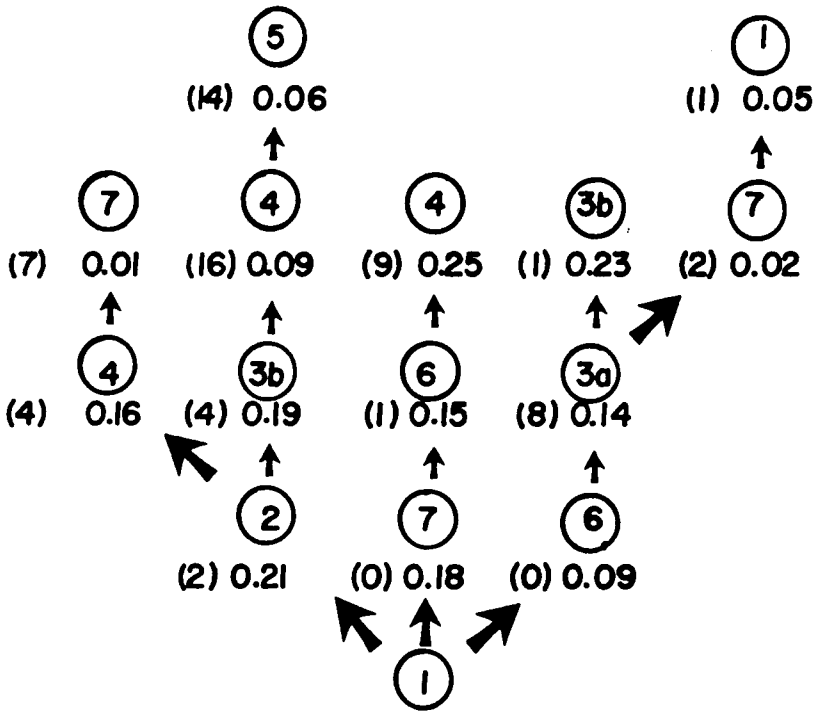
Figure 5.7A and 5.7B exhibits the facies transitions (visual observation, all four measured sections), and the more probable facies transitions derived from Figure 5.6A and B. This diagram indicates that there is no relationship between the probabilities observed in Figure 5.6B and the actual occurrence of facies in the sections. Only a few facies transitions with high probability (Figs. 5.6B, 5.6A) display high frequency of actual occurrences. For example, transition of facies 6 to 4, and transition of facies 6 to 3a.

In order to evaluation the presence of cycle or orderly events more objectively the modified Markov Method (Log-Linear Model) was applied, using the same set of data. The data (composite of all four sections) are compiled in a two way frequency table, where prior zeros are present in the diagonal of the matrix. The predefined zeros in the diagonal are simply because one facies being overlain by itself is impossible. The observed frequency matrix is tested against the quasi-independent or random model, using Pearson's chi-square

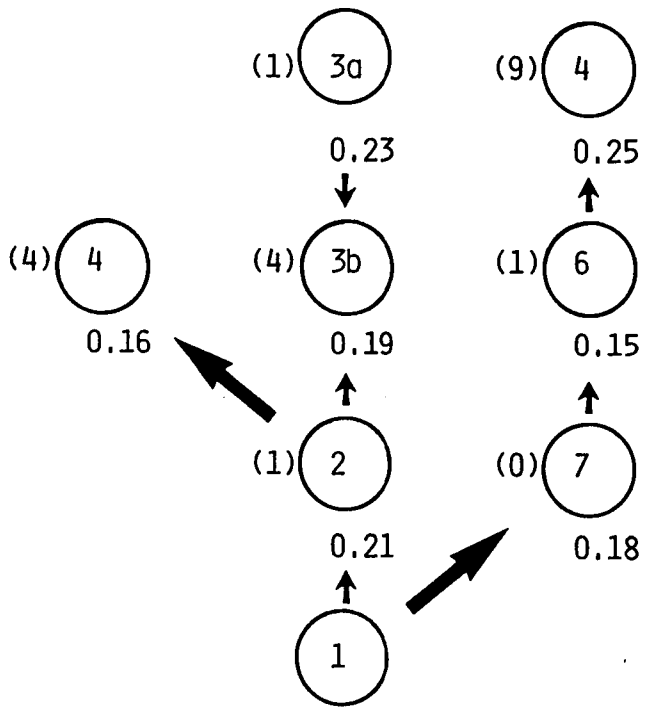
Figure 5.7. Probabilities of facies transition.

A. Probabilities of facies transitions diagram of Figure 5.6A, and the actual occurrence of lithofacies in the measured sections. Frequencies of actual occurrences are shown in parentheses and probabilities of facies transitions without parentheses.

B. Probabilities of facies transitions diagram of Figure 5.6B, and the actual occurrence of lithofacies on the measured sections. Frequency of actual occurrences are shown in parentheses and probabilities of facies transitions without parentheses.


5
(14) 0.06
1
(1) 0.05
7
(7) 0.01
4
(16) 0.09
4
(9) 0.25
3b
(1) 0.23
7
(2) 0.02
4
(4) 0.16
3b
(4) 0.19
6
(1) 0.15
3a
(8) 0.14
2
(2) 0.21
7
(0) 0.18
6
(0) 0.09
1

(A)


(1) 3a
0.23
(9) 4
0.25
(4) 4
0.16
(4) 3b
0.19
(1) 6
0.15
(1) 2
0.21
(0) 7
0.18
1

(B)

Figure 5.7.

statistic. Thus, a more meaningful understanding of vertical facies transitions can be derived by avoiding overemphasizing on the cyclicity concept. Figure 5.1 (p. 215) exhibits the facies transition tally matrix for 197 transition counts of the Lower and Middle Ordovician in the study area. A stepwise procedure was used (BMDP-2F) which is an extension of the Log-Linear Model (Brown, 1974), used to identify both positive and negative departures from the expected frequency under the quasi-independent concept.

This stepwise procedure identified two cells (Fig. 5.8), using an α value of 0.2 which indicate an 80% level of significance. This tally matrix (Fig. 5.8) indicates that the selected facies transitions have greater observed frequency than the expected values.

The facies transitions recognized in this study do not indicate cyclic sedimentation within this complex tidal flat-subtidal system. Facies transitions derived from the modified Markov model (Log-Linear Model) are different from the results of the Gingerich method (1969), and represent a smaller number of probable facies transitions (Fig. 5.8) than the Gingerich results. However, the probable facies transitions derived from Carr's (1982) method are not surprising, because based on the stratigraphic sections, the transitions between subtidal channel, intertidal channel, and intertidal pond can be easily detected. These transitions exist because within this complex tidal flat-subtidal system, some of the channels extended from the subtidal into the intertidal zone where they connected to intertidal ponds.

SIGNIFICANT FACIES TRANSITIONS (CARR'S METHOD,1982), $\alpha = 0.2$

Step No.	Observ. Freq.	Expect. Freq.	Chi-Square	Prob.	Transition Type
1	10.0	2.72	46.81	0.1826	Intertidal Channel(F-3a) ▲ Subtidal Channel (F-6)
2	8.0	2.07	40.01	0.3810	Intertidal Pond (F-3b) ▲ Intertidal Channel (F-3a)

FLOW CHART SUMMARY OF FACIES TRANSITIONS

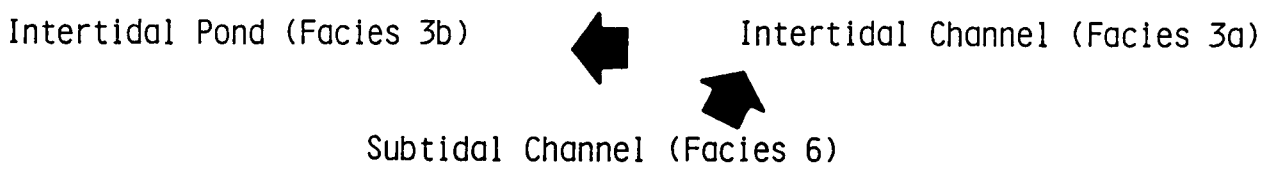


Figure 5.8. Facies transitions selected as significant after analysis of Figure 5.1 (p. 215).

Therefore, this transition does not seem to present a strong or cyclic pattern.

Finally, if the level of significance or confidence level in Brown's stepwise procedure (1974) is changed from 80 to 60 or less, the number of facies transitions would increase from two to four, and a more complex facies transition pattern is derived (Table 5.1 and Fig. 5.9). This more complex pattern which is statistically insignificant, is similar to the transitions derived from the Gingerich method.

Summary and Conclusions

1. Based on petrographic analysis (Chapter III), the Lower and Middle Ordovician carbonate rocks in the study area consist of fourteen lithofacies and subfacies, characteristic of a very complex tidal flat and subtidal environments.

2. In order to determine the presence or absence of orderly events or cyclicity (that is the result of "cyclic sedimentation"), and to clarify the lithofacies relationships by defining these relationships statistically, two mathematical (statistical) methods were used: (1) Markov Chain Analysis (Gingerich, 1969; Harbough and Bonham-Carter, 1970), and (2) the modified Markov method or Log-Linear Model (Carr, 1982).

3. To reduce the number of empty cells within the tally matrix in this study, a composite facies transition count (197 counts in all four measured sections) was prepared and facies within the same depositional

Table 5.1. Facies transition selected as significance level changes from $\alpha = 0.4$ to $\alpha = 0.9$ after analysis of Figure 5.1.

Step No.	Observ. Freq.	Expect. Freq.	Chi-Square	Transition Type
		$\alpha = 0.4$		
1	10.0	2.72	46.81	6 to 3a
2	8.0	2.07	40.01	3a to 3b
3	22.0	5.40	31.91	6 to 4
		$\alpha = 0.9$		
1	10.0	2.72	46.81	6 to 3a
2	8.0	2.07	40.0	3a to 3b
3	22.0	5.40	31.91	6 to 4
4	1.0	0.13	25.86	1 to 2

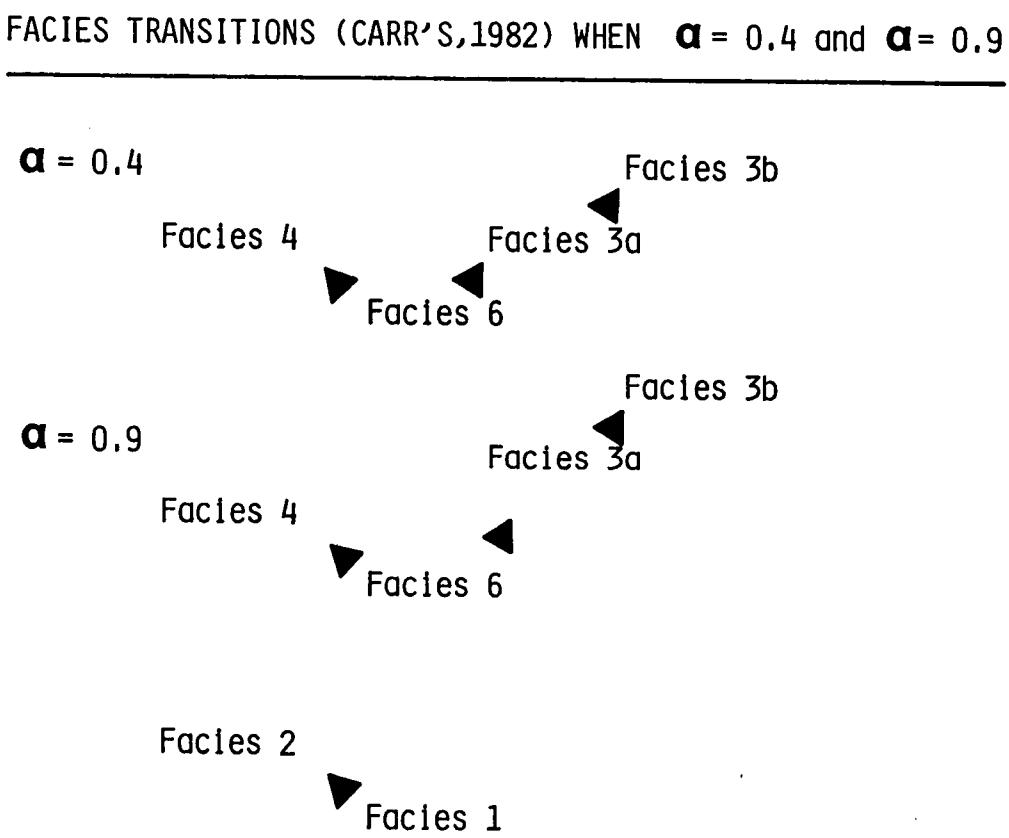


Figure 5.9. Facies transitions, using modified Markov Analysis.

environments were combined as follows: (1) Facies 2 (2a and 2b), (2) Facies 4 represents facies (4a, 4b, 4c), and (3) Facies 5 (5a, 5d).

4. The results of Markov Chain Analysis (Gingerich, 1969) indicate the existence of a very complex Markovian process. However, based on the total probabilities of the positive elements of the facies transitions, no conclusive interpretation can be made. The extraction of the probabilities of positive elements greater than 0.10 from the tally matrix, makes a more meaningful facies transition model which more likely reflects the natural system.

5. The modified Markov Analysis (Carr, 1982), applied to the same set of data, verified the presence of only two facies transitions of high probability. The facies transitions consist of subtidal channel to intertidal channel, and intertidal channel to intertidal ponds. This facies transition does not represent cyclic or orderly pattern within these Middle Ordovician carbonate sediments, but simply reflects the continuity of channel systems within the subtidal and intertidal environments which are adjacent to the intertidal ponds.

6. The validity or rejection of the two Markov Chain Analysis methods applied here require further examination. However, this study provides a ground for future investigation of the concept of cyclicity in sedimentary sequences and the accuracy and applicability of the Markov method in geology.

CHAPTER VI

CONCLUSIONS

1. Field studies of four measured stratigraphic sections (Goodfield, Center Point, Ten Mile, Barnardsville) in the Kingston allochthon of Eastern Tennessee, along with detailed petrographic analysis of 700 thin sections of lower Middle Ordovician carbonate rocks from the sections indicate these sediments were deposited in a complex of tidal flat and shallow, subtidal-lagoonal depositional environments. These environments are represented by fourteen volumetrically important lithofacies.

2. Due to the complex facies pattern, and the absence of time-stratigraphic markers such as bentonite beds or biostratigraphic evidence (conodont biozones), neither the formal rock stratigraphic units recognized by previous workers in the strike belts northwest and southeast of the study area, nor Milici and Smith's (1969) description of the type section rocks is used in this study. Thus, the approach of this study was to look at the lithic type in the context of a depositional environment, regardless of their stratigraphic position and previously proposed lithostratigraphic nomenclature.

3. The environmental framework of these Middle Ordovician rocks is believed to have been very similar to a combination of the following modern carbonate environments: Tidal flats and interior platform of the Greet Bahamian Bank, Florida Bay, Trucial Coast of the Persian Gulf, Shark Bay, and Belize (Ambergris Cay).

4. A combination of fluctuations in sea level, tidal currents, basin subsidence, tectonic activity, and geometry of the basin caused lateral migration of these environments, resulting in a patternless series of complex facies relationships, repeated several times during deposition of the entire Middle Ordovician in the study area.

5. Diagenetic features of these rocks represent several distinct events. These diagenetic features, in approximate order of formation, are: (1) evidence of biological activity (boring, burrowing, micritization), (2) crystal silts, (3) micrite cement, (4) fringe cement, (5) syntaxial overgrowth cement, (6) equant-drusy calcite mosaic cement, (7) neomorphism, (8) dissolution, (9) replacement (silica and dolomite), (10) physical compaction, and (11) pressure solution.

6. Primary and secondary porosity such as inter- and intraparticle, shelter, fenestral, moldic, shrinkage-crack, and fracture porosity was present in these rocks. However, not much of this porosity is now preserved because of cementation and occlusion of these pores.

7. Petrographic and geochemical data provide enough evidence to interpret the process responsible for the concentration of trace elements in these rocks. Correlation coefficient and factor analysis indicate that much of the trace elements such as Na, Mn, and Fe in the Center Point samples have been controlled by detrital minerals, high Mg content of some samples by stylolitization and dolomitization. High Mn/Fe ratios possibly indicate the presence of manganese-bearing

carbonate minerals. The inverse relationship between Sr and I.R. was controlled by original mineralogy of the carbonate sediments (aragonite and calcite).

8. Discriminant function analysis based on geochemical data (three and six parameters), and Mn vs Fe plot, all indicate that two distinct groups and a transitional group of samples are present in the samples analyzed geochemically.

9. Markov Analysis (Gingerich method) defined a very complex pattern characteristic of cyclic sedimentation within these lower Middle Ordovician carbonate sediments. On the other hand, Carr's (1982) modified Markov method has only shown two facies transitions, neither of which are representative of cyclic sedimentation.

REFERENCES

REFERENCES

Aitken, J. D., 1966, Middle Cambrian to Middle Ordovician cyclic sedimentation, southern Rocky Mountains of Alberta: Bull. of Canadian Petrol. Geol., v. 16, p. 275-287.

Alberstadt, L. P., 1973, Depositional environment and origin of the Bigby-Cannon Formation (Middle Ordovician), Central Basin, Tennessee: Jour. Sed. Pet., v. 43, p. 621-633.

Ashworth, J. K., 1982, Depositional environments and paleoecology of the Middle Ordovician rocks in Union County, Tennessee: Univ. of Tennessee, Master's Thesis, 176 p.

Bas Becking, L. G. M., Kaplan, I. R., and Moore, D., 1960, Limits of the natural environment in term of pH and oxidation-reduction potential: Jour. Geol., v. 68, p. 243-284.

Badiozamani, K., 1973, The dorag dolomitization model-application to the Middle Ordovician of Wisconsin: Jour. Sed. Pet., v. 43, p. 965-984.

Ball, M. M., 1976, Carbonate sand bodies of Florida and the Bahamas: Jour. Sed. Pet., v. 37, p. 556-591.

Ball, M. M, Shinn, E. A., and Stockman, K. W., 1967, The geologic effects of hurricane Donna in South Florida: Jour. Geol., v. 75, p. 583-597.

Bambach, R. K., Scotese, C. R., and Ziegler, A. M., 1980, Before Pangea: The geographies of the Paleozoic world: Amer. Sci., v. 68, p. 26-38.

Bassler, R. S., 1932, The stratigraphy of the Central Basin of Tennessee: Tennessee Div. of Geol. Bull. No. 38, 268 pp.

Bathurst, R. G. C., 1958, Diagenetic fabrics in some Dinantian limestone: Liverpool and Manchester Geol. Jour., v. 2, p. 11-36.

_____, 1966, Boring algae, micritic envelopes, and lithification of molluscan biosparities: Geol. Jour., v. 5, p. 15-32.

_____, 1967, Subtidal gelatinous mat, sand stabilizer and food, Great Bahama Bank: Jour. Geol., v. 75, p. 736-738.

_____, 1975, Carbonate Sediments and Their Diagenesis: Developments in Sedimentology 12, Second Edition, Elsevier, New York, 658 p.

Bausch, W. M., 1968, Outlines of distribution of strontium in marine limestone. In Muller, G., and Friedman, G. M. (eds.), Recent Developments in Carbonate Sedimentology in Central Europe: Springer-Verlag, New York, pp. 106-115.

Belvin, William, 1975, Sedimentary environments of the Basal Chickamauga Group in a portion of Raccoon Valley, Anderson County, Tennessee: Univ. of Tennessee, Masters Thesis, 124 p.

Bencini, A., and Turi, A., 1974, Mn distribution in the Mesozoic Carbonate rocks from Lima Valley, Northern Appenines: Jour. Sed. Pet., v. 44, p. 774-782.

Benedict, G. L., and Walker, K. R., 1978, Paleobathymetric analysis in Paleozoic sequence, and its geodynamic significance: Amer. Jour. Sci., v. 278, p. 579-607.

Bergstrom, S. M., 1971, Conodont biostratigraphy of the Middle and Upper Ordovician of Europe and Eastern North America. In Sweet, W. C., and Bergstrom, S. M. (eds.), Symposium on conodont biostratigraphy: Geol. Soc. Amer., Memoir 172, p. 83-162.

_____, 1973, Biostratigraphy and facies relations in the Lower Middle Ordovician of easternmost Tennessee: Amer. Jour. Sci., v. 273-A (Cooper Volume), p. 261-293.

_____, and Carnes, J. B., 1976, Conodont biostratigraphy and paleoecology of the Holston Formation (Middle Ordovician) and associated strata in eastern Tennessee. In Barnes, C. R. (ed.), Conodont paleoecology: Geol. Assoc. Canada Spec. Publ. 15, p. 27-58.

_____, and Line, C., 1979, Biostratigraphy and facies relationships of the Middle Ordovician Holston skeletal and bank complex in eastern Tennessee: Geol. Soc. Amer. Abstracts with Programs, v. 11, p. 171.

Billingsly, P., 1961, Statistical methods in chains: Ann. Math. Stat., v. 32, p. 12-40.

Bird, J. M., and Dewey, J. F., 1970, Lithosphere plate-continental margin tectonics and the evolution of the Appalachian Orogen: Geol. Soc. Amer. Bull., v. 81, p. 1031-1060.

Bishop, Y. A., Fienberg, S. E., and Holland, P. W., 1975, Discrete multivariate analysis: Cambridge, Massachusetts, MIT Press, 557 p.

Blyth, E. W., 1974, Environmental study of a portion of the Middle Ordovician in Sequatchie Valley, eastern Tennessee: Univ. of Tennessee, Dissertation, 197 p.

Bonatti, E., 1966, Deep-Sea authigenic calcite and dolomite: Science, v. 153, p. 534-537.

Boothroyd, J. C., and Hubbard, D. K., 1971, Genesis of estuarine bedforms and cross-bedding: Geol. Soc. Amer. Bull., v. 3, p. 509-510.

Borowski, W. S., 1982, Petrology, depositional environments, and stratigraphic analysis of a part of the Middle Ordovician Chickamauga Group limestones near Clinton, Tennessee: Univ. of Tennessee, Master's Thesis, 239 p.

Brand, U., and Veizer, J., 1980, Chemical diagenesis of a multicomponent carbonate system-1: Trace elements: Jour. Sed. Pet., v. 50, p. 1219-1236.

_____, 1981, Chemical diagenesis of a multicomponent carbonate system-2: Stable isotopes: Jour. Sed. Pet., v. 51, p. 987-998.

Braun, M., and Friedman, G. M., 1969, Carbonate lithofacies and environment of the Tribe Hill Formation (Lower Ordovician) of the Mohawk Valley, New York: Jour. Sed. Pet., v. 39, p. 113-135.

Breland, F. C., 1980, Stratigraphic, paleoenvironmental, and echinoderm distribution patterns in an unfaulted Middle Ordovician (Chickamauga Group) shelf-edge to on-shelf transect in east Tennessee: Univ. of Tennessee, Dissertation, 217 p.

Bricker, O. P., 1971, Carbonate cements: Johns Hopkins Univ. Stud. Geol. 19, 376 p., John Hopkins Press, Baltimore-London.

Brown, M. B., 1974, Identification of sources of significance in two-way contingency tables: Applied Statistics, v. 23, p. 405-413.

Butts, C., 1926, The Paleozoic rocks. In Adams, G. I., Butts, C., Stephenson, L. W., and Cook, W. (eds.), Geology of Alabama: Geol. Survey of Alabama Spec. Rept. 14, p. 41-230.

_____, and Gildersleeve, B., 1948, Geology and mineral resources of the Paleozoic area in northwest Georgia: Georgia Geol. Survey, Bull. 54, 176 p.

Carr, T. R., 1982, Log-Linear model, Markov Chains, and cyclic sedimentation: Jour. Sed. Pet., v. 52, p. 905-912.

Casshyyap, S. M., 1970, Sedimentary cycles and environment of deposition of the Barakar Coal Measures of Lower Gondwana, India: Jour. Sed. Pet., v. 40, p. 1302-1317.

_____, and Khan, Z. A., 1982, Discrete Markov analysis of Permian Coal Measures of East Bakara Basin, Bihar, India: Jour. Ind. Earth Sci., v. 9, p. 99-107.

Cattermole, J. M., 1958, Geology of the Knoxville Quadrangle, Tennessee: U.S.G.S. Geological Quadrangle Maps of the United States, Map GQ 115.

Causey, M. E., Jr., 1956, The Chickamauga rocks of a portion of Raccoon Valley, Western Knox County, Tennessee: Univ. of Tennessee Masters Thesis, 45 p.

Chave, K. E., 1964, Skeletal durability and preservation. In Imbrie, J., and Newell, N. (eds.), Approaches to Paleoecology: John Wiley and Sons, Inc., New York, p. 377-387.

Chayes, F., 1954, The theory of thin-section analysis: Jour. Geol., v. 62, p. 92-101.

Choquette, P. W., and Pray, L. C., 1970, Geologic nomenclature and classification of porosity in sedimentary carbonates: Amer. Assoc. Petrol. Geol. Bull., v. 54, p. 207-250.

Clifton, H. E., 1971, Orientation of empty pelecypod shells and shell fragments in quiet water: Jour. Sed. Pet., v. 41, p. 671-682.

Cloud, P. E., 1962, Environment of calcium carbonate deposition west of Andros Island, Bahamas: U.S. Geol. Surv. Prof. Papers, v. 350, p. 1-138.

Cooper, G. A., 1956, Chazyan and related brachiopods: Smithsonian Inst. Misc. Coll., Pt. I, 1024 p.

Correns, C. W., 1941, Beitrage zur geochemie des eisens und mangans: Nachr. Akad. Wiss. Gothingen, Math-Physik. Klasse, p. 219.

Cotter, E., 1966, Limestone diagenesis and dolomitization in Mississippian carbonate banks in Montana: Jour. Sed. Pet., v. 36, p. 764-774.

Davidson, D. F., and Lakin, H. W., 1961, Metal content of some black shales of the Western United States: U.S.G.S. Prof. Paper, 424-C, p. 329-331.

Davies, G. R., 1970a, Carbonate bank sedimentation, Eastern Shark Bay, Western Australia. In Logan, B. W., Davies, G. R., Read, J. R., and Cebulski, D. E. (eds.), Carbonate sedimentation and environments, Shark Bay, Western Australia: Amer. Assoc. Petrol. Geol. Memoir 13, p. 85-168.

_____, 1970b, Algal laminated sediments, Gladstone Embayment, Shark Bay, Western Australia. In Logan, B. W., Davies, G. R., Read, J. R., and Cebulski, D. E. (eds.), Carbonate sedimentation and environments, Shark Bay, Western Australia: Amer. Assoc. Petrol. Geol. Memoir 13, p. 169-205.

Davies, P. J., 1972, Trace element distribution in reef and subreef rocks of Jurassic age in Britain and Switzerland: Jour. Sed. Pet., v. 42, p. 183-194.

Davis, J. C., 1973, Statistics and data analysis in geology: John Wiley and Sons, Inc., New York, 550 p.

Dayton, P., 1971, Competition, disturbance and community organization: The provision and subsequent utilization of space in a rocky intertidal community: Ecol. Monographs, 41, p. 351-389.

Dickson, J. A. D., 1965, A modified staining technique for carbonates in thin section: Nature, v. 205, p. 587.

Dixon, W. J., and Massey, F. J., Jr., 1957, Introduction to statistical analysis, 2nd ed.: New York, McGraw-Hill Book Co., 488 p.

Doveton, J. H., 1971, An application of Markov chain analysis to the Ayrshire Coal Measures Succession: Scotish Jour. of Geol., v. 7, p. 11-27.

_____, and Skipper, K., 1974, Markov chain and substitutability analysis of a turbidite succession, Cloridorme Formation (Middle Ordovician), Gaspe, Quebec: Canadian Jour. Earth Sci., v. 11, p. 472-488.

Driese, S. G., and Dott, R. H., Jr., 1984, Model for sandstone-carbonate "Cyclothems" based on Upper Member of Morgan Formation (Middle Pennsylvania) of Northern Utah and Colorado: Amer. Assoc. Petrol. Geol., v. 68, p. 574-597.

Duff, P. McL. D., and Walton, E. K., 1962, Statistical basis for cyclothems: A quantitative study of the sedimentary succession in the east Pennine Coal field: Sedimentology, v. 1, p. 235-255.

_____, Hallam, A., and Walton, E. K., 1967, Cyclic sedimentation: Elsevier, Amsterdam, 280 p.

Dunham, R. J., 1962, Classification of carbonate rocks according to depositional textures. In Hamm, W., (ed.), Classification of carbonate rock: Amer. Assoc., Petrol. Geol., Memoir 1, p. 108-121.

_____, 1969, Early vadose silt in Townsend Mound (reef), New Mexico. In Friedman, G. M. (ed.), Depositional environment in carbonate rocks: Soc. Econ. Pale. Min. Spec. Publ. 14, p. 139-181.

_____, 1970, Keystone vugs in carbonate beach deposits: Amer. Assoc. Petrol Geol., Bull, v. 54, p. 845.

Durum, W. H., and Haffty, J., 1961, Occurrence of minor elements in water: United States Geol. Surv. Cir. No. 445, p. 1-11.

Ebanks, W. J., Jr., 1967, Recent carbonate sedimentation and diagenesis, Ambergris Cay, British Honduras: Rice University, Dissertation, 189 p.

Enos, P., and Perkins, R. D., 1979, Evolution of Florida Bay from island stratigraphy: Geol. Soc. Amer. Bull., v. 90, p. 59-83.

Ethier, V. G., 1975, Application of Markov analysis to the Banff Formation (Mississippian), Alberta: International Association for Mathematical Geology Journal, v. 7, p. 47-61.

Evamy, B. D., and Shearman, D. J., 1969, Early stages in development of overgrowth on echinoderm fragments in limestone: Sedimentology, v. 12, p. 317-323.

Evans, G., Kendall, C. G., and Skipwith, P. A., 1964a. Origin of the coastal flats, the Sabkha, of the Trucial Coast, Persian Gulf: Nature, v. 202, p. 759-761.

_____, 1965, Intertidal flat sediments and their environments of deposition in the Washington: Quart. J. Geol. Soc. Lond., v. 121, p. 209-245.

_____, Schmidt, V., Bush, P., and Nelson, H., 1969, Stratigraphy and geologic history of the Sabkha, Abu Dhabi, Persian Gulf: Sedimentology, v. 12, p. 145-159.

Fienberg, S. E., 1977, The analysis of cross-classified categorical data: Cambridge, Massachussetts, MIT Press, 151 p.

Fischer, A. G., 1964, The Lofer Cyclothems of the Alpine Triassic: Kansas Geol. Surv. Bull. 196, p. 107-149.

Folk, R. L., 1959, Practical petrographic classification of limestone: Bull. Amer. Assoc. Petrol. Geol., v. 43, p. 1-38.

_____, 1962, Spectral subdivision of limestone types. In Hamm, W. (ed.), Classification of carbonate rocks: Amer. Assoc. Petrol. Geol., Memoir 1, p. 62-84.

_____, 1965, Some aspects of recrystallization in ancient limestone. In Pray, L. C., and Murray, R. C. (eds.), Dolomitization and limestone diagenesis: A symposium: Soc. Econ. Paleon. and Mineral, Sp. Publ. 13, p. 14-49.

_____, Assereto, R., 1970, Comparative fabrics of length-slow and length fast calcite and calcitized aragonite in a Holocene Spelethem, Carlsbad Carverns, New Mexico: Jour. Sed. Petrol., v. 46, p. 486-496.

Folk, R. L., and Pittman, S. J., 1971, Length-slow chalcedony: A new testament for vanished evaporites: Jour. Sed. Pet., v. 41, p. 1045-1058.

_____, 1974, The natural history of crystalline calcium carbonate: Effect of magnesium content and salinity: Jour. Sed. Pet., v. 44, p. 40-53.

Friedman, G. M., 1959, Identification of carbonate minerals by staining methods: Jour. Sed. Pet., v. 29, p. 87-97.

_____, 1964, Early diagenesis and lithification in carbonate sediments: Jour. Sed. Pet., v. 34, p. 777-813.

_____, 1969, Recognizing tidal environments in carbonate rocks with particular references to those of the Lower Paleozoic in the Northern Appalachian (Abs.): Geol. Soc. America Abs. with programs, v. 15, p. 20-21.

_____, 1969, Trace elements as possible environmental indicators in carbonate sediments. In Friedman, G. M. (ed.), Depositional environments in carbonate rocks: Soc. Econ. Paleontologist Mineralogists, Spec. Publ. No. 14, p. 193-200.

_____, 1970, The Bahamas and South Florida--a model for carbonate deposition: Shale Shaker, v. 21, p. 4-12; discussion p. 17-20.

_____, Barzel, A., and Derim, B., 1971, Paleoenvironments of the Jurassic in the Coastal Belt of Northern and Central Israel and their significance in the search for petroleum reservoir: Geol. Survey Israel, Report OD/1/71, 26 p.

_____, 1972, "Sedimentary Facies" Products of sedimentary environments in Catskill Mountain, Mohawk Valley and Taconic Sequence, Eastern New York State: Guidebook Soc. Econ. Paleontol. Mineral., Eastern Sect., 48 p.

Fritz, P., and Katz, A., 1972, The sodium distribution of dolomite crystals: Chemical Geology, v. 10, p. 237-244.

Garrels, R. M., and Christ, C. L., 1965, Solution, minerals and equilibrium: Harper and Row, New York, 450 p.

Garrett, P., 1970, Phanerozoic Stromatolites: Noncompetitive ecologic restriction by grazing and burrowing animals: Science, 169, 171-173.

_____, 1975, Biological communities and their sedimentary record. In Hardie, L. A. (ed.), Sedimentation on the Modern Carbonate Tidal Flats of Northwest Andros Island, Bahamas: The Johns Hopkins University Press, Baltimore, p. 124-158.

Gavish, E., and Friedman, G. F., 1969, Progressive diagenesis in Quaternary to Late Tertiary carbonate sediments: Sequence and time scale: Jour. Sed. Pet., v. 39, p. 980-1006.

Gebelein, C. D., 1969, Distribution, morphology, and accretion rate of recent subtidal algal stomatolites, Bermuda: Jour. Sed. Pet., v. 39, p. 49-69.

_____, and Hoffman, P., 1971, Algal origin of dolomite in interlaminated limestone-dolomite sedimentary rocks. In Bricker, O. P. (ed.), Carbonate Cements: The Johns Hopkins Univ. Pres, Baltimore, p. 319-326.

Gibbs, R. J., 1973, Mechanisms of trace metal transport in river: Science, v. 180, p. 71-73.

Gingerich, P. D., 1969, Markov analysis of cyclic alluvial sediments: Jour. Sed. Pet., v. 39, p. 330-332.

Ginsburg, R. N., Isham, L. V., Bein, S. J., and Kuperberg, J., 1954, Laminated algal sediments of South Florida and their recognition in the fossil record: Marine Lab., Univ. Miami, Report 54-21, 33 p.

_____, 1956, Environment relationship of grain size and constituent particles in some South Florida carbonate sediments: Amer. Assoc. Petrol. Geol. Bull, v. 40, p. 2384-2427.

_____, 1957, Early diagenesis and lithification of shallow water carbonate sediments in South Florida. In Le Blanc, R. J., and Breeding, J. G. (ed.), Regional aspect of carbonate deposition: Soc. Econ. Paleontol. Mineral. Spec. Publ. No. 5, p. 80-100.

_____, ed., (1964), South Florida carbonate sediments: Ann. Mtg., Miami, Fla., Geol. Soc. America Guidebook for Field Trip No. 1, 72 p.

_____, and Garrett, P., 1969, Seminar on organism-sediment interrelationships: Bermuda Biol. Sta., Res., Spec. Publ. 2, 151 p.

_____, Marszalek, D. S., and Schneiderman, N., 1971, Ultrastructure of carbonate cements in a Holocene algal reef of Bermuda: Jour. Sed. Petrol., v. 41, p. 472-482.

_____, 1971a, Landward movement of carbonate mud: New model for regressive cycles in carbonates (abstr.): Amer. Assoc. Petrol. Geol. Bull, v. 55, p. 34.

_____, 1974, Introduction to comparative sedimentology of carbonate: Bull. Amer. Assoc. Petrol. Geol., v. 58, p. 781-786.

_____, and James, N. P., 1974, Holocene carbonate sediments of continental shelves. In Burk, C. A., and Drake, C. L. (eds.), The Geology of Continental Margin (p. 137-155): Springer-Verlag, Inc., New York, 1009 p.

_____, ed., 1975, Tidal Deposits: A Casebook of Recent Examples and Fossil Cuonterparts: Springer-Verlag Inc., New York, p. 428.

_____, and James, N. P., 1976, Submarine botyroidal aragonite in Holocene Reef limestone, Belize: Geology, v. 4, p. 431-436.

_____, Hardie, L. A., Bricker, O. P., Garrett, P., and Wanless, H., 1977, Exposure index: A quantitative approach to defining position within the tidal zone. In Hardie, L. A. (ed.), Sedimentation on the Modern Carbonate Tidal Flats of Northwest Andros Island, Bahamas: John Hopkins Univ. Press, Baltimore, p. 7-11.

Grover, G., and Read, J. F., 1978, Fenestral and associated vadose diagenetic fabric of tidal flat carbonate, Middle Ordovician New Market limestone, Southwestern Virginia: Jour. Sed. Petrol., v. 84, p. 543-573.

Harbough, J. W., and Bonham-Carter, G. F., 1970, Computer Simulation in Geology: Wiley Interscience, New York, 575 p.

Hardeman, W. D., Miller, R. L., and Swingle, G. D., 1966, Geologic map of Tennessee, east sheet: Tenn. Div. Geology, Scale 1:250,000.

Hardie, L. A., and Ginsburg, R. N., 1975, Layering: The origin and environmental significance of lamination and thin bedding. In Hardie, L. A. (ed.), Sedimentation on the Modern Carbonate Tidal Flats of Northwest Andros Island, Bahamas: The Johns Hopkins University Press, Baltimore, p. 50-123.

_____, and Garrett, P., 1975, General environmental setting. In Hardie, L. A. (ed.), Sedimentation on the Modern Carbonate Tidal Flats of Northwest Andros Island, Bahamas: The Johns Hopkins University Press, Baltimore, p. 12-49.

_____, 1975, Sedimentation on the modern carbonate tidal flats of Northwest Andros Island, Bahamas: The John Hopkins University Press, Baltimore 202 p.

_____, Smoot, J. P., Eugster, H. P., 1978, Saline lakes and their deposits: A sedimentological approach: Spec. Publ. Int. Assoc. Sed., 2, p. 7-41.

Harvell, G., 1954, A geologic study of the Chickamauga Formation of Raccoon Valley, Anderson County, Tennessee: Masters Thesis, Univ. of Tennessee, 40 p.

Hattori, I., 1976, Entropy in Markov chain and discrimination of cyclic patterns in lithologic succession: Jour. Math. Geol., v. 8, p. 477-497.

Hayes, C. W., 1981, The overthrust faults of the Southern Appalachian: Geol. Soc. Amer. Bull., v. 2, p. 141-154.

Heald, M. T., 1956, Significance of stylolites in permeable sandstone: Jour. Sed. Petrol., v. 29, p. 251.

Heckel, P. H., 1972, Recognition of ancient shallow marine environments. In Rigby, J. K., and Hamblin, W. K. (eds.), Recognition of ancient sedimentary environments: Soc. Econ. Paleon. and Min. Spec. Publ. 16, p. 226.

Hirst, D. M., and Nocholls, G. D., 1958, Techniques in sedimentary geochemistar 1. Separation of detrital and nondetrital fraction of limestone: Jour. Sed. Petrol., v. 28, p. 468-481.

Hiscott, R. N., 1981, Chi-square tests for Markov chain analysis: Mathematical Geology, v. 13, p. 69-80.

Hoskin, C. M., 1968, Magnesium and strontium in mud fraction of recent carbonate sediment, Alacran Reef, Mexico: Bull. Amer. Assoc. Petrol. Geol., v. 52, p. 2170-2177.

Illing, L. V., 1954, Bahamian calcareous sands: Bull. Amer. Assoc. Petrol. Geol., v. 38, p. 1-95.

_____, Wel, A. J., and Taylor, J. C. M., 1965, Penecontemporary dolomite in the Persian Gulf, in dolomitization and limestone diagenesis: Soc. Econ. Paleon. and Min. Spec. Publ. 13, p. 89-111.

Irwin, M. L., 1965, General theory of epeiric clear water sedimentation: Bull. Amer. Assoc. Petrol. Geol., v. 49, p. 445-449.

James, N. P., 1972, Holocene and Pleistocene calcareous crust (Caliche) profiles: Criteria for subaerial exposure: Jour. Sed. Petrol., v. 42, p. 817-836.

_____, Ginsburg, R. N., Marszalek, D. S., and Choquette, P. W., 1976, Facies and fabric specifidity of early subsea cement in shallow Belize (British Honduras) reefs: Jour. Sed. Petrol., v. 46, p. 523-544.

_____, and Ginsburg, R. N., 1979, The seaward margin of Belize barrier and atoll reefs: Intern. Assoc. Sediment., Spec. Publ. 3, 191 p.

Jernigan, D. G., 1987, Comparative diagenetic history of the Holston and Rockdell Formation Middle Ordovician of northeastern Tennessee: Univ. of Tennessee, Masters Thesis, 235 p.

Johnson, J. H., 1961, Limestone building algae and algal limestone: Colorado School Mines, 197 p.

Jull, R. K., 1976, Septal development during Hystero-Ontogeny in the Ordovician tabulate coral Foerstephyllum: Jour. of Paleon., v. 50, p. 380-391.

Kalkowsky, E., 1908, Oolith and stromatolith in Nordleutschen Bantsandstein: Dtsch. Geol. Ges., v. 60, p. 68-125.

Katz, A., and Friedman, G. M., 1965, The preparation of stained acetate peels for the study of carbonate rocks: Jour. Sed. Petrol., v. 35, p. 248-249.

Keith, A., 1895, Knoxville folio, Tennessee-North Carolina: U.S. Geol. Surv., Geologic Atlas, Folio No. 16.

Kemeny, J. C., and Snell, J. L., 1960, Finite Markov chains: Van Nostrand, Princeton, N.J., 210 p.

Kendall, C. G., and Skipwith, P. A., 1968, Recent algal mats of a Persian Gulf Lagoon: Jour. Sed. Petrol., v. 38, p. 830-840.

_____, 1969, Holocene shallow-water carbonate and evaporite sediments of Khor Al Bazam, Abu Dhabi, Southwest Persian Gulf: Amer. Assoc. Petrol. Geol. Bull. 53, p. 841-869.

Kendall, A. C., 1975, Postcompactional calcitization of molluscan aragonite in a Jurassic Limestone from Saskatchewan, Canada: Jour. Sed. Petrol., v. 45, p. 891-893.

Kennedy, V. C., 1965, Mineralogy and cation exchange capacity of sediments from selected streams: U.S. Geological Survey Professional Paper 433-D, 28 p.

Kepper, J. C., 1972, Paleoenvironmental pattern in Middle to Lower Upper Cambrian interval in Eastern Great Basin: Amer. Assoc. Petrol. Geol. Bull., v. 56, p. 503-527.

Kinsman, D. J. J., 1969, Interpretation of Sr^{+2} concentration in carbonate minerals and rocks: Jour. Sed. Petrol., v. 39, p. 486-508.

Klein, G. D., 1970, Paleotidal sedimentation: Geol. Soc. Amer. Abstr. with Programs, v. 2, p. 598.

Klovan, J. E., Billing, G. K., 1967, Classification of geological samples by discriminant function analysis: Bull. Canadian Petrol. Geol., v. 3, p. 313-330.

Krumbein, W. C., and Garrels, R. M., 1952, Origin and classification of chemical sediments in terms of Ph and oxidation-reduction potential: Jour. Geol., v. 60, pp. 1-33.

_____, 1965, An introduction to statistical models in geology: McGraw-Hill, New York, 475 p.

_____, 1967, Fortran IV computer programs for Markov chain experiments in geology: Kansas Geol. Survey Computer Centr. 13, 38 p.

_____, 1968, Computer simulation of transgressive and regressive deposits with a discrete-state continuous-time Markov model: Kansas Geol. Survey Computer Contr. 22, p. 11-18.

_____, and Dacey, M. F., 1969, Markov chains and embedded Markov chains in geology: Jour. Math. Geology, v. 1, p. 79-96.

Krauskopf, K. B., 1967, Introduction to Geochemistry: McGraw-Hill, New York, 721 p.

Kumar, N., and Sanders, J. E., 1976, Characteristics of shoreface storm deposits: Modern and ancient examples: Jour. Sed. Petrol., v. 46, p. 393-401.

Land, L. S., and Goreau, T. F., 1970, Submarine lithification of Jamaican reefs: Jour. Sed. Petrol., v. 40, p. 457-462.

_____, 1973, Holocene meteoric dolomitization of Pleistocene limestone, North Jamaica: Sedimentology, v. 20, p. 411-424.

_____, and Hoops, G. K., 1973, Sodium in carbonate sediments and rocks: A possible index to the salinity of diagenetic solutions: Jour. Sed. Petrol., v. 43, p. 614-617.

Laporte, L. F., 1967, Carbonate deposition near mean sea-level and resultant facies mosaic: Manilus Formation (Lower Devonian) of New York State: Amer. Assoc. Petrol. Geol. Bull., v. 51, p. 73-101.

_____, 1971, Paleozoic carbonate facies of the Central Appalachian Shelf: Jour. Sed. Petrol., v. 41, p. 724-740.

Lindholm, R. C., and Finkelman, R. B., 1972, Calcite staining: Semiquantitative determination of ferrous iron: Jour. Sed. Petrol., v. 42, p. 239-242.

Logan, B. W., Rezak, R., and Ginsburg, R. N., 1964, Classification and environmental significance of algal Stromatolites: Jour. Geol., v. 72, p. 68-83.

_____, Davies, G. R., Read, J. F., and Cebulski, D. E., eds., 1970, Carbonate sedimentation and environment, Shark Bay, Western Australia: Amer. Assoc. Petrol. Geol. Memoir 13, 223 p.

_____, Hoffman, P., and Gebelein, C. D., 1974, Algal mats, cryptalgal fabric and structures, Hamelin Pool, Western Australia. In Logan, B. W., Read, J. F., Hagan, G. M., Hoffman, P., Brown, R. G., Woods, P. J., and Gebelein, C. D., (eds.), Evolution and diagenesis of Quaternary Carbonate Sequence, Shark Bay, Western Australia: Amer. Assoc. Petrol Geol. Memoir 22, p. 140-194.

Logman, M. W., 1980, Carbonate diagenetic textures from nearshore diagenetic environments: Amer. Assoc. Petrol Geol., v. 64, p. 24-32.

Lohman, K. C., and Meyers, W. J., 1977, Microdolomite inclusion in cloudy prismatic calcites: A proposed criterion for former high magnesium calcite (abstr.): Geol. Soc. Am. Abst. Programs, v. 8, p. 983.

Lomenick, T. R., 1958, The geology of the Chickamauga Group of a portion of Raccoon Valley, Knox County, Tennessee: Univ. of Tennessee, Masters Thesis, 39 p.

Longman, M. W., 1980, Carbonate diagenetic textures from near-surface diagenetic environments: Amer. Assoc. Petrol. Geol. Bull., v. 64, p. 461-487.

Lowestam, H. A., 1954, Environmental relations of modification composition of certain carbonate secreting marine invertebrates: Natl. Acad. Sci. Proc., v. 40, p. 39-49.

Lucia, F. J., 1962, Diagenesis of a crinoidal sediment: Jour. Sed. Petrol., v. 32, p. 848-865.

_____, 1968, Recent sediments and diagenesis of South Bonaire, Netherland Antilles: Jour. Sed. Petrol., v. 38, p. 945-958.

_____, 1972, Recognition of evaporite-carbonate shoreline sedimentation. In Rigby, J. K., and Hamblin, W. K. (eds.), Recognition of ancient sedimentary environments: Soc. Econ. Paleontol. Mineral. Spec. Publ. 16, p. 160-191.

Lynn, D. C., and Bonatti, E., 1965, Mobility of manganese in diagenesis of deep-sea sediment: Mar. Geol., v. 3, p. 457-474.

MacIntyre, J. G., Mountjoy, E. W., and d'Anglejam, B. F., 1968, An occurrence of submarine cementation of carbonte sediment off the West Coast of Barbados, W.I.: Jour. Sed. Petrol., v. 38, p. 660-664.

_____, 1977, Distribution of submarine cements in a modern Caribbean Fringing Reef, Goleta Point, Panama: Jour. Sed. Petrol., v. 47, p. 503-516.

Mason, B. H., 1966, Principles of Geochemistry: John Wiley and Sons, Inc., New York, 329 p.

Matter, A., 1967, Tidal flat deposits in the Ordovician of Western Maryland: Jour. Sed. Petrol., v. 37, p. 601-609.

Mathews, R. K., 1966, Genesis of recent lime mud in Southern British Honduras: Jour. Sed. Petrol., v. 36, p. 428-454.

_____, 1974, A process approach to diagenesis of reefs and reef associated limestones. In Laporte, L. F. (ed.), Reefs in time and space: Soc. Econ. Paleon. Mineral. Spec. Publ. 18, Tulsa, 256 p.

Mazzullo, S. J., and Friedman, G. M., 1975, Conceptual model of tidally influenced deposition on margins of epeiric seas: Lower Ordovician (Canadian) of Eastern New York and Southwestern Vermont: Amer. Assoc. Petrol. Geol., v. 59, p. 2123-2141.

McGill, M., 1982, Study of the diagenesis of a portion of the Holston Limestone Paragenesis of cements and evaluation of geochemistry: Univ. of Tennessee, Masters Thesis, 103 p.

McLauglin, R. E., 1973, Observation on the biostratigraphy and stratigraphy of Knox County, Tennessee and vicinity: Tennessee Div. Geol. Bull., v. 70, p. 25-62.

Meyers, M. J., 1974, Carbonate cement stratigraphy of the Lake Valley Formation (Mississippian), Sacramentto Mountains, New Mexico: Jour. Sed. Petrol., v. 44, p. 837-861.

_____, 1978, Carbonate cements: Their regional distribution and interpretaton in Mississippian Limestones of Southeastern New Mexico: Sedimentology, v. 25, p. 371-400.

_____, 1980, Compaction in Mississippian skeletal limestones, Southwestern New Mexico: Jour. Sed. Petrol., v. 50, p. 457-474.

Miall, A. D., 1973, Markov Chain analysis applied to an ancient alluvial plain succession: Sedimentology, v. 20, p. 347-364.

Milici, R. C., and Smith, J. W., 1969, The stratigraphy of the Chickamauga Supergroup in its type area: Georgia Geol. Surv. Bull., v. 80, p. 1-35, and Tenn. Div. Geol. Rept. Invs. No. 24.

_____, 1970, Middle Ordovician stratigraphy in Central Sequatchie Valley, Tennessee: Southeastern Geology, v. 11, p. 111-127.

_____, 1973, The stratigraphy of Knox County: Tenn. Div. Geol. Bull., v. 70, p. 9-24.

Monty, C. L. V., 1967, Distribution and structure of recent Stromatolitic algal mats, Eastern Andros Island, Bahamas: Ann. Soc. Geologique de Belgique, v. 90, p. 55-100.

Moore, C. H., 1971, Pseudospar dolomite "Cement" of evaporite solution collapse breccia. In Bricker, O. P. (ed.), Carbonate Cements: The John Hopkins Univ. Press, Baltimore and London, p. 347-351.

_____, Smitherman, J. M., and Allen, S. H., 1972, Pore system evolution in a Cretaceous carbonate beach sequence: Proce. 24th Int. Geol. Congress, Section 6, p. 124-136.

Morrow, D. J., and Mayers, I. R., 1978, Simulation of limestone diagenesis-models based on strontium depletion: Can. Jour. Earth Sci., v. 15, p. 376-396.

Moss, T., 1981, A comparative study of the trace element distribution in limestone, dolomite and breccias in the Upper Knox Group of the Copper Ridge zinc district, East Tennessee: Unpub. Thesis, Univ. of Tennessee, Knoxville, 174 p.

Neuman, R. B., 1955, Middle Ordovician rocks of the Tellico-Sevier belt Eastern Tennessee: U.S. Geol. Survey Prof. Paper 274-F, p. 141-177.

Neuman, A. C., Gebelein, C. D., Scoffin, T. P., 1970, Composition, structure and erodability of subtidal mats, Abaco, Bahamas: Jour. Sed. Petrol., v. 40, p. 274-297.

Newell, N. D., Imbrie, J., Purdy, E. G., and Thurber, D. L., 1959, Organism communities and bottom facies, Great Bahama Bank: Bull. Amer. Mus. Nat. Hist., v. 117, p. 177-228.

Olershaw, A. E., 1971, The significance of ferroan and nonferroan calcite cements in the Halkin and Wenlock Limestone (Great Britain). In Bricker, O. P. (ed.), Carbonate Cements: The John Hopkins Univ. Press, Baltimore, p. 225-232.

Parekh, P. P., Moller, P., and Dulski, P., 1977, Distribution of trace elements between carbonate and noncarbonate phases of limestone: Earth and Planatery Science Letters, v. 34, p. 39-50.

Perkins, R. D., and Enos, P., 1968, Hurricane Betsy in the Florida-Bahamas area. Geologic effects and comparison with hurricane Donna: Jour. Geol., v. 76, p. 710-717.

Pilky, O. H., and Harriss, R. C., 1966, The effects of intertidal environment on the composition of calcareous skeletal material: Limnol. Ocenog., v. 11, p. 381-385.

_____, and Blackwelder, B. W., 1969, Mineralogy of the sand-size carbonate fraction of some recent marine terrigenous and carbonate sediments: Jour. Sed. Pet., v. 38, p. 799-810.

Pinta, M., 1975, Atomic absorption sepctrometry (English, ed.): John Wiley and Sons, New York, 418 p.

Pray, L. C., and Murray, R. C., 1965, Dolomitization and limestone diagenesis: A symposium: Soc. Econ. Paleontol. Mineral. spec. Publ. No. 13, p. 1-18.

Prouty, C. E., 1946, Lower Middle Ordovician of Southwest Virginia and Northeast Tennessee: Amer. Assoc. Petrol Geol. Bull., v. 30, p. 1140-1191.

Purdy, E. G., 1963, Recent calcium carbonate faceis of the Great Bahama Banks. 1. Petrography and reaction groups, and 2. Sedimentary facies: Jour. Geol., v. 71, p. 344-355; 472-497.

Purser, D. H., 1969, Syn-sedimentary marine lithification of Middle Jurassic Limestone in the Paris Basin: Sedimentology, v. 12, p. 205-230.

Radke, B. M., 1978, Carbonate sedimentation in tidal and epeiric environments and diagenetic overprint: The Nimmaroo Formation (Upper Cambrian-Lower Ordovician), Central Australia: Unpubl. Doctoral Dissertation, Rensselaer Polytechnic Institute, 254 p.

Rankama, K., and Sahama, T. G., 1950, Geochemistry: University of Chicago Press, Chicago, 912 p.

Rao, C. P., Naqvi, J. H., 1977, Petrography, geochemistry and factor analysis of a Lower Orodivian subsurface sequence, Tasmania, Australia: Jour. Sed. Pet., v. 47, p. 1036-1055.

Reeckman, A., and Friedman, G. M., 1982, Exploration for carbonate petroleum reservoirs: Elf-Aquitain, Center de Recherches Boussens et de Pau, John Wiley and Sons, New York, 213 p.

Rhoads, D. C., 1967, Biogenic reworking of intertidal and subtidal sediments in Barnstable Harbor and Buzzards Bay, Massachusetts: Jour. Geol., v. 75, p. 461-476.

Robinson, P., 1980, Determination of calcium, Mg, Mn, Sr, Na, and Fe in the carbonate fraction of limestone and dolomites: Chemical Geology, v. 28, p. 135-146.

Rodgers, J., 1953, Geologic map of east Tennessee with explanatory text: State of Tenn., Dept. of Conserv., Div. of Geol. Bulll, v. 58, pt. 1I, 168 p.

_____, 1970, The Taconic Orogeny: Geol. Soc. Amer. Bull., v. 82, p. 1141-1178.

Roeder, D., and Witherspoon, W. D., 1978, Palinspastic map of east Tennessee: Amer. Jour. of Science, v. 278, p. 543-550.

Roehl, P. O., 1967, Stony Mountain (Ordovician) and Interlake (Silurian) Facies analogs of recent low-energy marine and subaerial carbonates, Bahamas: Amer. Assoc. Petrol. Geol. Bull., v. 51, p. 1979-2032.

Ronov, A. B., and Ermishkina, A. I., 1959, Distribution of manganese in sedimentary rocks: Geochemistry, v. 3, p. 254-278.

Ruppel, S. C., and Walker, K. R., ed., 1977, The ecostratigraphy of Middle Ordovician of the Southern Appalachians (Kentucky, Tennessee, and Virginia U.S.A.): A field excursion: Univ. of Tennessee, Dept. of Geological Sciences Studies in Geology No. 77-1, 171 p.

Safford, J. M., 1869, Geology of Tennessee: Nashville: State of Tennessee, 550, p.

Schlanger, S. O., 1963, Subsurface geology of Eniwetok Atoll: U.S. Geol. Surv. Prof. Pap. 260-BG, p. 991-1038.

Schwarzacher, W., 1975, Sedimentary models and quantitative stratigraphy: Elsevier, Amsterdam, 382 p.

Seliacher, A., 1964, Biogenic sedimentary structures. In Imbrie, J., and Newell, N. D. (eds.), Appraoches to Paleoecology: John Wiley and Sons, Inc., New York, p. 296-316.

Shinn, E. A., 1964, Recent dolomite, Sugarloaf Key. In Guidebook for field trip No. 1 Geol. Soc. Am., Convention: Geol. Soc. Am., New York, p. 62-67.

_____, Ginsburg, R. N., and Lloyd, M. W., 1965, Formation of Recent dolomite in Florida and the Bahamas. In Pray, L. C., and Murray, R. C. (eds.), Dolomitizaton and limestone diagenesis: A symposium: Soc. Econ. Pale. Min. Spec. Publ. 13, p. 112-123.

_____, 196, Practical significance of birdseye structures in carbonate rocks: Jour. Sed. Petrol., v. 38, p. 215-223.

_____, Lloyd, R. M., and Ginsburg, R. N., 1969, Anatomy of a modern carbonate tidal flat, Andros Islands, Bahamas: Jour. Sed. Petrol., v. 39, p. 1202-1228.

_____, 1973, Carbonate coastal accretion in an area of longshore transport, Notheast Qater, Persian Gulf. In Purser, B. H., (ed.), The Persian Gulf: Springer Verlag, New York, p. 179-191.

Silk, John, 1979, Statistical concept in Geograpgy: George Allen and Unwin, London, 276 p.

Spears, D. A., 1973, Relationship between exchangeable cations and paleosalinity: Geochimica et Cosmochimica Acta, v. 37, p. 77-85.

Spencer, D. W., 1966, Factor affecting element distributions in a Silurian Graptolite band: Chem. Geol., v. 1, p. 221-249.

Steinen, R. R., 1974, Phreatic and vadose diagenetic modification of Pleistocene Limestone: Petrographic observation from subsurface Barbadose, West Indies: Amer. Assoc. Petrol. Geol., v. 58, p. 1008-1024.

Swingle, G. D., 1964, Elevation of the Chickamauga Group status in East Tennessee (abstract): Tennessee Academy of Science Journal, v. 39, p. 66.

Tebbutt, G. E., Conley, C. D., and Boyd, D. W., 1965, Lithogenesis of a distinctive carbonate rock fabric. Univ. Wyoming Contr. Geol., v. 4, p. 1-13.

Tewari, R. C., and Casshyah, S. M., 1983, Cyclicity in Early Permian fluviatile Gondwana Coal measures: An example from Giridith an Saharjari Bains, Bihar, India: Sedimentary Geology, v. 35, p. 297-312.

Thompson, T. G., and Chow, T. J., 1955, The strotium-calcium ratio in carbonate-secreting marine organisms, in papers in marine biology and oceanograph: Deep-Sea Research, Supp. to v. 3, p. 20-39.

Turnel, R. J., and Swanson, R. G., 1976, The development of Rodriguez Bank, a Holocene mudbank in the Florida reef tract: Jour. Sed. Petrol., v. 46, p. 497-518.

Twnehofel, W. H., Bridge, J., Cloud, P. E., Cooper, B. N., Cooper, G. A., Cummings, E. R., Cullison, J. S., Dunbar, C. O., Kay, G. M., Liberty, B. A., McFarland, A. C., Rodgers, J., Whittington, H. B., Wilson, C. W., 1954, Correlation of the Ordovician Formation of North America: Geol. Soc. Amer., v. 65, p. 247-298.

Urban, H., 1960, Bildugsbedingungen und Faziesverhaltnisse der marin-sedimentaren Eisenerzlageistatte an Kahlenberg bei Ringsheim: Baden. Jahrb. Geol. Landesamt. Baden-Wurtt., v. 8, p. 125-267.

Ulrich, E. O., 1911, Revision of the Paleozoic systems: Geol. Soc. Amer. Bull., v. 22, p. 281-680. Index: v. 24, p. 625-668, 1913.

Van der Plas, L., and Tobi, A. C., 1965, A chart for judging the reliability of point counting results: Amer. Jour. Sci., v. 263, p. 87-90.

Veizer, J., and Demovie, R., 1979, Strontium as a tool in facies analysis: Jour. Sed. Petrol., v. 44, p. 93-115.

_____, 1977, Diagenesis of prequarternary carbonate as indicated by tracer studies: Jour. Sed. Petrol., v. 47, p. 565-581.

_____, Lemieux, J., Jones, B., Gibling, M. R., Savelle, J., 1978, Paleosalinity and dolomitization of a Lower Paleozoic carbonate sequence, Somerset and Prince of Wales Islands, Artic Canada: Can. Jour. Earth Sci., v. 15, p. 1448-1460.

Walker, K. R., 1970, The stratigraphy, environmental sedimentology and community ecology of the Middle Ordovician Black River Group of New York State: Yale Univ., Dissertation, 214 p.

_____, 1973, Stratigraphy and environmental sedimentology of Middle Ordovician Black River Group in the type area-New York State. New York State Mus. Sci. Serv. Bull. No. 419.

_____, and Alberstadt, L. P., 1973, A new facies hypothesis concerning the Middle Ordovician of the Southern Appalachian (abst.): Geol. Soc. Amer., Southeastern Section Meeting, p. 447-448.

_____, 1977, A brief introduction to the ecostratigraphy of the Middle Ordovician of Tennessee (Southern Appalachian, U.S.A.). In Ruppel, S. C., and Walker, K. R. (ed.), The ecostratigraphy of the Middle Ordovician of the Southern Appalachian (Kentucky, Tennessee, and Virginia), U.S.A.: A field excursion: Univ. of Tennesse, Dept. of Geological Sciences, Studies in Geology No. 77-1, p. 12-17.

_____, 1980, Introduction to the stratigraphy and paleoenvironments of the Middle Ordovician of Tennessee (Southern Appalachian, U.S.A.). In Walker, K. R., Broadhead, T. W., and Keller, F. B. (eds.), Middle Ordovician carbonate shelf to deep water deposition in the Southern Appalachian: Univ. of Tennessee, Dept. Geological Sciences, Studies in Geology No. 4, p. 4-12.

_____, Shanmugam, G., and Ruppel, S. C., 1983, A model for carbonate to terrigenous clastic sequences: Geol. Soc. Amer. Bull., v. 94, p. 700-712.

_____, and Diehl, W. W., 1986, The effect of synsedimentary substrate modification on the composition of paleocommunities: Paleoecologic succession revisited: Palaios, v. 1, p. 65-75.

Wanless, H. R., 1979, Limestone response to stress: Pressure solution and dolomitization: Jour. Sed. Pet., v. 49, p. 437-462.

Warme, J. E., 1975, Borings as trace fossils and the processes of marine bioenvironment. In Frey, R. W. (ed.), The Study of Trace Fossils (p. 181-227): Springer-Verlag, New York, 625 p.

Weiss, E. A., 1981, Environmental sedimentology of the Middle Ordovician and paleoecology of a portion of the Witten Formation at Solway, Tennessee: Univ. of Tennessee, Masters Thesis, 229 p.

Wentworth, C. K., 1922, A scale of grade and class terms for clastic sediments: Jour. Geol., v. 30, p. 377-392.

Weyl, P. K., 1961, The carbonate saturometer: Jour. Geol., v. 69, p. 32-44.

Wilson, C. W., 1948, The geology of Nashville, Tennessee: Tenn. Div. Geol. Bull. No. 53, 172 p.

_____, 1949, Pre-Chattanooga stratigraphy in Central Tennessee: Tenn. Div. of Geol. Bull., v. 56, 407 p.

_____, 1962, Stratigraphy and geologic history of Middle Ordovician rocks on Central Tennessee: Tenn. Div. of Geol. Rept. of Inv. No. 15, p. 481-504.

Winland, H. D., 1968, The role of high-magnesium calcite in the preservation of micrite envelopes and textural features of aragonite sediments: Jour. Sed. Petrol, v. 38, p. 1320-1325.

Wong, R. K., and Oldershaw, A., 1981, Burial cementation in the Devonian Kaybob reef complex, Alberta, Canada: Jour. Sed. Petrol, v. 51, p. 507-520.

APPENDICES

APPENDIX A

DESCRIPTION OF MEASURED STRATIGRAPHIC SECTIONS

In this study, four stratigraphic sections, exposed along Highway 58, Tennessee, were measured. These sections are named according to their closeness to the nearest town as follows: Goodfield, Center Point, Ten Mile, and Barnardsville. Thickness of these sections ranges from 425 to 585 meters and measurements were done from the Knox/ Chickamauga contact to the base of the Moccasin Formation. Sample numbers are given with measured thickness from the base of the sections. For convenience of readers, formal rock stratigraphic names of Milici and Smith (1969) are used, but they are only approximations. Note: the numbers of samples which were point counted are underlined with a solid line and samples where thin sections were prepared but not point counted are underlined with dotted line. The thin sections from this study are housed in the collections of the University of Tennessee Department of Geological Sciences.

Measurement Conventions

Grain size descriptions are after the terminology of Wentworth (1922). Terminology for the bed thicknesses used in the field description are based on McKee and Weir (1953), and Ingram (1954). The carbonate rock classification used in the field is the standardized classification of Dunham (1962) and Folk (1962).

Grain Size

Pebbles	4-64 mm
Granules	2-4 mm
Sand	
Very Coarse	1-2 mm
Coarse	1/2-1 mm
Medium	1/4-1/2 mm
Fine	1/8-1/4 mm
Very Fine	1/16-1/8 mm
Silt	1/256-1/16 mm
Clay	less than 1/256 mm

Bed Thickness

Very thick bedded	Greater than 1.0 m
Thick bedded	0.3-1.0 m
Medium bedded	0.1-0.3 m
Thin bedded	0.03-0.1 m
Very thin bedded	0.01-0.03 m
Laminated	0.003-0.01 m
Thin laminated	less than 0.003 m

Location of Goodfield Section (GF)

Chattanooga sheet, Eastern United States 1:25,000 Topographic map, N1 16-3, Series V 501. Section exposed along Goodfield Creek and in pastures on both sides of Highway 58, Tennessee, approximately one mile north of town of Goodfield, Meigs County. Five hundred thirty-two meters of the "Chickamauga Group" carbonate sediments are exposed from the Knox/Chickamauga contact (on the northwest side of Highway 58, Tennessee) to the lower part of the Moccasin Formation (on the southeast side of Highway 58, Tennessee, close to No Pone Ridge).

Goodfield Section (GF)

Unit	Unit Thk (m)	Cum. Thk (M)	Description
1	13.5	13.5	Pond Spring Formation. Well exposed, dark purple to brownish maroon, thin, wavy-bedded, fine-grained dolostone. Rock is sometimes mottled. Macrofossils and stylolites are absent. Chert clasts and mudcracks are abundant. Weathers into thin slabs, some blocky. Contact with the Knox below is well exposed. Samples: GF1A, 6.0 m; GF2A, 12.0 m.
2	37.5	51.0	Pond Spring Formation. Very light, greenish gray and red-green mottled, thin to medium, wavy-bedded, well exposed, fine-grained mudstone and fine- to coarse-grained wackestone/packstones. Lower portion of unit is very fossiliferous with articulated and disarticulated ostracodes, gastropods, trilobites, Hedstroemia, and bivalves (articulated and disarticulated). Fossils become less abundant near top of unit. Bryozoan fragments, pelmatozoan plates, cephalopods, pellets, and intraclasts are also present in the middle and upper portions of unit. Fragmentation is displayed by bryozoans and pelmatozoans. Weathers to yellowish gray, rounded protrusions from ground. Solution-recrystallization, micrite envelope quartz silt, and pelmatozoan plates replaced by silica are also common in the middle and upper part of unit. Horizontal, irregular stylolites and black chert nodules (5%) are present in the middle of unit. Samples: GF3, 15.5 m; GF4, 23.0 m; GF5, 31.5 m; GF6, 36.0 m; GF7, 40.5 m; GF8, 43.5 m; GF9, 49.5 m.
	65.0	116.0	COVERED INTERVAL
3	6.0	122.0	Pond Spring Formation. Greenish gray to reddish, mottled, poorly exposed, thin, wavy-bedded, fine-grained wackestone. Weathers to blocky, rounded protrusions from ground. Fossil allochems include ostracodes,

			bivalves, gastropods, and trilobites. Ostracodes usually display varying degrees of fragmentation and abrasion. Quartz silt also observed. Sample: GF10, 120.5 m.
4	18.0	140.0	Pond Spring Formation. Maroonish dark red to green, very thin-bedded, poorly exposed, fine-grained, red, silty mudstone and green mudstone. Fossils are rare, except for a few unidentifiable fragments. Angular quartz silt, few irregular burrows, and irregular stylolites are also present throughout the unit. Weathers to yellowish, thin slabs. Samples: GF11, 125.0 m; GF12, 135.5 m.
5	4.5	144.5	Murfreesboro Limestone. Dark gray, thin- to medium-bedded, poorly exposed, fine-grained mudstone. Fossil allochems consist mostly of disarticulated ostracodes. Rocks in this unit are slightly bioturbated; vertical burrows are common. Horizontal and irregular stylolites with brownish black insoluble residue are also present. Sample: GF13, 143.0 m.
6	4.5	149.0	Murfreesboro Limestone. Yellowish, light gray to reddish maroon, mottled, poorly exposed, medium-bedded, fine-grained, silty mudstone. Weathers to reddish, thin, flat chips. Fossil allochems are mostly broken and fragmented ostracodes. Angular quartz silt and horizontal and vertical stylolites are abundant. Rock is thoroughly bioturbated, horizontal and irregular burrows are filled with mud, spar, and very small peloids. Sample: GF14, 149.0 m.
7	13.5	162.	Murfreesboro Limestone. Yellowish gray, mottled, poorly exposed, thin- to medium-bedded, fine-grained, silty wackestone. Weathers to yellowish-green, thin slabs. Fossil allochems are dominated by Tetradium and articulated and disarticulated ostracodes. Tetradium specimens are up to 8.0 mm high and are broken, but not abraded. Trilobites, bryozoans, Hedstroemia, and bivalves are present but rare. No preferred orientation is exhibited by allochems. Angular

quartz silt, calcite stringers, and horizontal burrows are observed throughout the unit, but solution-recrystallization of bivalve shells and Tetradium, encrustation by Hedstroemia, and drusy calcite cement are also present.
Sample: GF15, 159.5 m.

8	16.5	179.0	Murfreesboro Limestone. Dark gray to brownish gray, well exposed, thin, wavy- to medium-bedded, fine-grained, laminated mudstone. Laminae are .5 mm in thickness, and thicken on topographic highs. Macrofossils are absent. Fossils are rare but include disarticulated ostracodes. Mudstones are bioturbated with inclined and vertical burrows greater in number than horizontal burrows. Vertical burrows disrupt laminae to varying degrees. Top surfaces of some mudstones display boring. Desiccation fenestrae, quartz silts, vertical calcite stringers, and horizontal, irregular stylolites with brownish black insoluble residue are also present throughout the unit. Weathers to brownish, massive, some lumpy bedding, not real cobbles. Samples: GF16, 173.0 m; GF17, 179.0 m.
9	1.5	180.5	Murfreesboro Limestone. Dark gray, poorly exposed, thin, wavy-bedded, fine- to medium-grained silty wackestone/packstone. Weathers to brownish, thin slabs and chips. Few 0.3 to 0.6 mm diameter oncolites are also present. Scattered fossiliferous patches contain: trilobites, ostracodes, pelmatozoans, and bryozoans. Pellets (unsorted), angular quartz silt solution-recrystallization of moluscan shells, encrustation and micrite envelopes are also observed. Sample: GF18, 180.5 m.
10	29.8	210.3	Murfreesboro Limestone. Maroonish, dark red to greenish gray, poorly exposed, thin-bedded, fine-grained silty red mudstone and greenish gray peloid-fossil wackestone and dolostone. Upper portion of unit is somewhat mottled. Weathers to yellowish green, thin slabs and chips. Fabric is thoroughly bioturbated; horizontal, vertical, and inclined burrows are all common. Burrow walls are

distinct and sharp. Any physical sedimentary structures have been destroyed by burrowing. Near the bottom of the unit some beds show evidence of coarsening upward grain sizes: mud-supported matrix at bottom to peloid-fossil rich, grain-supported matrix on top. Peloids in some places are sorted. Fossil allochems include disarticulated and articulated ostracodes, bryozoan fragments, unabraded trilobites, Hedstroemia and Solenopora sp. Silt-sized, unidentifiable fossil debris is also present throughout the unit. Quartz silt, horizontal and vertical stylolites, pellets, and calcite stringers are observed. Near top of unit wavy lamination is a common structure.

Samples: GF19, 181.8 m; GF20, 184.8 m; GF21, 187.3 m; GF22, 188.8 m; GF23, 191.8 m; GF24, 196.3 m; GF25, 199.3 m; GF26, 206.8 m; GF27, 210.3 m.

	13.5	223.8	COVERED INTERVAL
11	26.5	250.3	Ridley Formation. Light to dark gray, well exposed, thin, wavy- to thick-bedded, fine- to medium-grained wackestone/packstone. Weathers to brownish, dark gray, somewhat cobbly appearance. Horizontal and irregular stylolites with brownish black insoluble residue are relatively abundant. Very fossiliferous: brachiopods, ostracodes, and bivalves are abundant. Gastropods, trilobites, cephalopods, Hedstroemia, Tetradium, pelmatozoans, an bryozoans are present. Allochems have no preferred orientation, but fragmentation and abrasion of bryozoan and Pelmatozoan grains is severe. Bivalves, ostracodes, gastropods, brachiopods, and Tetradium are not abraded or fragmented. Pellets and intraclasts are also present near the lower and middle portions of the unit. Calcite stringers only observed near the top of unit. Scour surfaces, vadose silt, current-oriented shells (convex up), coated grains (pelmatozoan), and intraclasts are common in the middle of unit (GF30).

			Samples: GF28, 225.3 m; GF29, 226.8 m; GF30, 234.3 m; GF31, 239.8 m; GF32, 247.3 m.
12	8.5	258.8	Ridley Formation. Light to dark gray to brownish, well exposed, thin- to medium-bedded, fine-grained wackestone and mudstone. Weathers to dark gray, thin slabs. Calcite stringers, horizontal and irregular stylolites, desiccation fenestrae, current-oriented shell (ostracodes--convex up), and spar- and pellets-filled, horizontal and vertical burrows are present in the lower portion of unit. Algal lamination is prominent in the upper portion of unit. Fossil allochems consist of disarticulated and fragmented ostracodes. Silt-sized, unidentifiable fossil debris is also present in lower portion of unit. Wackestones in the lower portion are composed of coarsening upward grain sizes with basal micrite succeeded by plane lamination and unidentifiable fossil debris. Samples: GF33, 251.8 m; GF34, 257.8 m.
13	9.0	267.8	Ridley Formation. Dark gray, well exposed, medium, wavy- to thick-bedded, fine-grained wackestone/packstone. Weathers into brownish, massive or nodular wackestone. Fossil allochems include trilobites articulated brachiopods, pelmatozoan debris, bryozoans, gastropods, and bivalves. Allochems exhibit varying degree of fragmentation. Micrite envelope, horizontal and inclined stylolites, solution-recrystallization of shell (bivalve and gastropod), vadose silt, drusy cement, and geopetal structures are also observed. Samples: GF35, 262.8 m; GF36, 267.3 m.
14	4.5	272.3	Ridley Formation. Light to dark gray, poorly exposed, fine-grained wackestone. Medium-bedded, somewhat cobbly weathering in portions of unit. Horizontal, irregular stylolites are abundant. Fossil allochems consist mostly of pelmatozoans, ostracodes, and gastropods. Silt- to sand-sized, unidentifiable fossil debris is also present. Rocks in this unit are thoroughly bioturbated; horizontal burrows are more abundant than vertical burrows. Sample: GF37, 271.8 m.

15	3.5	275.8	Ridley Formation. Dark gray to brownish, poorly exposed, thin- to very thin-bedded, fine-grained wackestone. Macrofossils absent. Fossil allochems include trilobites, ostracodes, pelmatozoans, and brachiopod fragments. Pellets and horizontal stylolites are also present. Sample: GF38, 274.8 m.
16	22.5	298.3	Lebanon Limestone. Light to dark gray to greenish gray, well exposed, thin, wavy- to medium-bedded, fine-grained dismicrite/ mudstone and fine- to medium-grained wackestone. Lithologies weather to yellowish gray, thin slabs with scattered beds of chert nodules (%5, upper portion of unit-GF41). Contains birdseyes, horizontal, irregular stylolites, and burrows. Wackestones in the middle and upper portions of unit are slightly fossiliferous: Hedstroemia, articulated and disarticulated ostracodes, pelmatozoan debris, bryozoan fragments, and bivalves. Abraded, current-oriented intraclasts and rounded, sorted pellets are present in the middle of unit, becoming more abundant toward the top. Scour surfaces are also observed in the middle of unit (GF40,41). Samples: GF39, 278.8 m; GF40, 282,3 m; GF41, 293.3 m; GF42, 296.3 m; GF43, 298.3 m.
17	5.1	303.4	Lebanon Limestone. Maroon to red, poorly exposed, very thin- to thin-bedded, fine-grained, red mudstone. Fabric is thoroughly bioturbated; horizontal and vertical burrows are common. Fenestral fabric (parallel to bedding) are also observed. Typical fossil components are disarticulated ostracodes and silt sized, unidentifiable fossil debris. Sample: GF44, 302.8 m.
	20.0	323.4	COVERED INTERVAL
18	1.5	324.9	Lebanon Limestone. Light gray, well exposed, thin to laminated, fine-grained dismicrite. Macrofossils absent. Horizontal birdseyes and fine, crenulated laminae are present. Some laminae are disrupted by vertical

			burrows. Irregular and vertical stylolites with brownish black insoluble residue are common throughout the unit. Sample: GF45, 324.9 m.
19	6.5	331.4	Lebanon Limestone. Light to dark gray, well exposed, thin-bedded, fine-grained wackestone. Somewhat mottled. Horizontal and irregular stylolites and solution-recrystallization are observed. Upper portion of unit is thoroughly bioturbated; horizontal burrows are the dominant type. Fossil allochems dominated by bryozoans, trilobite fragments, articulated and disarticulated ostracodes, Hedstroemia, bivalves, pelmatozoans, and Tetradium are also present. No preferred orientation is exhibited by allochems. All organisms show very little fragmentation and abrasion. Samples: GF46, 327.4 m; GF47, 331.4 m.
20	21.5	352.9	Carters Limestone. Tan to dark gray to brownish gray, well exposed, medium- to thin, wavy-bedded, fine-grained dismicrite to dolomitic mudstone to dolostone. Lower portion weathers somewhat nodular and cobbly. Middle and upper portions of unit weather to a brownish color with beds of black nodular chert protruding from the outcrop. Calcite stringers with black insoluble residue, horizontal, irregular stylolites, and vertical burrows are common throughout the unit. Lamination is present throughout the unit, becoming more abundant toward the top. Middle and upper portions of unit are somewhat mottled and contain mudcracks. Pellets and disarticulated ostracodes are also observed. Samples: GF48, 334.4 m; GF49, 338.4 m; GF50, 342.9 m; GF51, 348.4 m; GF52, 352.9 m.
21	14.0	366.9	Carters Limestone. Dark gray to brown, well exposed, thin, wavy- to medium-bedded, fine-grained mudstone and fine- to medium-grained wackestone/packstone. Weathers into yellowish brown, thick blocks and thin slabs, sometimes cobbly. Contains abundant horizontal and irregular stylolites, calcite stringers, and geopetal structures. Not very fossiliferous near the base of the unit, but fossil

			content increases toward the top. Fossils include bryozoans, articulated and disarticulated brachiopods and ostracodes, trilobites, pelmatozoans, gastropods, Tetradium, and Hedstroemia. Fragmentation and abrasion are displayed by bryozoan, trilobite, and pelmatozoans. Tetradium is present only in the upper portion of unit (GF57). Hedstroemia is also present throughout the unit, becoming more abundant toward the top (GF57). Algal encrustation (on trilobite, bryozoans, Tetradium, and molluscan shells), horizontal and vertical burrows, micrite envelope, and oncolites (?) are also observed in the upper part of unit (GF57). Top surfaces of some wackestone/packstones exhibit scouring. Samples: GF53, 354.4 m; GF54, 355.9 m; GF55, 358.9 m; GF56, 362.4 m; GF57, 365.9 m.
22	20.2	386.9	Carters Limestone. Dark gray to brown, well exposed, thin, wavy-bedded, fine-grained wackestone/packstone. Weathers into yellowish green to gray, thin, small chips. Contains irregular shale laminae, calcite stringers, and stylolites with black insoluble residue. Pyrite nodule is present throughout the unit. Wackestones are composed of disarticulated ostracodes, bryozoans, and brachiopod fragments. Upper portion of unit contains packages that show fining upward grain sizes with a basal lag of coarse, sand-size fossil debris, succeeded by plane lamination (unidentifiable silt-size fossil debris), and homogeneous lime mud. Horizontal and vertical pellets and pyrite-filled burrows are common throughout the unit. Samples: GF58, 374.4 m; GF59, 382.4 m.
23	8.5	395.4	Carters Limestone. Tan to gray, medium- to thick-bedded, medium- to coarse-grained packstone/grainstone. Weathers blocky and massive with a brownish red surface. Very fossiliferous unit, containing articulated and disarticulated brachiopods and ostracodes, Hedstroemia, Solenopora, bivalves, and pelmatozoans. Bryozoans dominate lower and upper portions of unit. Allochems have no preferred orientation or any evidence of

			fragmentation or abrasion. A single Stromatoporoides sp. was observed in lower portion of unit. Pellets, solution-recrystallization, blocky, drusy cement, geopetal structures, and syntaxial overgrowth cement on pelmatozoan fragments were also present. Samples: GF60, 389.9 m; GF61, 391.4 m; GF62, 395.4 m.
24	4.5	399.9	Carters Limestone. Light gray, well exposed, medium, wavy-bedded, fine-grained wackestone. Weathers cobbly, abundant horizontal, vertical, and irregular stylolites. Lower portion of unit is mottled, decreasing toward the top. Fossils include ostracodes, bryozoans, brachiopods, pelmatozoans, trilobites, and abundant silt-size, unidentifiable fossil debris. Horizontal burrows and calcite stringers are also present. Fragmentation and abrasion are severe on all shells. Samples: GF63, 396.9 m; GF64, 399.9 m.
25	13.5	413.4	Carters Limestone. Dark gray to brown, well exposed, medium- to thick-bedded, fine- to medium-grained wackestone/packstone. Weathers cobbly, with abundant stylolites. Shale laminae and horizontal burrows are present in the middle of unit. Wackestones in the lower portion of unit exhibit scouring and coarsening upward grain size; mud at bottom is succeeded by plane lamination (pellets, intraclasts, fossil fragments). Fossil allochems are present in the lower portion of unit becoming more abundant toward the top. Fossils include bivalves, gastropods, bryozoans, pelmatozoans, trilobite, ostracodes, cephalopods, and Tetradium. Articulated brachiopods, gastropods, and intraclasts are dominating allochems in upper portion of unit. Solution-recrystallization, syntaxial overgrowth cement, and encrustation by algae are common near top of unit. All allochems exhibit very little evidence of fragmentation, abrasion, transportation. Samples: GF65, 401.4 m; GF66, 402.9 m; GF67, 404.4 m; GF68, 408.9 m; GF69, 413.4 m.
26	6.0	417.9	Carters Limestone. Dark gray, well exposed, thin-bedded, fine-grained mudstone. Weathers

			cobbly. Stylolites and calcite stringers are present. Fabric is thoroughly bioturbated; horizontal burrows are very abundant. Fossils include bryozoan and ostracode fragments. Sample: GF70, 416.4 m.
27	15.0	432.9	Hermitage Formation. Dark gray to brown, well exposed, medium-grained wackestone/packstone to fine-grained wackestone/mudstone. Weathers to yellowish, thin slabs, sometimes cobbly. Unit appears to have abundant fining upward grain-size packages near base. These packages have a basal peloid/fossil portion succeeded by plane lamination; fragmented, unidentifiable, silt-size fossil debris, and micrite. Wackestone/packstones are in erosive contact with wackestone/mudstone. Borings on erosive surfaces or "hardgrounds" are evident. Trilobites dominate the fossil allochems in the lower portion of unit. Brachiopods, gastropods, bivalves, and bryozoans are allochems present, listed according to abundance throughout the unit. Solution-recrystallization, horizontal and vertical stylolites, calcite stringers, micrite envelope, vadose silt, drusy, bladed calcite, and syntaxial overgrowth cements are also present. Samples: GF71, 420.9 m; GF72, 425.4 m; GF73, 431.4 m.
28	4.5	437.4	Hermitage Formation. Dark gray to light brown to tan, poorly exposed, thin- to medium-bedded, medium-grained wackestone. Horizontal and vertical stylolites and burrows are common. Macrofossils are present, but rare. Fossil allochems consists of fragmented, abraded ostracodes, bryozoans, and clams. Algal encrustation of molluscan grains is also present, but only observed on three grains. Sample: GF74, 435.9 m.
29	4.5	441.9	Hermitage Formation. Light gray to greenish gray, well exposed, medium-bedded, fine- to medium-grained wackestone. Few irregular shale laminae are present in the lower portion of unit. Somewhat mottled. Weathers

			into yellowish, cobbly slabs. Irregular stylolites are abundant. Fossil constituents include bryozoans, ostracodes, bivalves, and gastropods. Sample: GF75, 440.4 m.
30	10.5	452.4	Hermitage Formation. Dark gray to light brown, poorly exposed, thin- to medium-bedded, fine-grained wackestone. Irregular shale laminae, calcite stringers, horizontal and vertical stylolites, and horizontal burrows are also observed throughout the unit. Upper portion of unit contains few laminae exhibiting fining upward grain sizes; fossil-peloid lag at the base is succeeded by micrite. Fossils consist of brachiopods, ostracodes, trilobites, bryozoans, gastropods, and bivalves. Pellets and intraclasts are also common in the upper part of unit. All fossil allochems show very little fragmentation or abrasion. Geopetal structures are also present. Samples: GF76, 449.4 m; GF77, 452.4 m.
31	3.0	455.4	Cannon Limestone. Dark gray to brownish gray, poorly exposed, thin-bedded, fine-grained wackestone/packstone. Weathers into a brownish smooth surface. Unit contains few laminae exhibiting coarsening upward grain sizes: unidentifiable, silt-size fossil debris at base succeeded by plane lamination of fossils and peloids. Contains quartz silt, ripple marks, and geopetal structures. Fossiliferous beds contain: brachiopods, bivalves, bryozoans, ostracodes, and pelmatozoans. Sample: GF78, 455.4 m.
32	15.0	470.4	Cannon Limestone. Light and dark gray, well exposed, thin- to medium-bedded, medium-grained wackestone/packstone at base, mudstone in middle, and fine- to medium-grained packstone toward the top of unit. Weathers into reddish, thin slabs and, in places, into small chips. Rocks in the middle of unit (GF80) are thoroughly bioturbated; inclined burrows are predominant type. Fossils include pelmatozoans, bryozoans (ramose), brachiopods, trilobites, ostracodes, bivalves, and gastropods. Fossils (except pelmatozoans) exhibit little evidence of

			fragmentation or abrasion. Bryozoans and pelmatozoans dominate in the lower portion, pellets and intraclasts in the middle (GF80), and Strophomenid brachiopods in the upper portion of the unit. Planar lamination peloids), solution-recrystallization, syntaxial overgrowth cement, and horizontal, irregular stylolites are present. Samples: GF79, 458.4 m; GF80, 462.9 m; GF81, 465.9 m; GF82, 470.4 m.
33	7.5	477.9	Cannon Limestone. Dark gray, well exposed, thin-bedded, fine-grained mudstone. Weathers to a yellowish, somewhat cobbly appearance. Fossil allochems are mostly brachiopods. Horizontal and vertical burrows and stylolites are abundant. Samples: GF83, 473.4 m; GF84, 476.4 m.
34	48.5	526.4	Catheys Limestone. Greenish gray, poorly exposed, thin to laminated, fine-grained dismicrite/mudstone and medium-grained packstone. Weathers to small chips. Upper portion of unit contains fossiliferous beds (GF91). Fossils include disarticulated and fragmented ostracodes, pelmatozoan debris, brachiopods, trilobites, gastropods, and bryozoans. Rocks in this unit are somewhat mottled. Burrows (horizontal and vertical) and birdseyes are abundant in the lower and middle portions of unit, becoming less abundant toward the top. Mudcrack polygons (5 to 10 cm in diameter), calcite stringers, irregular and vertical stylolites, shale laminae, pellets and intraclasts are all common throughout the unit. Samples: GF85, 479.4 m; GF86, 486.9 m; GF87, 489.9 m; GF88, 442.9 m; GF89, 498.9 m; GF90, 501.9 m; GF91, 510.4 m; GF92, 514.4 m; GF93, 522.4 m.
35	8.0	534.4	Catheys Limestone. Dark gray to reddish brown, well exposed, medium-bedded, medium- to coarse-grained packstone/grainstone and fine- to medium-grained wackestone/packstone. Lithologies weather into reddish rough surfaces. Pelmatozoans, bryozoans, trilobites,

			and gastropods occur as randomly oriented grain. Current-oriented brachiopods (convex up) are abundant near top of unit. Planar-lamination (peloid-fossil laminae) are also observed near the base of unit. Intraclasts, calcite stringers, syntaxial overgrowth, and drusy spar cements are also present. Samples: GF94, 530.4 m; GF95, 532.4 m; GF96, 534.4 m.
36	21.5	555.9	Catheys Limestone. Light gray, well exposed, thin- to medium-bedded, fine- to medium-grained wackestone/packstone. Packstones are present as layers 50 cm thick in the upper portion of unit. Allochems include peloids, intraclasts, highly fragmented and abraded bryozoans and pelmatozoans, articulated and disarticulated brachiopods, abraded Hedstroemia plates, ostracodes, bivalves, and whole or broken gastropods. Middle of unit contains few laminae of fining upward grain sizes, fossil fragments as basal lag succeeded by plane lamination consists of peloid/unidentifiable fossil debris. Inclined burrows, irregular shale laminae, geopetal structures, drusy and syntaxial overgrowth cements are also observed. Samples: GF97, 549.4 m; GF98, 554.5 m; GF99, 555.9 m.
			Moccasin Formation. Not measured. No sample taken.

Location of Center Point Section (CP)

Chattanooga sheet, Eastern United States 1:25,000 Topographic map, N1 16-3, Series V 501. Five hundred ninety-two meters of "Chickamauga Group" exposed along Sewee Creek and in the pastures on the south side of Highway 68, Tennessee, from Highway 58, Tennessee (where Knox/Chickamauga contact is located in the Sewee Creek), to the intersection of Big Sewee Creek and Highway 68, Tennessee, Meigs County

(near the bridge, one mile southeast of town of Center Point where Moccasin Formation is poorly exposed on top of the hill on the river bank).

Center Point Section (CP)

Unit	Unit Thk (m)	Cum. Thk (M)	Description
			KNOX GROUP
			UNCONFORMITY
			CHICKAMAUGA GROUP
1	5.5	5.5	Pond Spring Formation. Bluish dark gray to greenish yellow gray, medium bedded, well exposed (located along edge of Sewee Creek), fine grained cherty dolostone. Abundant red and gray color chert clasts. Macrofossils are absent. No stylolites or burrows were observed. Sharp contact with underlying Knox. Samples: CP1A, 25. m; CP1B1, 5.5 m.
2	3.5	9.0	Pond Spring Formation. Dark gray to brownish and bluish light gray, thin to medium bedded, well exposed, very fine to fine grained silty dolostone. Macrofossils absent. Fossil allochems not abundant, a few ostracodes and trilobites. Weathers to thin slabs, abundant horizontal stylolites. Contains algal laminations, mud cracks, vertical burrows. Algal laminations appear to be more abundant near top of unit. Samples: CP1B, 6.5 m; CP1C, 9.0 m.
	68.5	77.5	COVERED INTERVAL (POND SPRING FORMATION).
3	56.0	133.5	Pond Spring Formation. Intercalated, thin beds of fine grained, dark red silty mudstones with internal green coloration and green, silty calcareous shales. Lower portion not well exposed, weathers to thin slabs. Mudstones display prominent burrow mottling produced by vertical burrows.

			Pellets, quartz-silt filled vertical burrows with distinct walls are prominent. Horizontal burrows are also present. Mudcrack polygons, and desiccation fenestrae are present in the middle portion of this unit. The fabric is usually completely bioturbated, but some samples possess relict laminae. Fossils are rare, except a few disarticulated ostracodes, bryozoans, and Hedstroemia fragments. Fossils display abrasion and breakage. Quartz silt is also abundant. Samples: CP1D, 78.5 m; CP1E, 82.5 m; CP1F, 83.5 m; CP1G, 88.5 m; CP1H, 95.0 m; CP1I, 108.0 m; CP1J, 133.5 m.
4	3.2	136.7	Murfreesboro Limestone. Dark gray, poorly exposed, thin bedded, very fine grained mudstone. Horizontal and vertical stylolites are abundant. Very fine algal laminations present in the upper part of this unit. Quartz silt is also present. Macrofossils are absent. Sample: CP3A, 135.0 m.
5	43.8	180.5	Murfreesboro Limestone. Dark gray to light brown, thin to medium bedded. In the lower portion of the unit beds tend to be wavy, fine to medium grained mudstone/wackestone. Contains few irregular shale laminae, horizontal and vertical stylolites. Weathers to cobbly thin slabs. Quartz silt forming fine crenulated laminae is present in the middle of the unit but much less abundant than in previous unit. Some layers (middle of the unit) fairly fossiliferous; large flat brachiopods, trilobites, pelmatozoan debris, ostracodes, gastropods, algal fragments (unidentifiable), Tetradium, worm tubes, and bivalves. Wackestones contain intraclasts and pellets. Mudstones in the lower portion of the unit contain horizontal and vertical burrows filled with mud, spar, and pellets. Unabraded, unbroken, articulated and disarticulated ostracodes and whole gastropods are the most abundant fossil allochems in the middle of the unit. Fossils are very sparse, only ostracode valves are present in the upper portion of the unit.

Samples: CP5-1A, 150.7 m; CP5,1B, 159.7 m; CP5,1C, 168.7 m; CP5A, 177.2 m.

6	5.0	185.5	Murfreesboro Limestone. Light gray to greenish-gray, poorly exposed, fine grained argillaceous wackestone. Thin, wavy bedded. Quartz silt, and irregular stylolites are present. Fabric is thoroughly bioturbated-inclined burrows filled with pellets and spar. These wackestones are sometimes mottled. Fossils include trilobite, ostracodes, bivalves, Hedstroemia, Solenopora, pelmatozoan debris, and sponge spicules. Scattered fossiliferous patches show varying degrees of abrasion and fragmentation. Samples: CP5B, 184.0 m; CP5C, 185.5 m.
7	.50	186.0	Murfreesboro Limestone. Dark gray to bluish gray, poorly exposed, thin to wavy bedded, fine grained wackestone. Horizontal and vertical burrows (filled with spar), ripple cross laminated, horizontal stylolites, and quartz silts are present. Fossil allochems include ostracodes, trilobites, Hedstroemia, brachiopods and bryozoans. Peloids and intraclasts are present. Peloids are sorted, rounded, fine to medium grained, and show preferred orientation (parallel to bedding). Intraclasts are also rounded and contain abundant fossil fragments. Sample: CP6-1A, 186.0 m.
8	.40	186.4	Murfreesboro Limestone. Dark gray, poorly exposed, thin to medium bedded, fine grained wackestone. Weathers to a light gray-bluish gray with some scattered black chert nodules. Wackestone contains specimens of bryozoan fragments, ostracodes, and abundant sponge spicules. This rock is thoroughly bioturbated (inclined and horizontal burrows), burrow walls are not distinct. Sample: CP6A, 186.4 m.
9	1.5	187.9	Murfreesboro Limestone. Light gray to tan, thin-wavy bedded, poorly exposed, fine grained wackestone-packstone. fossils include trilobite fragments, bivalves (with micrite envelope), articulated and disarticulated ostracodes, bryozoan fragments, and

			minor amount of Hedstroemia clasts. In situ Tetradium corallites dominate this lithology. Moldic fabric due to leaching and recrystallization of Tetradium skeleton is prominent. Hedstroemia-encrusted Tetradium corallites are also present. This rock weathers somewhat nodular-cobbly. Sample: CP7A, 187.9 m.
10	6.0	193.9	Ridley Formation. Greenish gray and brown-red, very thin to thin-wavy bedded, not well exposed, fine grained argillaceous wackestone/silty red mudstone. Contains abundant quartz silt and inclined-vertical burrows (prominent in the upper portion of the unit). Fossil constituents are ostracodes, trilobites, and sponge spicules. All taxa exhibit abrasion and fragmentation. Samples: CP81A, 189.2 m; CP9A, 193.9 m.
11	4.8	198.7	Ridley Formation. Dark gray, thin to medium bedded, well exposed, fine to medium grained packstone. Weathers to thin slabs. Abundant stylo-bedding. Mud content increases toward the top of the unit. Very fossiliferous unit containing flat brachiopods, whole gastropods, articulated and disarticulated unabraded ostracodes, trilobite pieces, bivalves, algal fragments, and abundant pelmatozoan debris. Horizontal and vertical burrows are also present. Fossils (restricted and open marine) exhibit little transportion effects. Moldic fabric; leaching and recrystallization of molluscan shells, and micrite envelopes on bivalve shells are also present. Sample: CP10A, 197.2 m.
12	15.	214.7	Ridley Formation. Greenish to gray, poorly exposed, thin bedded, fine grained argillaceous wackestone and silty-laminated mudstone. Upper portion of this unit is thoroughly bioturbated. Vertical burrows with distinct burrow walls are much more common than horizontal burrows. Coarser constituent particles consist mainly of ostracodes, trilobites, and bryozoans. Weathers to thin yellowish-greenish slabs. Laminations composed of quartz silt dominate in the upper

			portion of the unit. Laminae are about 1 mm or less in thickness and fairly continuous. Samples: CP11A, 203.2 m; CP12A, 213.2 m; CP12B, 214.7 m.
13	8.3	224.1	Ridley Formation. Dark gray to brownish gray, thin to medium bedded, well exposed, fine grained silty wackestone and silty mudstone. Fossil constituents are mostly silt size, unidentifiable fragments and broken-abraded ostracodes and trilobite fragments. Peloids and vertical burrows with diffused walls are also present. Weathering characteristic are such that surface is light yellowish and nodular. General increase in mud vertically in the unit. Wackestones contain planar and cross-ripple laminations; these are much more common in the lower portion of the unit. Samples: CP13A, 219.8 m; CP13B, 224.1 m.
14	2.2	226.3	Ridley Formation. Dark gray, thin-wavy bedded, well exposed, fine to medium grained wackestone/packstone. This unit contains abundant horizontal-irregular stylolites, and is very fossiliferous; articulated brachiopods, ostracodes, pelmatozoan plates, trilobites, whole gastropods, bivalves. Hedstroemia, Solenopora, and a few bryozoan fragments. Fossil allochems show various degrees of abrasion and fragmentation. Solution-recrystallization of gastropod and bivalve shells and encrustation by Hedstroemia (on brachiopod and bivalve shells) are also observed. Sample: CP14A, 226.3 m.
15	25.1	251.4	Ridley Formation. Light-dark gray, dark brownish and greenish gray, thin to medium bedded, fine to medium grained wackestone/packstone. Irregular stylolites fairly abundant. Lower portion not well exposed. Middle and upper portions fairly well exposed. In the middle portion of the unit fossil and intraclast packstone beds are intercalated with mud rich layers. Top of the unit has layers composed of fining upward grains, grain size varies from medium grained

			packstone to fine grained mudstone. This is a very fossiliferous unit. Allochems include peloids, intraclasts, unabraded-fragmented ramose bryozoans, articulated brachiopods, broken trilobites, Hedstroemia plates, ostracode valves, and pelmatozoan plates. Mudstones are always bioturbated with horizontal burrows much more abundant than vertical burrows. Solution-recrystallization of molluscan shells, micrite envelope on brachiopod shells, and syntaxial overgrowth cement on pelmatozoan plates is also common in the middle and upper portion of the unit. Samples: CP14B, 230.0 m; CP15A, 235.6 m; CP16A, 251.4 m.
16	46.5	297.9	Ridley Formation. Greenish gray, dark gray, and brownish; thin to medium bedded, well exposed, fine grained mudstone. Weathers to yellowish, somewhat cobbly thin slabs. Irregular and horizontal, discontinuous stylolites are abundant. Allochems include broken, fragmented and abraded pelmatozoan debris, bryozoans, ostracodes, trilobites, and pellets. Burrows (horizontal and vertical), planar and ripple-cross laminations are common throughout the middle and upper portions of the unit. Encrustation by bryozoans on echinoderm fragments is also observed. Samples: CP16B, 266.4 m; CP16C, 281.4 m; CP16D, 285.9 m; CP16E1-16E2, 297.9 m.
17	13.6	311.5	Lebanon Limestone. Greenish gray, thin to medium-wavy bedded, poorly exposed, fine grained dismicrite/mudstone. Weathers to light yellowish gray, thin flat chips. Birdseyes, fine crenulated laminae (in the upper portion of unit), mudcracks, calcite stringers, and burrows (inclined and horizontal) are present. Constituent particles consist mostly of ostracode and trilobite fragments. Samples: CP17A, 300.9 m; CP17B, 305.4 m; CP18A, 309.9 m.
18	21.7	332.2	Lebanon Limestone. Intercalated thin to medium beds of red mudstones and greenish

			gray argillaceous wackestones. This unit is thoroughly bioturbated; horizontal burrows greater in number than vertical burrows. Burrow walls are distinct. Fossil allochems are less common and are represented by ostracode, bryozoan, and trilobite fragments. Detrital quartz silt is ubiquitous. Wackestones near the top of the unit contain numerous laminae of storm accumulated fossil fragments which are cut by vertical burrows. Samples: CP19A, 314.0 m; CP19B, 316.5 m; CP20A, 318.0 m; CP20A2, 319.5 m; CP21A2, 324.9 m; CP22A, 327.9 m; CP22B, 331.4 m; CP22C, 332.2 m.
19	5.1	338.1	Lebanon Limestone. Greenish gray, poorly exposed, fine grained dismicrite/mudstone. Thin bedded, weathers to yellowish-greenish, thin, flat chips. Fossil allochems include broken, abraded, unidentifiable sand to silt size fragments. Birdseyes, mudcracks, horizontal and vertical burrows, quartz silt, pellets, and algal laminations are present. Samples: CP23A, 333.7 m; CP24A1, 336.7 m; CP24B, 338.2 m.
20	18	356.2	Carters Limestone. Light bluish to light gray, very well exposed, medium bedded, fine grained cherty packstone-wackestone. Weathers to a light gray with beds of black, nodular chert protruding from the outcrop. Contains few irregular, vertical and discontinuous stylolites, articulated and disarticulated ostracodes with geopetal structures, quartz silts, algal fragments, birdseye, and burrows (irregular). Sponge spicules is also present and comprise 10 to 15% of thin sections. Samples: CP25A, 341.2 m; CP25B, 346.2 m; CP25C, 351.2 m; CP25D, 356.2 m.
21	10.0	366.2	Carters Limestone. Light gray to bluish gray, very well exposed, very thin-wavy bedded, fine grained mudstone. Fossil allochems consist mainly of disarticulated ostracodes. Weathers to a greenish-gray

			cobbly, thin slabs. Few quartz silt grains, vertical-irregular, discontinuous stylolites, and fine crenulated internal laminae are also present. Sample: CP26A, 359.2 m.
22	37.5	403.7	Carters Limestone. Light gray to bluish, well exposed, very thin bedded, fine grained wackestone/mudstone. Vertical burrows are dominated in the lower portion of the unit and are spar, mud, and pellet filled. Vertical burrows are represented by 0.5 to 15 mm tubules with distinct walls. Ostracodes are represented by valves and valve fragments. Hedstroemia plates, horizontal stylolites and calcite stringers are also present. Samples: CP26B, 369.2 m; CP26C, 376.7 m; CP26D, 294.7 m; CP26E, 401.7 m.
23	8.2	411.9	Carters Limestone. Greenish to light gray, well exposed, medium bedded, fine grained wackestone. Fossil allochems mostly articulated and disarticulated, mud and spar filled ostracodes, few gastropods, and Hedstroemia fragments. Abundant horizontal and vertical stylolites. Pink-reddish calcite stringers and few inclined burrows are observed. Sample: CP26F, 409.9 m.
24	2.70	414.6	Hermitage Formation. Maroon-brownish to dark red, thin to medium bedded, well exposed, fine grained wackestone/mudstone. Dominant fossil allochems consist of ostracode fragments (abundant in the lower portion of the unit). Somewhat mottled. Vertical burrows, mudcracks, quartz silts abundant. Sample: CP27R, 412.6 m.
	50.0	464.6	COVERED INTERVAL.
25	64	528.6	Cannon Limestone. Dark gray to brownish, medium-wavy (lower portion of the unit) to thick bedded (middle and upper portions), very well exposed, medium to coarse grained packstone/grainstone and fine to medium grained wackestone. Horizontal stylolites with black-brownish organic residue fairly abundant. Scour surfaces, shale laminae,

			calcite stringers and planar laminations are also present. Lower and middle portions of this unit are very fossiliferous and contain articulated brachiopods, whole gastropods, unabraded-unbroken trilobites, bivalves, pelmatozoans, ostracodes, bryozoans and few Tetradium fragments. Not very fossiliferous near the top of the unit; fossil allochems near top are mostly of whole gastropods. Bored gastropods shells and horizontal and vertical burrows are also present in the upper portion of unit. Packstone and grainstones in the lower portion of the unit have abundant layers of coarsening and fining upward grain size, whereas packstone/wackestones in the upper portion of unit show only fining upward grain size. Restricted and open marine fauna display very little evidence of transportation. Pellets, intraclasts, and current oriented grains are observed in packstone/grainstone in the middle of unit (CP-E, CP-F). Other features include micrite envelopes, geopetal structures, and solution-recrystallization of molluscan shells. Samples: CP28A, 470.1 m; CP28B, 475.7 m; CP28C, 481.7 m; CP28D, 488.2 m; CP28E, 493.8 m; CP28F, 500.3 m; CP28G, 507.3 m; CP28H, 514.9 m.
26	4.5	533.1	Cannon Limestone. Greenish gray to dark brownish red, poorly exposed, thin to medium bedded, fine grained argillaceous wackestone and red mudstone. Allochems consist mostly of broken ostracodes and few bryozoan fragments. Mudstone is thoroughly bioturbated; horizontal, vertical and inclined. Burrow tubes are spar, mud, and pellet-filled with distinct walls. Horizontal burrows display high density and are much more abundant than the vertical burrows. Argillaceous wackestone is somewhat mottled. Samples: CP29A, 531.1 m; CP29A2, 533.1 m.
27	24.3	557.4	Cannon Limestone. Dark gray to brownish, well exposed, medium to thick bedded, fine to medium grained packstone/wackestone. Weathers to reddish-yellowish cobbles. Horizontal

			and vertical burrows and irregular-discontinuous stylolites are present. In upper portion of unit bioturbation has disturbed layering. Fossil allochems consist of fragmented, broken and abraded brachiopods, pelmatozoans, ostracodes, bryozoans, and Hedstroemia. Packstones are composed of moderately to well sorted, fine-grained peloids and abraded, fragmented and sorted fossil fragments. Grains (fossils and pellets) near bed bottom tend to be oriented parallel to laminae. Samples: CP29B, 541.2 m; CP29C, 549.3 m; CP29D, 557.4 m.
28	16.2	573.6	Catheys Formation. Dark gray to brownish, well exposed, thin bedded, fine grained wackestone and fine to medium grained peloids wackestone/packstone. Abundant irregular, vertical and horizontal stylolites with black organic rich residue. Calcite stringers are also present. Fossil allochems are much fewer than in underlying unit. Allochems include ostracodes, pelmatozoan debris, trilobite fragments, brachiopods, Hedstroemia plates, and unidentifiable silt-size fossil fragments. Intraclasts and pellets are abundant in the upper portion of unit. Fine to medium grained peloidal wackestone/packstone display faint lamination and gradual change from pelbiosparite to pelbiomicrite within some of the laminae. Solution-recrystallization and replacement of shells (molluscan) by silica is also observed. Samples: CP29E, 565.6 m; CP29F, 573.6 m.
29	24.3	597.9	Catheys Formation. Greenish to gray, poorly exposed, thin bedded, fine grained mudstone/dismicrite. Horizontal, vertical, and inclined burrows are common. Vertical burrows much more abundant than others and destroyed primary sedimentary structures (lamination). Desiccation fenestrae and mudcracks are notable (CP29H). Fossils are rare, disarticulated, fragmented ostracodes are present in the lower and middle of the unit. Intraclasts, algal lamination, current oriented shells (convex up) are also present. Middle portion of the unit contains packstone

			laminae. Some laminae display fining upward grains size, storm accumulated shells, homogeneous mud, and birdseyes. Birdseyes and mudcracks are less common near the top of the unit. Samples: CP29G, 581.7 m; CP29H, 589.8 m; CP29I, 597.9 m.
30	24.3	622.2	Catheys Formation. Light gray-tan, to dark gray, thin bedded, well exposed, fine to medium grained wackestone/packstone. In upper portion of the unit layers are truncated by scour surfaces and are overlain by peloid-fossil packstone which display planar laminations. Horizontal stylolites abundant. Macrofossils absent. Horizontal and inclined burrows (lower portion of unit), and calcite stringers are also present. Bryozoan, ostracodes, trilobites, brachiopods, pelmatozoan debris, pellets and intraclasts are common. All fossils are fragmented and abraded. Unidentifiable silt-size fossil debris is common and this together with the fragmented nature of all fossils suggests transportation. The lower and upper portions of this unit are composed of several low amplitude ripples with intervening mud layers and mud drapes. Upper portions of some samples are laminated, with laminae disturbed by vertical burrows. Samples: CP29J, 606.0 m; CP29K, 614,1 m; CP29I, 622.2 m.
31	5.0	627.2	Catheys Formation. Gray to bluish, thin bedded, well exposed, coarse grained packstone. Fossil allochems include brachiopods, algae (Hedstroemia ?), trilobites and whole gastropods. Unabraded, unfragmented ramose bryozoans present in significant number. Rocks in the lower portion of the unit (wackestones) were probably "firm ground" when bored and scoured. Irregular stylolites, intraclasts, rounded peloids, geopetal structures, and drusy spar cement are also present throughout the unit. Sample: CP30, 627.2 m.

32	3.0	630.2	Catheys Formation. Maroon-dark red and greenish gray, well exposed, very thin bedded, fine to medium grained peloids-fossils packstone/wackestone. Current-oriented fossils consist mostly of brachiopods. Fossils become more fragmented and less abundant at top of unit. Birdseye and planar laminations are common toward the top. Sample: CP31, 630.2 m.
			Moccasin Formation. Not measured. No sample taken.

Location of Ten Mile Section (TM)

Chattanooga sheet, Eastern United States 1:25,000 Topographic map, N1 16-3, Series V 501. Four hundred ninety-two meters of Middle Ordovician, "Chickamauga Group," are exposed on both sides of Highway 58, Tennessee, and along Ten Mile road from approximately 25 meters south of Ten Mile Post Office (Ten Mile Quarry or Hurricane Creek) to approximately 180 meters on the northwest side of Highway 58, Tennessee, Meigs County (from the intersection of Highway 58, Tennessee, and Ten Mile road). Section is measured from the Knox/Chickamauga contact on the northwest side of Highway 58 to the axis of Ten Mile Ridge (syncline).

Ten Mile Creek Section

Unit	Unit Thk (m)	Cum. Thk (M)	Description
			KNOX GROUP
			UNCONFORMITY
			CHICKAMAUGA GROUP

1	25.5	25.5	Pond Spring Formation. Greenish gray and red-maroon, fine-grained, poorly exposed, thin-bedded; clayey mudstone, red quartz-silt mudstone and argillaceous wackestone. Fabric is thoroughly bioturbated, vertical burrows being more abundant than horizontal burrows. Weathers to greenish-yellowish, sometimes pinkish, thin slabs and small chips. Wackestones in the upper portion of unit contain articulated and disarticulated ostracodes, Solenopora, bryozoan fragments, and trilobites. Severe fragmentation and abrasion are clearly evident in all organisms. Stylolites, quartz-silt, irregular-discontinuous birdseyes, and geopetal structures are present. Contact with unconformity is sharp and well exposed. Samples: TM1, 1.5 m; TM2, 7.5 m; TM3, 13.5 m; TM4, 15.0 m; TM5, 16.5 m; TM6, 19.5 m; TM7, 25.5 m.
2	3.0	28.5	Pond Spring Formation. Medium gray, fine-grained, well exposed, thin-bedded mudstone/dismicrite. Weather surface is greenish-yellowish. Vertical stylolites, discontinuous birdseyes, quartz-silt, calcite stringers, vertical-inclined burrows, and broken ostracodes are observed. Sample: TM8, 28.5 m.
3	7.5	36.0	Pond Spring Formation. Green and maroon to dark red, poorly exposed, fine-grained, medium- to thick-bedded, red and green, quartz-silt and shaley mudstones. Horizontal and vertical burrows and stylolites are present. Fossils include bryozoans, disarticulated ostracodes, and trilobite fragments. Worm tubes are also present in upper portion of unit. Samples: TM9, 31.5 m; TM10, 36.0 m.
	10.5	46.5	Covered Interval.
4	6.0	52.5	Pond Spring Formation. Dark gray, poorly exposed, fine-grained mudstone. Weathers into thin beds. Stylolites are abundant; chert and iron oxide nodules can be observed

			near top of unit. Disarticulated ostracodes, bryozoans, quartz-silt, and calcite stringers are also present throughout the unit. Sample: TM11, 51.0 m.
5	27.75	80.25	Pond Spring Formation. Intercalated green, very thin-bedded mudstone and red, thin-bedded, silty mudstones. Weathers cobbly. Upper portion of unit has wackestone beds. Rocks in lower portion of unit (TM12,13) are alternating 1 mm laminae of mud and quartz-silt. Vertical burrows with distinct burrow walls and mudcracks are present. Wackestones in upper portion of unit contain specimens of crinoid columns, bryozoans (ramose), trilobites, brachiopods, and fragmented and disarticulated ostracodes. Hedstroemia and Solenopora sp. are present in amounts. Samples: TM12, 58.5 m; TM13, 66.0 m; TM14, 69.5 m; TM15, 71.0 m; TM16-1, 72.75 m; TM16-2, 75.75 m.
	19.5	99.75	Covered Interval.
6	18.0	117.75	Murfreesboro Limestone. Light gray, fine-grained, medium- to thick-bedded, mudstone/wackestone-packstones. Rocks in upper portion of unit (TM18-2) are bioturbated mudstone, while lower and middle portions are gastropod-ostracode-Tetradium wackestone or packstones. Tetradiums are broken but not abraded. Pelmatozoans and bryozoans are present and exhibit a high degree of fragmentation and abrasion. Gastropods are whole, and ostracodes are both articulated and disarticulated. Trilobites, clams, brachiopods, and worm tubes are present in small amounts. Peloids are common, and range from 0.1 to 0.2 mm in size. Wackestones in upper portion of unit weather cobbly and exhibit fining-upward sequences: fossils as lag at bottom, succeeded by homogeneous mud on top. Solution-recrystallization of molluscan and Tetradium skeletons, geopetal structures, calcite stringers, stylolites, horizontal burrows, and drusy calcite cement are common throughout the unit. Samples: TM17-1, 102.75 m; TM17-2, 107.25 m; TM18-1, 111.75 m; TM18-2, 114,75 m.

7	9.0	126.75	Murfreesboro Limestone. Dark gray, well exposed, fine- to medium-grained wackestone-packstone. Rocks in this unit become coarser grained near top of unit. Weathers cobbly. Stylolites are abundant. Fossil allochems include pelmatozoans, ostracodes, trilobites, brachiopods, gastropods, cephalopods, bivalves, and worm tubes. Drusy calcite cement and geopetal structures are present throughout the unit. Sample; TM19-1, 123.75 m.
	13.0	139.75	Covered Interval.
8	15.0	154.75	Murfreesboro Limestone. Gray and yellowish-gray, poorly exposed, fine-grained wackestone and mudstone/dismicrite. Very thin- to thin-bedded. Weathers to light, olive gray, thin chips. Fossil fragments, primarily ostracodes, Solenopora, gastropods, pelmatozoan plates, and a few brachiopods, are common. Vertical burrows, mudcracks (near top of unit), and geopetal structures are present. desiccation fenestrae are present throughout the unit, becoming more abundant toward the top. Samples: TM20, 141.25 m; TM20-1, 144.25 m; TM20-2, 147.25 m; TM21, 148.75 m; TM22, 153.25 m.
9	12.0	166.75	Murfreesboro Limestone. Dark gray to brownish gray, medium-bedded wackestone/packstone and gray mudstone/dismicrite. Wackestone/packstones are largely composed of intraclasts, abraded bryozoans, pelmatozoans, gastropods, brachiopods, trilobites, articulated bivalves, and disarticulated ostracodes. Peloids are common; intraclasts are bored. Allochems exhibit varying degrees of abrasion and fragmentation. Vertical and horizontal burrows, stylolites, solution-recrystallization, calcite stringers, and geopetal structures are present throughout the unit. Rocks in the upper portion of unit contain fining-upward grain sizes (TM23-3). Samples: TM23, 156.25 m; TM23-1, 157.75 m; TM23-2, 159.25 m; TM23-3, 162.25 m.

10	6.0	172.75	Murfreesboro Limestone. Light gray to yellowish gray, well exposed, fine-grained wackestone/mudstone. Very thin- to thin-bedded, weathers to small, flat chips. Horizontal stylolites, and horizontal, inclined burrows with distinct walls are abundant. Macrofossils are scarce. Some Solenopora sp. fragments and disarticulated ostracodes are present. Sample: TM23-4, 169.75 m.
11	13.75	186.25	Murfreesboro Limestone. Light gray to greenish gray, poorly exposed, very thin, wavy-bedded, fine-grained, argillaceous-bioturbated wackestone/mudstones intercalated with medium- to thin-bedded, dark red-maroon bioturbated mudstones. Weathers to light, yellowish gray, pale green and pinkish, thin chips. Some layers are slightly fossiliferous, the most abundant being, Tetradium, disarticulated and fragmented ostracodes, Solenopora sp., gastropods, pelmatozoans and worm tubes. Fabric is thoroughly bioturbated; vertical, inclined, and horizontal burrows are all common. Vertical burrows with distinct walls in upper portion of unit (TM28) are short and stubby. Ostracodes in middle of unit exhibit preferred orientation, parallel to bedding. Solution-recrystallization and vertical, calcite stringers are also observed. Samples: TM25, 175,75 m; TM26, 180.25 m; TM27, 183.25 m; TM28, 185.0 m; TM29, 186.25 m.
12	3.0	189.25	Murfreesboro Limestone. Gray, well exposed, medium- to thick-bedded, fine-grained wackestone/packstone. Restricted water fauna, ostracodes and gastropods exhibit little transportation effects, Solenopora sp., Hedstroemia, and trilobites display varying degrees of abrasion and fragmentation. worm tubes are common throughout the unit. Horizontal, irregular stylolites are very abundant in lower part of unit. Sample: TM30, 188.0 m.

13	30.0	219.25	Ridley Limestone. Light gray to light brown, poorly exposed, thin- to medium-bedded, fine-grained, ostracode-Tetradium, wackestone/packstone. Ten cm thick lenses of peloidal packstones also occur at middle of unit (TM32). Bioturbated fabric is present near upper part of unit (TM34); however, some relict, current-emplaced and current-oriented allochems are present. Dolomites are common and associated with stylolites. Irregular birdseyes are also present. Lower portion of unit (TM32) weathers to yellowish-gray, thin slabs. Ostracodes, trilobites, bivalves, gastropods, Tetradium, rounded pelmatozoan debris, bryozoans, and Solenopora sp. are present throughout the unit. However, restricted marine fauna display less fragmentation and are more abundant than open marine forms, such as bryozoans and pelmatozoans. Samples: TM31, 195.25 m; TM32, 202.75 m; TM33, 208.75 m; TM34, 216.25 m.
14	3.0	222.25	Ridley Limestone. Light gray, very well exposed, medium-grained, Tetradium-intraclast packstone. Interlaminar, continuous fenestral fabrics are present at bottom of beds. Fossils include articulated and disarticulated ostracodes, abraded pelmatozoans, and trilobites. Green intraclasts and fine- to medium-grained pellets are very abundant. Sample: TM35, 222.25 m.
15	9.0	231.25	Ridley Limestone. Dark gray to light brown, well exposed, fine-grained wackestone. Weathering characteristics are such that thin to medium beds produce resistant ledges in the creek. Rocks in this unit break with concoidal fractures. Fossils include ostracodes, rounded pelmatozoans, gastropods, Tetradium fragments, a few articulated bivalves, brachiopods, and trilobites. Rounded to subangular, fine- to medium-grained peloids are abundant in upper part of unit, whereas unidentifiable fossil fragments are predominant in lower part. Inclined and horizontal, peloid-spar-filled burrows, stylolites, and irregular birdseyes are abundant throughout the unit.

			Samples: TM36, 223,75 m; TM37, 226.75 m; TM37-1, 229.75 m.
16	10.5	241.75	Ridley Limestone. Gray to light brown, well exposed, thin- to medium-bedded, fine-grained wackestone and bioturbated mudstones. Vertical and horizontal burrows are abundant. Middle of unit (TM39A) contains few 5 cm thick brachiopod-pelmatozoan grainstone laminae (storm-accumulated skeletal fragments). Fossils include Solenopora sp., trilobites, bivalves, brachiopods, gastropods, and pelmatozoans. Worm tubes, pellets, intraclasts, and unidentifiable fossil debris are also present. Upper part of unit (TM39B) contains large, orthocone cephalopods. Weathers cobbly. Vertical calcite stringers are also observed. Samples: TM38, 232.75 m; TM39A, 238.75 m; TM39B, 241.75 m.
17	6.0	247.75	Ridley Limestone. Dark gray, well exposed, medium-bedded, fine-grained, bioturbated wackestone. Bioturbation is very intense; burrowing has apparently destroyed any current-orientation display by allochems. Fossils include brachiopods, bryozoans, pelmatozoans, gastropods, bivalves, trilobites, Solenopora sp., and Hedstroemia. Allochems display no preferred orientation. All fossils exhibit fragmentation and abrasion. Samples: TM39C, 244.75 m; TM39D, 247.75 m.
18	6.0	253.75	Ridley Limestone. Light gray, very well exposed, thin- to medium-bedded, fine-grained packstone. Constituents include peloids, pelmatozoan debris, gastropods, trilobites, disarticulated brachiopods, and unidentifiable fossil debris. Particles show varying degrees of roundness and are well sorted. Horizontal burrows are very abundant near the base of unit. Sample: TM39E, 252.25 m.
19	18.0	271.75	Ridley Limestone. Brown to dark gray, well exposed, thin-bedded, fine-grained bioturbated wackestone/mudstone. Horizontal and

			vertical burrows are prominent, horizontal burrows being more common. Vertical burrows are short and stubby. Bioturbation decreases toward the top of unit. Weathers to dark gray, very indurated, rounded protrusions from the ground. Stylolitization is abundant. Scattered fossiliferous patches contain disarticulated ostracodes, Tetradium fragments, trilobites, gastropods, and brachiopods. Unidentifiable fossil debris is also present throughout the unit. Samples: TM38F, 258.25 m; TM39G, 262,75 m; TM39H, 267.25 m.
20	21.0	292.75	Lebanon Limestone. Light gray to bluish gray to dark brown, well exposed, fine-grained, thin, wavy-bedded packstone/wackestone in lower and upper part, and medium- to coarse-grained, medium-bedded packstone in middle of unit. Both irregular and horizontal, peloid-spar filled burrows occur. Allochems have no preferred orientation. Peloids in upper part of unit (TM39J) are well sorted. Fossils include bored bryozoans, algal-coated brachiopods, Solenopora sp., pelmatozoan debris, trilobites, gastropods, and bivalves. Pelmatozoans are abundant in middle of unit. Boring, solution-recrystallization, algal encrustation, and strophominid brachiopods are present only in lower portion of unit (TM39I). Weathers blocky and massive. Stylolites are abundant. Samples: TM39I, 273.25 m; TM39J, 280.75 m; TM39K, 288.25 m.
21	22.5	315.25	Lebanon Limestone. Light brown to light gray, well exposed, thin, wavy- to medium-bedded, fine-grained mudstone and medium- to coarse-grained packstone. Small scale, planar and cross lamination, and megascopic fining-upward sequences are observed (TM39M, 39N). Allochems include pellets, ostracodes, pelmatozoans, bryozoans, gastropods, brachiopods, bivalves, trilobites, Solenopora sp., and intraclasts. Physical, soft-sediment, deformation features (slump structure, TM39-O), vertical calcite stringers, geopetal

			structures, and solution-recrystallization are also present throughout the unit. Lower part of some beds are heavily bioturbated with horizontal burrows more common than vertical burrows. Packstones are in erosive contact with mud-supported beds near the top of unit and display planar and cross laminations. Top surfaces of some mudstone beds are "hardground" or omission surfaces. Samples: TM39L, 294.25 m; TM39M, 297.25 m; TM39N, 300.25 m; TM39-0, 303.25 m; TM39P, 307.75 m; TM39Q, 312.25 m; TM39R, 315.25 m.
22	1.5	316.75	Lebanon Limestone. Light gray to light blue, medium-bedded, well exposed, fine-grained wackestone. Allochems include unidentifiable, fossil debris. Vertical and horizontal burrows are present. Weathers massive and breaks with concoidal fractures. Sample: TM39S, 316.75 m.
23	14.5	329.75	Lebanon Limestone. Light gray to yellowish-greenish gray, poorly exposed, thin- to medium-bedded, fine-grained argillaceous wackestone interbedded with greenish-yellow, thin-bedded shale. Shale weathers to small flat chips. Continuous, horizontal birdseyes, mudcracks, vertical burrows, and horizontal stylolites are present. Bottom of some beds contains fossiliferous horizon of ostracodes, trilobites, worm tubes, and sorted pellets (storm deposit). Contact between shale and fossiliferous beds is sharp. Burrows are present throughout the unit but become more abundant toward the top (TM40A). Samples: TM39T, 318.25 m; TM40,, 323.75 m; TM40A, 329.75 m.
24	24.9	353.75	Carters Limestone. Light brown to dark gray to tan, thin, wavy-bedded, poorly exposed, fine-grained bioturbated wackestone and fine- to medium-grained packstone. Numerous horizontal and irregular stylolites are present. Rocks weather to a yellowish gray color with pitted surfaces. Sediment in the lower part of unit is bioturbated; horizontal and vertical burrows are common. Unidentifiable

fossil debris is abundant throughout the unit. Identifiable fossils include brachiopods, bryozoans, pelmatozoans (with overgrowth cement), trilobites, coated molluscan skeletons, worm tubes, gastropods, and disarticulated ostracodes. Current-generated, planar lamination (brachiopod shells are convex up), geopetal structures, and silicification (brachiopods) are present in middle of unit (TM41A).
Samples: TM41, 340.25 m; TM41A, 349.25 m; TM41B, 353.75 m.

25 12.0 365.75 Carters Limestone. Light gray and brownish gray, well exposed, fine-grained, thin, wavy- to medium-bedded packstone, and medium- to coarse-grained, medium- to thick-bedded, brachiopod-gastropod grainstone. Both packstones and grainstones display planar and cross laminations and fining-upward sequences with a basal lag of coarse sand to pebble fossil debris (brachiopod and gastropods), succeeded by bioturbated mud. Horizontal burrows are prominent at top of unit. Fossils are all fragmented and abraded. Allochems present, listed in order of decreasing abundance, are: brachiopods, gastropods, ostracodes, trilobites, bryozoans, pelmatozoans, Solenopora sp., Hedstroemia, and Kazakstanelia (?). Rocks in this unit weather into a gray, massive bedding with a reddish stain. Geopetal structures, syntaxial overgrowth cement on pelmatozoan grains, shelter cavities (brachiopod) and silica-replacement of brachiopod shells are common throughout the unit.
Samples: TM41C, 356.75 m; TM41D, 359.75 m; TM41E, 364,25 m; TM41F, 365.75 m.

26 13.5 379.25 Carters Limestone. Greenish gray to yellowish gray, poorly exposed, thin-bedded, very fine-grained, argillaceous wackestone and mudstone. Weathers to pale green, thin slabs and small chips. Macrofossils are scarce. Some disarticulated ostracodes, horizontal birdseyes, fine, crenulated laminae, mudcracks, worm tubes, and burrows (vertical and horizontal) are present.

Samples: TM42, 368.75 m; TM42A, 373.25 m; TM42B, 377.75 m.

27	7.5	386.75	Carters Limestone. Dove to bluish gray, well exposed, thin, wavy- to medium-bedded, medium-grained packstone. Several fossiliferous laminae with sharp and irregular contact with underlying beds are present in middle of unit. Horizontal and irregular stylolites, pellets, and bored intraclasts are common throughout the unit. Fossils include brachiopods, bryozoans, pelmatozoans, trilobites, ostracodes, worm tubes, and Solenopora sp. Fossils show varying degrees of fragmentation and abrasion. Weathers blocky with a light brown to reddish color and rough surfaces. Sample: TM42C, 385.25 m.
28	13.5	400.25	Carters Limestone. Dark gray to light brown, well exposed, fine-grained, thin- to medium-bedded wackestone/packstone. Weathers massive and blocky. Horizontal and irregular stylolites are abundant. Fossils include brachiopods and ostracodes mostly. Fossils are heavily fragmented and abraded. Pellets and unidentifiable fossil debris are abundant throughout the unit. Rocks in this unit are thoroughly bioturbated; only horizontal burrows with diffuse walls occur. Bioturbation decreases toward the top of unit. Current-formed laminae of unidentifiable fossil debris are common near the top of unit (TM43B,43C). Samples: TM43, 394.25 m; TM43A, 397.25 m; TM43B, 298.75 m; TM43C, 400.25 m.
29	13.5	413.75	Carters Limestone. Dove to light, bluish gray, well exposed, thin- to medium-bedded, fine- to medium-grained packstone and fine-grained mudstones. Mudstones are thoroughly bioturbated, displaying prominent vertical and less numerous horizontal burrows. Many beds in upper part of unit exhibit planar and cross laminations and fining-upward sequences. All fossil allochems are abraded and fragmented to some degree. Organisms include brachiopods, ostracodes, gastropods,

			pelmatozoans, and molluscs. Rounded, ellipsoidal, fine-grained peloids and intraclasts are also present throughout the unit. Samples: TM43D, 401.75 m; TM44, 407.75 m; TM44B, 410.75 m; TM44C, 412.25 m.
30	27	440.75	Hermitage Formation. Light green to light gray, well exposed, thin- to medium-bedded, fine- to medium-grained peloidal packstone and maroon to red, thin-bedded, very fine-grained, bioturbated mudstones. Both vertical and horizontal, pellet-filled burrows occur. Peloids are of uniform size between 0.03-0.04 mm. Allochems have no preferred orientation. Fossils include fragmented Tetradium, and disarticulated ostracodes. Angular intraclasts, large mudcracks, horizontal, irregular fenestrae, and pink, calcite stringers are also present throughout the unit but are more abundant toward the top of unit. Rocks weather into a maroonish or brownish color, taking a cubic or rectangular form in lower part of unit and forming small, flat chips in upper part. Some beds in upper portion are also slightly mottled (TM44C). Samples: TM45A, 421.25 m; TM45B, 425.75 m; TM45C, 430.25 m; TM45D, 433.25 m; TM45E, 436.25 m.
	13.5	454.25	Covered Interval.
31	21.0	475.25	Cannon Limestone. Bluish gray, well exposed, thin, wavy- to medium-bedded, medium- to coarse-grained, bryozoan-pelmatozoan packstone and fine- to medium-grained wackestones. Wackestones are abundant in upper part of unit (TM46E,46F). Unit displays both current-oriented allochems in planar laminae and fining-upward sequences, molluscan debris as a lag, succeeded by fossil debris on top. Bed surfaces in middle of unit (TM46C) display rugose corals and strophominid brachiopods. Open-marine fossils are greater in abundance than restricted water fauna. All fossils exhibit fragmentation and abrasion. Fossils include pelmatozoans, bryozoans,

brachiopods, trilobites, bivalves, gastropods, ostracodes, and Solenopora sp. Irregular stylolites, overgrowth calcite cement on pelmatozoan plates, drusy-blocky calcite cements, coated grains (bryozoan, mollusc), and silica-replacement of brachiopod skeletons are also observed throughout the unit. Rocks in this unit weather blocky and cobbly.
Samples: TM46, 454.25 m; TM46B, 458.75 m; TM46C, 463.25 m; TM46D, 466.25 m; TM46E, 467.75 m; TM46F, 470.75 m.

32 6.0 481.25 Cannon Limestone. Dark gray to brownish gray, well exposed, fine-grained, thin- to medium-bedded, mollusca wackestone. Weathers blocky and at surface is flaggy and nodular. Fossil constituents are mostly unabraded and unbroken clams, but broken, abraded, and fragmented ostracodes, bryozoans, and pelmatozoans are also present. Clam skeletons are current-oriented, parallel to bed, and convex-up. Irregular stylolites, vertical burrows, and silica replacement of clam shells are also observed throughout the unit. Rocks in this unit display moldic fabric due to leaching and recrystallization of clam skeletons.
Samples: TM46G, 437.75 m; TM46H, 476.75 m.

33 18.5 499.75 Cannon-Catheys Formation (?). Light gray to tan, well exposed, medium- to thick-bedded, medium- to coarse-grained, pelmatozoan-brachiopod-bryozoan packstones and gastopod packstones. Very fossiliferous: articulated and disarticulated brachiopods, whole and broken gastropods, foliated bryozoans, pelmatozoans, ostracodes, trilobites, Solenopora sp., and Hedstroemia. Fossils become more fragmented at top of unit. Brachiopods, gastropods, bryozoans, and pelmatozoans are the dominant organisms throughout the unit. Also common in this unit are: solution-recrystallization of molluscan skeletons, syntaxial overgrowth cement on pelmatozoan plates, drusy-blocky calcite cements, adhered mud (on brachiopods and trilobites), boring of brachiopod shells, algal encrustation on gastropod and brachiopod skeletons, shelter

cavities, and horizontal stylolites. Rocks weather massive with rough surface and concoidal fractures.
Samples: TM46I, 482.75 m; TM46J, 488.75 m; TM46K, 492.75 m; TM46L, 495.75 m.

Moccasin Formation. No measurement. No sample taken.

Location of Barnardsville Section (B)

Chattanooga sheet, Eastern United States 1:25,000 Topographic map, N1 16-3, Series V 501. Four hundred fifty-eight meters of "Chickamauga Group" (from approximately 6 meters above the Knox/Chickamauga contact to the axis of Ten Mile Ridge (syncline)) is exposed on both sides of Highway 58, Tennessee, Roan County (mainly on the southeast side of Highway 58), near the town of Barnardsville, 2.5 miles south of intersection of Highway 72 and 58, Tennessee.

Barnardsville Section

Unit	Unit Thk (m)	Cum. Thk (M)	Description
			KNOX GROUP
			UNCONFORMITY
			CHICKAMAUGA GROUP
	9.0	9.0	Covered Interval.
1.	33.0	42.0	Pond Spring Formation. Dark red-maroon or greenish gray, well exposed, thin- to medium-bedded, fine-grained, red and green quartz-silt mudstone/wackestone-packstones, and quartz-silt ostracode wackestone-packstones. Fabric is thoroughly bioturbated: vertical, inclined, and horizontal

burrows all are common. U-shaped burrows are also present in the upper part of unit (B-99). Mudstones in lower part of unit (B-106, 105, 104) display prominent burrow mottling produced by vertical burrows. Vertical burrows are pellet-spar filled, and burrow walls are distinct but not sharp. Mudcracks, irregular stylolites, calcite stringers, and irregular fenestral fabric are present throughout the unit. Fossils are rare but include articulated and disarticulated ostracodes, trilobite and brachiopod fragments, worm tubes, pelmatozoan debris (B-103), and Hedstroemia plates (B-97). Weathers to pale green and light red, thin slabs and small flat chips.

Samples: B105, 13.5 m; B104, 19.5 m; B103, 22.5 m; B102, 24.0 m; B101, 27.0 m; B100, 28.5 m; B99, 33.0 m; B98, 34.5 m; B97, 42.0 m.

2	10.5	52.5	Pond Spring Formation. Gray and greenish-gray, well exposed, medium-bedded, fine-grained green mudstone, ostracode wackestone, and quartz-silt, red and green mudstone/ wackestone-packstone. Allochems within this unit are randomly oriented due to bioturbation. Ostracodes are articulated, disarticulated, and fragmented and dominate the fossil allochems. Trilobites, bryozoans, and Hedstroemia are fragmented and abraded. Gastropods and worm tubes are rare. Any physical sedimentary structures have been destroyed by burrowing. Both vertical and horizontal, pellet-spar filled burrows occur. Irregular birdseyes, calcite stringers, coated grains (molluscs), quartz-silt, unidentifiable fossil debris, and mud cracks can be observed throughout the unit. Weathers to small flat chips.

Samples: B96, 43.5 m; B95, 45.0 m; B94, 46.5 m; B93, 48.0 m; B92, 49.5 m; B91, 52.5 m.

	4.5	57.0	Covered Interval.

3	13.5	70.5	Pond Spring Formation. Greenish gray, well exposed, thin- to medium-bedded, fine-grained, green mudstone/wackestone-packstones. Both horizontal and vertical burrows are present; both are pellet-spar filled. Fabric is bioturbated, but some samples possess relict laminae. One to .5 mm mud-rich and quartz-silt laminae are intercalated (B90). Fossils are few in number but include disarticulated ostracodes, trilobite fragments, and unidentifiable fossil debris. Lithologies weather to light yellowish green, thin, small flat chips. Quartz-silt and mud cracks are present. Samples: B90, 58.5 m; B89, 60.0 m; B88, 69.0 m.
	7.5	78.0	Covered Interval.
4	3.0	81.0	Murfreesboro Limestone. Dark gray to bluish gray, well exposed, medium-bedded, medium-grained pelmatozoan packstone-grainstones. Constituents include bryozoan, pelmatozoan debris, trilobites, brachiopods, algae (Hedstroemia, Solenopora, Nuia), algal oncolite (?), intraclasts, and molluscan fragments. Pelmatozoans and bryozoans are well rounded and sorted. Throughout the unit the following are observed: algal encrustation on echinoderm plates; micrite envelope (on trilobite and mollusc skeletons); marine fibrous, blocky and syntaxial overgrowth calcite cements; silicified fossils (brachiopods, bryozoans, pelmatozoans); and silt-sized unidentifiable fossil debris. Sample: B87, 81.0 m.
	7.5	88.5	Covered Interval.
5	6.0	94.5	Murfreesboro Limestone. Light-medium gray to bluish gray, well exposed, thin-bedded, medium-grained packstone. Dobbles are produced on weathering. Constituents include peloids, pelmatozoan debris, gastropods, trilobites, ostracodes (articulated and disarticulated), brachiopods, bivalves, and worm tubes. rocks in this unit exhibit megascopic small scale fining-upward sequences in some horizons:

			peloid-fossil debris at bottom, succeeded by gastropod-molluscan and bioturbated mud. Vertical burrows are common, but horizontal burrows rare. All fossil groups exhibit varying degrees of fragmentation and abrasions. Sample: B86, 93.0 m.
	36.0	130.5	Covered Interval.
6	9.0	139.5	Murfreesboro Limestone. Bluish light gray to medium, dark gray, well exposed, thin, wavy-bedded, fine- to medium-grained, gastropod packstones. Allochems include gastropods (up to 50% volume), bivalve, tribite fragments, a few bryozoans, articulated brachiopods, pellets, and a few pieces of Hedstroemia. Gastropods are present as whole or broken fragments. Some beds exhibit coarsening-upward sequences: bioturbated mud at bottom, succeeded by gastropod-rich horizon. Geopetal structures and solution-recrystallization are common throughout the unit. Weathers cobbly. Samples: B85, 132.0 m; B84, 139.5 m.
7	13.5	151.5	Murfreesboro Limestone. Dark gray to light, brownish gray, well exposed, thin, wavy- to medium-bedded, medium-grained Tetradium-pelmatozoan packstone-grainstones. Thickness of beds in the upper part of unit increases (medium to thick). Bioturbation is present (horizontal and vertical). Most fossils are fragmented. In order of decreasing abundance, fossils include: Tetradium, pelmatozoan debris, trilobites, bryozoans, brachiopods, Hedstroemia, molluscs and worm tubes. Horizontal and vertical stylolites and mud cracks are present in upper part of unit (B80). some shale laminae are present in lower part where they weather to small flat chips. Samples: B83, 142.5 m; B82, 145.5 m; B81, 150.0 m; B80, 151.5 m.
8	13.5	165.0	Murfreesboro Limestone. Medium dark gray to light brown, well exposed, medium, wavy-bedded, fine- to medium-grained mollusc

			wackestone-packstone, and bioturbated mudstones. In lower part of unit, few, very thin, shale laminae interbedded with dark gray-brown mollusc packstone are present. Constituents include articulated and disarticulated ostracodes, molluscs, trilobite fragments, few bryozoans, brachiopods and pellets. Most fossils, both open marine and restricted fauna, are fragmented and abraded. Horizontal stylolites are abundant on outcrop. Weathering of irregularly spaced shale drapes in lower part produces cobbly appearance. Wackestone in lower and middle portion of unit exhibits small fining-upward sequences in some horizons. Tabular cross beds are present only in upper part of unit (B77). Burrows, horizontal, inclined, and vertical, vadose silts, solution-recrystallization of molluscan shells, calcite stringers, and unidentifiable fossil debris are observed throughout the unit. Fossil debris becomes more abundant upsection. Samples: B79, 153.0 m; B78, 156.0 m; B77, 162.0 m.
9	3.0	168.0	Murfreesboro Limestone. Light gray to bluish gray, well exposed, very thin, wavy-bedded to laminated, fine-grained quartz-silt wackestone and wackestone-packstone. Laminae are 1 mm or less in thickness and are continuous. Mud-rich laminae and quartz-silt laminae are intercalated and are common only near the top of the unit (B75). Vertical burrows disrupt laminae to varying degree. Allochems include disarticulated ostracodes, Hedstroemia, unidentifiable fossil debris and quartz-silt. Irregular birdseyes, and horizontal burrows with diffuse walls are also present throughout the unit. Samples: B76, 166.5 m; B75, 168.0 m.
10	2.0	170.0	Murfreesboro Limestone. Gray, thin- to medium-bedded, fine- to medium-grained wackestone and Tetradium packstones. Fossils include disarticulated and fragmented ostracodes, and Tetradium corals as single coralites or heads. Moldic porosity due to leaching and recrystallization of Tetradium skeletons is

			common on top of unit (B73). Horizontal and inclined burrows and stylolites are also observed in this rock. Samples: B75, 169.5 m; B73, 170.0 m.
11	1.5	171.5	Murfreesboro Limestone. Medium gray to bluish gray, well exposed, medium-bedded, coarse-grained, intraclast-packstone-grainstones. Constituents include intraclasts (with fossil debris), Tetardium, bryozoans, brachiopods, ostracodes, trilobites, pelmatozoans, and Hedstroemia. All fossil groups exhibit varying degrees of abrasion and fragmentation. Sample: B72, 171.5 m.
12	.5	172.0	Murfreesboro Limestone. Dark gray, well exposed, medium- to thick-bedded, medium-grained cherty packstone. Black chert nodules and lenses are common. Allochems include trilobites, ostracodes, and sponge spicules. Cobbles are produced on weathering. Calcite stringers are also present. Sample: B71B, 172.0 m.
13	4.0	176.0	Murfreesboro Limestone. Red-maroon and green, well exposed, medium-bedded, fine-grained, red wackestone and green, quartz-silt mudstones. Allochems include disarticulated and broken ostracodes, and unidentifiable fossil debris. Beds weather into small, thin chips. Rocks are thoroughly bioturbated; vertical burrows are greater in number than horizontal burrows at lower part of unit, whereas in upper part, horizontal burrows are more common. Burrow walls are distinct and sharp. Angular quartz-silt is common in upper part of unit (B70). Samples: B71, 174.5 m; B70, 176.0 m.
14	19.5	195.5	Ridley Limestone. Tan to light gray, well exposed, thin- to medium-bedded, fine-grained wackestone/Tetradium wackestone and thin, wavy bedded bioturbated wackestone-mudstones. Both wackestone and mudstones display burrowing; vertical, inclined, and horizontal burrows are all common. Any physical sedimentary structures have been destroyed by burrowing. Trilobites, bryozoans, gastropods,

			brachiopods, and Hedstroemia are always fragmented and abraded. Ostracodes are abraded and unabraded, articulated and disarticulated. Tetradium usually display fragmentation and abrasion. Orthocone cephalopods are only present in upper part of unit (B66). Pellets worm tubes, calcites stringers, stylolites, and irregular-discontinuous birdseyes are also present throughout the unit. Moldic fabric due to solution and recrystallization of Tetradium and gastropods and geopetal structures are common in lower part of unit (B69, 68), Weathers cobbly. Samples: B69, 179.0 m; B68, 182.0 m; B67, 188.0 m; B66, 192.0 m.
15	12.0	207.5	Ridley Limestone. Light to dark gray, well exposed, medium, wavy- to thick-bedded, medium-grained packstone-wackestones. Fossils include abraded bryozoans, articulated and disarticulated ostracodes, strophominid brachiopods, trilobite fragments, Hedstroemia, gastropods (whole and broken), bivalves, and pelmatozoan debris. Pellets, calcite stringers, and unidentifiable fossil debris are also present throughout the unit. Packstones in upper part of unit exhibit fining-upward sequences with a basal lag of medium sand to silt-sized fossil debris succeeded by bioturbated mud. Packstone in middle part of unit (B64) also contains low amplitude (0.1-0.2 mm) ripple cross-laminations. Samples: B65, 198.5 m; B64, 200.0 m; B63, 204.5 m.
16	17.0	224.5	Ridley Limestone. Dark gray, well exposed, thin- to medium-bedded wackestone; and light gray to bluish gray, thin-bedded ostracodes packstone; thin, wavy-bedded peloid-fossil packstones and tan, bioturbated mudstones. Packstones exhibit packages of fining-upward sequences with a basal lag of coarse sand sized, fossil debris, succeeded by plane-laminated peloids or ostracodes and bioturbated mud (B61). Coarsening-upward packages are also observed in middle of unit (B60): bioturbated mud at bottom, succeeded by

peloids-fossil packstone. Fossils include fragmented bryozoans and Tetradium, articulated and disarticulated ostracodes, trilobites, strophominid brachiopods, Hedstroemia, bivalves, gastropods (whole and broken), and unidentifiable fossil debris. Molluscs predominant in upper part of unit (B59). Pellets, intraclasts, burrows, horizontal and vertical, and calcite stringers are also present throughout the unit. Weather into thin slabs in lower part of unit and cobbles toward the top.
Samples: B62, 209.5 m; B61, 211.0 m; B60, 212.5 m; B59, 216.5 m; B58, 224.5 m.

	34.0	258.5	Covered Interval.
17	19.5	281.0	Ridley Limestone. Medium to dark gray to light brown-tan, well exposed, medium-bedded grainstone. Some shale laminae are present in upper part of section. Beds weather blocky. Horizontal stylolites are present. Allochems within this unit are oriented parallel to beds. Planar and cross laminations and low amplitude ripples are present throughout the unit. Brachiopods, bryozoans, and cephalopods are unbroken and unabraded, and brachiopods may be either articulated or disarticulated. Pelmatozoans, trilobites, ostracodes, bivalves and Hedstroemia exhibit varying degree of fragmentation and abrasions. Pelmatozoans and bryozoans are the dominant allochems in upper part of unit (B55,54). Sorted peloids and rounded intraclasts with fossil debris are present and probably are transported grains. Syntaxial overgrowth cement (on pelmatozoans), pore-filling drusy and blocky calcite cements and micrite rim (on molluscs skeletons) are also present throughout the unit. Samples: B57, 261.5 m; B56, 268.5 m; B55, 274.0 m; B54, 281.0 m.
18	5.0	286.0	Lebanon Limestone. Tan to light gray-bluish gray, well exposed, thin, wavy- to medium, wavy-bedded, fine-grained wackestone. Burrows are present; horizontal burrows outnumber vertical burrows. Burrow walls are

			distinct. Allochems include trilobites, molluscs, brachiopods, pelmatozoan debris, and unidentifiable fossil debris. Fossils are all broken and fragmented. Current-oriented fossil debris (planar lamination) is common. Samples: B53, 284.5 m; B52, 286.0 m.
19	6.0	292.0	Lebanon Limestone. Light gray to bluish, dark gray, tan, well exposed, thin, wavy to medium-bedded, medium- to coarse-grained, brachiopod-bryozoan packstone. Bryozoans, pelmatozoans and brachiopods are dominant allochems; bryozoans are unbroken-unabraded, brachiopods (strophominids) are articulated or disarticulated, and pelmatozoans are abraded and exhibit syntaxial overgrowth cement. Disarticulated ostracodes, trilobite fragments, and molluscs are also present. Rounded intraclasts are present upsection. Geopetal structures (in brachiopod shells), pore-filling drusy-blocky calcite cements, horizontal stylolites, and shale laminae are also present. Weathers nodular with a bluish-yellowish color. Samples: B51, 288.0 m; B50, 290.0 m; B49, 292.0 m.
20	5.5	297.5	Lebanon Limestone. Dark gray to light brown, well exposed, medium- to thick-bedded, medium- to fine-grained bryozoan wackestone. Weathers to bluish, sometimes yellowish, cobbly, thin slabs. Bryozoans are dominant allochems. Trilobites, ostracodes and pelmatozoans are also present. Vertical burrows and stylolites are present throughout the unit. Sample: B48, 295.5 m.
21	7.0	304.5	Lebanon Limestone. Light gray to yellowish gray, poorly exposed, very thin- to medium-bedded, very fine-grained mudstone-dismicrite. Macrofossils are scarce. Some disarticulated and fragmented ostracodes. Weathers to light yellowish thin chips. Horizontal and irregular birdseyes, fine crenulated laminae, mudcracks, and vertical burrows are abundant in this unit. Samples: B47, 299.5 m; B46, 303.0 m.

22	13.5	318.0	Carters Limestone. Dark gray to light, bluish gray, well exposed, medium- to thick-bedded, medium-grained peloids-fossil packstone-grainstone; and medium, wavy-bedded, fine-grained wackestone-packstone (B42,41). Packstone-grainstones exhibit fining-upward sequence with a basal lag of medium to coarse sand, fossil debris, succeeded by well sorted, rounded planar-laminated peloids. Shale laminae and flaser bedding are common in upper part of unit (B42,41). Fossils include bryozoans, ostracodes (articulated), pelmatozoan debris, worm tubes, trilobites, Hedstroemia, articulated and disarticulated brachiopods, gastropods, and molluscs. Planar and cross laminations, stylolites, and burrows are present throughout the unit but are more abundant in lower part. Upper portion of unit weathers into small flat chips, whereas lower and middle portions weather massive and blocky. Samples: B45, 310.5 m; B44, 313.5 m; B43, 314.0 m; B42, 314.5 m; B41, 318.0 m.
23	2.0	318.0	Carters Limestone. Dove to light brown to light gray, thick-bedded, well exposed, coarse-grained gastropod packstone-grainstone. Rocks exhibit fining-upward sequences. Geopetal structures, stylolites, and pore-filling drusy calcite cement are present. Allochems include gastropods (whole), pelmatozoan debris, bryozoans, trilobites, Hedstroemia, ostracodes, and brachiopods. Fossils are all broken, fragmented and abraded, except gastropods. Sample: B40, 318.0 m.
24	11.5	329.5	Carters Limestone. Intercalated dark gray to light brown, medium, wavy-bedded peloids packstone-grainstone; and thin-bedded, pelmatozoan, quartz-silt-intraclast, brachiopod packstones and bioturbated mudstones. Mudstone possesses both horizontal and vertical burrows. Peloidal packstones form the lower 2.0 m of this unit. Abraded and fragmented pelmatozoan plates, trilobites, ostracodes, articulated and disarticulated brachiopods, broken gastropods, Hedstroemia, and bryozoans

			are the fossil allochems present. Some shale laminae are present in lower part of unit (B39). Weathers cobbly with abundant stylolization. Calcite stringers, shelter cavity (brachiopod), solution-recrystallization (gastropods), and planar and cross laminations are common throughout the unit. Samples: B39, 320.0 m; B38, 323.5 m; B37, 327.0 m; B35, 328.0 m; B34, 329.5 m.
25	2.0	331.5	Carters Limestone. Dark gray, well exposed, thin-bedded, cherty wackestone-packstone. Allochems include sponge spicules, gastropod fragments, ostracodes, and brachiopods. Vertical burrows, pellets and calcite stringers are common. Chert is black and are in the form of nodules and lenses. Sample: B33, 331.5 m.
26	2.0	333.5	Carters Limestone. Light brown to tan, fine-grained, thin, wavy-bedded bioturbated mudstone, interbedded with fine-grained, dark gray, medium-bedded wackestone-packstone. Shale laminae are present in lower part of this unit. Fossils include disarticulated and broken ostracodes and unidentifiable fossil debris. Burrows, horizontal and vertical, and irregular stylolites are abundant. Samples: B32, 332.5 m; B31, 333.5 m.
27	1.5	335.0	Carters Limestone. Greenish to yellowish gray, well exposed, thin-bedded, fine-grained wackestone Cobbles are produced on weathering. Allochems include disarticulated and fragmented ostracodes and pellets. Birdseyes, vertical burrows with distinct walls, and mud-cracks are present. Sample: B30, 335.0 m.
28	15.0	350.0	Carters Limestone. Dove to light brown, medium-bedded, medium-grained wackestone interbedded with dove to light gray, fine-grained, thin, wavy-bedded packstone. Shale laminae are present throughout the unit. Lower and middle portion of unit contains packages of coarsening-upward sequences; bioturbated wackestone at bottom, succeeded by peloids-fossil packstone on top. Wackestone layers are truncated by a sharp scour

			surface and are overlain by pelloid-fossil packstone. Grains are current-oriented in packstone layers but lose their preferred orientation where horizontal and vertical burrows are common (B27). Most fossils are fragmented and abraded. Fossils include bryozoans, gastropods, pelmatozoan debris, trilobites, ostracodes, Hedstroemia, and unidentifiable fossil debris weather nodular and cobbly. Vertical calcite stringers, and irregular stylolites are present. Samples: B29, 338.0 m; B28, 344.0 m; B27, 348.5 m.
29	1.5	351.5	Carters Limestone. Dark gray to light, brownish gray, medium-bedded, fine-grained, cherty wackestone-packstone. Laminae of black chert are commonly interbedded with the carbonates. Constituents include gastropods, peloids, trilobites, ostracodes, brachiopods, bryozoans, and Hedstroemia. Cobbles are produced on weathering. Silicification is common in all fossils (brachiopods, trilobites, bryozoans, ostracodes). Geopetal structures are common. Sample: B26, 351.5 m.
30	13.57	365.07	Hermitage Formation. Intercalated green and red, medium-bedded, fine- to medium-grained peloidal packstone, peloid-intraclast packstone, and bioturbated mudstones. Contact between mudstone and packstones is erosive. Mudstones are prominent in upper part of unit. Vertical burrows with distinct walls are abundant, and horizontal burrows are present but rare. Allochems (intraclasts and peloids) tend to possess preferred orientation, parallel to bed. Disarticulated and broken ostracodes and Tetradium are present, but Tetradium is less common. Pelloids are rounded and sorted and range in size from 0.05-0.20 mm. Long, continuous interlaminar and irregular desiccation fenestrae are present throughout the unit. Mud-cracks (small polygons) are common. Intraclasts are angular and in situ. Weathers into small flat chips with a greenish yellow or a reddish color.

			Samples: B25, 353.0 m; B24, 354.87 m; B23, 356.07 m; B22, 357.57 m; B21, 360.57 m; B20, 363.57 m.
	4.5	369.57	Covered Interval.
31	22.5	392.07	Cannon Limestone. Dark gray to light blue, well exposed, medium- to coarse-grained, medium- to thick, wavy-bedded, bryozoan-brachiopod-mollusc packstone. Bryozoans dominate in lower portion, brachiopods in middle portion, and molluscs in upper portion of section. Weathers cobbly and nodular. shale laminae are present throughout the unit. Silicification of skeletal fragments is present, increasing upsection. Other fossil allochems include pelmatozoan debris, articulated and disarticulated ostracodes, bivalves, gastropods, and Hedstroemia. Fossils are all broken and fragmented. Also common are micrite rim (on mollusc skeletons), syntaxial overgrowth and pore-filling drusy-blocky calcite cements, and horizontal burrows. Samples: B18, 372.57 m; B17, 378.57 m; B16, 384.45 m; B15, 389.07 m.
32	9.0	401.07	Cannon Limestone. Dark gray, thick, wavy-bedded, medium-grained, Tetardium packstone. Fossil allochems include Tetradium, articulated and disarticulated ostracodes, bryozoan and trilobite fragments, whole and broken gastropods, disarticulated brachiopods, and pelmatozoan debris. In situ Tetradium coral-lites dominate this lithology. Weathers nodular. Samples: B14, 393.57 m; B13, 401.07 m.
33	11.5	412.57	Cannon Limestone. Light gray to bluish gray, well exposed, medium, wavy-bedded, medium-grained packstone; gastropod-brachiopod, and gastropods. Gastropods are whole or broken and are dominant fossil allochems, comprising 80-90% of allochems. Brachiopods are articulated or disarticulated and are the second most abundant. Other fossils are broken and fragmented and include Hedstroemia, trilobite, bivalves, and bryozoans. Rocks in

			lower part of unit contain packages of fining-upward sequences. Geopetal structures and stylolites are common. Samples: B12, 408.57 m; B11, 412.07 m; B10, 412.57 m.
34	19.5	432.07	Cannon-Catheys Formation (?). Brownish gray to dark gray, medium- to thick-bedded, well exposed, medium- to coarse-grained, gastropod packstone, pelmatozoan packstone-grainstone, and molluscs packstone-grainstones. Unit is very fossiliferous; molluscs (gastropods and bivalves) are predominant fossil allochems. Pelmatozoans are rounded and sorted and are the most abundant allochems in lower part of unit (B8). Strophominid brachiopods are also abundant (B9). Other fossils, such as bryozoans, trilobites, and Hedstroemia, are present and exhibit varying degree of fragmentation and abrasion. Micrite rim (on bryozoans and molluscs), syntaxial overgrowth and pore-filling drusy-blocky cements, and silicification of skeletal fragments (molluscs, brachiopods, bryozoans, pelmatozoans) are present throughout the unit. Samples: B9, 414.07 m; B8, 418.57 m; B7, 426.07 m; B6, 429.07 m; B5, 432.07 m.
35	3.0	435.07	Cannon-Catheys Formation (?). Dark gray to tan, well exposed, medium, wavy- to thick-bedded, medium- to coarse-grained packstone, either mollusc-gastropod or pelmatozoan. some shale laminae are also present. Allochems include articulated and disarticulated brachiopods, bryozoans, pelmatozoan debris, trilobites, whole and broken gastropods, and articulated bivalves. Fragmentation and abrasion is severe on bryozoan, trilobites, and pelmatozoans. Pelmatozoans are present only in middle of unit (B3). Weathers cobbly and nodular. Samples: B4, 433.07 m; B3, 433.57 m; B2, 434.07 m; B1, 435.07 m.
			Moccasin Formation. Not measured. No sample taken.

APPENDIX B

PETROGRAPHIC CONSTITUENT ANALYSIS

In order to determine the percentage of constituent particles within each sample, 212 petrographic thin sections, representative of the samples taken in this study, were analyzed, using a technique described by Chayes (1954). Also, to reach a 95% confidence level in the point count analyses (Van der Plus and Tobi, 1965), a minimum of 350 points were counted on each slide. Constituent particles not observed in a given thin section are designated by a dash line in the point count.

Table B.1. Center Point section point count analysis of samples 1A-1E (volume percent of constituents).

Constituents	Sample Numbers					
	1A	1B	$1B_1$	1C	1D	1E
Micrite	4.65	25.89	-	33.81	56.30	58.72
Spar	-	19.13	-	14.38	2.92	18.18
Intraclasts	-	1.07	-	-	-	-
Peloids	-	-	-	-	-	-
Brachiopods	-	-	-	-	-	-
Gastropods	-	-	-	-	-	-
Ostracods	-	1.88	-	4.55	-	-
Trilobites	-	-	-	-	-	-
Molluscan debris	-	-	-	-	-	-
Pelmatozoans	-	-	-	-	-	-
Bryozoans	-	-	-	-	-	-
Algae	-	-	-	-	-	-
Oncolite	-	-	-	-	-	-
Sponge	-	-	-	-	-	-
Unidentifiable Fossile debris	-	0.80	-	0.23	-	-
Dolomite	74.9	44.47	90.08	46.28	1.57	-
Quartz	19.12	4.04	9.06	-	33.10	23.09
Tetradium	-	-	-	-	-	-
Worm Tube	-	-	-	-	-	-
Stylolite	1.03	2.69	0.84	0.71	6.08	-

*Note: Algae (Hedstroemia = H; Solenopora = S; Kazakstanelia = K; Girvanelia = G; Nuia = N).

Table B.2. Center Point section point count analysis of samples 1F-5_1A (volume percent of constituents).

Constituents	Sample Numbers					
	1F	1G	1H	1I	3A	5_1A
Micrite	63.78	60.92	28.65	36.17	82.79	72.87
Spar	-	22.67	5.73	26.06	-	10.37
Intraclasts	-	-	-	-	-	-
Peloids	-	-	-	-	-	-
Brachiopods	-	-	-	-	-	-
Gastropods	-	-	-	-	-	-
Ostracods	-	-	-	2.39	-	-
Trilobites	-	-	-	-	-	-
Molluscan debris	-	-	-	-	-	-
Pelmatozoans	-	-	-	-	-	-
Bryozoans	-	-	-	-	-	-
Algae	-	-	-	6.11(H)	-	-
Oncolite	-	-	-	-	-	-
Sponge	-	-	-	-	-	-
Unidentifiable Fossile debris	-	-	2.57	-	-	-
Dolomite	-	-	-	-	-	12.23
Quartz	36.21	16.39	62.17	-	4.48	-
Tetradium	-	-	-	-	-	-
Worm Tube	-	-	-	-	-	-
Stylolite	-	-	0.85	-	12.71	4.52

*Note: Algae (Hedstroemia = H; Solenopora = S; Kazakstanelia = K; Girvanelia = G; Nuia = N).

Table B.3. Center Point section point count analysis of samples 5A-6A (volume percent of constituents).

Constituents	Sample Numbers					
	5A	5_1B	5B	5C	5_1C	6A
Micrite	75.42	61.69	48.03	55.82	19.17	30.08
Spar	9.42	2.04	14.32	24.47	33.69	2.57
Intraclasts	-	0.87	-	-	2.46	-
Peloids	-	1.46	-	-	21.09	-
Brachiopods	-	2.63	0.56	1.19	1.90	-
Gastropods	-	0.29	-	0.29	6.57	-
Ostracods	-	2.63	1.68	3.88	3.83	-
Trilobites	-	4.09	0.28	0.29	0.82	-
Molluscan debris	-	-	-	-	1.91	-
Pelmatozoans	-	2.33	0.84	-	2.73	-
Bryozoans	-	-	0.54	-	-	-
Algae	-	-	-	-	-	-
Oncolite	-	-	-	-	-	-
Sponge	-	-	7.02	-	-	20.63 (silica + 46.70 spicules)
Unidentifiable Fossile debris	-	-	-	14.02	3.0	-
Dolomite	15.14	17.25	-	-	3.56	-
Quartz	-	-	26.68	-	-	-
Tetradium	-	-	-	-	-	-
Worm Tube	-	-	-	-	-	-
Stylolite	-	4.67	-	-	-	-

*Note: Algae (Hedstroemia = H; Solenopora = S; Kazakstanelia = K; Girvanelia = G; Nuia = N).

Table B.4. Center Point section point count analysis of samples 6_1A-11A (volume percent of constituents).

Constituents	Sample Numbers					
	6_1A	7A	8A	9A	10A	11A
Micrite	6.56	35.93	52.55	18.57	18.71	22.02
Spar	57.61	3.24	15.62	8.85	12.5	14.44
Intraclasts	0.29	-	-	-	1.67	0.18
Peloids	29.25	-	-	-	0.55	-
Brachiopods	-	-	-	-	10.33	6.67
Gastropods	-	-	-	-	5.30	3.42
Ostracods	2.38	1.29	1.13	-	5.86	5.95
Trilobites	-	-	-	-	2.23	3.42
Molluscan debris	-	-	-	-	12.29	8.48
Pelmatozoans	-	-	-	-	8.37	4.69
Bryozoans	-	-	-	-	-	0.18
Algae	-	2.81(H)	-	-	-	-
Oncolite	-	-	-	-	-	-
Sponge	-	-	30.68	-	-	-
Unidentifiable Fossile debris	1.79	1.94	-	0.57	6.42	14.98
Dolomite	2.08	-	-	0.28	7.54	4.87
Quartz	-	-	-	71.71	-	4.15
Tetradium	-	54.76	-	-	-	-
Worm Tube	-	-	-	-	-	-
Stylolite	-	-	-	-	8.10	6.49

*Note: Algae (Hedstroemia = H; Solenopora = S; Kazakstanelia = K; Girvanelia = G; Nuia = N).

Table B.5. Center Point section point count analysis of samples 12B-15A (volume percent of constituents).

Constituents	Sample Numbers					
	12B	13A	13B	14A	14B	15A
Micrite	42.89	6.33	3.48	30.63	27.54	0.92
Spar	29.82	44.06	48.25	3.75	19	30.86
Intraclasts	-	-	-	-	1.65	16.97
Peloids	-	11.60	5.23	-	0.55	-
Brachiopods	-	-	-	2.89	0.82	8.64
Gastropods	-	-	-	7.22	-	-
Ostracods	-	-	-	6.06	0.55	0.92
Trilobites	-	-	-	1.73	0.82	1.54
Molluscan debris	-	-	-	6.64	-	-
Pelmatozoans	-	-	-	6.06	13.77	12.65
Bryozoans	-	-	-	2.02	3.85	21.60
Algae	-	-	-	5.78	3.85(H)	-
Oncolite	-	-	-	-	-	-
Sponge	-	-	-	-	-	-
Unidentifiable Fossile debris	5.11	-	2.32	12.42	11.83	5.86
Dolomite	-	-	-	1.15	1.37	-
Quartz	22.15	37.99	40.40	-	-	-
Tetradium	-	-	-	-	-	-
Worm Tube	-	-	-	-	-	-
Stylolite	-	-	0.29	13.58	14.32	-

*Note: Algae (Hedstroemia = H; Solenopora = S; Kazakstanelia = K; Girvanelia = G; Nuia = N).

Table B.6. Center Point section point count analysis of samples 16A-16E_2 (volume percent of constituents).

Constituents	Sample Numbers					
	16A	16B	16C	16D	16E_1	16E_2
Micrite	33.24	88.79	56.57	87.65	49.03	84.61
Spar	6.89	3.92	19.42	3.01	1.61	9.89
Intraclasts	10.34	-	-	-	0.64	-
Peloids	-	-	-	0.90	6.12	-
Brachiopods	18.51	-	-	-	0.96	-
Gastropods	-	-	-	-	-	-
Ostracods	3.1	-	1.14	-	-	-
Trilobites	3.1	-	2.28	-	0.64	-
Molluscan debris	2.41	-	-	-	-	-
Pelmatozoans	12.06	-	-	-	0.32	-
Bryozoans	3.79	-	-	-	0.64	-
Algae	-	-	-	-	1.64 (H+S)	-
Oncolite	-	-	-	-	-	-
Sponge	-	-	-	-	-	-
Unidentifiable Fossile debris	6.55	7.28	8.57	-	1.61	3.29
Dolomite	-	-	12	-	-	2.19
Quartz	-	-	-	4.51	8.06	-
Tetradium	-	-	-	-	-	-
Worm Tube	-	-	-	-	-	-
Stylolite	-	-	-	3.91	28.70	-

*Note: Algae (Hedstroemia = H; Solenopora = S; Kazakstanelia = K; Girvanelia = G; Nuia = N).

Table B.7. Center Point section point count analysis of samples 17A-$20A_2$ (volume percent of constituents).

Constituents	Sample Numbers					
	17A	17B	$18A_1$	19A	19B	$20A_2$
Micrite	50.78	45.33	55.04	55.61	48.10	42.61
Spar	35.73	32.80	30.51	15.71	9.03	28.13
Intraclasts	-	-	-	-	-	-
Peloids	-	-	-	-	-	2.78
Brachiopods	-	-	-	-	-	-
Gastropods	-	-	-	-	-	-
Ostracods	0.62	2.66	7.35	1.99	-	0.55
Trilobites	-	-	2.45	-	-	-
Molluscan debris	-	3.20	-	-	-	-
Pelmatozoans	-	-	-	-	-	0.27
Bryozoans	-	-	-	-	-	-
Algae	-	-	-	-	-	-
Oncolite	-	-	-	-	-	-
Sponge	-	-	-	-	-	-
Unidentifiable Fossile debris	0.38	9.33	-	-	-	7.52
Dolomite	1.02	-	-	-	-	-
Quartz	2.02	3.46	-	26.68	37.90	10.58
Tetradium	-	-	-	-	-	-
Worm Tube	-	3.20	4.63	-	-	-
Stylolite	5.95	-	-	-	4.95	7.52

*Note: Algae (Hedstroemia = H; Solenopora = S; Kazakstanelia = K; Girvanelia = G; Nuia = N).

Table B.8. Center Point section point count analysis of samples $21A_1$-25A (volume percent of constituents).

Constituents	Sample Numbers					
	$21A_1$	22A	22B	23A	24BR	25A
Micrite	55.55	44.29	50.40	36.36	59.94	34.30
Spar	15.80	7.33	8.08	35.15	27.62	14.59
Intraclasts	-	-	-	-	-	-
Peloids	-	-	-	9.09	-	-
Brachiopods	-	-	-	0.30	-	-
Gastropods	-	-	-	-	-	-
Ostracods	1.48	13.04	20.21	0.30	-	4.13
Trilobites	0.49	0.81	4.85	-	-	-
Molluscan debris	-	-	-	-	-	-
Pelmatozoans	-	-	-	-	-	-
Bryozoans	-	-	-	-	-	-
Algae	-	-	-	-	-	0.72(H)
Oncolite	-	-	-	-	-	-
Sponge	-	-	-	-	-	36.25
Unidentifiable Fossile debris	-	34.51	16.44	14.24	10.76	-
Dolomite	-	-	-	-	-	-
Quartz	26.66	-	-	-	-	9.24
Tetradium	-	-	-	-	-	-
Worm Tube	-	-	-	-	-	-
Stylolite	-	-	-	4.54	1.65	-

*Note: Algae (Hedstroemia = H; Solenopora = S; Kazakstanelia = K; Girvanelia = G; Nuia = N).

Table B.9. Center Point section point count analysis of samples 25B-27R (volume percent of constituents).

Constituents	Sample Numbers					
	25B	25D	26A	26B	26F	27R
Micrite	82.67	35.60	79.82	41.86	58.96	38.15
Spar	3.40	29.72	19.31	18.31	30.39	27.07
Intraclasts	-	-	-	-	-	-
Peloids	-	2.16	-	-	-	7.38
Brachiopods	-	-	-	-	-	-
Gastropods	-	-	-	-	-	-
Ostracods	10.51	2.47	0.85	-	1.21	0
Trilobites	1.13	-	-	-	-	-
Molluscan debris	-	-	-	-	-	-
Pelmatozoans	-	-	-	-	-	-
Bryozoans	-	-	-	-	-	-
Algae	-	-	-	-	2.12 (H+S)	-
Oncolite	-	-	-	-	-	-
Sponge	-	-	-	-	-	-
Unidentifiable Fossile debris	2.27	7.43	-	30.22	3.34	10.76
Dolomite	-	-	-	-	-	-
Quartz	-	21.67	-	-	-	14.15
Tetradium	-	-	-	-	-	-
Worm Tube	-	-	-	-	-	-
Stylolite	-	0.92	-	9.59	-	2.46

*Note: Algae (Hedstroemia = H; Solenopora = S; Kazakstanelia = K; Girvanelia = G; Nuia = N).

Table B.10. Center Point section point count analysis of samples 28A-28H (volume percent of constituents).

Constituents	Sample Numbers					
	28A	28B	28D	28F	28G	28H
Micrite	34.10	47.66	46.65	1.53	56.35	35.36
Spar	12.71	6.21	15.77	36	6.62	22.89
Intraclasts	0.28	-	-	7.07	-	-
Peloids	-	11.39	-	15.69	-	-
Brachiopods	10.98	3.10	12.11	5.53	12.70	0.86
Gastropods	4.04	2.07	5.91	1.53	3.31	26.37
Ostracods	2.89	1.03	4.78	3.06	5.24	-
Trilobites	1.15	0.25	3.38	4.0	2.20	-
Molluscan debris	6.64	3.62	-	5.84	5.24	-
Pelmatozoans	2.02	3.10	-	12.0	2.76	-
Bryozoans	1.15	0.25	-	3.06	2.48	-
Algae	-	-	-	-	-	-
Oncolite	-	-	-	-	-	-
Sponge	-	-	-	-	-	-
Unidentifiable Fossile debris	8.09	6.73	1.97	3.69	3.03	13.62
Dolomite	8.67	1.29	-	-	-	0.28
Quartz	-	-	-	-	-	-
Tetradium	-	-	-	-	-	-
Worm Tube	-	-	-	-	-	-
Stylolite	7.22	13.21	-	0.92	-	0.57

*Note: Algae (Hedstroemia = H; Solenopora = S; Kazakstanelia = K; Girvanelia = G; Nuia = N).

Table B.11. Center Point section point count analysis of samples 29A-29G (volume percent of constituents).

Constituents	Sample Numbers					
	29A	$29A_2$	29C	29E	29F	29G
Micrite	60.45	57.45	27.35	44.44	-	74.60
Spar	11.58	20.49	23.52	20.10	29.20	22.22
Intraclasts	-	-	3.52	-	-	0.52
Peloids	-	0.93	17.35	14.81	64.76	-
Brachiopods	-	-	-	-	0.63	-
Gastropods	-	-	-	7.40	0.31	-
Ostracods	7.34	1.86	1.17	3.70	-	-
Trilobites	3.10	-	-	1.32	-	-
Molluscan debris	-	0.31	2.94	3.70	-	-
Pelmatozoans	2.25	-	6.76	-	0.31	-
Bryozoans	-	-	-	-	-	-
Algae	-	-	-	-	-	-
Oncolite	-	-	-	-	-	-
Sponge	-	-	-	-	-	-
Unidentifiable Fossile debris	15.25	13.04	15	4.49	4.76	-
Dolomite	-	-	-	-	-	-
Quartz	-	4.65	-	-	-	-
Tetradium	-	-	-	-	-	-
Worm Tube	-	-	-	-	-	-
Stylolite	-	1.24	2.35	-	-	2.64

*Note: Algae (Hedstroemia = H; Solenopora = S; Kazakstanelia = K; Girvanelia = G; Nuia = N).

Table B.12. Center Point section point count analysis of samples 29J-31 (volume percent of constituents).

Constituents	Sample Numbers				
	29J	29K	29L	30	31
Micrite	48.37	64.68	41.34	7.96	0.64
Spar	14.15	19.20	8.89	39.83	34.62
Intraclasts	1.47	-	2.64	16.20	13.59
Peloids	16.22	-	2.40	3.57	37.54
Brachiopods	1.17	0.28	0.72	4.94	0.97
Gastropods	0.29	0.28	0.48	0.27	-
Ostracods	1.17	6.21	0.96	0.54	0.32
Trilobites	0.29	0.56	0.24	-	-
Molluscan debris	-	-	0.48	-	10.67
Pelmatozoans	2.65	-	0.72	8.79	-
Bryozoans	0.88	-	0.48	7.14	-
Algae	-	-	-	-	-
Oncolite	-	-	-	-	-
Sponge	-	-	-	-	-
Unidentifiable Fossile debris	2.06	8.75	14.66	3.29	1.61
Dolomite	11.20	-	22.11	6.31	-
Quartz	-	-	-	-	-
Tetradium	-	-	-	-	-
Worm Tube	-	-	-	-	-
Stylolite	-	-	3.33	1.09	-

*Note: Algae (Hedstroemia = H; Solenopora = S; Kazakstanelia = K; Girvanelia = G; Nuia = N).

Table B.13. Goodfield section point count analysis of samples 1A-9 (volume percent of constituents).

Constituents	Sample Numbers					
	1A	2A	3	5	8	9
Micrite	-	-	16.74	15.70	16.98	36.18
Spar	-	-	0.44	31.63	5.42	7.45
Intraclasts	-	-	-	-	-	-
Peloids	-	-	-	5.75	-	-
Brachiopods	-	-	0.22	0.66	0.23	-
Gastropods	-	-	3.57	4.20	9.19	5.45
Ostracods	-	-	32.58	3.09	34.66	21.27
Trilobites	-	-	4.91	3.89	1.41	0.54
Molluscan debris	-	-	12.05	2.65	8.72	9.27
Pelmatozoans	-	-	-	5.30	-	0.72
Bryozoans	-	-	-	-	-	2.0
Algae	-	-	0.44	-	-	-
Oncolite	-	-	-	-	-	-
Sponge	-	-	-	-	-	-
Unidentifiable Fossile debris	-	-	2.90	20.35	13.20	4.72
Dolomite	90.53	100	26.11	-	-	3.63
Quartz	-	-	-	5.08	3.53	3.09
Tetradium	-	-	-	-	-	-
Worm Tube	-	-	-	-	-	-
Stylolite	9.46	-	-	1.54	10.14	5.63

*Note: Algae (Hedstroemia = H; Solenopora = S; Kazakstanelia = K; Girvanelia = G; Nuia = N).

Table B.14. Goodfield section point count analysis of samples 10-22 (volume percent of constituents).

Constituents	Sample Numbers					
	10	11	13	16	17	22
Micrite	18	31.82	73.26	73.44	13.87	27.79
Spar	14.09	38.95	21.30	25.17	52.52	40.25
Intraclasts	-	-	-	-	-	-
Peloids	0.21	-	-	-	12.18	4.41
Brachiopods	0.21	-	-	-	-	-
Gastropods	9.76	-	-	-	-	-
Ostracods	20.17	-	0.65	-	1.26	3.37
Trilobites	0.86	-	-	-	0.84	1.29
Molluscan debris	13.44	-	-	-	0.42	-
Pelmatozoans	1.30	-	-	-	1.05	-
Bryozoans	0.86	-	-	-	-	-
Algae	-	-	-	-	-	-
Oncolite	-	-	-	-	-	-
Sponge	-	-	-	-	-	-
Unidentifiable Fossile debris	12.14	-	-	-	2.73	9.09
Dolomite	-	0.69	-	-	-	-
Quartz	5.63	28.52	-	-	11.55	12.72
Tetradium	-	-	-	-	-	-
Worm Tube	-	-	-	-	-	-
Stylolite	3.25	-	4.35	1.39	-	1.03

*Note: Algae (Hedstroemia = H; Solenopora = S; Kazakstanelia = K; Girvanelia = G; Nuia = N).

Table B.15. Goodfield section point count analysis of samples 24-32 (volume percent of constituents).

Constituents	Sample Numbers					
	24	26	28	30	31	32
Micrite	33.78	16.67	32.05	17.12	31.23	64.46
Spar	10.51	41.67	12.17	26.15	7.67	14.89
Intraclasts	-	-	1.28	0.23	-	-
Peloids	1.57	-	1.70	29.16	0.54	0.21
Brachiopods	0.45	-	1.49	13.42	0.27	0.42
Gastropods	-	-	1.49	1.85	5.47	2.12
Ostracods	12.98	-	5.34	-	2.19	2.55
Trilobites	0.98	-	0.85	0.69	5.20	1.70
Molluscan debris	-	-	3.20	1.15	14.79	4.68
Pelmatozoans	1.79	-	7.47	1.15	15.89	0.85
Bryozoans	-	-	0.21	-	-	-
Algae	10.74(H)	-	0.42(H)	-	-	-
Oncolite	-	-	-	-	-	-
Sponge	-	-	-	-	-	-
Unidentifiable Fossile debris	25.50	-	4.70	1.62	2.19	2.34
Dolomite	-	41.67	7.05	1.38	12.05	3.61
Quartz	-	-	-	-	-	-
Tetradium	-	-	19.23	-	-	-
Worm Tube	-	-	-	-	-	-
Stylolite	1.34	-	1.28	1.85	2.46	2.12

*Note: Algae (Hedstroemia = H; Solenopora = S; Kazakstanelia = K; Girvanelia = G; Nuia = N).

Table B.16. Goodfield section point count analysis of samples 34-41 (volume percent of constituents).

Constituents	Sample Numbers					
	34	35	37	38	39	41
Micrite	50.10	8.47	21.27	3.57	51.68	17.63
Spar	14.43	15.21	16.13	27.23	46.87	23.18
Intraclasts	1.44	2.49	-	0.22	-	0.24
Peloids	-	10.72	9.53	13.16	-	25.84
Brachiopods	-	11.22	0.73	0.44	-	-
Gastropods	0.20	10.72	0.24	-	-	0.24
Ostracods	-	11.22	2.93	5.13	0.24	8.93
Trilobites	-	2.24	0.97	3.12	-	0.72
Molluscan debris	0.20	4.98	4.15	2.0	-	6.03
Pelmatozoans	-	2.99	2.93	18.52	-	6.28
Bryozoans	-	3.49	-	1.11	-	0.48
Algae	-	-	-	-	-	2.89(H)
Oncolite	-	-	-	-	-	-
Sponge	-	-	-	-	-	-
Unidentifiable Fossile debris	-	1.74	26.16	8.70	-	5.55
Dolomite	27.42	14.46	12.95	0.22	-	1.93
Quartz	-	-	-	-	-	-
Tetradium	-	-	-	-	-	-
Worm Tube	-	-	-	-	-	-
Stylolite	6.18	-	1.95	16.51	-	-

*Note: Algae (Hedstroemia = H; Solenopora = S; Kazakstanelia = K; Girvanelia = G; Nuia = N).

Table B.17. Goodfield section point count analysis of samples 44-53 (volume percent of constituents).

Constituents	Sample Numbers					
	44	45	46	47	50	53
Micrite	38.51	66.50	76.26	61.95	80.52	57.75
Spar	42.45	33.49	13.36	4.70	19.23	32.45
Intraclasts	-	-	0.69	-	0.24	-
Peloids	-	-	-	-	-	8.59
Brachiopods	-	-	-	0.37	-	-
Gastropods	-	-	-	-	-	-
Ostracods	1.39	-	0.46	5.08	-	1.19
Trilobites	-	-	-	0.18	-	-
Molluscan debris	-	-	-	0.37	-	-
Pelmatozoans	-	-	-	0.56	-	-
Bryozoans	-	-	-	0.18	-	-
Algae	-	-	-	0.75(H)	-	-
Oncolite	-	-	-	-	-	-
Sponge	-	-	-	-	-	-
Unidentifiable Fossile debris	16.0	-	-	0.37	-	-
Dolomite	-	-	-	-	-	-
Quartz	1.62	-	-	-	-	-
Tetradium	-	-	-	25.42	-	-
Worm Tube	-	-	-	-	-	-
Stylolite	-	-	9.21	-	-	-

*Note: Algae (Hedstroemia = H; Solenopora = S; Kazakstanelia = K; Girvanelia = G; Nuia = N).

Table B.18. Goodfield section point count analysis of samples 57-64 (volume percent of constituents).

Constituents	Sample Numbers				
	57	59	60	62	64
Micrite	8.14	83.02	2.54	-	49.09
Spar	34.61	6.19	45.95	51.87	17.34
Intraclasts	9.04	-	0.46	-	0.45
Peloids	5.20	-	-	-	3.15
Brachiopods	-	0.22	8.77	9.52	-
Gastropods	0.22	1.37	-	1.25	0.45
Ostracods	2.26	4.35	6.0	4.51	1.35
Trilobites	0.22	-	2.30	3.25	-
Molluscan debris	5.42	1.60	1.61	-	2.02
Pelmatozoans	6.78	-	3.0	0.75	0.45
Bryozoans	1.80	-	22.17	27.31	0.45
Algae	12.44(H)	0.45(H)	-	-	-
Stromataporoids	-	-	6.45	-	-
Sponge	-	-	-	-	-
Unidentifiable Fossile debris	4.97	2.75	0.69	1.50	12.61
Dolomite	0.45	-	-	-	6.98
Quartz	-	-	-	-	-
Tetradium	8.37	-	-	-	-
Worm Tube	-	-	-	-	-
Stylolite	-	-	-	-	5.63

*Note: Algae (Hedstroemia = H; Solenopora = S; Kazakstanelia = K; Girvanelia = G; Nuia = N).

Table B.19. Goodfield section point count analysis of samples 65-74 (volume percent of constituents).

Constituents	Sample Numbers					
	65	68	70	71	72	74
Micrite	33.75	6.18	74.39	1.82	2.69	38.64
Spar	15.72	21.63	11.69	27.05	32.59	11.70
Intraclasts	0.20	15.67	-	0.30	0.49	-
Peloids	5.45	17.66	0.22	36.17	1.22	2.10
Brachiopods	4.19	15.01	-	3.64	5.88	-
Gastropods	0.40	0.22	-	-	5.39	0.23
Ostracods	1.46	1.54	1.32	3.64	10.78	6.79
Trilobites	0.83	1.54	-	5.16	5.14	-
Molluscan debris	3.98	0.22	-	2.73	19.60	0.93
Pelmatozoans	0.83	1.54	-	14.58	6.61	-
Bryozoans	3.35	8.16	1.10	1.82	5.39	-
Algae	0.83(H)	-	-	-	-	-
Oncolite	-	-	-	-	-	-
Sponge	-	-	-	-	-	-
Unidentifiable Fossile debris	5.03	1.76	-	3.03	2.69	10.07
Dolomite	18.23	6.18	5.73	-	1.47	22.01
Quartz	-	-	-	-	-	-
Tetradium	-	-	-	-	-	-
Worm Tube	-	-	-	-	-	-
Stylolite	5.66	2.64	5.51	-	-	7.49

*Note: Algae (Hedstroemia = H; Solenopora = S; Kazakstanelia = K; Girvanelia = G; Nuia = N).

Table B.20. Goodfield section point count analysis of samples 75-81 (volume percent of constituents).

Constituents	Sample Numbers					
	75	76	78	79	80	81
Micrite	50	36.15	14.81	5.18	62.17	-
Spar	9.95	5.63	31.85	36.79	20.33	30.41
Intraclasts	0.21	1.17	-	0.47	-	-
Peloids	-	3.99	12.34	0.23	5.67	26.54
Brachiopods	-	12.44	13.08	10.37	-	2.31
Gastropods	-	12.20	-	1.17	-	-
Ostracods	2.33	6.10	7.90	0.47	1.65	5.67
Trilobites	-	3.05	1.72	5.42	-	4.63
Molluscan debris	0.21	0.46	-	1.17	2.60	3.35
Pelmatozoans	-	0.93	1.48	2.83	-	17.26
Bryozoans	1.27	3.05	0.98	31.60	-	6.18
Algae	-	-	-	-	-	-
Oncolite	-	-	-	-	-	-
Sponge	-	-	-	-	-	-
Unidentifiable Fossile debris	10.38	0.70	9.62	0.94	2.36	3.60
Dolomite	0.42	9.85	-	3.30	2.36	-
Quartz	-	-	6.17	-	-	-
Tetradium	20.97	-	-	-	-	-
Worm Tube	-	-	-	-	-	-
Stylolite	4.23	4.22	-	-	2.83	-

*Note: Algae (Hedstroemia = H; Solenopora = S; Kazakstanelia = K; Girvanelia = G; Nuia = N).

Table B.21. Goodfield section point count analysis of samples 82-95 (volume percent of constituents).

Constituents	Sample Numbers					
	82	84	86	91	92	95
Micrite	0.92	63.35	66.81	9.95	68.65	0.28
Spar	33.09	15.67	19.59	31.77	31.34	9.20
Intraclasts	0.70	-	-	2.75	-	2.73
Peloids	9.69	0.22	0.22	0.84	-	0.43
Brachiopods	25.76	-	-	18	-	36.83
Gastropods	1.18	0.22	-	1.48	-	0.43
Ostracods	3.07	-	1.11	1.27	-	0.28
Trilobites	5.91	-	-	2.96	-	0.71
Molluscan debris	0.70	-	-	7.62	-	-
Pelmatozoans	4.01	-	-	7.41	-	37.69
Bryozoans	13.94	-	-	5.72	-	8.63
Algae	-	-	-	-	-	-
Oncolite	-	-	-	-	-	-
Sponge	-	-	-	-	-	-
Unidentifiable Fossile debris	0.94	0.66	-	5.93	-	2.73
Dolomite	-	14.79	-	1.27	-	-
Quartz	-	-	-	-	-	-
Tetradium	-	-	-	-	-	-
Worm Tube	-	-	-	-	-	-
Stylolite	-	5.07	12.24	2.96	-	-

*Note: Algae (Hedstroemia = H; Solenopora = S; Kazakstanelia = K; Girvanelia = G; Nuia = N).

Table B.22. Goodfield section point count analysis of samples 97 & 99 (volume percent of constituents).

Constituents	Sample Numbers	
	97	99
Micrite	60.57	29.84
Spar	39.42	14.33
Intraclasts	-	3.03
Peloids	-	7.25
Brachiopods	-	6.23
Gastropods	-	2.19
Ostracods	-	2.19
Trilobites	-	1.51
Molluscan debris	-	1.51
Pelmatozoans	-	10.79
Bryozoans	-	15.51
Algae	-	-
Oncolite	-	-
Sponge	-	-
Unidentifiable Fossile debris	-	3.03
Dolomite	-	2.52
Quartz	-	-
Tetradium	-	-
Worm Tube	-	-
Stylolite	-	-

*Note: Algae (Hedstroemia = H; Solenopora = S; Kazakstanelia = K; Girvanelia = G; Nuia = N).

Table B.23. Barnardsville section point count analysis of samples 1-18 (volume percent of constituents).

Constituents	Sample Numbers					
	1	9	11	14	15	18
Micrite	31.97	4.82	35.89	21.79	43.15	2.66
Spar	3.52	31.53	5.47	2.45	2.58	24
Intraclasts	-	-	-	-	-	-
Peloids	-	2.55	-	-	-	-
Brachiopods	4.06	11.07	7.67	0.81	3.35	9.33
Gastropods	48.78	12.21	38.63	0.54	11.36	-
Ostracods	2.71	1.13	1.91	10.89	1.80	2.93
Trilobites	2.98	3.69	1.36	2.72	4.13	2.4
Molluscan debris	2.16	18.46	4.65	-	19.37	5.06
Pelmatozoans	-	1.98	-	4.90	2.06	23.46
Bryozoans	-	12.5	3.56	2.17	4.39	27.73
Algae	-	-	0.82(H)	-	-	-
Oncolite	-	-	-	-	-	-
Sponge	-	-	-	-	-	-
Unidentifiable Fossile debris	3.79	-	-	-	7.75	-
Dolomite	-	-	-	-	-	-
Quartz	-	-	-	-	-	-
Tetradium	-	-	-	53.67	-	-
Worm Tube	-	-	-	-	-	-
Stylolite	-	-	-	-	-	-

*Note: Algae (Hedstroemia = H; Solenopora = S; Kazakstanelia = K; Girvanelia = G; Nuia = N).

Table B.24. Barnardsville section point count analysis of samples 22-40 (volume percent of constituents).

Constituents	Sample Numbers					
	22	24	28	32	37	40
Micrite	65.27	33.42	29.81	85.14	3.82	8.57
Spar	13.61	28	8.44	14.85	25.13	27.34
Intraclasts	15	10	1.58	-	2.45	-
Peloids	6.1	28.57	15.56	-	21.03	26.27
Brachiopods	-	-	4.48	-	3.55	8.57
Gastropods	-	-	-	-	0.54	12.06
Ostracods	-	-	4.74	-	3.27	5.63
Trilobites	-	-	1.05	-	2.18	2.14
Molluscan debris	-	-	0.52	-	3.0	3.48
Pelmatozoans	-	-	10.55	-	26.77	1.34
Bryozoans	-	-	8.17	-	3.27	4.55
Algae	-	-	-	-	-	-
Oncolite	-	-	-	-	-	-
Sponge	-	-	-	-	-	-
Unidentifiable Fossile debris	-	-	8.17	-	3.27	-
Dolomite	-	-	6.86	-	1.63	-
Quartz	-	-	-	-	-	-
Tetradium	-	-	-	-	-	-
Worm Tube	-	-	-	-	-	-
Stylolite	-	-	-	-	-	-

*Note: Algae (Hedstroemia = H; Solenopora = S; Kazakstanelia = K; Girvanelia = G; Nuia = N).

Table B.25. Barnardsville section point count analysis of samples 45-56 (volume percent of constituents).

Constituents	Sample Numbers					
	45	47	48	51	52	56
Micrite	2.95	68.09	72.45	14.24	81.15	3.14
Spar	30.64	28.77	3.03	28.21	-	33.59
Intraclasts	2.15	-	-	1.64	-	5.77
Peloids	21.23	-	-	9.04	5.79	2.09
Brachiopods	4.30	-	-	12.05	-	12.59
Gastropods	0.80	-	-	1.64	-	-
Ostracods	4.30	3.13	3.30	4.38	4.34	4.46
Trilobites	3.22	-	1.37	6.57	-	2.62
Molluscan debris	2.41	-	-	1.36	-	6.03
Pelmatozoans	15.86	-	-	14.52	-	24.93
Bryozoans	8.60	-	19.83	-	-	4.19
Algae	-	-	-	-	-	-
Oncolite	-	-	-	-	-	-
Sponge	-	-	-	-	-	-
Unidentifiable Fossile debris	2.41	-	-	-	4.05	0.52
Dolomite	1.07	-	-	2.73	4.63	-
Quartz	-	-	-	-	-	-
Tetradium	-	-	-	-	-	-
Worm Tube	-	-	-	-	-	-
Stylolite	-	-	-	-	-	-

*Note: Algae (Hedstroemia = H; Solenopora = S; Kazakstanelia = K; Girvanelia = G; Nuia = N).

Table B.26. Barnardsville section point count analysis of samples 59-70 (volume percent of constituents).

Constituents	Sample Numbers					
	59	61	63	65	67	70
Micrite	46.11	58.68	55.34	30.46	55.05	50.38
Spar	19.79	13.67	10.69	24.73	37.07	25.31
Intraclasts	-	-	-	-	-	-
Peloids	8.27	-	-	2.60	-	-
Brachiopods	1.0	-	2.13	1.56	-	-
Gastropods	3.0	-	21.12	1.82	-	-
Ostracods	3.0	18.51	2.13	3.64	5.05	2.30
Trilobites	0.25	-	1.33	1.04	-	-
Molluscan debris	3.25	-	2.67	5.72	-	-
Pelmatozoans	0.50	-	0.26	5.98	-	-
Bryozoans	0.75	-	-	14.58	-	-
Algae	-	-	-	-	-	-
Oncolite	-	-	-	-	-	-
Sponge	-	-	-	-	-	-
Unidentifiable Fossile debris	4.01	9.11	-	6.77	2.80	7.67
Dolomite	7.01	-	4.27	1.04	-	-
Quartz	3.0	-	-	-	-	14.32
Tetradium	-	-	-	-	-	-
Worm Tube	-	-	-	-	-	-
Stylolite	-	-	-	-	-	-

*Note: Algae (Hedstroemia = H; Solenopora = S; Kazakstanelia = K; Girvanelia = G; Nuia = N).

Table B.27. Barnardsville section point count analysis of samples 75-86 (volume percent of constituents).

Constituents	Sample Numbers					
	75	76	79	80	84	86
Micrite	58.19	36.46	54.15	67.50	16.79	36.49
Spar	39.54	39.77	2.01	30.25	13.12	16.58
Intraclasts	-	-	-	-	-	-
Peloids	-	-	0.50	-	2.09	15.16
Brachiopods	-	-	1.25	-	7.87	2.13
Gastropods	-	-	8.06	-	11.54	5.68
Ostracods	2.25	5.52	7.80	2.27	1.31	2.36
Trilobites	-	-	-	-	1.83	3.08
Molluscan debris	-	1.65	13.60	-	38.58	1.89
Pelmatozoans	-	0.55	-	-	1.31	-
Bryozoans	-	-	1.51	-	5.51	2.13
Algae	-	0.55 (H+S)	-	-	-	-
Oncolite	-	-	-	-	-	-
Stromatoporoids	-	4.97	-	-	-	-
Unidentifiable Fossile debris	-	-	-	-	-	-
Dolomite	-	-	11.08	-	-	14.45
Quartz	-	10.49	-	-	-	-
Tetradium	-	-	-	-	-	-
Worm Tube	-	-	-	-	-	-
Stylolite	-	-	-	-	-	-

*Note: Algae (Hedstroemia = H; Solenopora = S; Kazakstanelia = K; Girvanelia = G; Nuia = N).

Table B.28. Barnardsville section point count analysis of samples 87-101 (volume percent of constituents).

Constituents	Sample Numbers					
	87	89	92	95	97	101
Micrite	1.99	65.28	79.78	58.80	48.56	57.68
Spar	32.83	8.04	13.66	22.72	14.88	12.12
Intraclasts	5.97	-	-	-	-	-
Peloids	1.49	5.74	-	-	7.31	-
Brachiopods	2.98	-	-	-	-	-
Gastropods	-	-	-	-	-	-
Ostracods	1.49	1.37	2.18	8.23	16.97	-
Trilobites	3.48	-	-	-	-	-
Molluscan debris	8.20	-	-	-	-	-
Pelmatozoans	26.36	-	-	-	-	-
Bryozoans	11.19	-	-	-	-	-
Algae	3.23 (H+N)	-	-	-	-	-
Oncolite	-	-	-	-	-	-
Sponge	-	-	-	-	-	-
Unidentifiable Fossile debris	-	-	-	10.22	8.35	7.54
Dolomite	0.74	-	-	-	-	-
Quartz	-	19.54	-	-	3.91	22.64
Tetradium	-	-	-	-	-	-
Worm Tube	-	-	-	-	-	-
Stylolite	-	-	4.37	-	-	-

*Note: Algae (Hedstroemia = H; Solenopora = S; Kazakstanelia = K; Girvanelia = G; Nuia = N).

Table B.29. Barnardsville section point count analysis of samples 103-105 (volume percent of constituents).

Constituents	Sample Numbers	
	103	105
Micrite	58.10	24.43
Spar	6.75	32.16
Intraclasts	-	-
Peloids	-	2.49
Brachiopods	1.62	-
Gastropods	-	-
Ostracods	9.45	3.24
Trilobites	0.81	-
Molluscan debris	8.37	-
Pelmatozoans	1.35	-
Bryozoans	-	-
Algae	-	-
Oncolite	-	-
Sponge	-	-
Unidentifiable Fossile debris	8.10	6.98
Dolomite	-	-
Quartz	5.40	30.67
Tetradium	-	-
Worm Tube	-	-
Stylolite	-	-

*Note: Algae (Hedstroemia = H; Solenopora = S; Kazakstanelia = K; Girvanelia = G; Nuia = N).

Table B.30. Ten Mile section point count analysis of samples 1-8 (volume percent of constituents).

Constituents	Sample Numbers					
	1	3	4	5	6	8
Micrite	57.45	39.94	29.80	50.25	54.73	70.03
Spar	33.43	24.39	29.23	7.73	3.06	18.99
Intraclasts	-	-	-	1.03	-	-
Peloids	-	-	12.61	7.98	11.76	-
Brachiopods	-	-	-	-	-	-
Gastropods	-	-	-	-	-	-
Ostracods	0.30	-	-	5.15	9.71	-
Trilobites	-	-	-	2.31	1.53	-
Molluscan debris	-	-	-	-	2.04	-
Pelmatozoans	-	-	-	0.51	-	-
Bryozoans	-	-	-	-	-	-
Algae	-	-	-	2.06(H)	-	-
Oncolite	-	-	-	-	-	-
Sponge	-	-	-	-	-	-
Unidentifiable Fossile debris	3.34	-	-	4.63	2.55	-
Dolomite	-	-	-	-	-	-
Quartz	4.26	35.67	18.62	18.29	14.57	-
Tetradium	-	-	-	-	-	-
Worm Tube	-	-	-	-	-	-
Stylolite	1.22	-	9.75	-	-	10.09

*Note: Algae (Hedstroemia = H; Solenopora = S; Kazakstanelia = K; Girvanelia = G; Nuia = N).

Table B.31. Ten Mile section point count analysis of samples 10 through 19-1 (volume percent of constituents).

Constituents	Sample Numbers					
	10	11	14	16-2	17-2	19-1
Micrite	32.03	77.59	20.45	21.22	37.19	30.29
Spar	25.49	6.44	40.26	28.38	1.93	3.66
Intraclasts	-	-	-	-	-	-
Peloids	-	-	-	-	-	-
Brachiopods	-	-	-	-	4.13	15.14
Gastropods	-	-	-	-	6.89	2.09
Ostracods	-	-	-	3.18	2.20	2.87
Trilobites	-	-	-	-	0.28	2.87
Molluscan debris	-	-	-	-	1.65	3.66
Pelmatozoans	-	-	-	-	-	2.87
Bryozoans	0.98	-	-	-	-	-
Algae	-	-	-	-	-	-
Oncolite	-	-	-	-	-	-
Sponge	-	-	-	-	-	-
Unidentifiable Fossile debris	-	-	-	23.61	4.96	4.44
Dolomite	-	-	-	-	-	27.94
Quartz	39.21	-	31.17	19.10	-	-
Tetradium	-	-	-	-	29.75	-
Worm Tube	-	-	-	-	10.47	3.39
Stylolite	2.29	15.97	8.12	4.51	-	0.78

*Note: Algae (Hedstroemia = H; Solenopora = S; Kazakstanelia = K; Girvanelia = G; Nuia = N).

Table B.32. Ten Mile section point count analysis of samples 20 through 23-4B (volume percent of constituents).

Constituents	Sample Numbers					
	20	20-1	22	23-1	23-3	23-4B
Micrite	69.79	57.21	48.08	30.28	34.17	67.46
Spar	17.01	5.24	43.27	7.63	14.93	15.52
Intraclasts	-	-	-	-	4.81	-
Peloids	-	1.04	-	3.82	10.37	-
Brachiopods	-	-	-	9.41	1.26	-
Gastropods	-	-	-	3.82	1.01	-
Ostracods	2.35	25.45	3.85	5.85	3.54	8.36
Trilobites	-	2.62	-	4.33	1.01	-
Molluscan debris	-	0.78	-	5.85	2.02	-
Pelmatozoans	-	-	-	3.05	4.05	-
Bryozoans	-	-	-	-	0.50	-
Algae	-	6.82 (H)	-	-	12.65 (H)	0.90 (H)
Oncolite	-	-	-	-	-	-
Sponge	-	-	-	-	-	-
Unidentifiable Fossile debris	-	0.78	4.80	6.11	4.30	3.58
Dolomite	-	-	-	16.79	5.31	-
Quartz	-	-	-	-	-	-
Tetradium	-	-	-	-	-	-
Worm Tube	-	-	-	-	-	-
Stylolite	8.80	-	-	3.05	-	4.18

*Note: Algae (Hedstroemia = H; Solenopora = S; Kazakstanelia = K; Girvanelia = G; Nuia = N).

Table B.33. Ten Mile section point count analysis of samples 27-37 (volume percent of constituents).

Constituents	Sample Numbers					
	27	30	32	35	36	37
Micrite	45.14	45.68	47.30	8.67	50.38	58.17
Spar	11.43	5.41	3.34	20.87	13.17	14.04
Intraclasts	-	-	0.77	3.52	-	-
Peloids	-	-	2.05	27.10	1.80	0.86
Brachiopods	-	-	1.03	1.08	0.51	-
Gastropods	-	4.05	-	0.54	-	1.43
Ostracods	11.43	13.51	7.20	8.13	6.71	3.44
Trilobites	-	0.54	1.80	2.44	-	0.57
Molluscan debris	-	1.62	0.77	5.69	1.02	3.72
Pelmatozoans	-	-	-	4.61	0.51	1.72
Bryozoans	-	2.05(S)	10.03	-	-	-
Algae	-	-	1.54(S)	-	1.02(H)	-
Oncolite	-	-	-	-	-	-
Sponge	-	-	-	-	10.33	-
Unidentifiable Fossile debris	27.43	8.14	9.25	2.71	10.85	10.89
Dolomite	-	-	-	-	3.60	1.43
Quartz	-	-	-	-	-	-
Tetradium	-	10.56	10.03	14.63	-	2.29
Worm Tube	-	11.76	1.54	-	-	0.57
Stylolite	4.57	1.64	3.34	-	-	0.86

*Note: Algae (Hedstroemia = H; Solenopora = S; Kazakstanelia = K; Girvanelia = G; Nuia = N).

Table B.34. Ten Mile section point count analysis of samples 38-39M (volume percent of constituents).

Constituents	Sample Numbers					
	38	39A	39D	39G	39J	39M
Micrite	38.48	50.42	45.38	51.65	-	45.82
Spar	17.34	11.33	7.61	35.74	9.58	8.89
Intraclasts	0.81	-	-	-	23.05	-
Peloids	5.42	-	1.09	-	11.08	-
Brachiopods	0.81	14.16	2.17	-	7.49	12.40
Gastropods	1.89	-	1.63	-	-	7.55
Ostracods	3.25	3.40	2.72	-	2.99	1.62
Trilobites	0.81	3.12	1.09	-	0.60	0.54
Molluscan debris	1.08	3.68	6.79	-	-	4.85
Pelmatozoans	2.98	1.42	2.17	-	35.33	1.62
Bryozoans	2.43	-	0.82	-	3.59	0.81
Algae	0.54(H)	-	0.54(S)	-	-	-
Oncolite	-	-	-	-	-	-
Sponge	-	-	-	-	-	-
Unidentifiable Fossile debris	17.61	11.61	19.29	2.40	-	6.20
Dolomite	3.79	-	5.98	10.21	6.29	8.09
Quartz	-	-	-	-	-	-
Tetradium	2.71	-	0.82	-	-	-
Worm Tube	-	-	-	-	-	1.61
Stylolite	-	0.85	1.90	-	-	-

*Note: Algae (Hedstroemia = H; Solenopora = S; Kazakstanelia = K; Girvanelia = G; Nuia = N).

Table B.35. Ten Mile section point count analysis of samples 39N-40 (volume percent of constituents).

Constituents	Sample Numbers					
	39N	39O	39R	39S	39T	40
Micrite	16.71	2.12	34.09	67.76	51.07	53
Spar	9.7	18.25	14.48	11.34	30.89	24
Intraclasts	2.42	4.23	1.13	-	-	2
Peloids	16.98	33.60	24.71	-	-	14.33
Brachiopods	8.08	7.94	1.13	-	-	-
Gastropods	0.80	-	1.13	-	-	-
Ostracods	3.23	3.97	12.78	-	11.62	5.33
Trilobites	3.77	3.97	5.39	-	-	1.33
Molluscan debris	3.23	0.53	2.55	-	-	-
Pelmatozoans	4.04	9.26	1.98	-	-	-
Bryozoans	2.15	9.26	-	-	-	-
Algae	0.53(H)	-	-	-	-	-
Oncolite	-	-	-	-	-	-
Sponge	-	-	-	-	-	-
Unidentifiable Fossile debris	3.77	6.87	0.56	9.55	-	-
Dolomite	24.52	-	-	11.34	0	0
Quartz	-	-	-	-	-	-
Tetradium	-	-	-	-	-	-
Worm Tube	-	-	-	-	-	-
Stylolite	-	-	-	-	6.42	-

*Note: Algae (Hedstroemia = H; Solenopora = S; Kazakstanelia = K; Girvanelia = G; Nuia = N).

Table B.36. Ten Mile section point count analysis of samples 41A-42B (volume percent of constituents).

Constituents	Sample Numbers					
	41A	41C	41E	41F	42	42B
Micrite	11.81	5.28	57	-	77.32	41.47
Spar	20.73	12.90	16	13.49	16.93	7.36
Intraclasts	2.36	0.59	-	4.11	-	-
Peloids	-	25.51	24.86	39	-	-
Brachiopods	17.32	17.60	12.57	2.93	-	-
Gastropods	1.05	0.59	0.57	0.88	-	-
Ostracods	1.31	4.69	8	4.11	5.75	13.71
Trilobites	5.77	2.35	2.86	0.88	-	-
Molluscan debris	-	2.64	12.86	17.59	-	-
Pelmatozoans	9.45	2.64	8	5.28	-	-
Bryozoans	24.15	5.87	5.71	2.93	-	-
Algae	0.26(S)	-	-	-	-	-
Oncolite	-	-	-	-	-	-
Sponge	-	-	-	-	-	-
Unidentifiable Fossile debris	1.31	17.88	8	8.80	-	-
Dolomite	2.89	-	-	-	-	-
Quartz	-	-	-	-	-	-
Tetradium	-	-	-	-	-	-
Worm Tube	1.57	0.59	-	-	-	37.46
Stylolite	-	0.87	-	-	-	-

*Note: Algae (Hedstroemia = H; Solenopora = S; Kazakstanelia = K; Girvanelia = G; Nuia = N).

Table B.37. Ten Mile section point count analysis of samples 42C-45B (volume percent of constituents).

Constituents	Sample Numbers					
	42C	43B	44	44C	45A	45B
Micrite	11.97	65.77	13.82	40.43	22.91	2.64
Spar	16.22	6.31	15.29	14.82	24.77	0.99
Intraclasts	9.57	-	7.06	3.77	4.33	46.20
Peloids	18.62	-	30	10.24	47.99	-
Brachiopods	0.80	1.20	6.18	1.62	-	-
Gastropods	0.53	0.60	2.06	-	-	-
Ostracods	5.85	2.10	5.29	2.43	-	4.95
Trilobites	1.33	2.70	2.35	1.35	-	0.66
Molluscan debris	-	-	3.53	-	-	-
Pelmatozoans	10.64	1.20	7.35	2.16	-	-
Bryozoans	4.52	6.31	2.35	2.43	-	-
Algae	1.60(S)	-	-	-	-	-
Oncolite	-	-	-	-	-	-
Sponge	-	-	-	-	-	-
Unidentifiable Fossile debris	10.64	1.80	4.71	16.17	-	-
Dolomite	5.32	7.21	-	3.23	-	-
Quartz	-	-	-	-	-	-
Tetradium	-	-	-	-	-	43.56
Worm Tube	-	-	-	-	-	-
Stylolite	2.39	4.80	-	-	-	0.99

*Note: Algae (Hedstroemia = H; Solenopora = S; Kazakstanelia = K; Girvanelia = G; Nuia = N).

Table B.38. Ten Mile section point count analysis of samples 45E-46K (volume percent of constituents).

Constituents	Sample Numbers					
	45E	46	46D	46E	46H	46K
Micrite	66.27	15.08	2.08	32.37	42.51	16.98
Spar	17.75	10.61	18.18	2.63	4.90	36.39
Intraclasts	-	0.84	2.60	0.26	-	-
Peloids	-	-	0.52	0.26	1.36	-
Brachiopods	-	9.78	8.05	7.37	0.54	12.13
Gastropods	-	-	0.26	1.32	1.63	3.50
Ostracods	4.73	2.79	4.16	2.63	7.63	0.54
Trilobites	-	7.54	2.60	5.26	1.36	2.70
Molluscan debris	-	1.68	1.30	11.84	3	4.85
Pelmatozoans	-	18.44	17.92	4.74	-	6.74
Bryozoans	-	18.72	35.84	3.68	-	11.32
Algae	-	-	-	0.79 (S)	1.36 (S)	-
Oncolite	-	-	-	-	-	-
Sponge	-	-	-	-	-	-
Unidentifiable Fossile debris	7.10	8.94	3.89	18.42	30.79	2.16
Dolomite	-	3.35	2.60	2.89	0.82	0.80
Quartz	-	-	-	-	-	-
Tetradium	-	-	-	-	3	-
Worm Tube	-	-	-	-	1.09	-
Stylolite	4.14	2.23	-	5.53	-	1.89

*Note: Algae (Hedstroemia = H; Solenopora = S; Kazakstanelia = K; Girvanelia = G; Nuia = N).

APPENDIX C

FACIES ASSIGNMENT OF SAMPLES IN THE FOUR MEASURED STRATIGRAPHIC SECTIONS

Table C.1. Stratigraphic section samples.

Facies	Center Point	Barnardsville	Ten Mile	Goodfield
1	1C, 1B, 1B1, 1A	------	------	1A, 2A, 26, 34, 51
2a	1D, 1E, 1F	------	------	------
2b	17A, 18A, 27R, 23A	96	39T, 42A	52
3a	15A, 16A1, 6-1A, 13A, 28A, 28B, 28C, 28F, 29C, 29D, 29F, 29G, 29H, 29I, 29J, 31	24, 39-1, 41, 42, 43, 44, 54, 55, 56	14, 20-1, 39L, 39M, 39O, 39R, 41F, 45A, 45B	38, 43, 91
3b	29K	20, 21, 22, 23, 25, 30, 46, 47, 60, 67, 69, 77, 90-1, 93, 95, 98, 100, 101, 103	8, 16, 26, 39S, 40A-1, 40, 42, 42B, 45C, 45D	33, 39, 45, 48, 49, 85, 86, 88, 89, 90, 92, 93
3c	------	75	------	------
4a	17B, 19A, 19B, 20A-1, 20A-2, 24A, 24B, 24B-2, 24BL, 29A-2	3, 7, 8, 26, 31, 48, 50, 51	3, 43A, 46G, 46C, 46D, 46L	5, 18, 21, 22, 23, 32, 37, 53, 56, 59, 64, 66, 69, 70, 74, 75, 80, 83
4b	10A, 28D, 28E, 28G	1, 2, 4, 5, 6, 9, 10, 11, 15, 19, 61, 76, 84, 88, 91, 94, 97	6, 16-1, 16-2, 17-1, 17-2, 18-1, 38, 39D, 41A, 46E, 46F, 46G, 46H, 46I, 46J, 46K	60, 61, 79

Table C.1 (continued)

Facies	Center Point	Barnardsville	Ten Mile	Goodfield
4c	11A, 14A, 14B, 22A, 22B, 22C, 25A, 26C, 26D, 26F, 29A, 6A, 25D, 25C	29, 38, 53, 62, 66, 71, 74, 89, 33	5, 22, 23, 23-4, 25, 25-1, 27, 28, 20, 32C, 33, 36, 37, 37-1, 39C, 39E, 39F, 39H, 41, 41B, 43, 44C, 45E	3, 4, 6, 7, 8, 9, 10, 15, 24, 31, 54, 98
4d	5-1B, 5-1C	63, 79, 78	19-1, 39A-1	------
5a	1G, 1H, 1I, 9A, 12A, 21A, 21A-2	70, 104, 105	1, 4, 9, 10, 12, 34, 39B, 43B-1	11, 12, 14, 19, 44, 8A
5b	3A, 5-1A, 5A, 5B, 16B, 16C, 16D, 16E-1, 16E-2, 26A, 25B	32, 58, 80, 82, 102	11, 18A02, 20A-2, 21, 39G	13, 16, 25, 77, 84
6	5b, 30	12, 16, 17, 18, 27, 28, 34, 35, 36, 37, 40, 45, 49, 52, 57, 59, 64, 65, 85, 86, 87	23-3, 23-1, 35, 39I, 39J, 39K, 39N, 41C, 41D, 41E, 42C, 43A, 44B, 44, 46	17, 30, 35, 41, 57, 62, 65, 67, 68, 71, 72, 73, 76, 78, 81, 82, 95, 96, 99, 100
7	7A	13, 14, 68, 72, 73, 80, 81, 83	29, 31	28, 29, 40, 47, 50

APPENDIX D

PROCEDURE AND SAMPLE PREPARATION FOR ATOMIC ABSORPTION ANALYSIS

ATOMIC ABSORPTION SAMPLE PREPARATION

In order to prepare a homogenous sample representative of the whole rock for geochemical analysis, several small portions of the four corners of the rock chips (approximately 1 cm squares, representative of sample of each thin section) were cut. These cuttings were polished to remove surface contamination. Samples were washed and rinsed with deionized water and dried. After drying, samples were ground to a fine powder. Each ground sample was stored in glass bottle; the morter and pestle were washed with a solution of $HCl:HNO_3:H_2O$ (ration of 12:4:9) to remove contaminants. One gram of each sample was digested for 12 hours in 50 ml acetic acid (25% volume/volume, Hirst and Nichols, 1958), filtered, and the solution brought up to a volume of 100 ml by additional acetic acid (25% volume/volume).

These solutions were stored in 100 ml plastic bottles and filters were oven-dried and weighed to the nearest .0001 g for calculation of the amount of insoluble residue and the actual amount of sample in solution. For analysis of elements such as Fe and Mg, where elemental concentration was very high, further dilution was necessary to reach the working range of the instrument.

In order to determine: (1) the precision of the sample preparation and procedure, (2) the standard prepration and precision, and (3) the instrument calibration and repeatability, standards were run after every third sample. A summary of the analytical conditions require for elements is given in Table D.1.

Table D.1. Analytical conditions.

Element	Wavelength (A)	Spectral Band Pass (A)	Flame Type	Lamp Current (ma)
Na	5890	10	Air/Acetylene	5
Mg	2852	10	Air/Acetylene	3-5
Fe	2483	2	Air/Acetylene	5
Mn	2795	2	Air/Acetylene	5
Sr	4607	5	Air/Acetylene	5

Also to reduce the amount of interference (Pinta, 1975) due to: (1) chemical, (2) physical, and (3) spectral, releasing agent ($LaCl_3$) and ionization buffer (HNO_3) was added to all the solution. Table D.2 summarizes the added releasing agent and/or ionization buffer for each element. The effect of physical (due to mineral salt formation) and spectral interferences (spectral band pass width) are probably minimal because in one gram sample the effect of physical interference is very low (Moss, 1981), and using a recommended (standard) spectral band width also eliminated this effect.

Table D.2. Chemical interferences for selected elements, and the recommended* releasing agent/ ionization buffer.

Element	Interference	Releasing Agent	Ionization Buffer
Mn	None	---	---
Fe	None	---	---
Mg	Some, no ionization	La^3 (10,000 mg/ml)	---
Sr	Partially ionized	---	K (2,000 mg/ml)
Ca	Yes	La^3 (10,000 mg/ml)	K (2,000 mg/ml)
Na	Yes	La^3 (10,000 mg/ml)	K (2,000 mg/ml)

*From Pinta (1975).

APPENDIX E

TWO DIMENSIONAL DIAGRAM OF TRACE ELEMENT IN RELATION TO VARIMAX ROTATION FACTORS

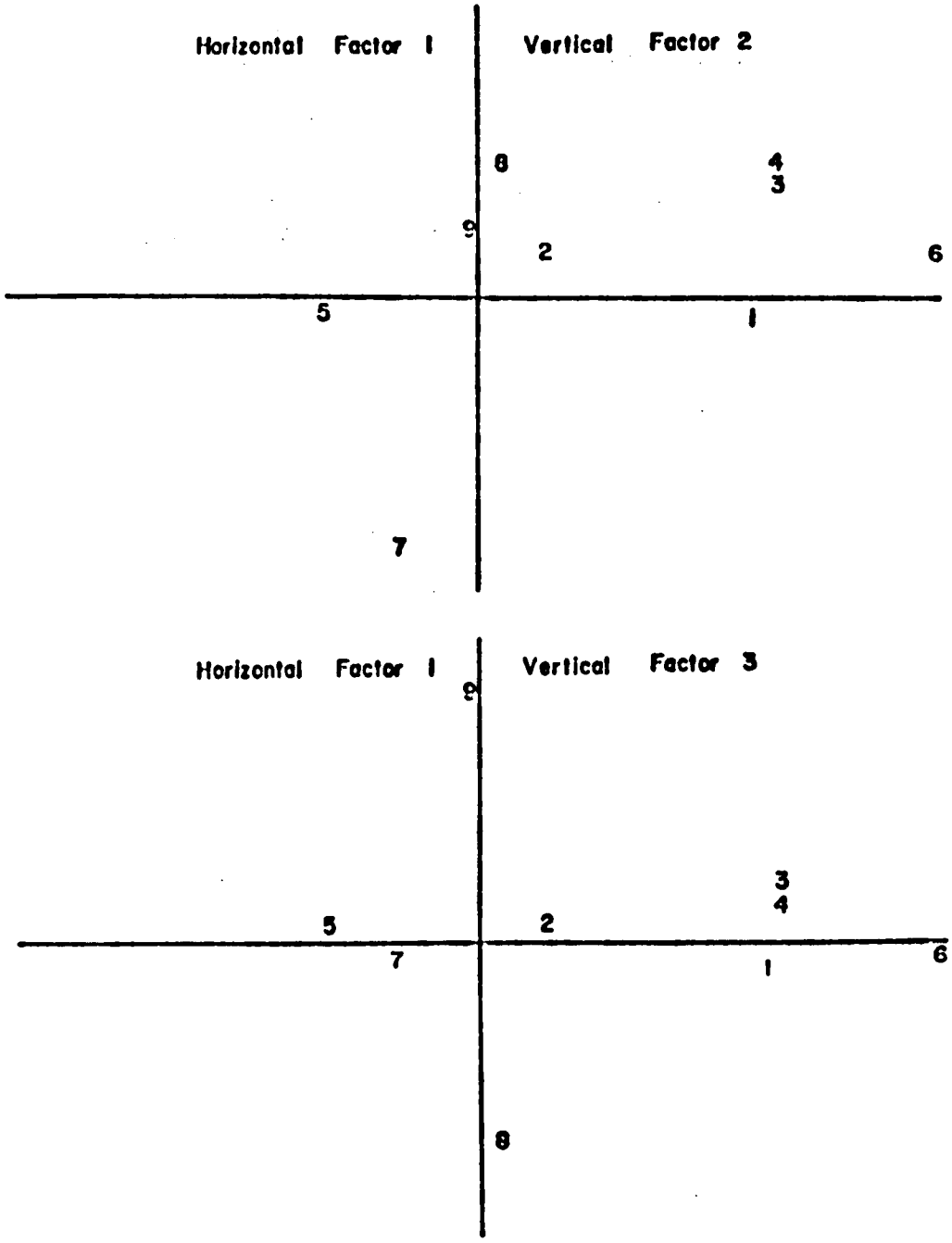


Figure E.1. Varimax rotation of Middle Ordovician data.

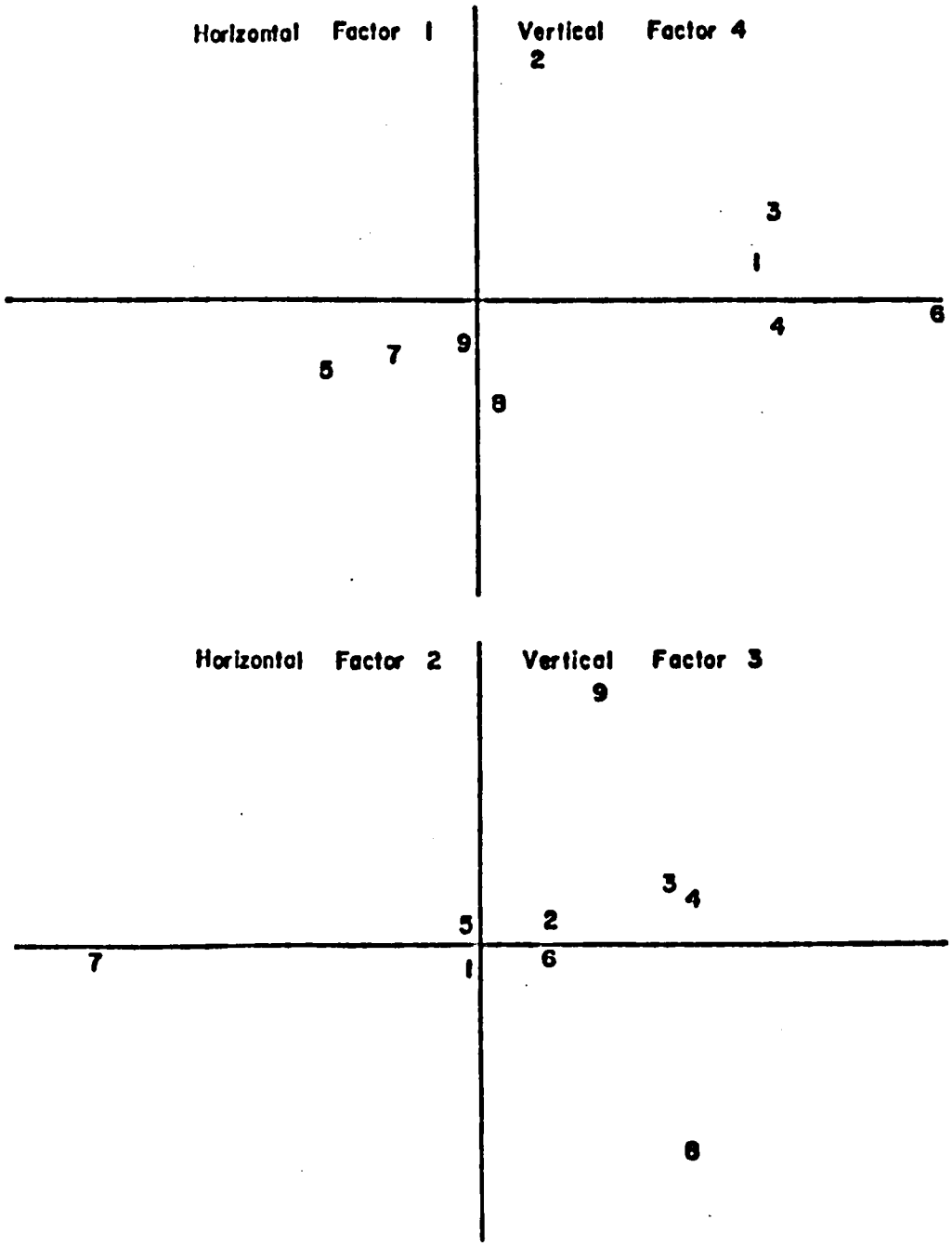
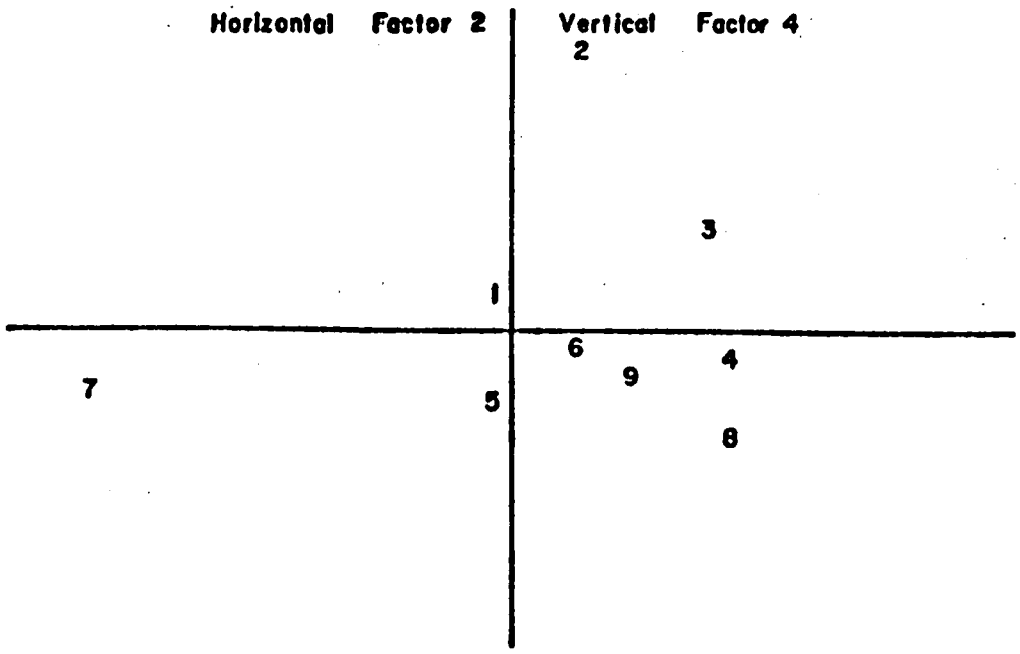


Figure E.1 (continued)



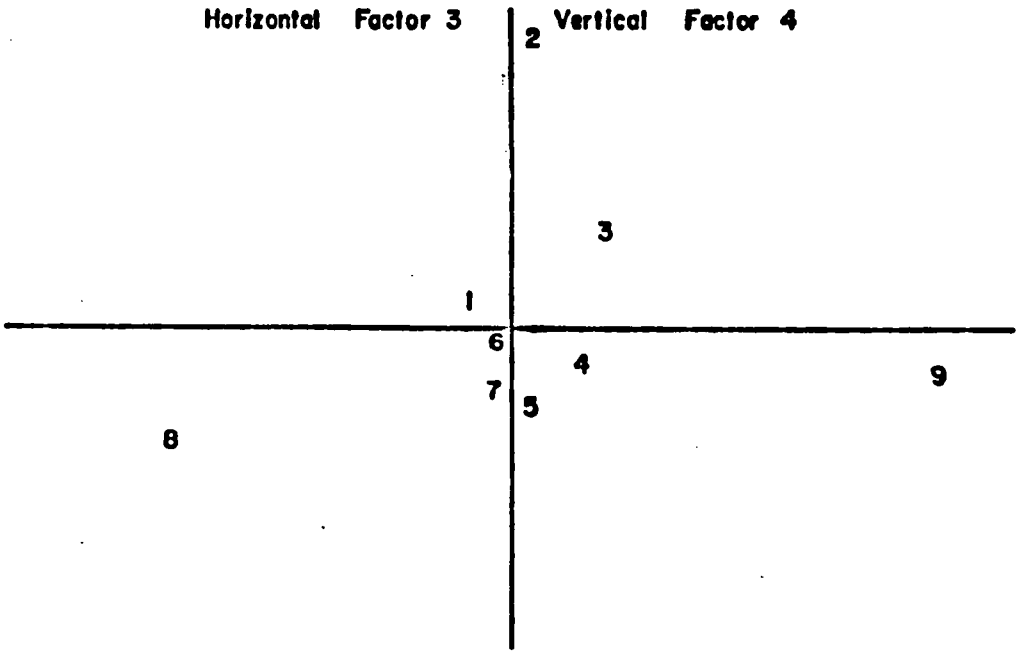


Figure E.1 (continued)

VITA

Mahmood Ghazizadeh, was born on October 22, 1948, in Abadan, Iran. He attended elementary school in Abadan, Iran, where he was graduated from Razi High School in May 1966. In the fall of that year, he entered the University of Isfahan, Iran, where he majored in geology and graduated with a Bachelor of Science degree in June 1970. He then continued his studies (in the United States of America) at Eastern new Mexico University, Portales, New Mexico, where he received a Master of Natural Science degree in December 1975, and at Northeast Louisiana University, Monroe, Louisiana, where he received a Master of Science degree in geology in August 1978. In March 1979 he enetered The University of Tennessee, Knoxville, and in August 1987 he was granted the Doctor of Philosophy degree.

Mahmood ("Moe") Ghazizadeh is currently employed by the TranEx Corporation in Lexington, Kentucky, as an exploration geologist. He is married to the former Shahnaz F. Davani of Abadan, Iran. They have two children: Lily and Jessica, 10 and 2 years.